Centro de Transferencia de Tecnología en Transportación
Departamento de Ingeniería Civil y Agrimensura
UPR-Recinto Universitario de Mayagüez
Call Box 9000 * Mayagüez, PR 00681
Tel. 787-834-6385 * Fax: 787-265-5695 * www.uprm.edu/prt2

30 Años de Excelencia en el Adiestramiento de Oficiales de Transportación a Nivel Municipal, Estatal, y Federal en Puerto Rico e Islas Vírgenes

Introducción a las Estructuras de Gaviones

Instructor

Dr. Ricardo Ramos Cabeza
Departamento de Ingeniería Civil y Agrimensura
UPR – Recinto Universitario de Mayagüez

7 de junio de 2016

Centro de Transferencia de Tecnología de Transportación

INTRODUCCIÓN

Curso corto: Diseño de Gaviones

Dr. Ricardo Ramos
Catedrático UPRM

Agenda

- Introducción
- Gaviones
- Revisión conceptos ingeniería geotécnica
  - Clasificación suelos
  - Exploración geotécnica
  - Resistencia al corte

Agenda

- Revisión presiones laterales
  - Estado en reposo
  - Teoría de Rankine – Estado Activo
  - Teoría de Rankine – Estado Pasivo
  - Teoría de Coulomb
  - Fluido Equivalente
  - Método de Equilibrio Límite
  - Fuerzas Dinámica - Mononobe-Okabe

Agenda

- Gaviones
  - Diseño
    - Criterios de diseño
    - Métodos de análisis
    - Modos de falla
    - Ejemplos
    - Ejercicios Prácticos
  - Compañías
  - Dimensiones y especificaciones típicas
  - Detalles de construcción

Gaviones (en ingles “Gabions”)

- Definición – canastas de malla de acero galvanizado en forma de caja.
- Estas canastas se rellenan con material pesado (generalmente roca, puede ser concreto triturado)
- Canastas vienen en varias dimensiones
- Uniendo varias canastas entre si se pueden obtener una variedad de geometrías.
- Las canastas se unen mediante el uso de amarres.

Definición según ASTM A974 - 97

❖A wire container, uniformly partitioned, of variable size, interconected with other similar containers, and filled with stone at the site of use, to form flexible, permanent, monolithic structures.

❖For example, retaining walls, sea walls, channel linings, revetments, and weir for erosion control.

Aspectos importantes de Gaviones como Material de Construcción

- Resistencia
- Flexibilidad
- Durabilidad
- Estética
- Permeabilidad
- Fácil Instalación
- Bajo Costo
- Minimiza Impacto Ambiental

Aspectos importantes de muros en gaviones como material de construcción

Resistencia

Aspectos importantes de muros en gaviones como material de construcción

Flexibilidad-pueden resistir grandes deformaciones

Aspectos importantes de muros en gaviones como material de construcción

Capacidad Drenante

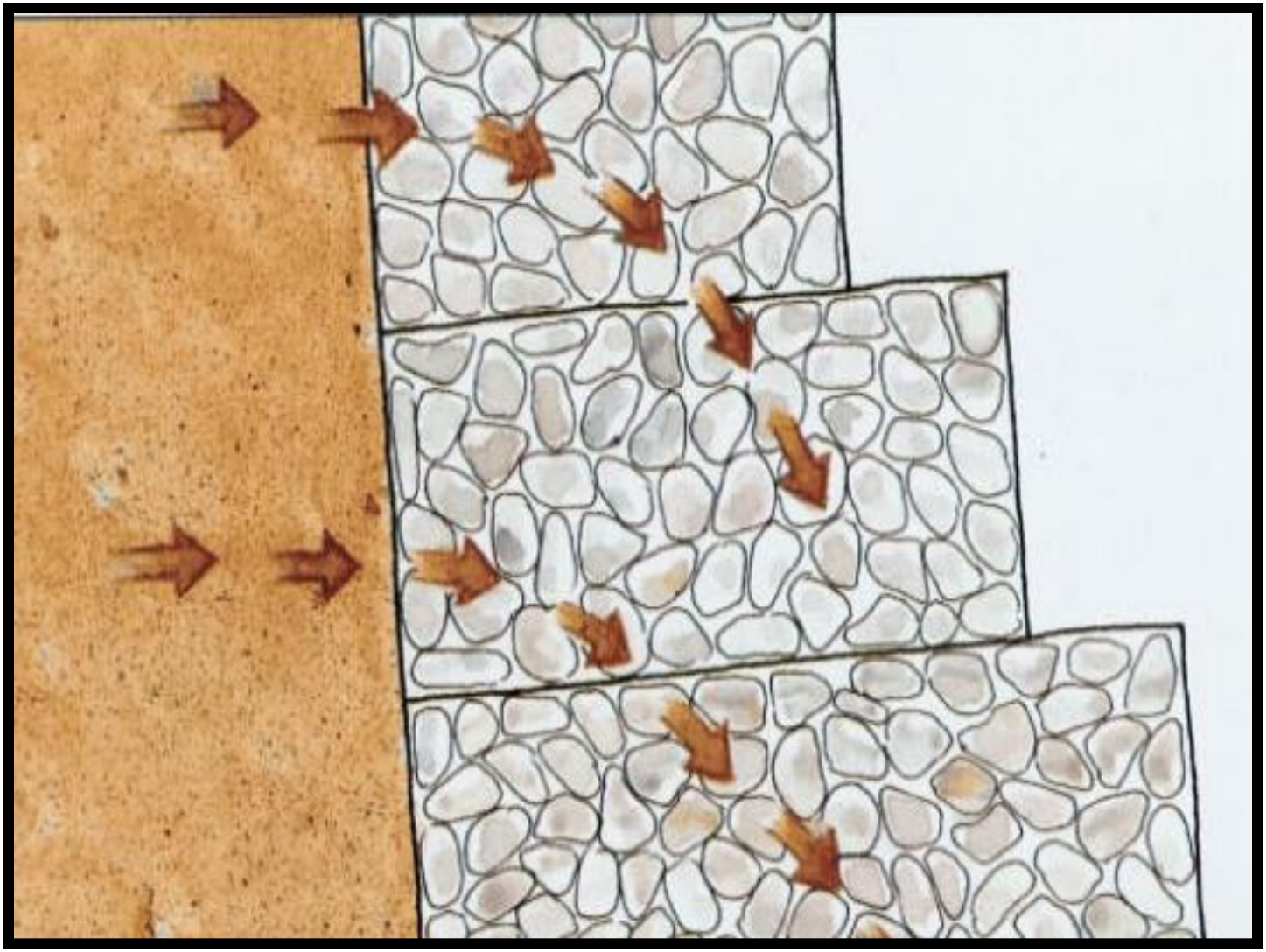

Aspectos importantes de muros en gaviones como material de construcción

Minimiza Impacto Ambiental

GAVIÓN PRE-ENSAMBLADO

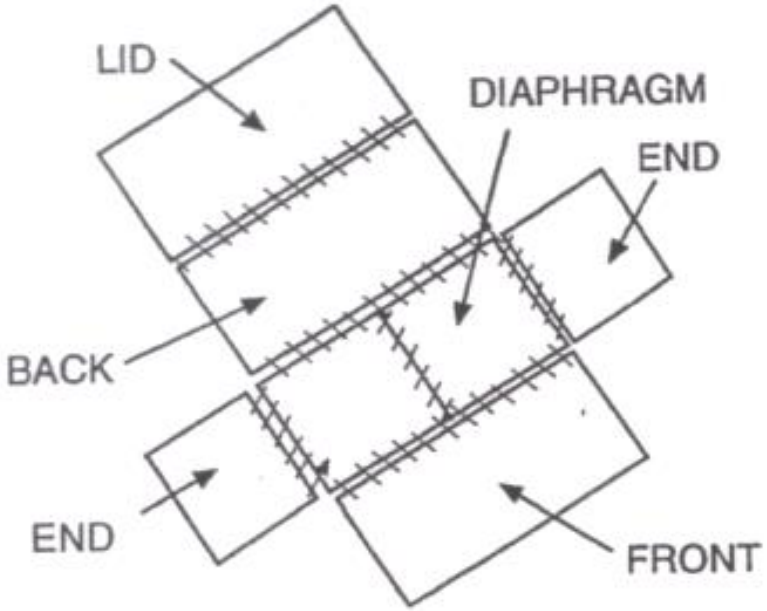

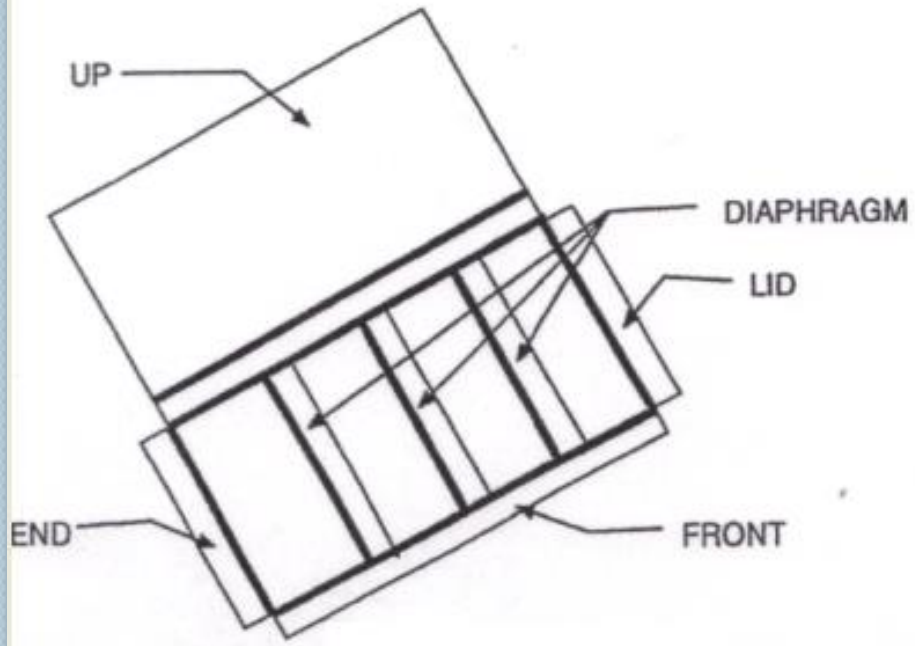

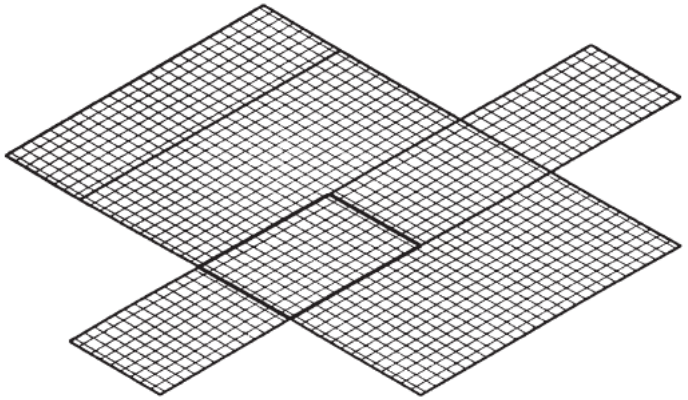

GAVIÓN

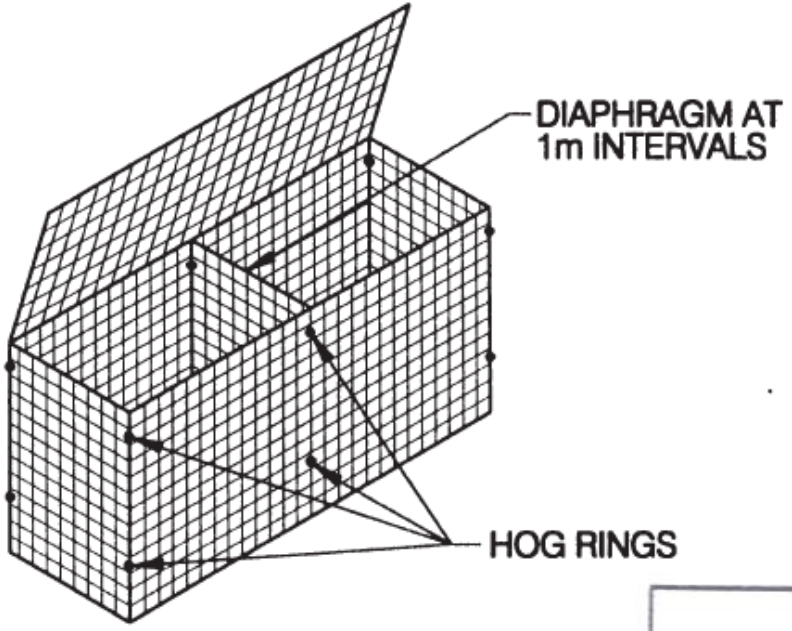
DIAPHRAGM AT
1m INTERVALS
HOG RINGS

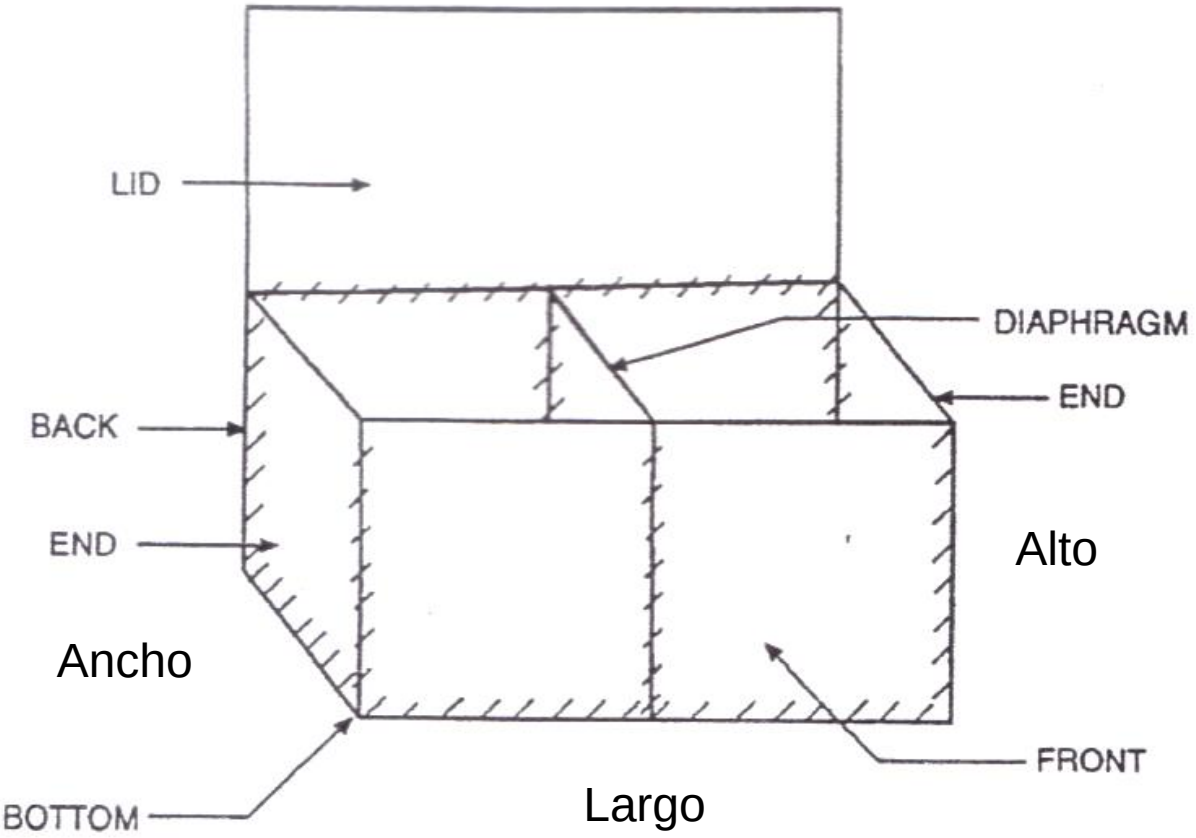
LID
DIAPHRAGM
END
BACK
END
Alto
Ancho
FRONT
BOTTOM
Largo

Tamaños típicos de gaviones (ASTM A974-97)

Tabla 1. Tamaños Típicos de Gaviones (after ASTM A 974, 1997)

Length, ft (cm)	Width, ft, (cm)	Height, ft (cm)	Number of Cells	Capacity, yd^3 (m^3)
6 (182.9)	3 (91.4)	3 (91.4)	2	2.0 (1.53)
9 (274.3)	3 (91.4)	3 (91.4)	3	3.0 (2.29)
12 (365.8)	3 (91.4)	3 (91.4)	4	4.0 (3.06)
6 (182.9)	3 (91.4)	1.5 (45.7)	2	1.0 (0.765)
9 (274.3)	3 (91.4)	1.5 (45.7)	3	1.5 (1.15)
12 (365.8)	3 (91.4)	1.5 (45.7)	4	2.0 (1.53)
6 (182.9)	3 (91.4)	1 (30.5)	2	0.66 (0.50)
9 (274.3)	3 (91.4)	1 (30.5)	3	1.0 (0.765)
12 (365.8)	3 (91.4)	1 (30.5)	4	1.33 (1.02)

“Mattress” de Gaviones

- Definición según ASTM A 974
  - Es un gavión cuya altura es relativamente pequeña en comparación con sus dimensiones laterales
- Se utilizan generalmente para revestimiento de canales

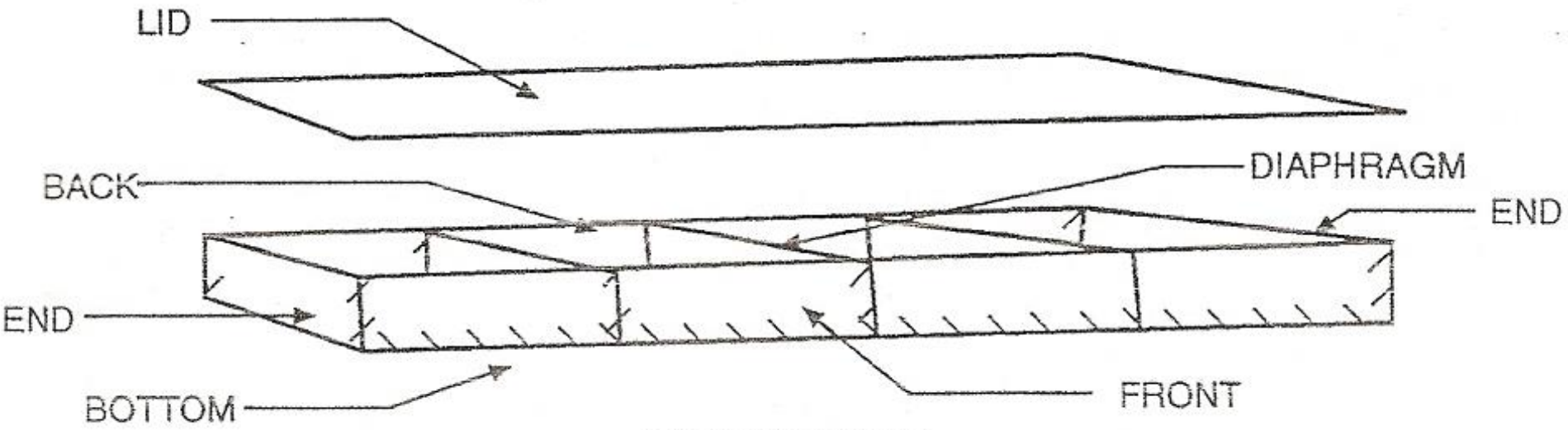

FIG. 2 Gabion Mattress **(from ASTM)**

Tamaños típicos de “mattress” de gaviones según (ASTM A974-97)

Tabla 2. Tamaños Típicos para Mattress de Gaviones (after ASTM A 974, 1997)

Length, ft (cm)	Width, ft, (cm)	Height, ft (cm)	Number of Cells	Area, yd^2, (m^2)
9 (274.3)	6 (182.9)	0.5 (15.2)	3	6.0 (5.2)
12 (365.8)	6 (182.9)	0.5 (15.2)	4	8.0 (6.69)
9 (274.3)	6 (182.9)	0.75 (22.9)	3	6.0 (5.2)
12 (365.8)	6 (182.9)	0.75 (22.9)	4	8.0 (6.69)
9 (274.3)	6 (182,9)	1.0 (30.0)	3	6.0 (5.2)
12 (365.8)	6 (182.9)	1.0 (30.0)	4	8.0 (6.69)

Amarrado de canastas según ASTM A974

- Dos tipos
  - “Lacing wire” – utilizado para ensamblar, cerrar, y/o conectar las canastas. Puede ser de acero galvanizado o recubierto con /C.

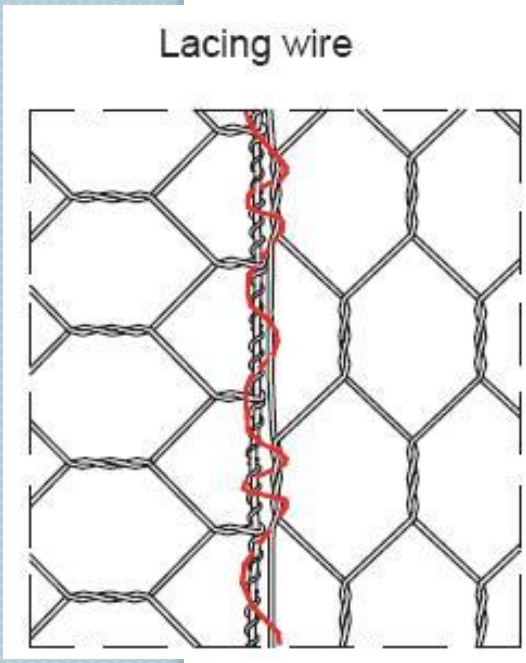

piral wire” – alambre preformado (forma e espiral) de acero galvanizado o cubierto con PVC, utilizado para ısamblaje, cierre y union de canastas.

(Imagen cortesía Macafferri)

Ejemplos de amarres utilizados para ensamblar e instalar gaviones

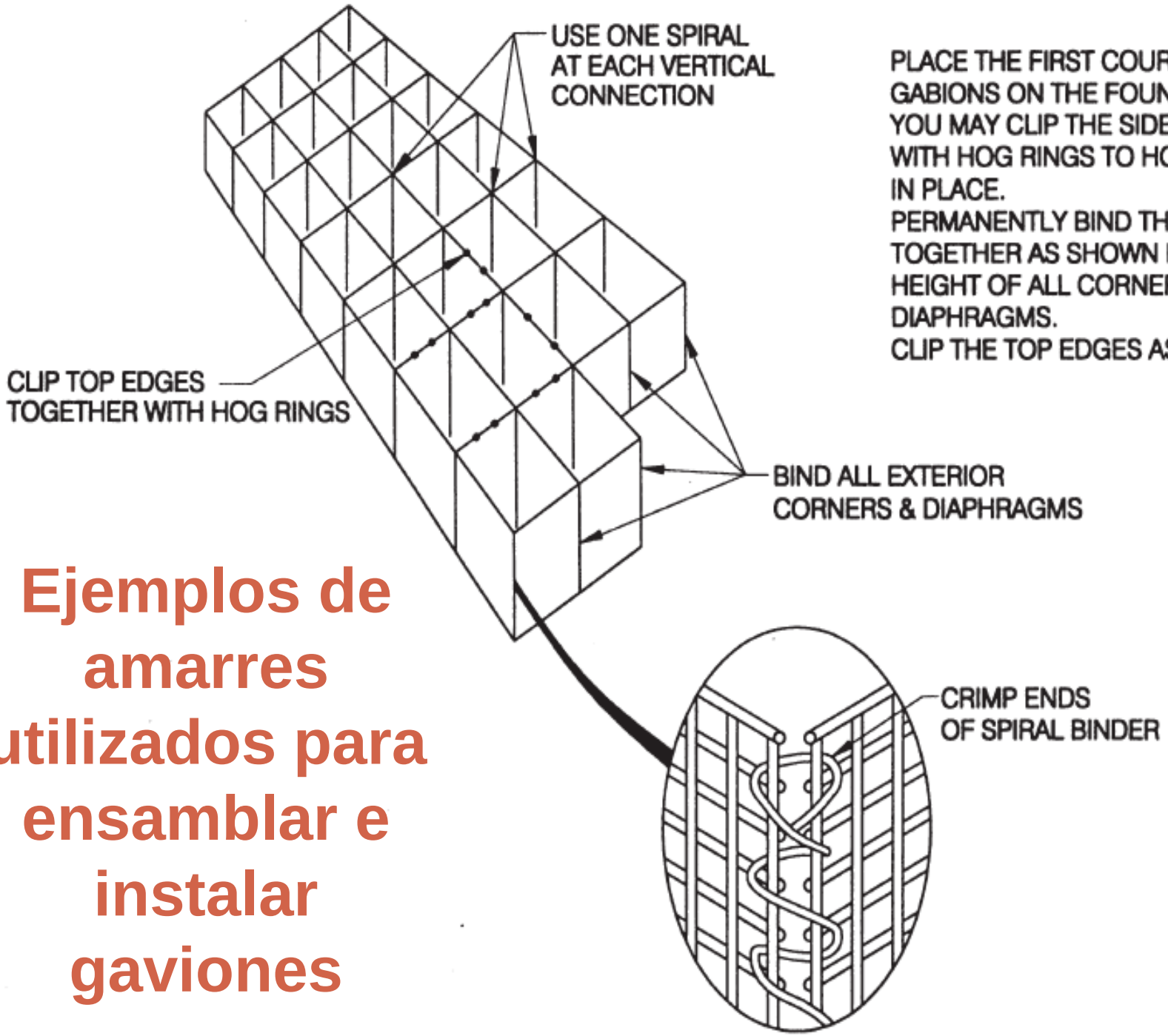

CLASIFICACION - ASTM A974 - 97

Welded wire gabions are classified according to coating:

- Style 1: Consists of welded wire fabric made of zinc coated wire before being welded into fabric.

- Style 2: Welded wire fabric made from uncoated wire. After fabrication it is zinc-coated.

- Style 3: Welded wire fabric made from wire which is coated with zonc-5% aluminum/mischmetal alloy (Zn-5AI-MM) before welded into fabric

- Style 4: Welded wire fabric made from wire which is aluminum coated before welded into fabric.

- Style 5: Welded wire fabric made from wire styles 1,2,3 or 4, and overcoated with PVC.

Orden típica según ASTM A974

- Incluir
  - Numero de unidades según planos
  - Gavión o matre
  - Dimensiones canasta
  - Estilo de alambre (amarre)
    - Citar especificaciones indicadas en ASTM

  Ejemplo:

  100 gaviones 6x3x3 pies como se indica en los planos; alambre estilo 1, con conectores, alambre y rigidizadores (“stiffeners”) según especificado en ASTM A 974.

Geometrías típicas de gaviones

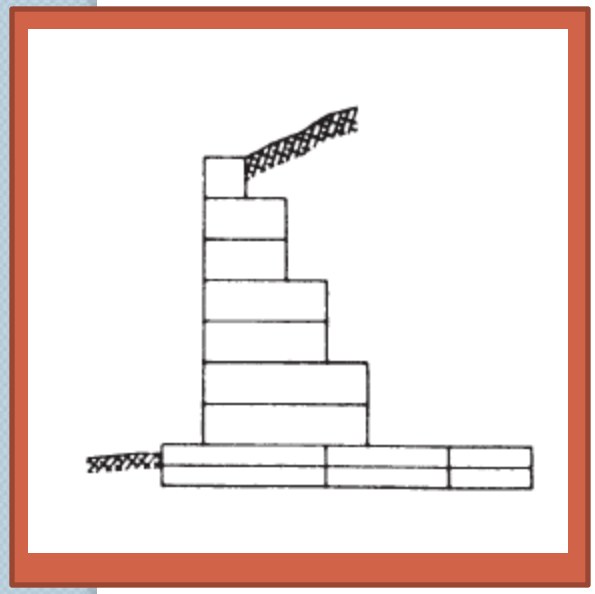

Escalonado hacia adentro y contrapeso (cohesivos)

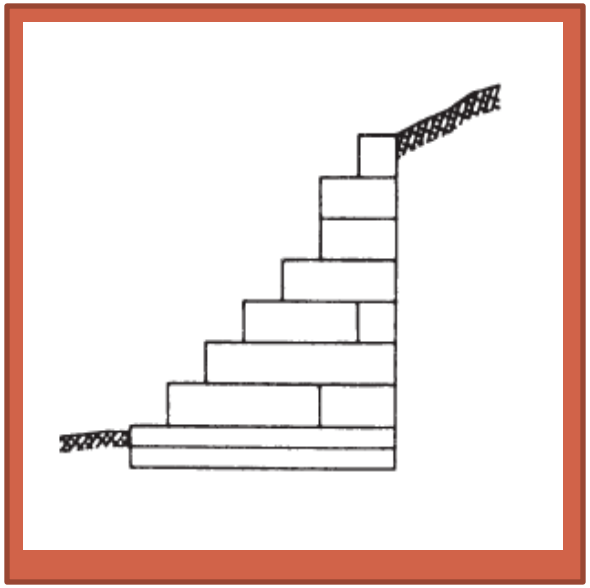

Escalonado hacia fuera

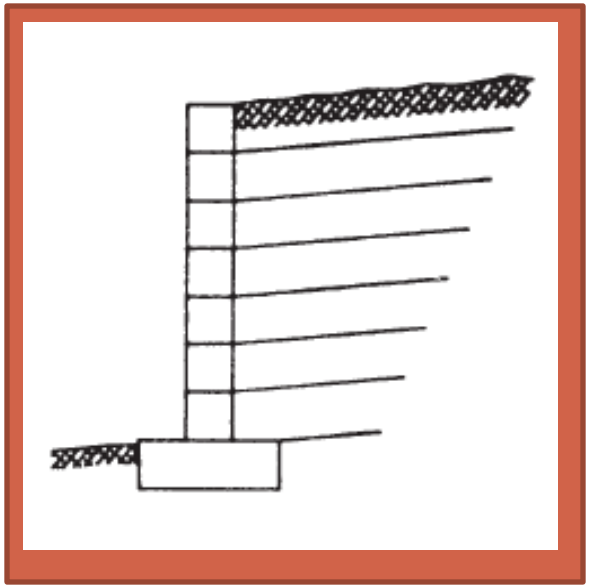

Gavión con refuerzo

-Muros pueden tener inclinación – hasta 8 grados (incrementar estabilidad)
-Colocado piedras en canasta, 1) manual o 2) maquinaria construcción

Algunos fabricantes de gaviones

- Macafferri
- Modular Gabion System (www.gabions.net)

Comentarios generales de gaviones

- Opción económica si se dispone de suficiente espacio
  - Ocupan área entre 40 y 60 % de su altura
- Económico si roca disponible
- Mayor desventaja – corrosión del alambre
  - Se ha mejorado con uso de acero galvanizado (tipo caliente) y el recubrimiento con PVC (PVC coated)
- Importante – controlar erosión interna del relleno
  - Practica común - geosintético cara interna del muro
  - Para relleno cohesivo añadir drenaje interno con chimenea
  - Para asegurar buen drenaje: tubo perforado a lo largo de la base del muro

ALGUNAS APPLICACIONES

Gaviones pueden ser utilizados para una gran variedad de aplicaciones tales como:

- Estructuras de Retención
- Estabilidad de taludes
- Estribos de puentes
- Protección contra erosión
  - Lagos y costas
- Revestimiento de canales
- "Culverts"
- Entre otros

REPUBLICA DOMINICANA

Muro contención
escalonado

Recubrimiento de Canales

foto cortesía Macafferri

Canal de Concreto - Kentucky

foto cortesía Macafferri

Canal de Concreto - Kentucky

foto cortesía Macafferri

foto cortesía Macafferri

Otra vista – Estructura Finalizada

foto cortesía Macafferri

MEXICO

Erosión costas


ITALIA


HONG KONG

AUSTRALIA

PR- #349, km 0.8

refuerzo

PR- #349, km 0.8

refuerzo


PR- #349, km 0.8
SE ALQUILA
JOHN DEERE


PR- #349, km 1.2


PR- #349, km 1.2


PR- #349, km 1.2


PR- #349, km 1.2

Revestimiento arroyo

Estabilizar flujo

Aplicaciones Innovadoras e Inusuales

IRLANDA

National Garden Exhibition Centre in County Wicklow

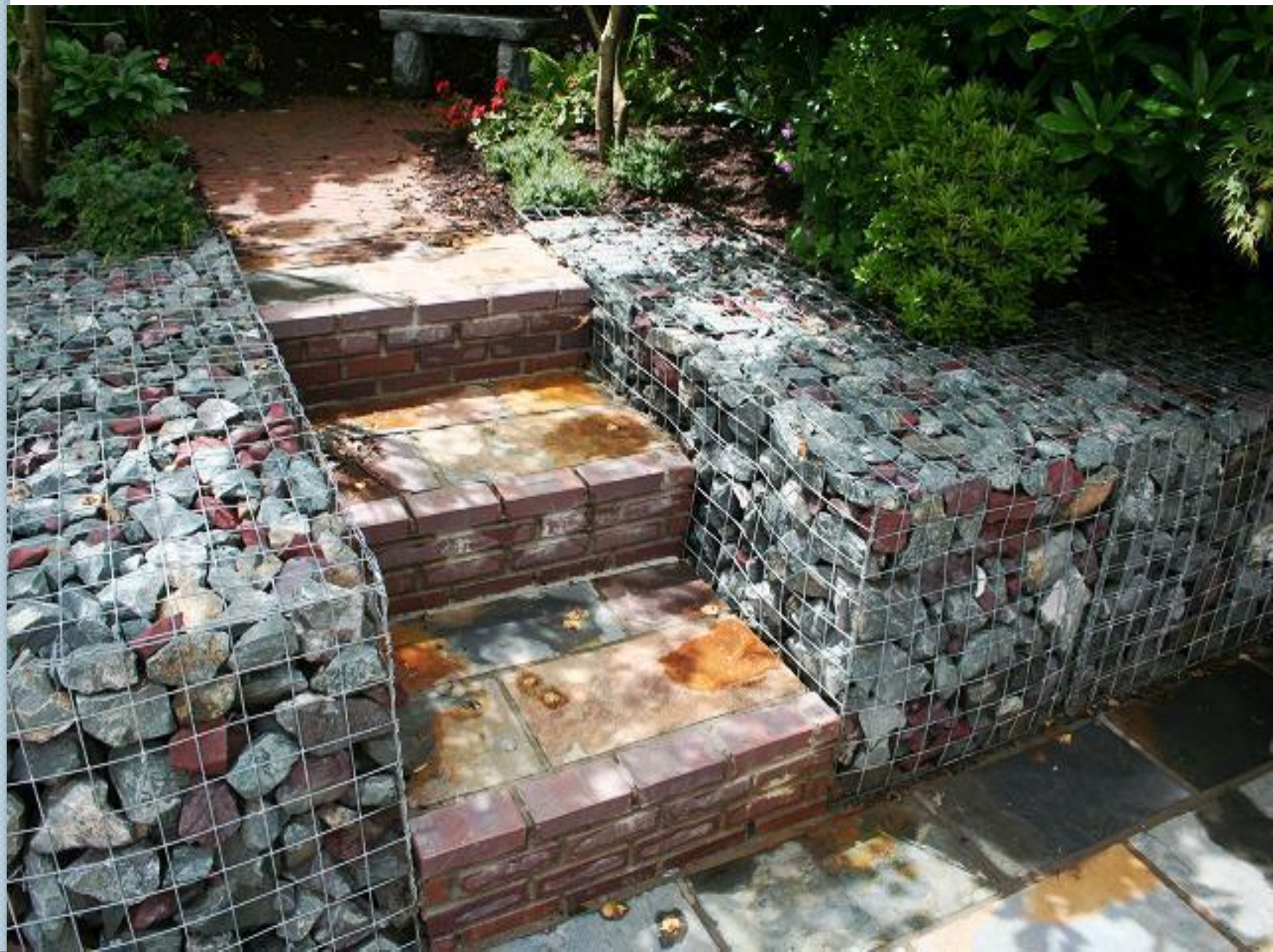

Jardinería-Irlanda

National Garden Exhibition Centre in County Wicklow

7m (~23ft) Sign Structure (Gabion / Steel Frame) – Melbourne, Australia (from Macafferri)

Presenta un uso innovador de un material inusual en la construcción de las paredes y el techo de esta hermosa residencia

Construida
2003

Bavaria – Alemania

40,000 toneladas de piedra, mantienen la casa cálida en invierno y fría en verano

4. SOIL CLASSIFICATION SYSTEMS: AASHTO AND USCS

INTRODUCTION

- Different soils with similar properties may be classified into groups and sub groups according to their engineering behavior. Classification systems provide a common language to concisely express the general characteristics of soils, which are infinitely varied, without detailed descriptions. Currently, two elaborate classification systems are commonly used by soils engineers. Both systems take into consideration the particle size distribution and Atterberg limits

CLASSIFICATION SYSTEMS

- **Two commonly used systems:**
  - Unified Soil Classification System (USCS).
  - American Association of State Highway and Transportation Officials (AASHTO) System

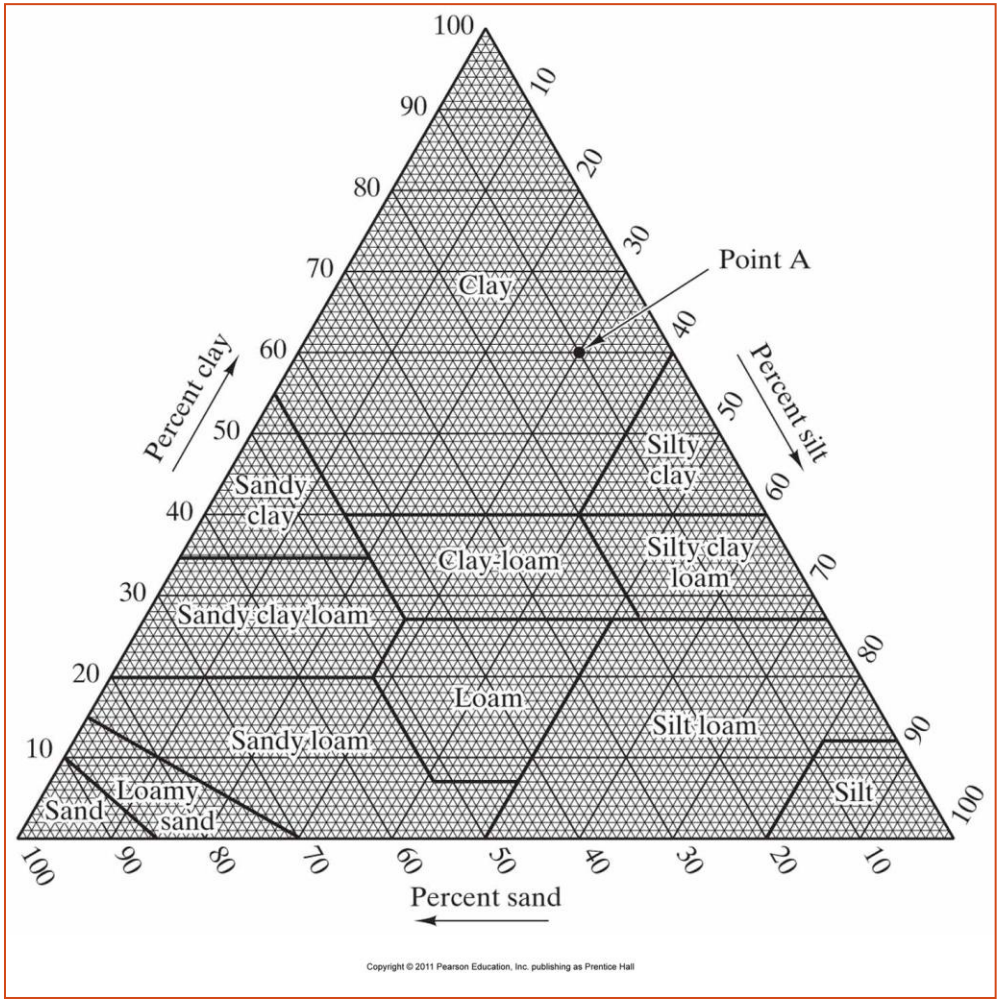

Figure 4.1a USDA soil classification triangle. There are three sets of lines in this diagram: The percent clay is represented by a series of horizontal lines, silt by lines inclined from upper right to lower left, and sand by lines inclined from lower right to upper left. For example, Point A represents 60% clay, 30% silt, and 10% sand. To classify a soil using this diagram, determine the percentages of clay, silt, and sand, and trace the appropriate lines until they meet.

4.1 AMERICAN ASSOCIATION OF STATE HIGHWAY AND TRANSPORTATION OFFICIALS SYSTEM (AASHTO)

AMERICAN ASSOCIATION OF STATE HIGHWAY AND TRANSPORTATION OFFICIALS SYSTEM (AASHTO)

- The AASTHO system of soil classification was developed in 1929 as the Public Road Administration Classification System. It has undergone several revisions, with the present version proposed by the Committee on Classification of Materials for Subgrades and Granular Type Roads of the Highway Research Board in 1945 (*ASTM designation D-3282; AASTHO method M-145*)

CLASSIFICATION

- Soil is classified into seven major groups: *A-1* through *A-7*.
- Soil classified under groups *A-1, A-2,* and *A-3* are granular materials of which 35% o less of the particles pass through the No. 200 sieve.
- Soils of which more than 35% pass through the No. 200 sieve are classified under groups *A-4, A-5, A-6* and *A-7*. These soils are mostly silt and clay materials.

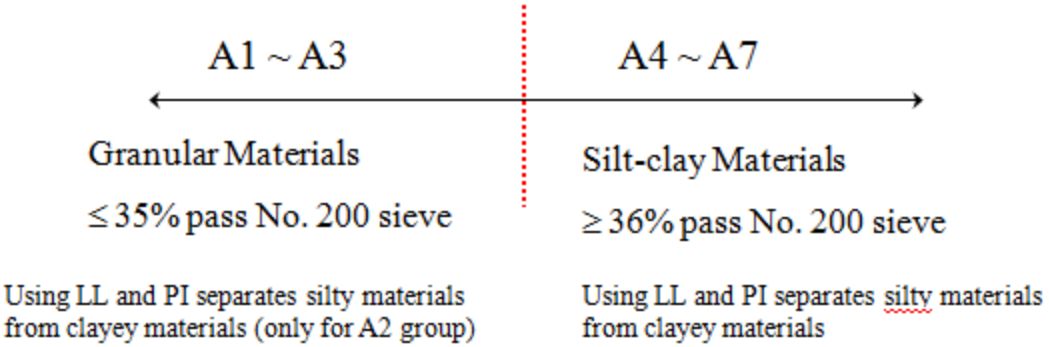

- The classification system is based on the following criteria:

1. Grain size

a. Gravel: fraction passing the 75mm (3in) sieve and retained on the No. 10 (2mm) US sieve

b. Sand: fraction passing the No. 10 (2mm) US sieve and retained on the No. 200(0.075 mm) US sieve

c. Silt and clay: fraction passing the No. 200 US sieve

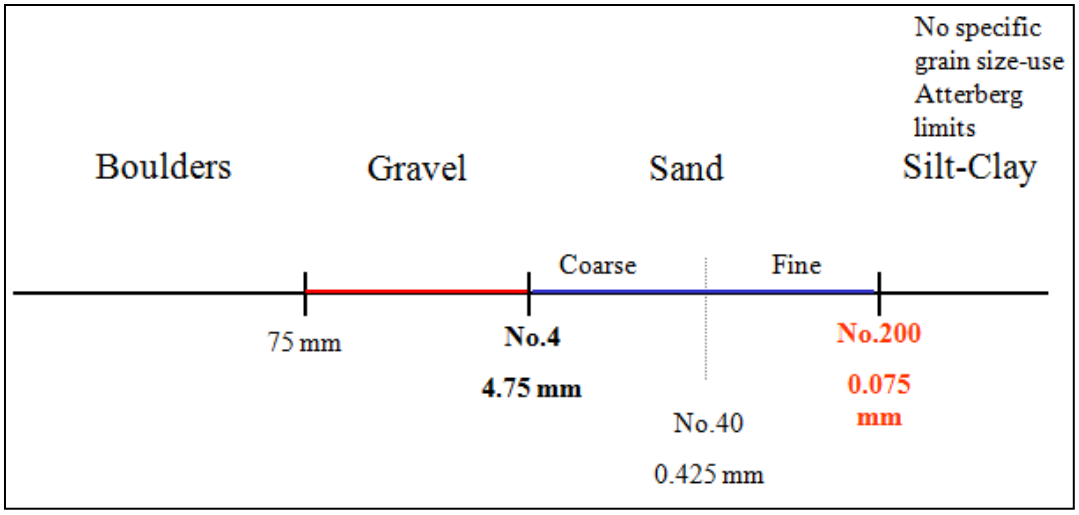

2. Plasticity: The term silty is applied when the fine fractions of the soil have a plasticity index of 10 or less. The term clayey is applied when the fine fractions have a plasticity index of 11 or more.

3. If cobbles and boulders (size larger than 75*mm*) are encountered, they are excluded from the portion of the soil sample from which classification is made. However, the percentage of such material is recorded.

TABLE 5.1 AASHTO Soil Classification System

General Classification	Granular Materials (35% or less passing No. 200 sieve)[c]							Silt-Clay Materials (more than 35% passing No. 200 sieve)				Highly Organic
Group Classification	A-1			A-2							A-7	
	A-1-a	A-1-b	A-3	A-2-4	A-2-5	A-2-6	A-2-7	A-4	A-5	A-6	A-7-5 A-7-6	A-8
Sieve analysis percent passing:												
#10	≤50											
#40	≤30	≤50	≥51									
#200	≤15	≤25	≤10	≤35	≤35	≤35	≤35	≥36	≥36	≥36	≥36	
Characteristics of fraction passing #40:											*b*	
Liquid limit				≤40	≥41	≤40	≥41	≤40	≥41	≤40	≥41	
Plasticity index	≤6		NP[a]	≤10	≤10	≥11	≥11	≤10	≤10	≥11	≥11	
Usual types of significant constituent materials	Stone fragments; gravel and sand		Fine sand	Silty or clayey gravel and sand				Silty soils		Clayey soils		Peat or muck
General rating as subgrade	Excellent to good							Fair to poor				Un-suitable

[a]NP indicates the soil is non-plastic (i.e., it has no clay).
[b]The plasticity index of A-7-5 soils is ≤ liquid limit −30. For A-7-6 soils, it is > than the liquid limit −30.
[c]The placement of A-3 before A-2 is necessary for the "left-to-right elimination process" and does not indicate superiority of A-3 over A-2.

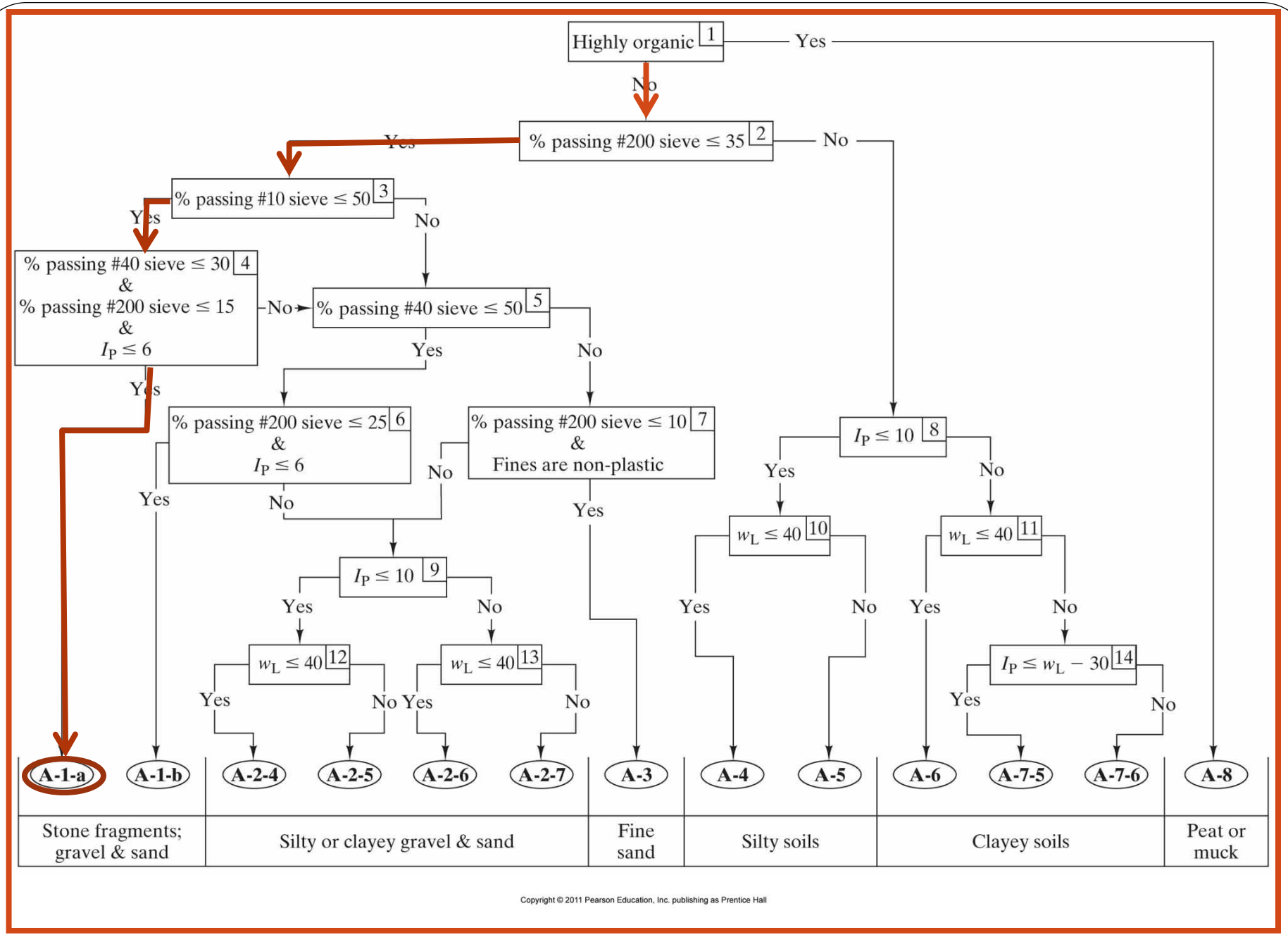

Figure 5.3 Flow chart for soil classification using the AASHTO system.

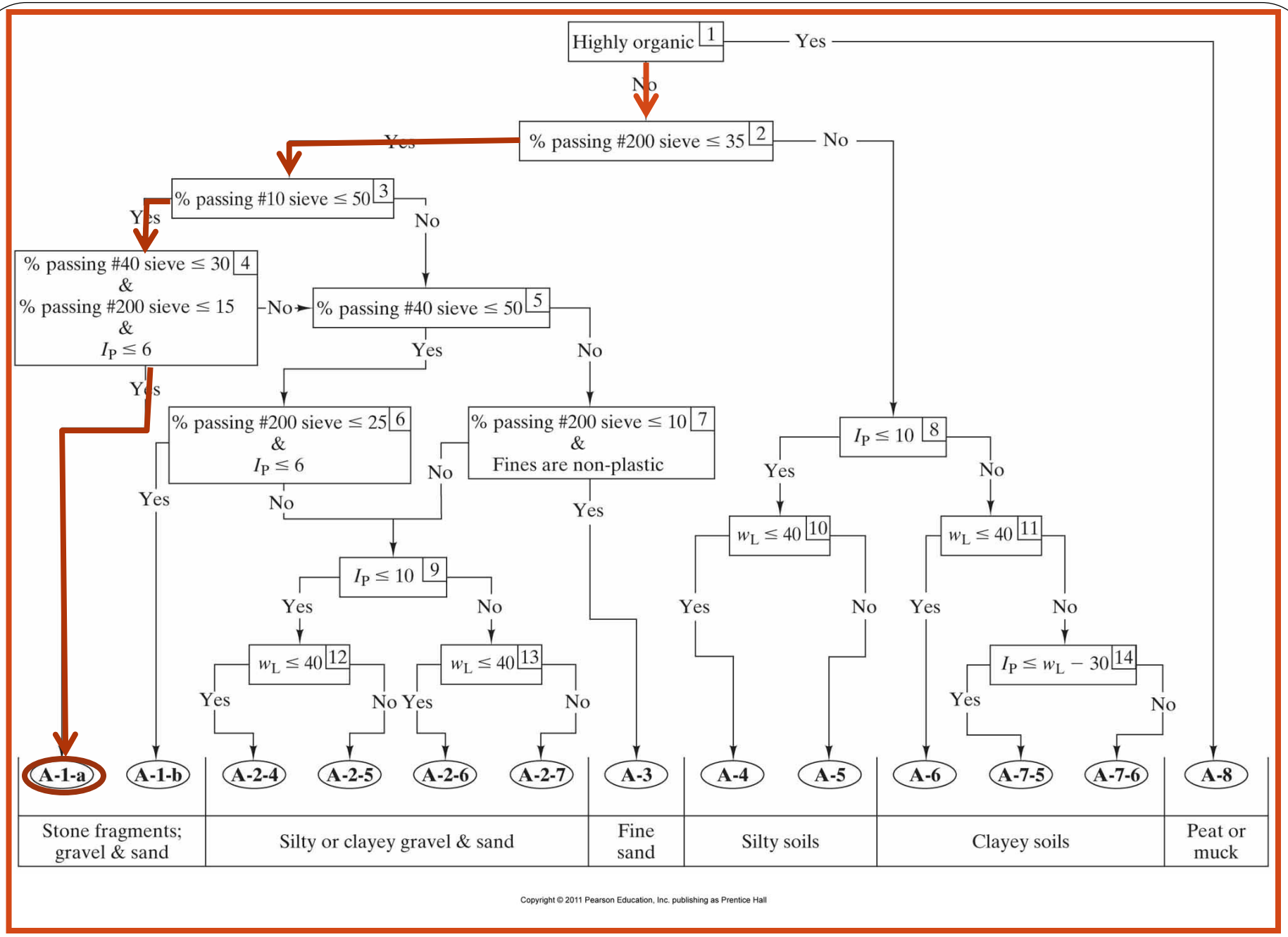

Figure 5.3 Flow chart for soil classification using the AASHTO system.

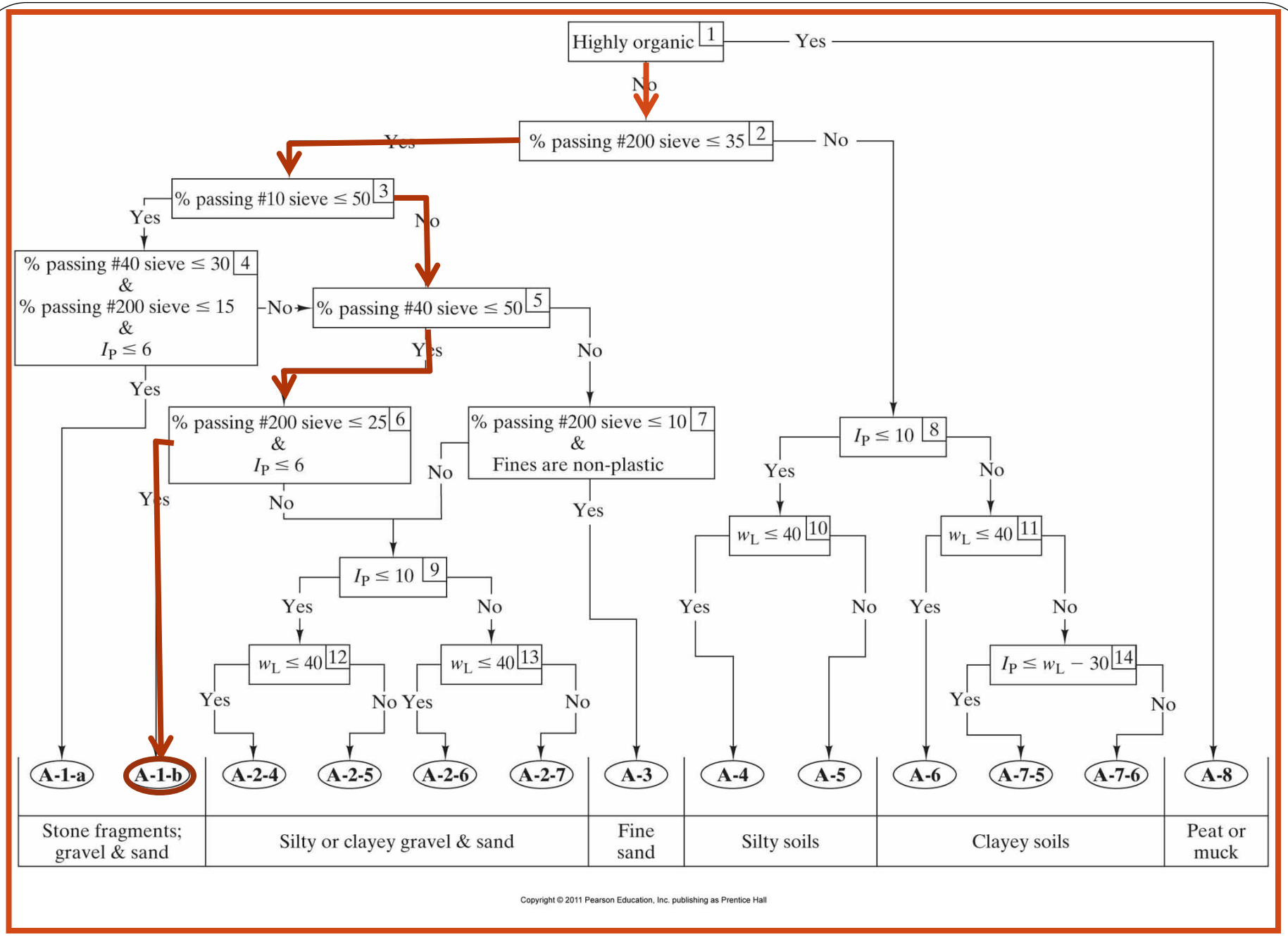

Figure 5.3 Flow chart for soil classification using the AASHTO system.

- ***Figures 4.1*** shows a plot of the range of the liquid limit and the plasticity index for soils that fall into groups *A-2, A-4, A-5, A-6 and A-7*.

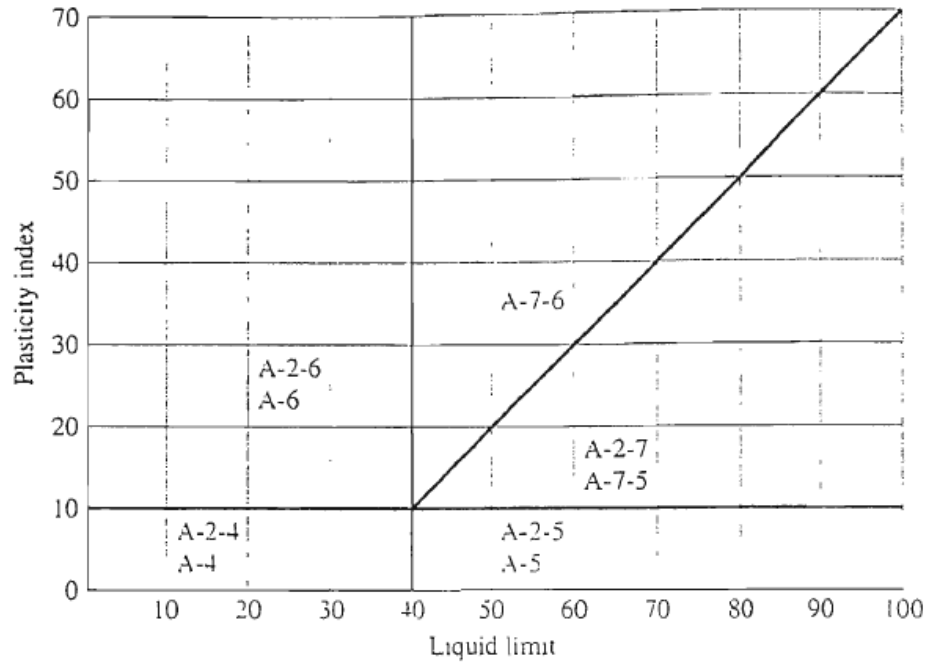

Figure 4.1 Range of liquid limit and plasticity index for soils in groups A-2, A-4, A-5, A-6, and A-7

GROUP INDEX

- The group index, an empirical formula, is used to further evaluate soils within a group (subgroups).

- To evaluate the quality of a soil as a highway subgrade material, one must also incorporate a number called the group index (GI) with the groups and subgroups of the soil. This index is written in parentheses after the group or subgroup designation. The group index is given by the Eq. (4.1):

$$GI = (F_{200} - 35)[0.2 + 0.005(LL - 40)] + 0.01(F_{200} - 15)(PI - 10)$$

Where

- F_{200}= Percentage passing through the No. 200 sieve
- LL= liquid limit
- PI=plasticity index

- The first term of Eq. (4.1)- that is: (F200 -35)[0.2+0.005(LL-40)] The partial group index determined from the liquid limit.

- The second term is the partial group index determined from the plastic limit. The second term that is, 0.01(F200-15)(PI-10), is the partial group index determined from the plasticity index. Following are some rules for determining the group index:

1. If Eq. (4.1) yields a negative value for GI, it is taken as 0
2. The group index calculated from Eq. (4.1) is rounded off to the nearest whole number.
3. There is no upper limit for the group index
4. The group index of soils belonging to groups ***A-1,a, A-1b, A-2-4, A-2-5,*** and A-3 always 0.

5. When calculating the group index for soils that belong to groups A-2-6 and A-2-7, use the partial group index for PI, Eq. (4.2)

$$GI = 0.01(F_{200} - 15)(PI - 10)$$

The quality of performance of a soil as a subgrade material is inversely proportional to the group index.

F = porcentaje pasando

R = porcentaje retenido

AASHTO

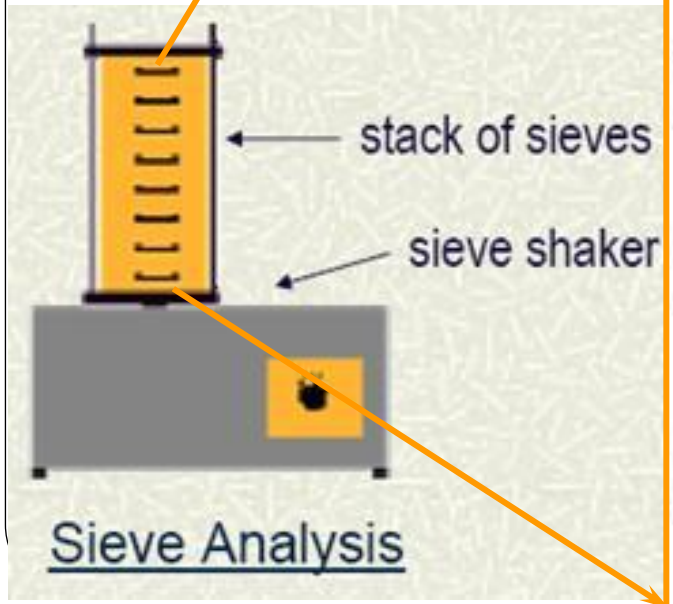

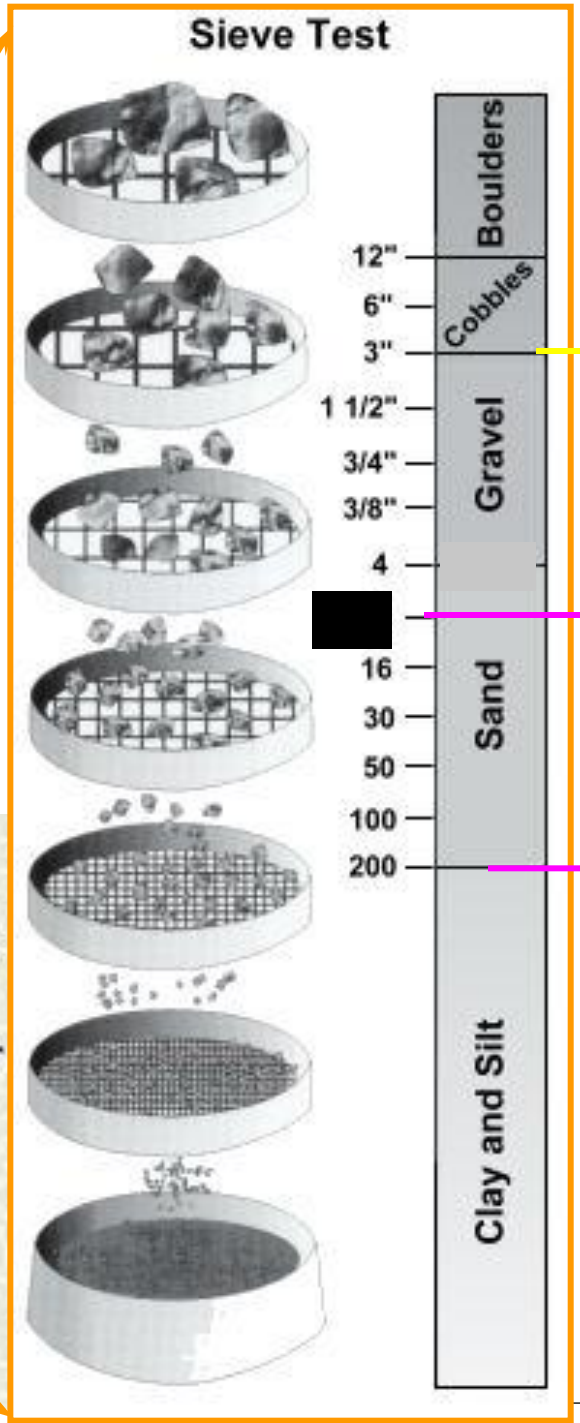

R_{200}= fracción gruesa

R_{10}= % grava

% arena

F_{200}= fracción fina

Example 4.1

Classify the following soils by the AASHTO classification system:

Description	Soil A	B	C	D	E
Percent finer than No. 10 sieve	83	100	48	90	100
Percent finer than No. 40 sieve	48	92	28	76	82
Percent finer than No. 200 sieve	20	86	6	34	38
Liquid Limit	20	70	-	37	42
Plasticity Index	5	32	Non plastic	12	23

[a] Plasticity for the minus 40 fraction

suelo A	
#10	83
#40	48
#200	20
LL	20
PI	5

Table 4.1 Classification of Highway Subgrade Materials

General classification	Granular materials (35% or less of total sample passing no. 200)					
	A-1					A-2
Group classification	A-1-a	A-1-b	A-3	A-2-4	A-2-5	A-2-
Sieve analysis (percent passing):						
No. 10	50 max.					
No. 40	30 max.	50 max.	51 min.			
No. 200	15 max.	25 max.	10 max.	35 max.	35 max.	35 m
Characteristics of fraction passing no. 40						
Liquid limit				40 max.	41 min.	40 m
Plasticity index	6 max.		NP	10 max.	10 max.	11 m

Not OK

OK

OK

OK

GI = 0, según las reglas, o calcularlo:

$$GI = (F_{200}-35)\,[0.2+0.005(LL-40)]+0.01(F_{200}-15)(PI-10)$$

$$= (20-35)[0.2+0.005(20-40)]+0.01(20-15)(5-10)$$

$$= -1.5 - 0.25 = -1.75 \rightarrow 0$$

Clasificación del Suelo A-1-b (0)

Example 4.1

Classify the following soils by the AASHTO classification system:

Description	Soil A	B	C	D	E
Percent finer than No. 10 sieve	83	100	48	90	100
Percent finer than No. 40 sieve	48	92	28	76	82
Percent finer than No. 200 sieve	20	86	6	34	38
Liquid Limit	20	70	-	37	42
Plasticity Index	5	32	Non plastic	12	23

[a] Plasticity for the minus 40 fraction

suelo B	
#10	100
#40	92
#200	86
LL	70
PI	32

Table 4.1 Classification of Highway Subgrade Material (continuación)

General classification	Silt-clay materials (More than 35% of total sample passing no. 200)			
Group classification	A-4	A-5	A-6	A-7 A-7-5[a] A-7-6[b]
Sieve analysis (percent passing)				
No. 10				
No. 40				
No. 200	36 min.	36 min.	36 min.	36 min.
				OK
				41 min.
				11 min.
				oils
				Fair to poor

[b] For A-7-6, $PI > LL - 30$

$$GI = (F_{200}-35)\,[0.2+0.005(LL-40)]+0.01(F_{200}-15)(PI-10)$$

$$= (86-35)[0.2+0.005(70-40)]+0.01(86-15)(32-10)$$

$$= 17.85 + 15.62 = 33.47 \rightarrow 33$$

Clasificación del suelo A-7-5 (33)

$PI \leq LL - 30$

$32 \leq 70-30=40 \rightarrow$ **OK**

Clasifica como:

A-7-5

EXAMPLE 4.1

The results of the particle size analysis of a soil are as follows:

Percent passing through the No. 10 sieve=100

Percent passing through the No. 40 sieve=80

Percent passing through the No. 200 sieve=58

The liquid limit and plasticity index of the minus No. 40 fraction of the soil are 30 and 10, respectively. Classify the soil by the AASTHO system.

SOLUTION

- Using table 4.1, since 58% of soil is passing through the No. 200 sieve, it falls under silt clay classifications, that is, it falls under group A-4, A-5, A-6 or A-7. Proceeding from left to right, it falls under group A-4

- From Eq. (4.1)

$$GI = (F_{200} - 35)[0.2 + 0.005(LL - 40)] + 0.01(F_{200} - 15)(PI - 10)$$
$$= (58 - 35)[0.2 + 0.005(30 - 40] + 0.01(58 - 15)(10 - 10)$$
$$= 3.45 \approx 3$$

So, the soil will be classified as A-4(3)

EXAMPLE 4.2

- Ninety five percent of a soil passes through the No. 200 sieve and has a liquid limit of 60 and plasticity index of 40. Classify the soil by the AASTHO system.

SOLUTION

- According to table 4.1 this soil falls under group A-7. (Proceed in a manner similar to Example 4.1) Since
- PI>LL-30
- 40>60-30
- This is an A-7-6 soil. Hence

$$GI = (F_{200} - 35)\left[0.2 + 0.005(LL - 40)\right] + 0.01(F_{200} - 15)(PI - 10)$$
$$= (95 - 35)\left[0.2 + 0.005(60 - 40)\right] + (0.01)(95 - 15)(40 - 10)$$
$$= 42$$

- So, the classification is A-7-6 (42)

EXAMPLE 4.3

- For a soil given

Sieve No.	Percent passing
4	90
10	76
200	34

- Liquid limit=37
- Plasticity index=12
- Classify the soil by the AASTHO system

SOLUTION

- The percentage passing through the No. 200 sieve is less than 35, so the soil is a granular material. From table 4.1, we see that is type A-2-6. From Eq. (4.2)

$$GI = 0.01(34-15)(12-10) = 0.38 \approx 0$$

- Thus, the soil is type A-2-6 (0)

4.2 UNITED SOIL CLASSIFICATION SYSTEM

4.2 UNITED SOIL CLASSIFICATION SYSTEM

- The original form of the Unified Soil Classification System was proposed by Casagrande in 1942 during World War II for use in airfield construction undertaken by the army Corps of Engineers. In cooperation with the U.S. Bureau of Reclamation (*ASTM designation D-2487*). The USCS is presented in ***Table 4.2.***
- In order to use the classification system, the following points must be kept in mind:

1. The classification is based on material passing a 75 *mm* (3*in*) sieve
2. Coarse fraction=percent retained above No. 200 sieve $R200=100-F_{200}$

3. Fine fraction= percent passing No. 200 sieve=F_{200}

4. Gravel fraction=percent retained above No. 4 sieve =R_4

According to the USCS, the soils are divided into two major Categories:

1. Coarse grained soils that are gravelly and sandy in nature with less than 50% passing through the No. 200 sieve (that is, $F_{200}<50$). The group symbols start with prefixes of either G or S. stands for gravel or gravelly soil, and S for sand or sandy soil.

2. Fine grained soils with 50% or more passing through the No. 200 sieve (that is, $F_{200}>50$). The group symbols start with prefixes of M, which stands for inorganic silt, C for inorganic clay, and O for organic silts and clays. The symbol P_t is used for peat, mulch, and other highly organic soils.

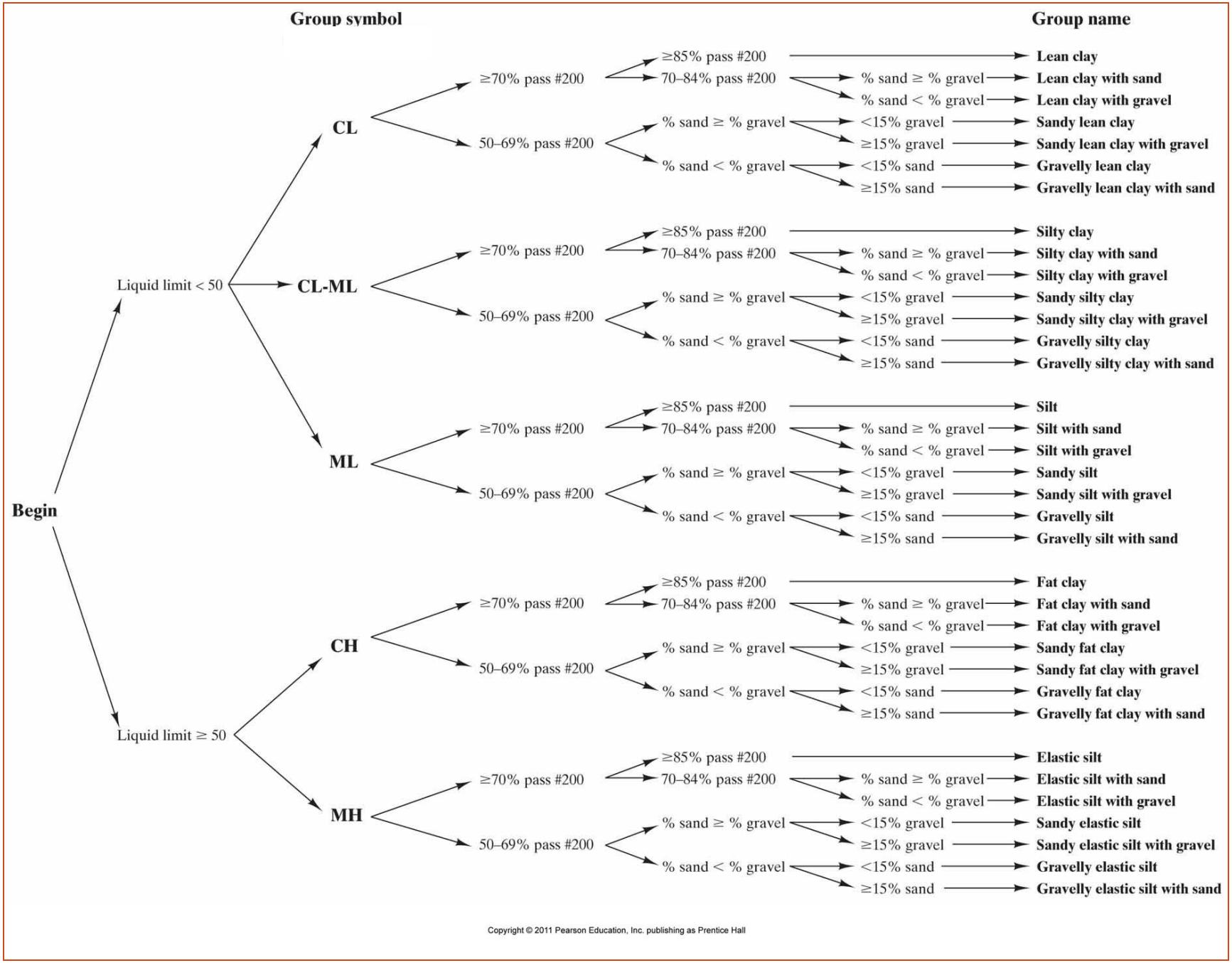

Figure 4.2a Flow chart for classification of inorganic fine-grained soils (≥50% passing #200 sieve). (Adapted from ASTM D2487.)

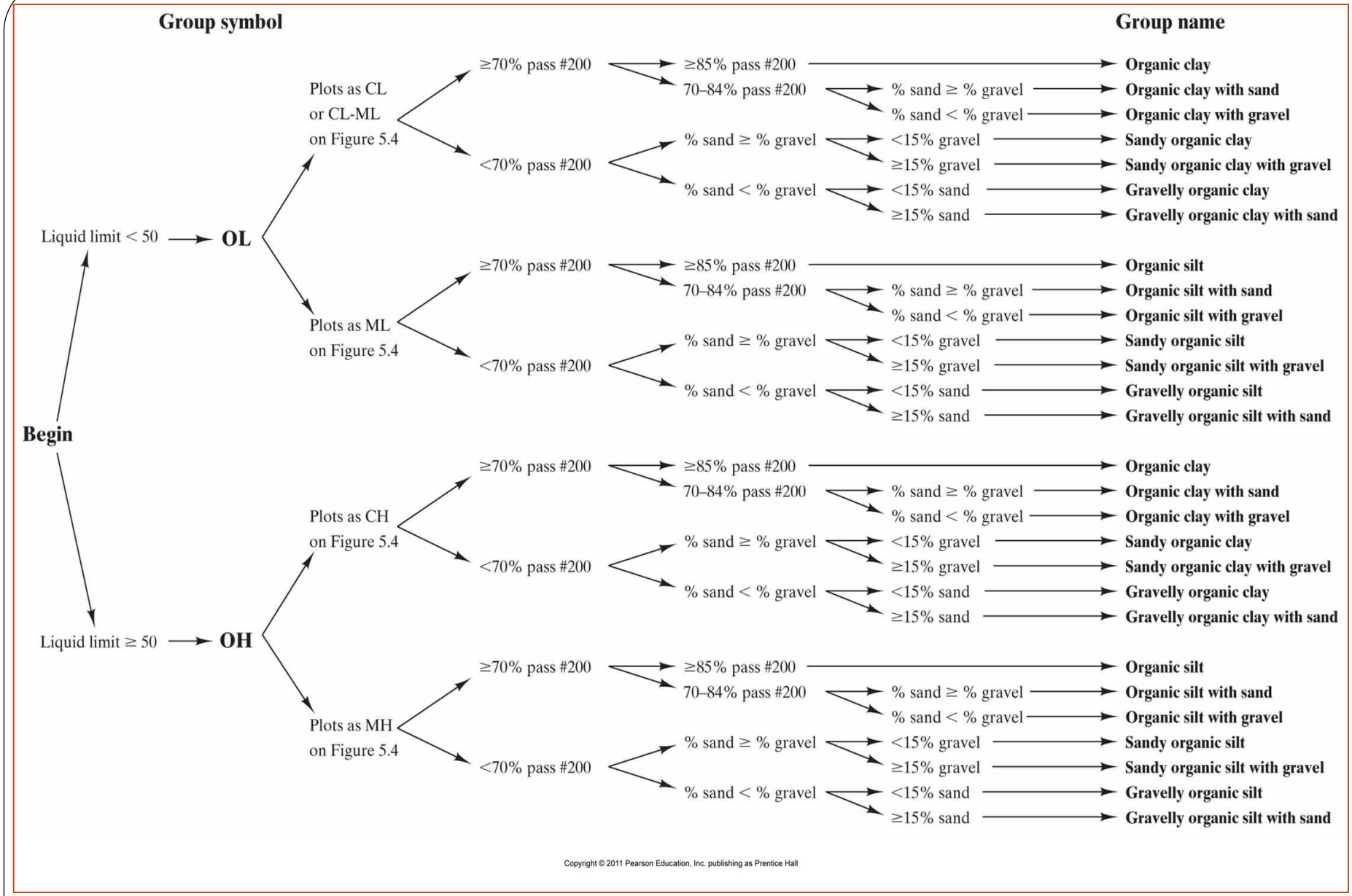

Figure 4.2b Flow chart for classification of organic fine-grained soils (≥50% passing #200 sieve). (Adapted from ASTM D2487.)

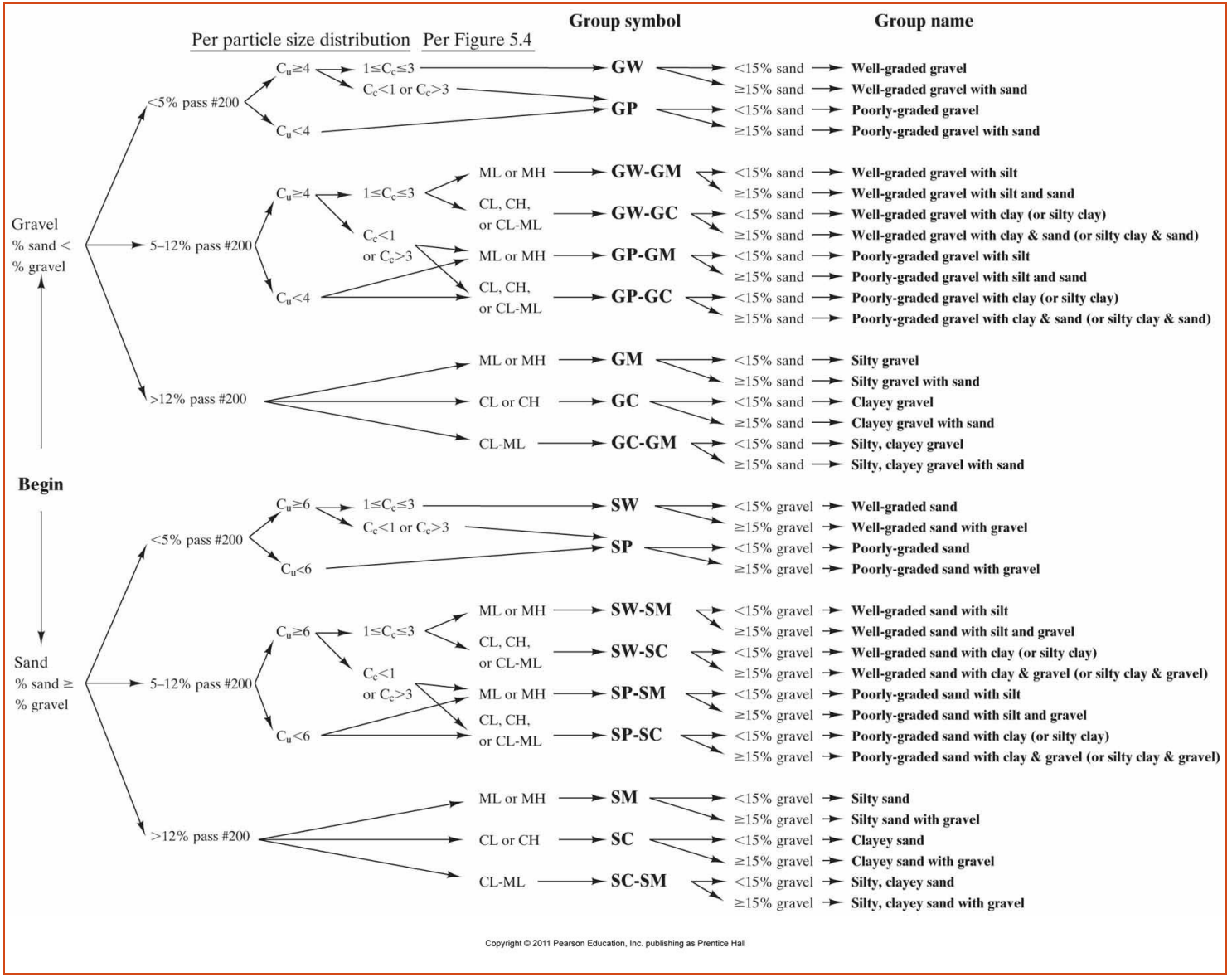

Figure 4.2c Flow chart for classification of coarse-grained soils (<50% passing #200 sieve). (Adapted from ASTM D2487.) C_u and C_c are the coefficients of uniformity and curvature, respectively, as defined in Chapter 4. The alternative endings for some group names (shown in parentheses) are for soils that plot as CL-ML on Figure 5.4.

F = porcentaje pasando

R = porcentaje retenido

USCS

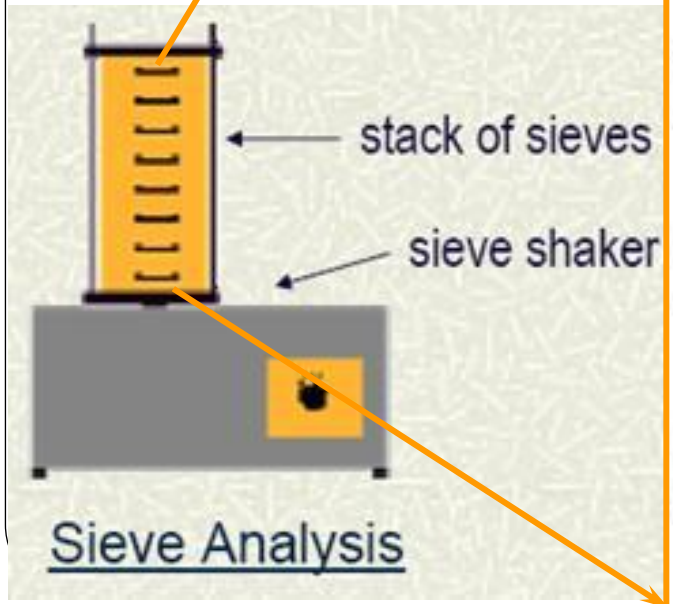

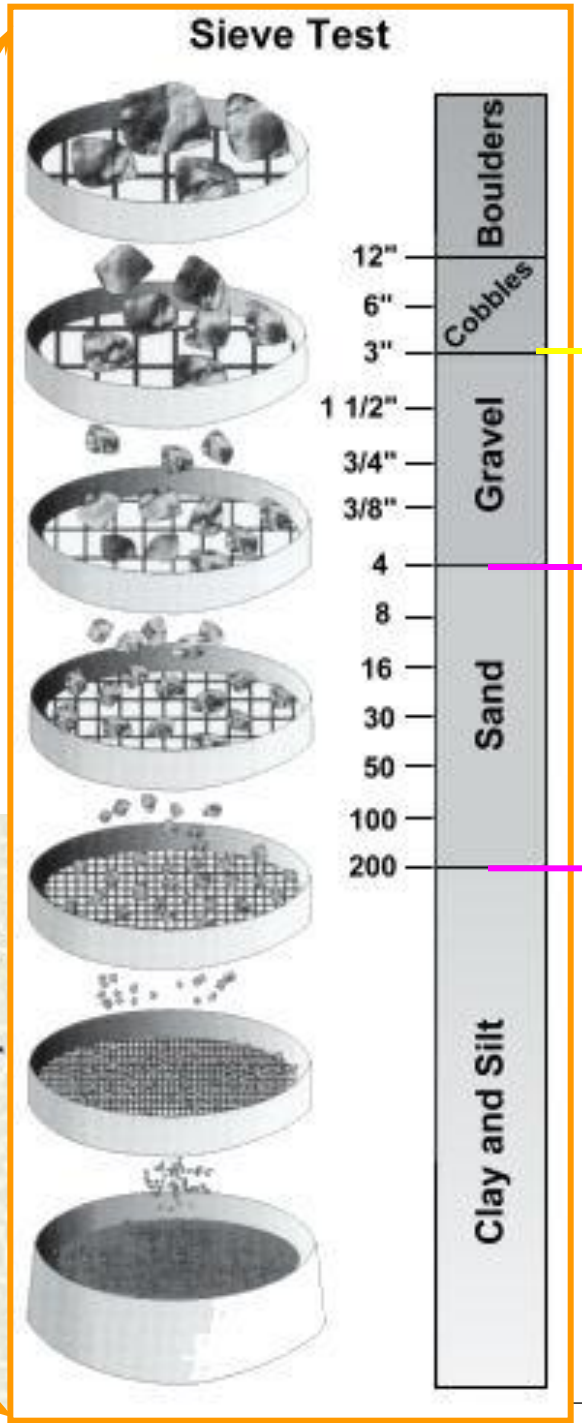

R_{200}= fracción gruesa

R_4= % grava

% arena

F_{200}= fracción fina

Table 4.2 Unified Soil Classification System (Based on Material Passing 76.2-mm Sieve)

Criteria for assigning group symbols				Group symbol
Coarse-grained soils More than 50% of retained on No. 4 sieve	**Gravels** More than 50% of coarse fraction retained on No. 4 sieve	Clean Gravels Less than 5% fines[a]	$C_u \geq 4$ and $1 \leq C_c \leq 3$[c]	GW
			$C_u < 4$ and/or $1 > C_c > 3$[c]	GP
		Gravels with Fines More than 12% fines[a,d]	$PI < 4$ or plots below "A" line (Figure 4.2)	GM
			$PI > 7$ and plots on or above "A" line (Figure 4.2)	GC
	Sands 50% or more of coarse fraction passes No. 4 sieve	Clean Sands Less than 5% fines[b]	$C_u \geq 6$ and $1 \leq C_c \leq 3$[c]	SW
			$C_u < 6$ and/or $1 > C_c > 3$[c]	SP
		Sands with Fines More than 12% fines[b,d]	$PI < 4$ or plots below "A" line (Figure 4.2)	SM
			$PI > 7$ and plots on or above "A" line (Figure 4.2)	SC
Fine-grained soils 50% or more passes No. 200 sieve	**Silts and clays** Liquid limit less than 50	Inorganic	$PI > 7$ and plots on or above "A" line (Figure 4.2)[e]	CL
			$PI < 4$ or plots below "A" line (Figure 4.2)[e]	ML
		Organic	$\frac{\text{Liquid limit — oven dried}}{\text{Liquid limit — not dried}} < 0.75$; see Figure 4.2; OL zone	OL
	Silts and clays Liquid limit 50 or more	Inorganic	PI plots on or above "A" line (Figure 4.2)	CH
			PI plots below "A" line (Figure 4.2)	MH
		Organic	$\frac{\text{Liquid limit — oven dried}}{\text{Liquid limit — not dried}} < 0.75$; see Figure 4.2; OH zone	OH
Highly Organic Soils	Primarily organic matter, dark in color, and organic odor			Pt

[a] Gravels with 5 to 12% fine require dual symbols: GW-GM, GW-GC, GP-GM, GP-GC.

[b] Sands with 5 to 12% fines require dual symbols: SW-SM, SW-SC, SP-SM, SP-SC.

[c] $C_u = \frac{D_{60}}{D_{10}}$; $C_c = \frac{(D_{30})^2}{D_{60} \times D_{10}}$

[d] If $4 \leq PI \leq 7$ and plots in the hatched area in Figure 4.2, use dual symbol GC-GM or SC-SM.

[e] If $4 \leq PI \leq 7$ and plots in the hatched area in Figure 4.2, use dual symbol CL-ML.

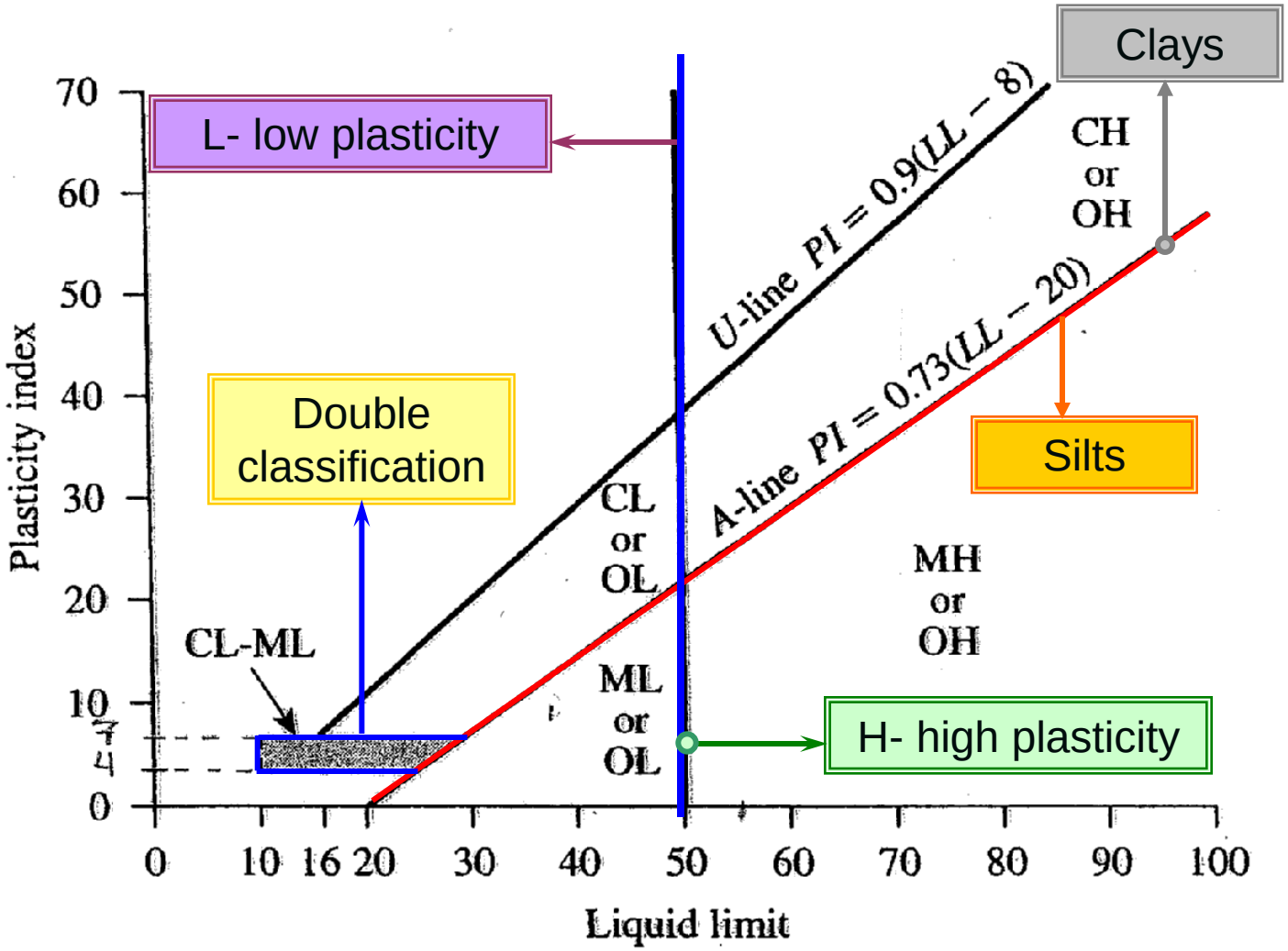

Figure 4.2 Plasticity chart

DEFINITION OF GRAIN SIZE

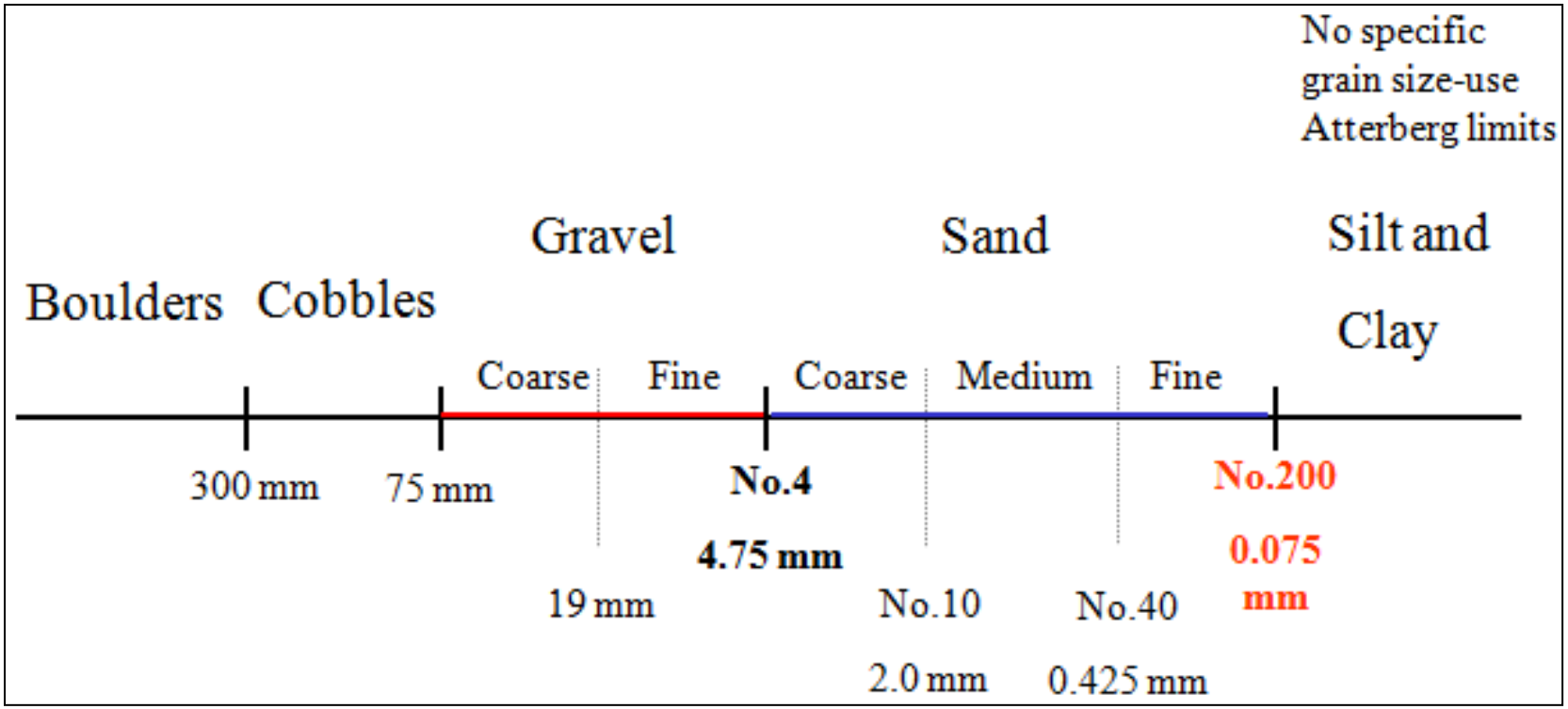

- Other symbols used for the classification are:
  - W-well graded
  - P-poorly graded
  - L-low plasticity (liquid limit less than 50)
  - H-high plasticity (liquid limit more than 50)

- ***Table 4.2*** gives the details of the soil classification system to determine the group symbols

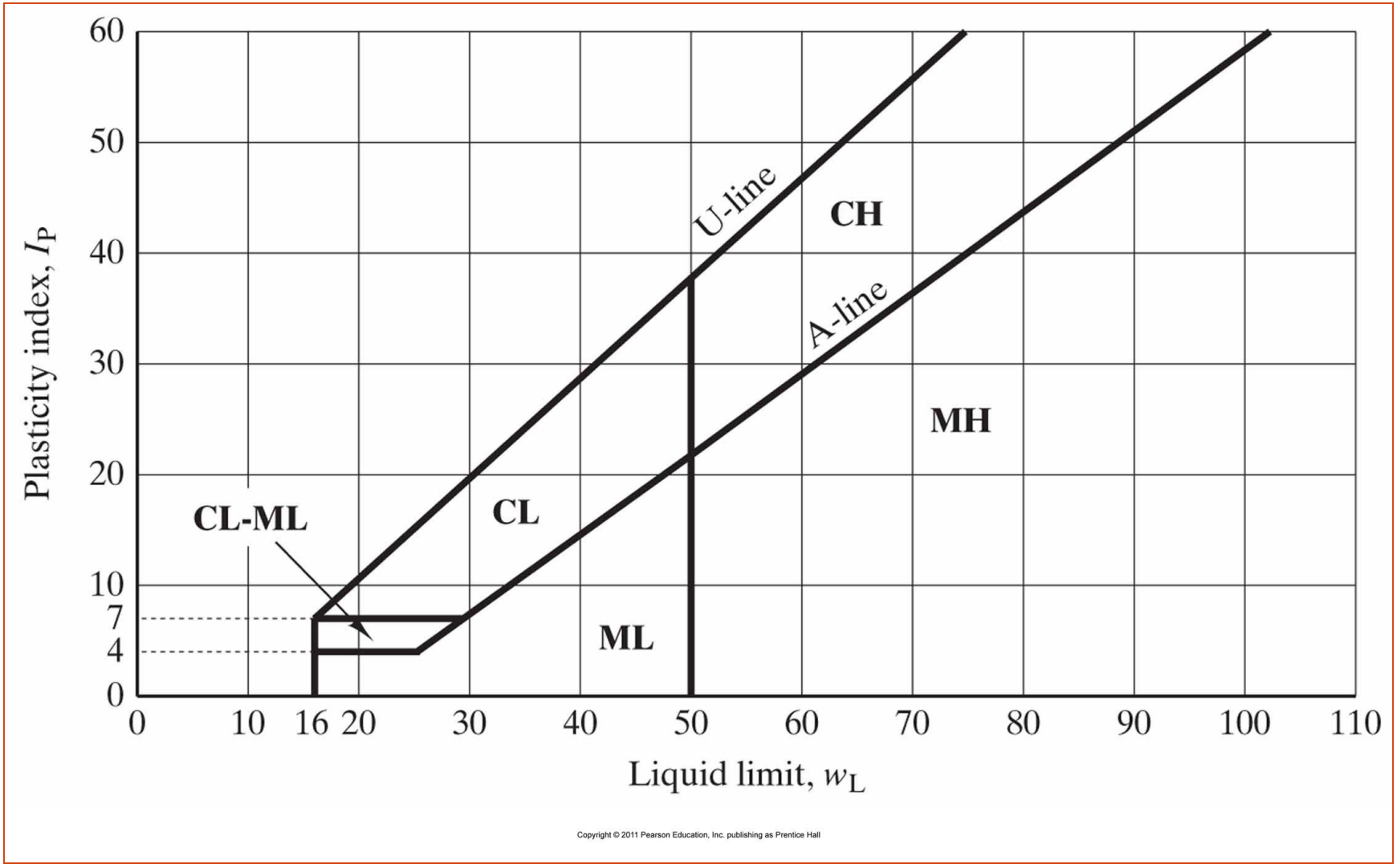

4.2 Plasticity chart

Figure 4.3 Flowchart group names for gravelly and sandy soil. *Source:* From "Annual Book of ASTM Standards, 04.08." Copyright © 1999 American Society for Testing and Materials. Reprinted with permission.

% pasando tamiz #	①	②	③	④	⑤	⑥
4	69	98	40	62	40	95
10	54	90	30	55	30	90
40	46	76	22	32	12	83
100	41	43	20	16	3	71
200	36	33	15	9	-	65
ω_L	39	37	35	30	NP	55
ω_p	27	12	22	24		24
C_u	12	15	7	53	22	-
C_c	4	5	1.8	0.4	12	-

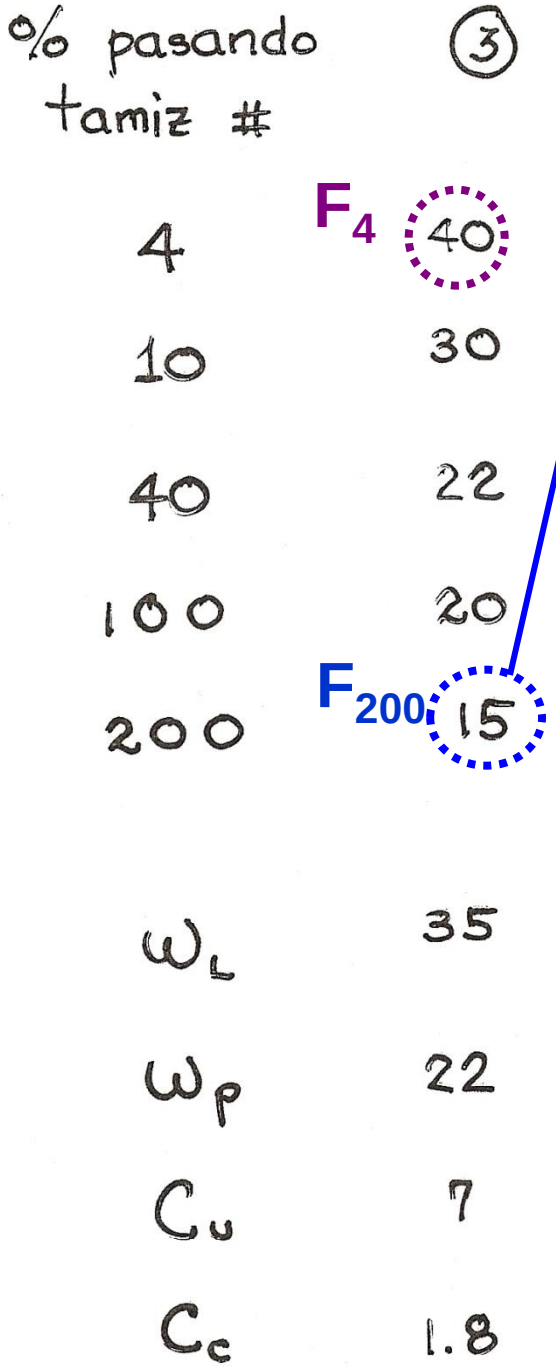

$F_{200} < 50\% \rightarrow$ suelo grueso

1ra letra G ó S

$R_4 / R_{200} > 0.5$

$R_4 = 100 - F_4$
$= 100 - 40 = 60\%$

$R_{200} = 100 - F_{200}$
$= 100 - 15 = 85\%$

$R_4 / R_{200} = 60/85 = 0.7 > 0.5 \rightarrow$ G

2da letra – verificar F_{200}

$F_{200} = 15 > 12\%$ → C ó M

Figura 4.2
w_L =35, w_P = 22
(PI = 35-22=13)

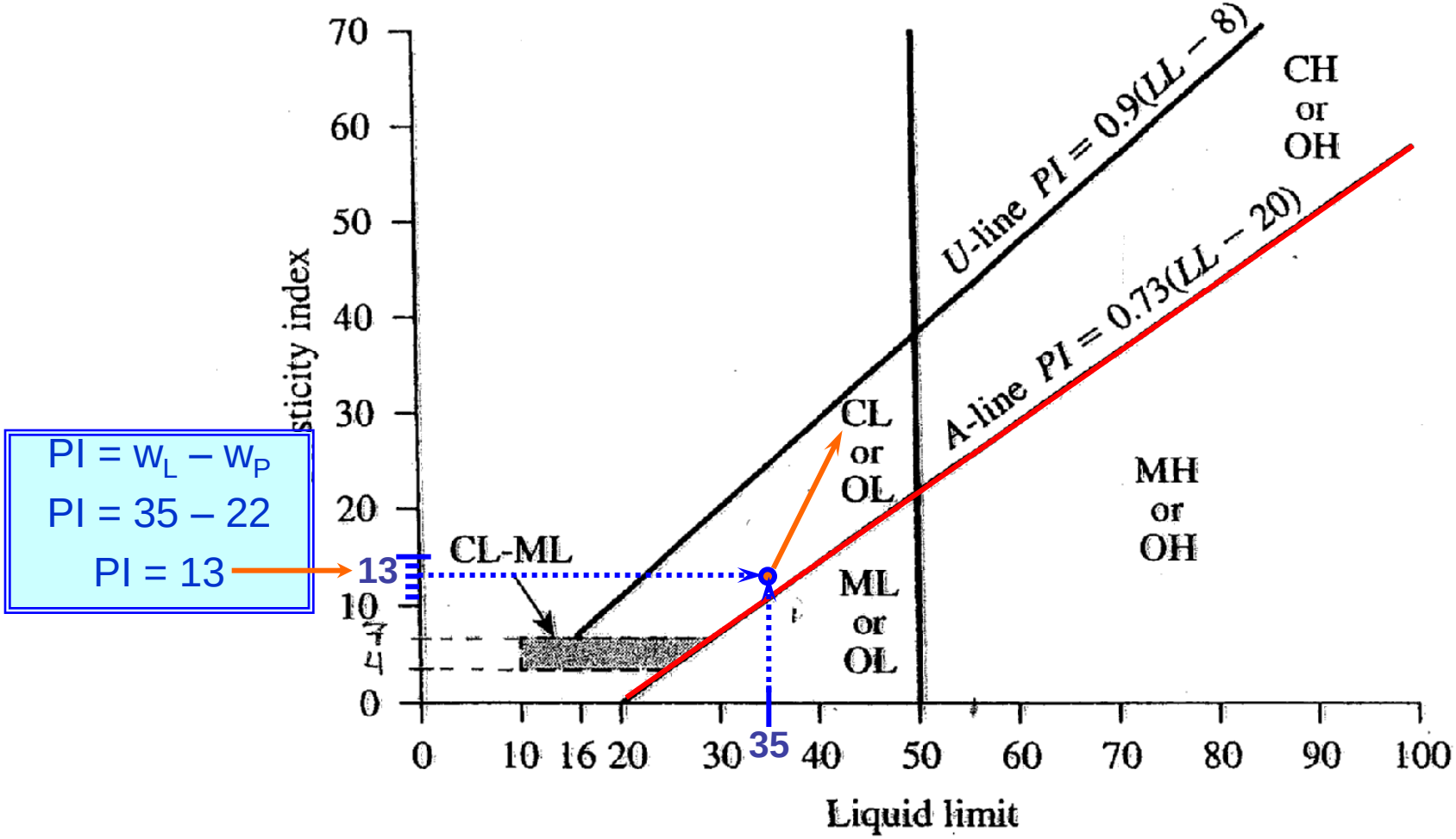

Figure 4.2 Plasticity chart

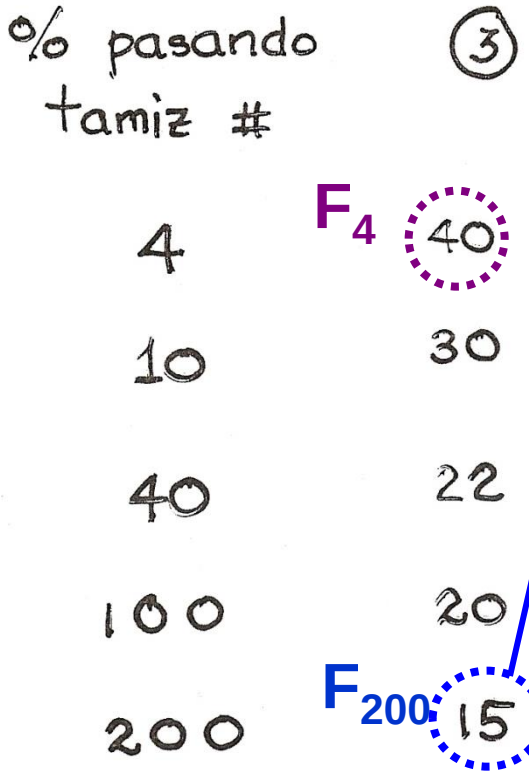

$F_{200} < 50 \rightarrow$ suelo grueso

1ra letra G ó S

$R_4 / R_{200} > 0.5$

$R_4 = 100 - F_4$
$= 100 - 40 = 60\%$

$R_{200} = 100 - F_{200}$
$= 100 - 15 = 85\%$

$R_4 / R_{200} = 60/85 = 0.7 > 0.5 \rightarrow$ G

2da letra – verificar F_{200}

$F_{200} = 15 > 12\%$ → C ó M

%arena = $R_{200} - R_4$

%arena = 85–60=25

25 (entre 15 y 29)
"con arena"

Figura 4.2
w_L =35, w_P = 22
(PI = 35-22=13

Suelo clasifica - GC

Verificar si %arena > 15

Clasificación final
GC, grava arcillosa
con arena

"clayey gravel with sand"

TABLE Assessment of Soil Properties Based on Group Symbol[a]

Group Symbol	Compaction Characteristics	Compressibility and Expansion	Drainage and Hydraulic Conductivity	Value as a Fill Material	Value as a Pavement Subgrade When Not Subject to Frost	Value as a Base Course for Pavement
GW	Good	Almost none	Good drainage; pervious	Very stable	Excellent	Good
GP	Good	Almost none	Good drainage; pervious	Reasonably stable	Excellent to good	Poor to fair
GM	Good	Slight	Poor drainage; semipervious	Reasonably stable	Excellent to good	Fair to poor
GC	Good to fair	Slight	Poor drainage; semipervious	Reasonably stable	Good	Good to fair; not suitable if subject to frost
SW	Good	Almost none	Good drainage; pervious	Very stable	Good	Fair to poor
SP	Good	Almost none	Good drainage; pervious	Reasonably stable when dense	Good to fair	Poor
SM	Good	Slight	Poor drainage; impervious	Reasonably stable when dense	Good to fair	Poor
SC	Good to fair	Slight to medium	Poor drainage; impervious	Reasonably stable	Good to fair	Fair to poor; not suitable if subject to frost

ML	Good to poor	Slight to medium	Poor drainage; impervious	Fair stability, good compaction required	Fair to poor	Not suitable
CL	Good to fair	Medium	No drainage; impervious	Good stability	Fair to poor	Not suitable
OL	Fair to poor	Medium to high	Poor drainage; impervious	Unstable; should not be used	Poor, not suitable	Not suitable
MH	Fair to poor	High	Poor drainage; impervious	Fair to poor stability, good compaction required	Poor	Not suitable
CH	Fair to poor	Very high	No drainage; impervious	Fair stability, expands, weakens, shrinks, cracks	Poor to very poor	Not suitable
OH	Fair to poor	High	No drainage; impervious	Unstable; should not be used	Very poor	Not suitable
Pt	Not suitable	Very high	Fair to poor drainage	Should not be used	Not suitable	Not suitable

[a] Adapted from Sowers, 1979.

EXAMPLE 4.4

- Figure 4.6 gives the grain size distribution of two soils. The liquid and plastic limits of minus No. 40 sieve fraction of the soil are as follow:

	Soil A	Soil B
Liquid limit	30	26
Plastic limit	22	20

- Determine the group symbols and group names according to the USCS.

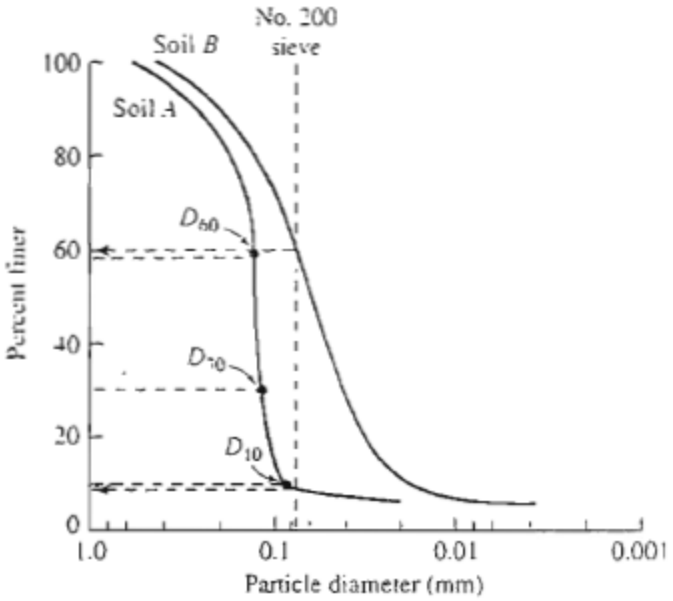

Figure 4.6 Particle-size distribution of two soils

SOLUTION

- Soil A

The grain size distribution curve indicates that ***F200***=8. So this is a coarse grained soil, and

$$R_{200} = 100 - F_{200} = 100 - 8 = 92$$

From Figure 4.6 $R_4 \approx 0$, therefore

$$\frac{R_4}{R_{200}} = \frac{0}{92} < 0.5$$

Hence, it is a sandy soil (***table 4.2***). From ***figure 4.6*** D_{10}=0.085mm, D_{30}=0.12, and D_{60}=0.135mm. thus

$$C_u = \frac{D_{60}}{D_{10}} = \frac{0.135}{0.085} = 1.59 < 6$$

$$C_z = \frac{D_{30}^2}{D_{60} \times D_{10}} = \frac{(0.12)^2}{(0.135)(0.085)} = 1.25 > 1$$

- With ***LL***=30 and ***PI***=30-22=8 (which is greater than 7), it plots above the A-line in ***Figure 4.2***. Hence, the group symbol is SP-SC. In order to determine the group name, we refer to ***Figure 4.3*** Percentage of gravel=R_4=0 (which is<15%). So, the group name is poorly graded sand with clay
- Soil B
- From group the grain size distribution curve, F200=61. Hence this is a fine grained soil. Given ***LL***= 26 and ***PI***=26-20=6 In ***figure 4.2*** the PI plots in the hatched area. So, from ***table 4.2***, the group symbol is ***CL-ML*** for group name, assuming that the soil is inorganic, we go to ***figure 4.4*** and obtain Plus No. 200 sieve R200=100 –F200=100-61= 39 (which is greater than 30)

- Percent of gravel=R_4=0, percentage of sand= R200-R_4=39

- Thus, because the percentage of sand is greater than the percentage of gravel, the soil is sandy silty clay

EXAMPLE 4.5

- The grain size analysis for a soil is given next:

Sieve no.	% passing
4	94
10	63
20	21
40	10
60	7
100	5
200	3

- Given that the soil is nonplastic, classify the soil by using the USCS

SOLUTION

$$F_{200} = 3$$

$$F_{200} = 100 - 3 = 97$$

$$R_4 = 100 - F_4 = 100 - 94 = 6$$

$$\frac{R_4}{R_{200}} = \frac{6}{97} < 0.5$$

- Thus, this oil is sandy. The grain size distribution is shown in Figure 4.7. From this figure, we obtain:

$$D_{60} = 1.41$$

$$D_{30} = 0.96mm$$

$$D_{10} = 0.41mm$$

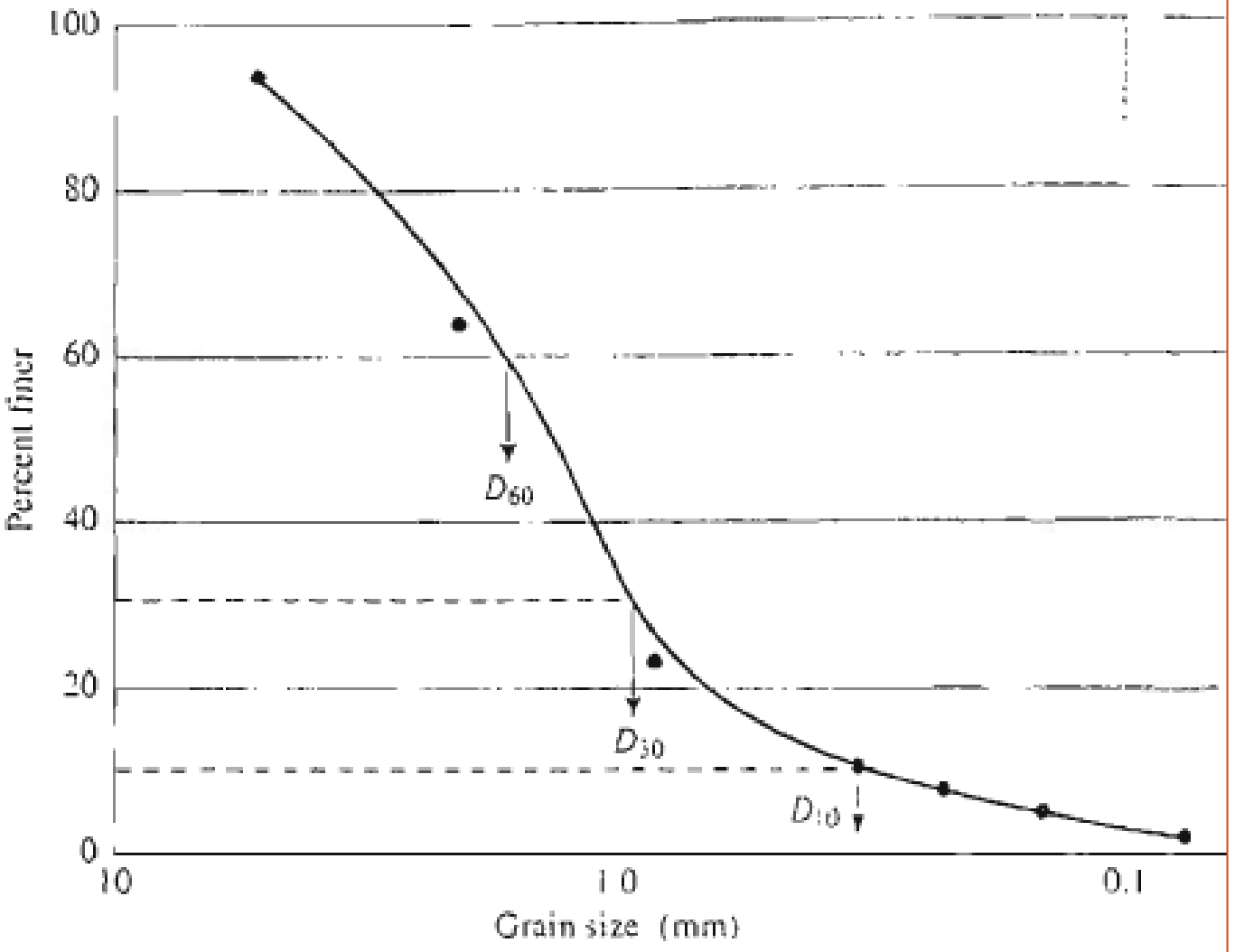

Figure 4.7 Grain-size distribution curve

- Thus

$$C_u = \frac{D_{60}}{D_{10}} = \frac{1.41}{0.41} = 3.44$$

$$C_z = \frac{D_{30}^2}{D_{60} \times D_{10}} = \frac{0.96^2}{1.41 \times 0.41} = 1.59$$

- From table 4.2 we see that the group symbol is SP. For this soil R_4=6. Referring to ***Figure 4.3***, we find that the group name is poorly grades sand.

4.3 SUMMARY AND COMPARISON BETWEEN THE AASTHO AND UNIFIED SYSTEMS

SUMMARY AND COMPARISON BETWEEN THE AASTHO AND UNIFIED SYSTEMS

- Both soil classification systems, are based on the texture and plasticity of soil. Also, both systems divide the soils into two major categories, coarse grained and fine grained, as separated by the No.200 sieve. According to the AASTHO, a soil is considered fine grained when more than 35% passes through the No. 200 sieve . According to the USCS, when more than 50% passes through the No. 200 sieve. A coarse grained soil that has about 35% fine grains will behave like a fine grained material. This is because enough fine grains exist to fill the voids between the coarse grains and hold them apart. In this respect, the AASHTO system appears to be more appropriate.

- In the AASTHO system the No. 10 sieve is used to separate gravel from the sand, in the USCS system, the No. 4 sieve is used. From the viewpoint of soil separate size limits, the No. 10 sieve is the more accepted upper limit for sand. This limit is used in concrete and highways base course technology.
- In the USCS, the gravelly and sandy soils are clearly separated; in the AASTHO system, they are not. The A-2 group, in particular, contains a large variety of soils. Symbols like GW, SM, CH, and others that are used in the USCS are more descriptive of the soil properties than the A symbols used in the AASTHO.
- The classification of organic soils as OL, OH, and Pt is provided in the USCS. Under AASTHO, there is no place for organic soils.

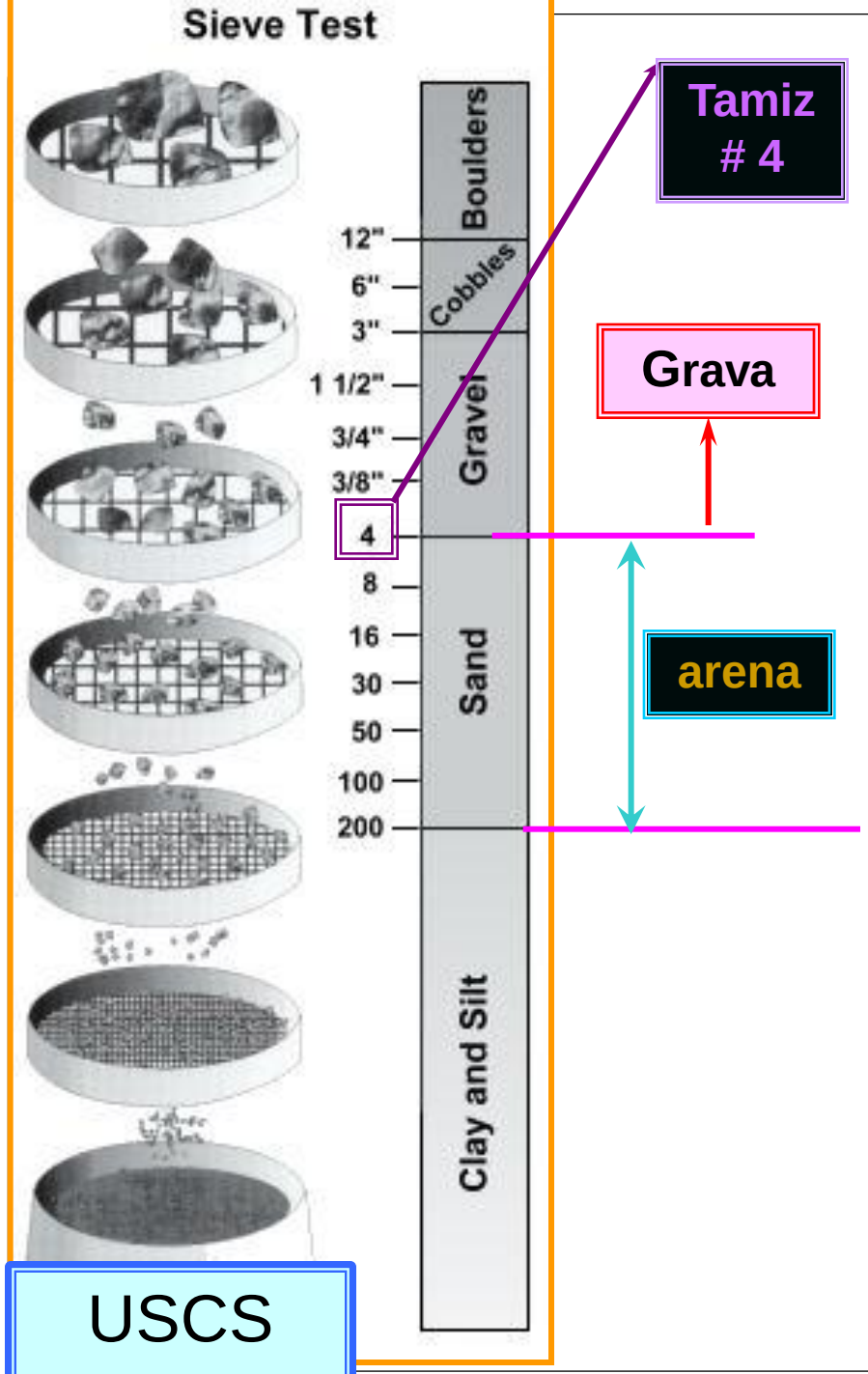
Sieve Test
Boulders
Cobbles
Gravel
Sand
Clay and Silt
12"
6"
3"
1 1/2"
3/4"
3/8"
4
8
16
30
50
100
200
Tamiz # 4
Grava
arena
USCS

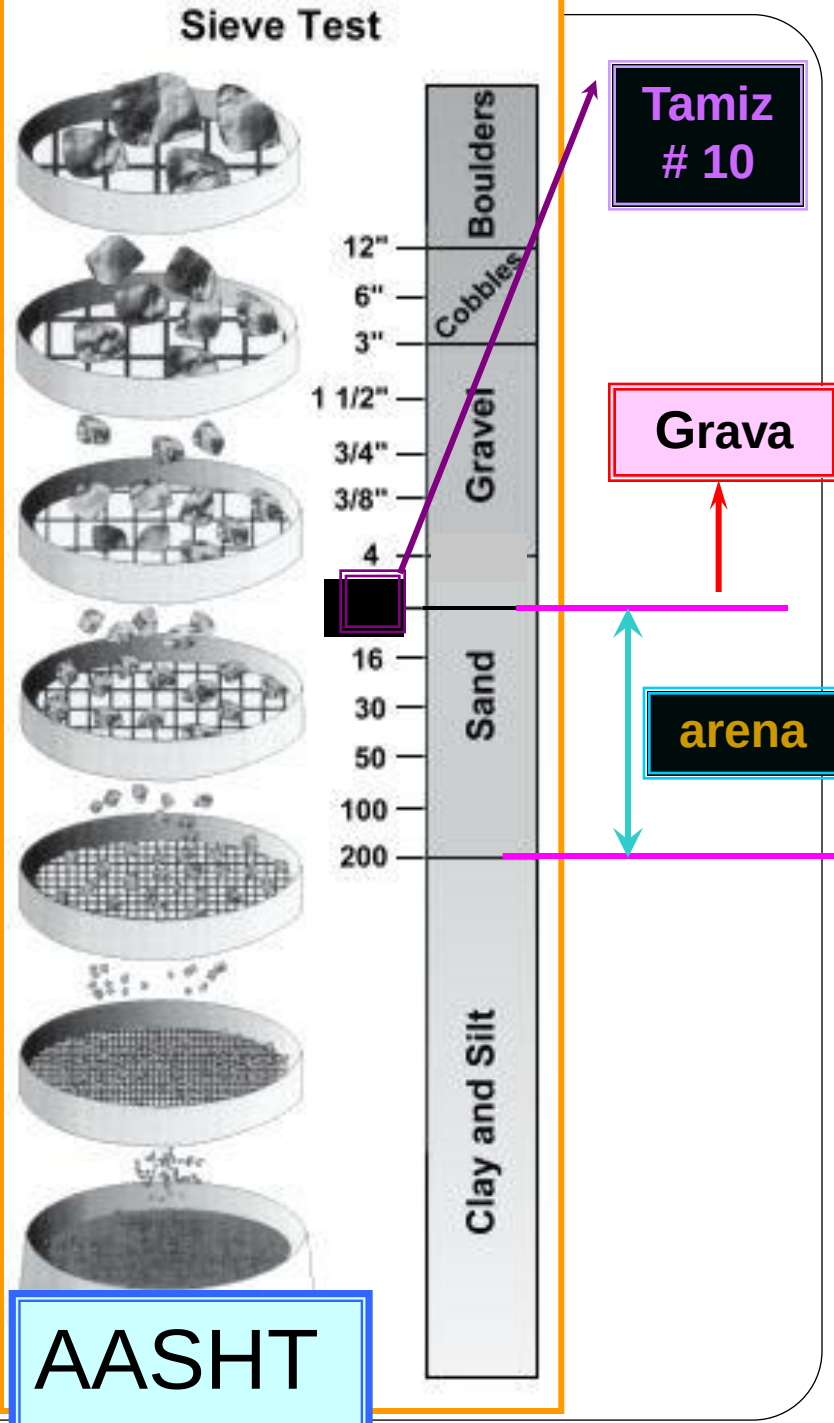
Sieve Test
Boulders
Cobbles
Gravel
Sand
Clay and Silt
12"
6"
3"
1 1/2"
3/4"
3/8"
4
16
30
50
100
200
Tamiz # 10
Grava
arena
AASHT

ORGANIC SOILS

- **Highly organic soils- Peat (Group symbol PT)**
  - A sample composed primarily of vegetable tissue in various stages of decomposition and has a fibrous to amorphous texture, a dark-brown to black color, and an organic odor should be designated as a highly organic soil and shall be classified as peat, PT.

- **Organic clay or silt(group symbol OL or OH):**
  - "The soil's liquid limit (LL) after oven drying is less than 75 % of its liquid limit before oven drying." If the above statement is true, then the first symbol is O.
  - The second symbol is obtained by locating the values of PI and LL (not oven dried) in the plasticity chart.

University of Puerto Rico at Mayaguez
Department of Civil Engineering and Surveying

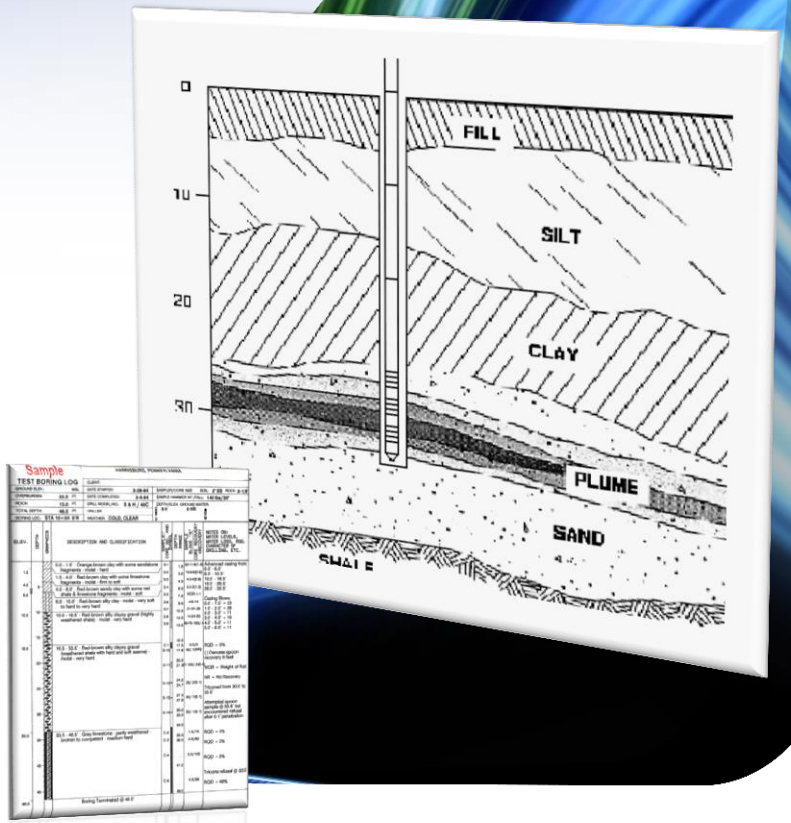

Borings and In-Situ Testing

By: Ricardo Ramos Cabeza

Borings

Drilling Methods

- Test pits
- Auguring
  - Solid Stem
  - Hollow Stem
- Rotary Drilling
- Percussion Drilling

Borings

- Test pits

Advantages	Disadvantages
– Provides detailed information on a stratigraphy – Large quantities of disturbed soil available – Large blocks of undisturbed specimens can be “carved” – Large- scale field tests can be conducted on exposed soils	– Depth limited to about 6 m with appropriate safety measures – Numerous or deep pits uneconomical – Excavation below groundwater level and into rock is difficult and costly

Borings

- Augurs
  - Truck-mounted and equipped with continuous-flight augers that bore a hole 100 to 250 mm in diameter. Augers can have a solid or hollow stem.

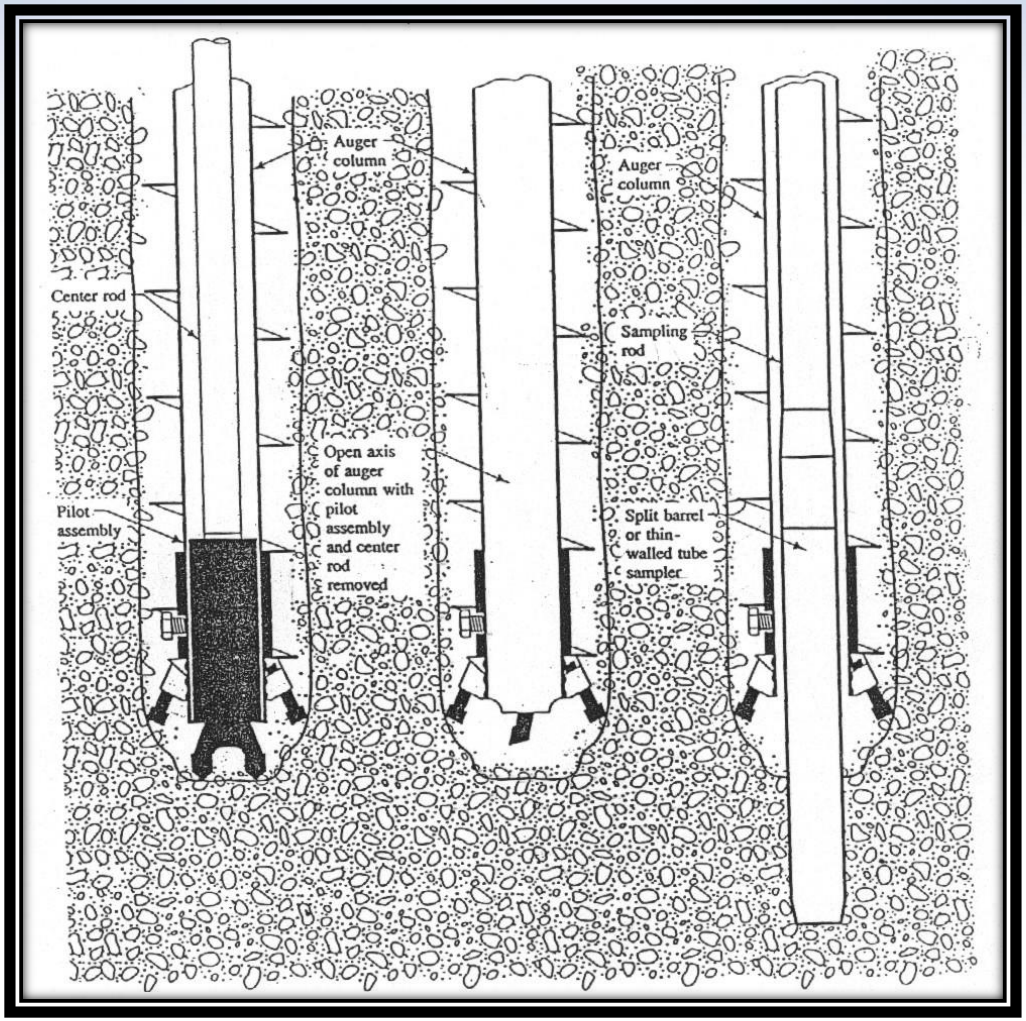

Borings

- Solid-Stem Augers

Advantages	Disadvantages
– Rapid – Inexpensive – Small- diameter boreholes possible	– Sampling difficult – Borehole collapse on removal – Limited depth – Cannot be used in rock

Borings

- Hollow-Stem Augers

(1) Hollow Stem Auger
(2) Auger Drive Cap
(3) Nut & Bolt for the Rod-to-Cap Adapter
(4) Auger Pilot Bit Connector
(5) Rod-to-Cap-Adapter
(6) Auger Drill Rod
(7) Auger Lock Bolts
(8) Auger Bushing Nuts
(9) Auger Drive Keys
(10) Auger Cutterheads .
(11) Auger Pilot Bits

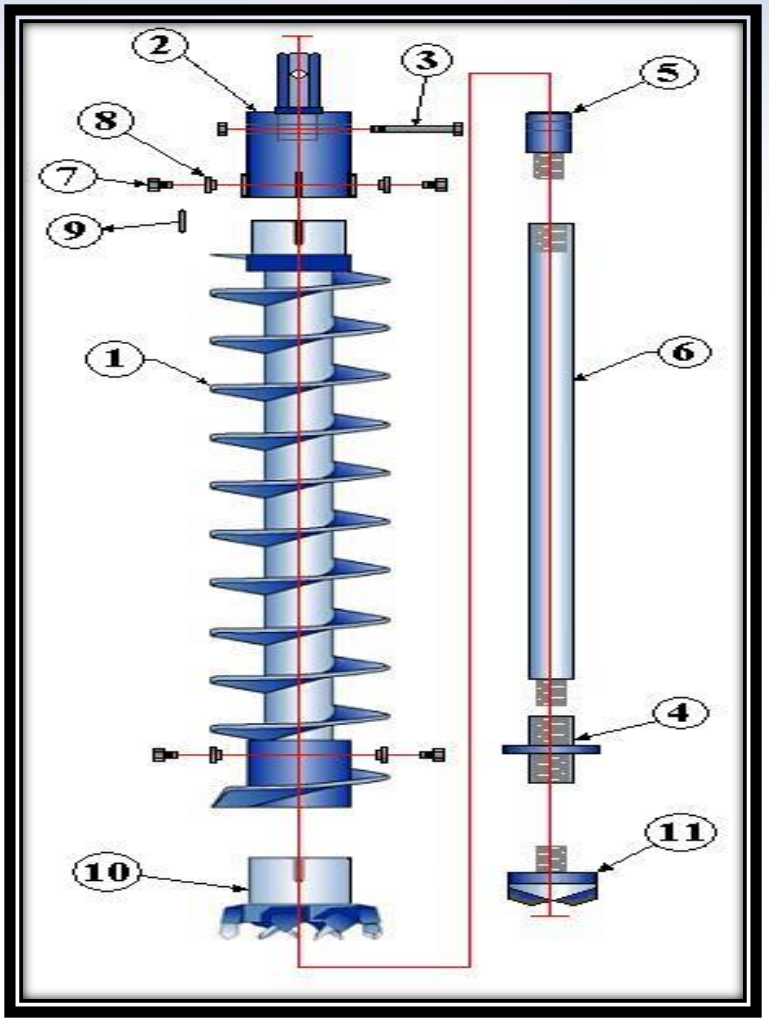

Borings

- Solid-Stem Augers

Advantages	Disadvantages
– Rapid – Inexpensive – Equipment readily available – Samples easily obtained – Drilling fluids not required – Groundwater levels easily obtained	– Depths limited to 15 to 45 m – Cannot be used in rock

Borings

- Direct Rotary Drilling
  - A drill bit is advanced by the weight of the drill string and down-force of the drilling rig and rotated by a motor. Drilling fluids are used to remove the cuttings and maintain the stability of the borehole.

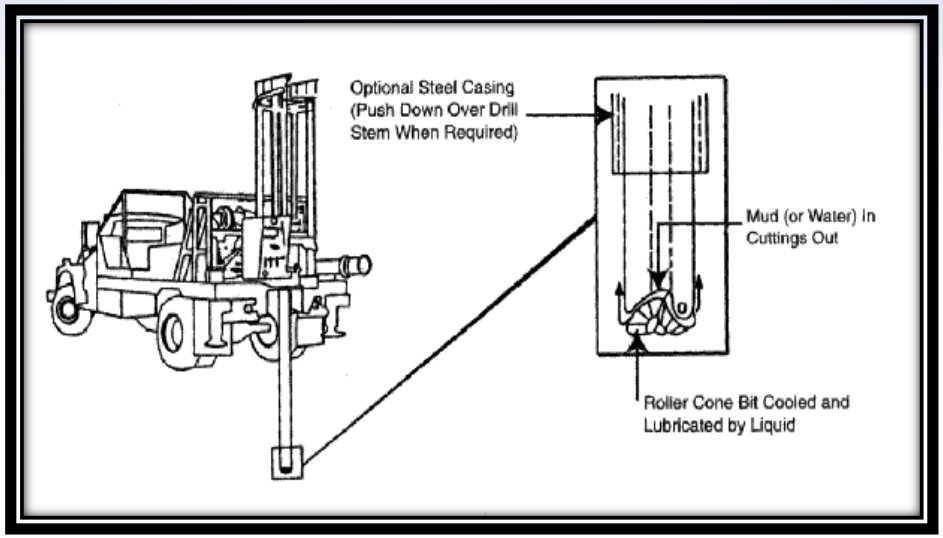

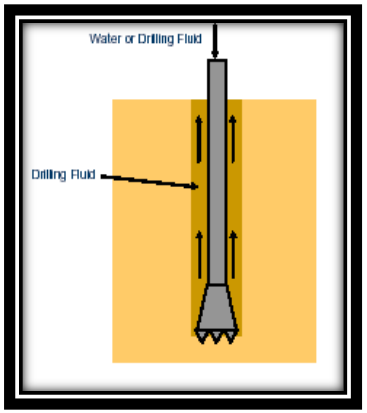

Borings

- Direct Rotary Drilling

Advantages	Disadvantages
– Rapid drilling – Drilling in soil and rock – Large depths possible – Casing not required	– Drilling fluid required with associated time and cost – Difficulty in identifying groundwater level during drilling – Sampling not possible during drilling

Borings

- Percussion Drilling
  - The percussion drill is one of the oldest known tools for making holes in the ground to get water. For most types of soil, the percussion drill is a solid, reliable, and fast way to make a low cost well.

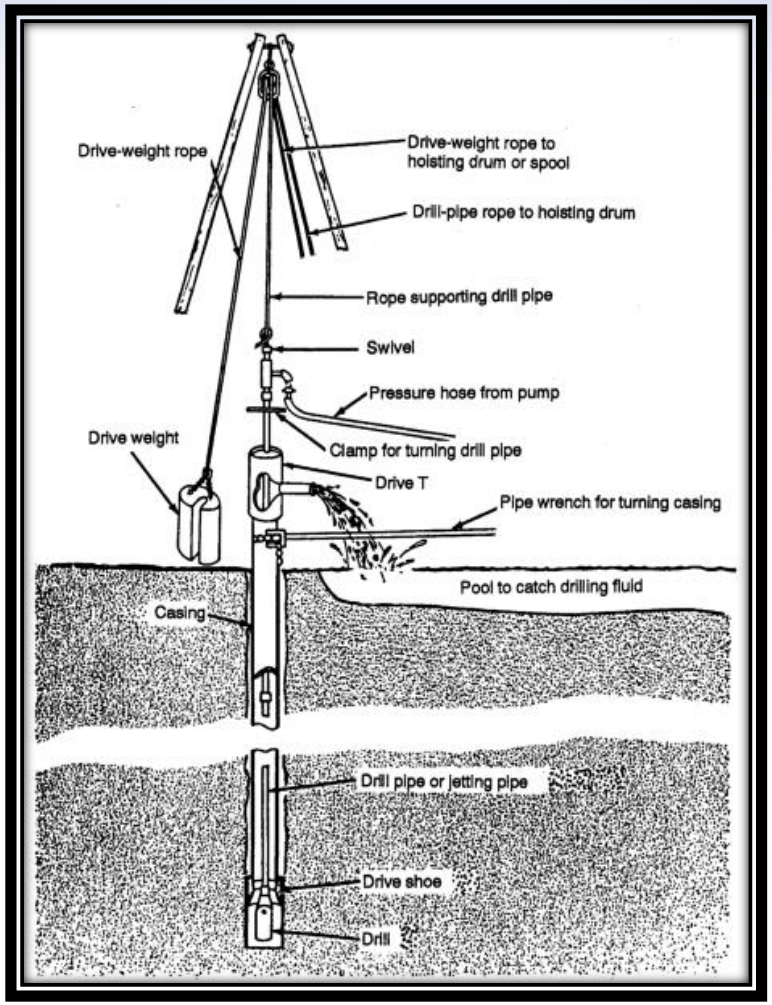

Borings

Sampling

- Disturbed samples
  - Bulk samples
  - Split- barrel (split- spoon) samples

  } Visual classification, Index tests, Compaction

- "Undisturbed" samples
  - Hand- trimmed samples
  - Thin- walled (Shelby) tube samples
  - Piston samples
  - Denison samples
  - Coring

  } Hydraulic Conductivity, Strength tests, Consolidation tests

Borings

Split-Barrel Samples

- Sampler is driven into the soil at the bottom of the boring using repeated blows of a 140-lb. hammer falling 30 in.
- Used in both coarse-grained and fine-grained soils
- Samples obtained as part of the Standard Penetration Test (SPT)

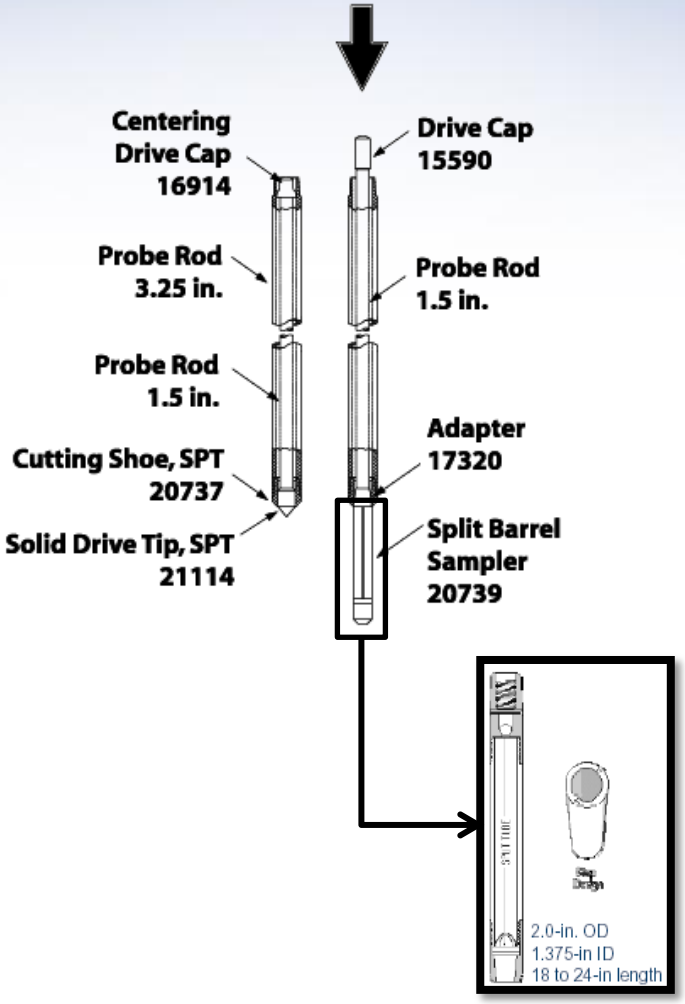

Borings

Shelby Tube Samples

- Sampler is pushed into the soil at the bottom of the boring using the hydraulic system on a drilling rig
- Most often used in fine-grained soils
- Amount of disturbance related to inside clearance ratio:

$$\frac{D_i - D_e}{D_e} \approx 1\%$$

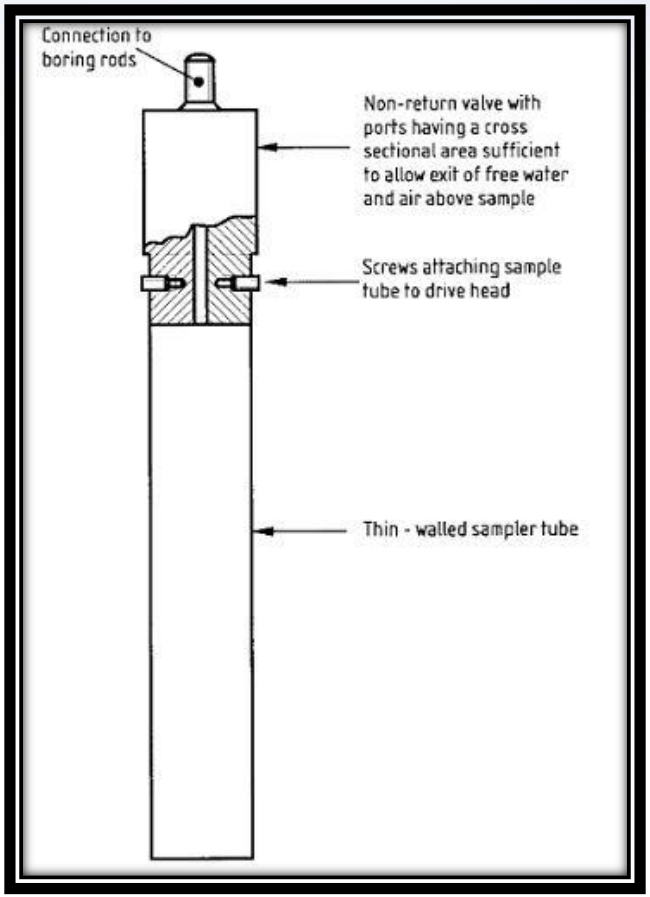

Borings

Boring Logs

- Holds important information of soil
- Identifies changes in soil properties
- Every Boring Log is produced from a single sample

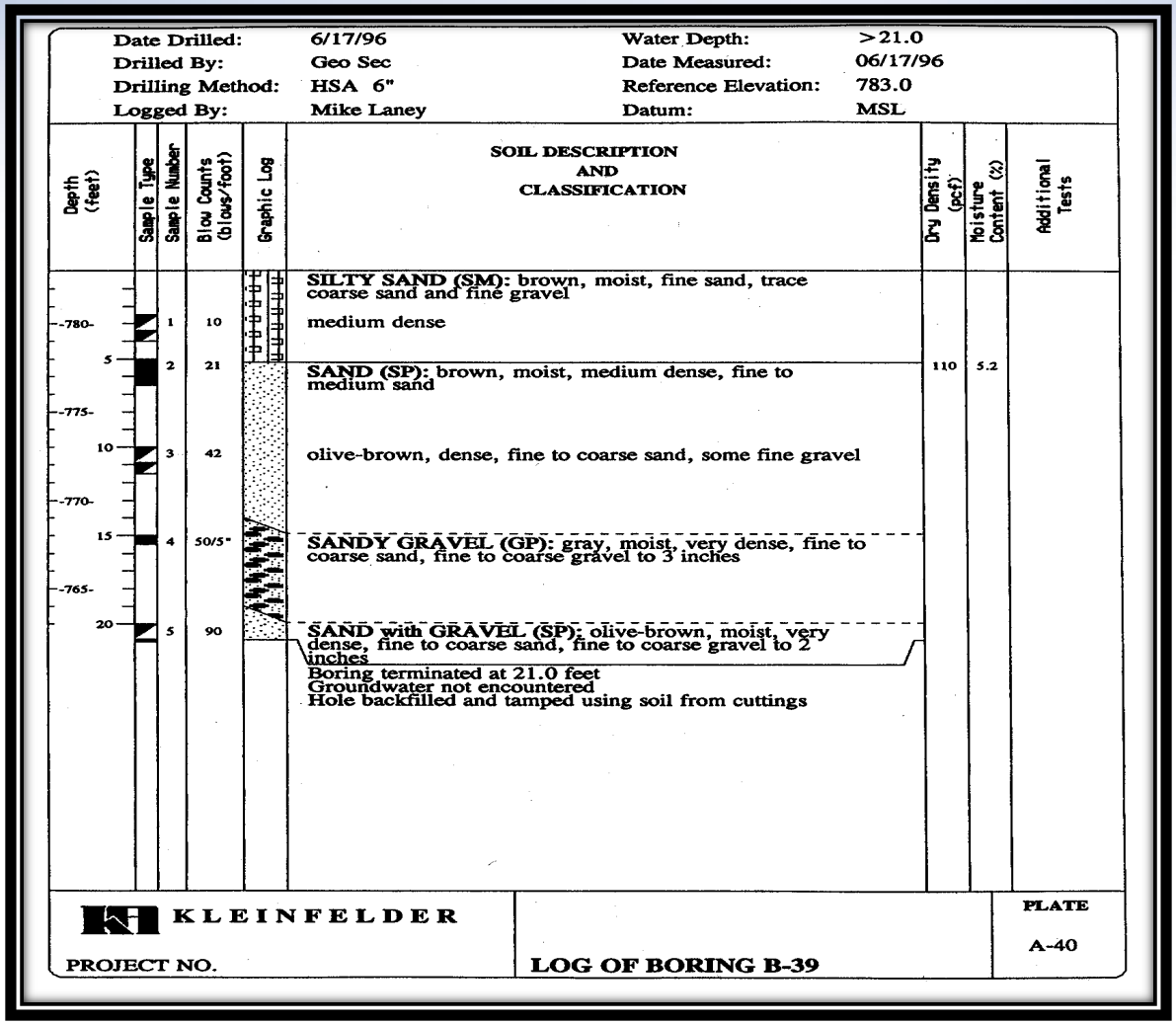

Date Drilled:	6/17/96	Water Depth:	>21.0
Drilled By:	Geo Sec	Date Measured:	06/17/96
Drilling Method:	HSA 6"	Reference Elevation:	783.0
Logged By:	Mike Laney	Datum:	MSL

Depth (feet)	Sample Type	Sample Number	Blow Counts (blows/foot)	Graphic Log	SOIL DESCRIPTION AND CLASSIFICATION	Dry Density (pcf)	Moisture Content (%)	Additional Tests
-780-		1	10		SILTY SAND (SM): brown, moist, fine sand, trace coarse sand and fine gravel medium dense			
5		2	21		SAND (SP): brown, moist, medium dense, fine to medium sand	110	5.2	
-775-								
10		3	42		olive-brown, dense, fine to coarse sand, some fine gravel			
-770-								
15		4	50/5"		SANDY GRAVEL (GP): gray, moist, very dense, fine to coarse sand, fine to coarse gravel to 3 inches			
-765-								
20		5	90		SAND with GRAVEL (SP): olive-brown, moist, very dense, fine to coarse sand, fine to coarse gravel to 2 inches Boring terminated at 21.0 feet Groundwater not encountered Hole backfilled and tamped using soil from cuttings			

KLEINFELDER

PROJECT NO.

LOG OF BORING B-39

PLATE A-40

Borings

TABLE 6

DESCRIPTIVE TERMS FOR COHESIONLESS SOILS TO BE USED IN FORMING THE SOIL NAME

Descriptive or qualifying terms as written	Range of proportions
Sandy, gravelly, etc.	35% to 50%
Some	20% to 35%
Little	10% to 20%
Trace	1% to 10%

Borings

Subsurface Profiles

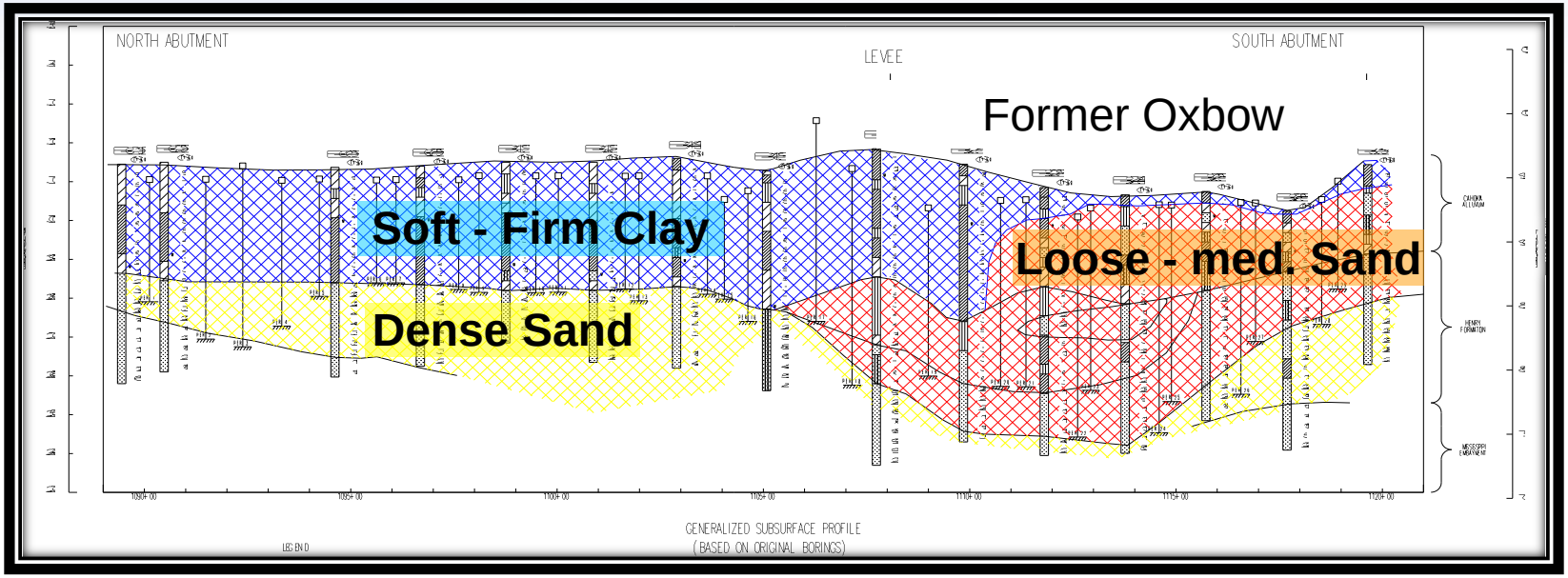

- Cahokia Formation = Clays
- Henry Formation = Loose to Medium Dense Sands
- Mississippi Embayment = Dense Sand
- GWT ~ 10ft below ground surface

Borings

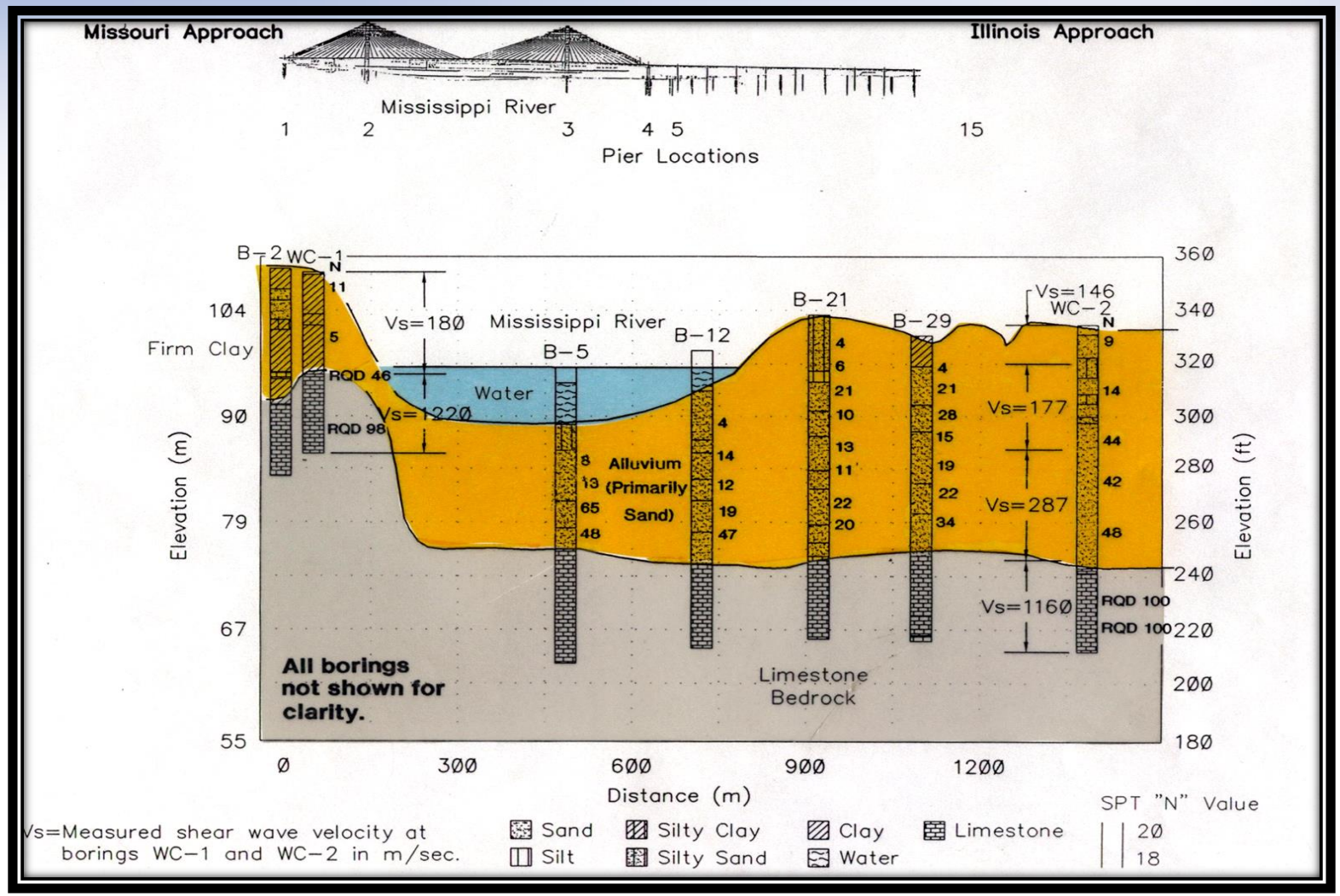
Missouri Approach
Illinois Approach
Mississippi River
1 2 3 4 5 15
Pier Locations
B-2 WC-1
B-5
B-12
B-21
B-29
Vs=146 WC-2
Vs=180
Vs=1220
Vs=177
Vs=287
Vs=1160
Water
Alluvium (Primarily Sand)
Firm Clay
Limestone Bedrock
All borings not shown for clarity.
RQD 46
RQD 98
RQD 100
RQD 100
Elevation (m)
Elevation (ft)
104
90
79
67
55
360
340
320
300
280
260
240
220
200
180
0
300
600
900
1200
Distance (m)
Vs=Measured shear wave velocity at borings WC-1 and WC-2 in m/sec.
Sand
Silt
Silty Clay
Silty Sand
Clay
Water
Limestone
SPT "N" Value
20
18

In-Situ Testing

In-Situ Testing

- Standard Penetration Test (SPT)
- Cone Penetration Test (CPT)
  - Seismic Cone Penetration Test (SCPT)
- Vane Shear Test (VST)
- Pressure Meter Test (PMT)
- Dilatometer Test (DMT)
- Becker Penetration Test (BPT)

In-Situ Testing

- Standard Penetration Tests (SPTs)
  - Most common in situ test worldwide.
  - 2.5 to 8 inches diameter (exploratory boring).
  - The Standard Penetration Tests aims to determine the SPT N value, which gives an indication of the soil stiffness and can be empirically related to many engineering properties.
  - Drive a thick-walled tube into the ground and measure the number of blows required to advance the tube 1 ft.
    - Developed in 1902 by Colonel Charles Gow of the Raymond Pile Company
    - Seating correction recommended by Karl Terzaghi in 1947
    - Improved “standardization” in past 25 years

In-Situ Testing

- SPT Split-Barret sampler is driven into the soil at the bottom of the boring using at 140-lb. hammer falling 30 in.
  - Rope cathead system
  - Trip
  - Semi-automatic
  - Automatic

In-Situ Testing

In-Situ Testing

– SPT Sampler

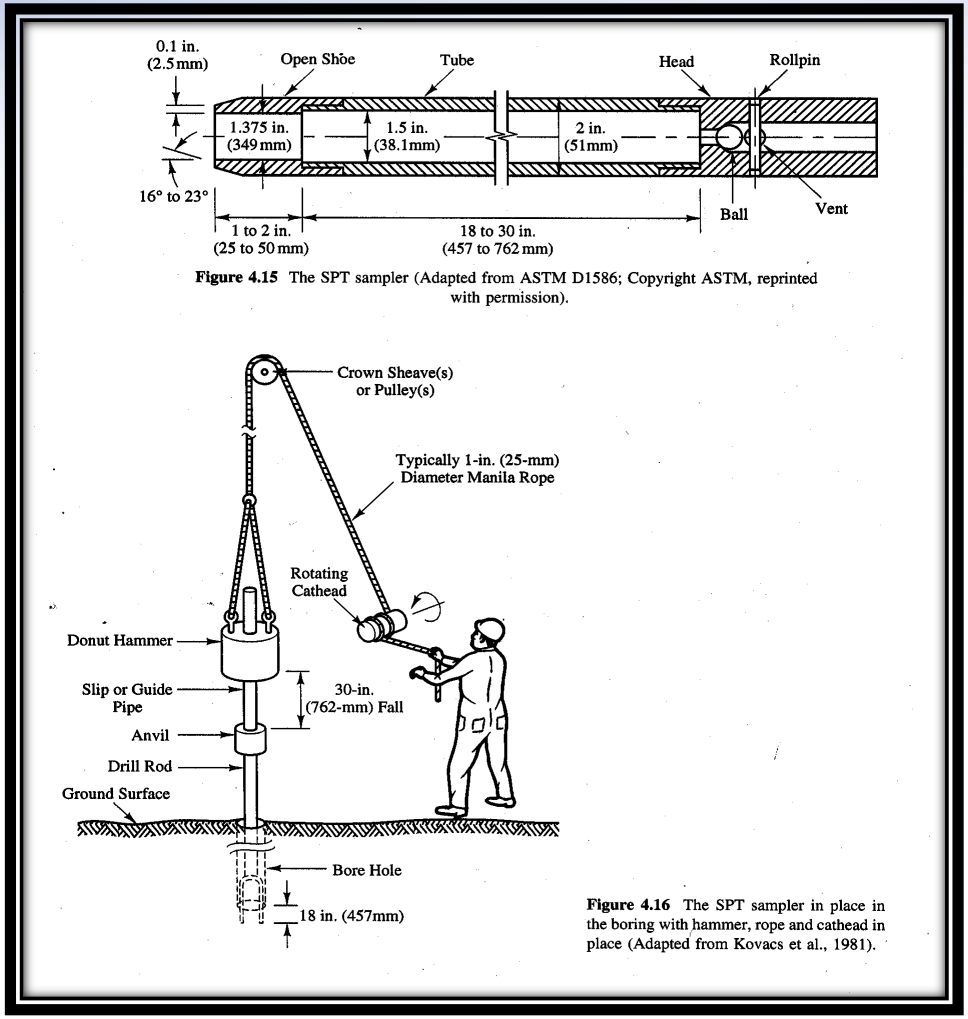

Figure 4.15 The SPT sampler (Adapted from ASTM D1586; Copyright ASTM, reprinted with permission).

Figure 4.16 The SPT sampler in place in the boring with hammer, rope and cathead in place (Adapted from Kovacs et al., 1981).

In-Situ Testing

In-Situ Testing

– SPT Hammers

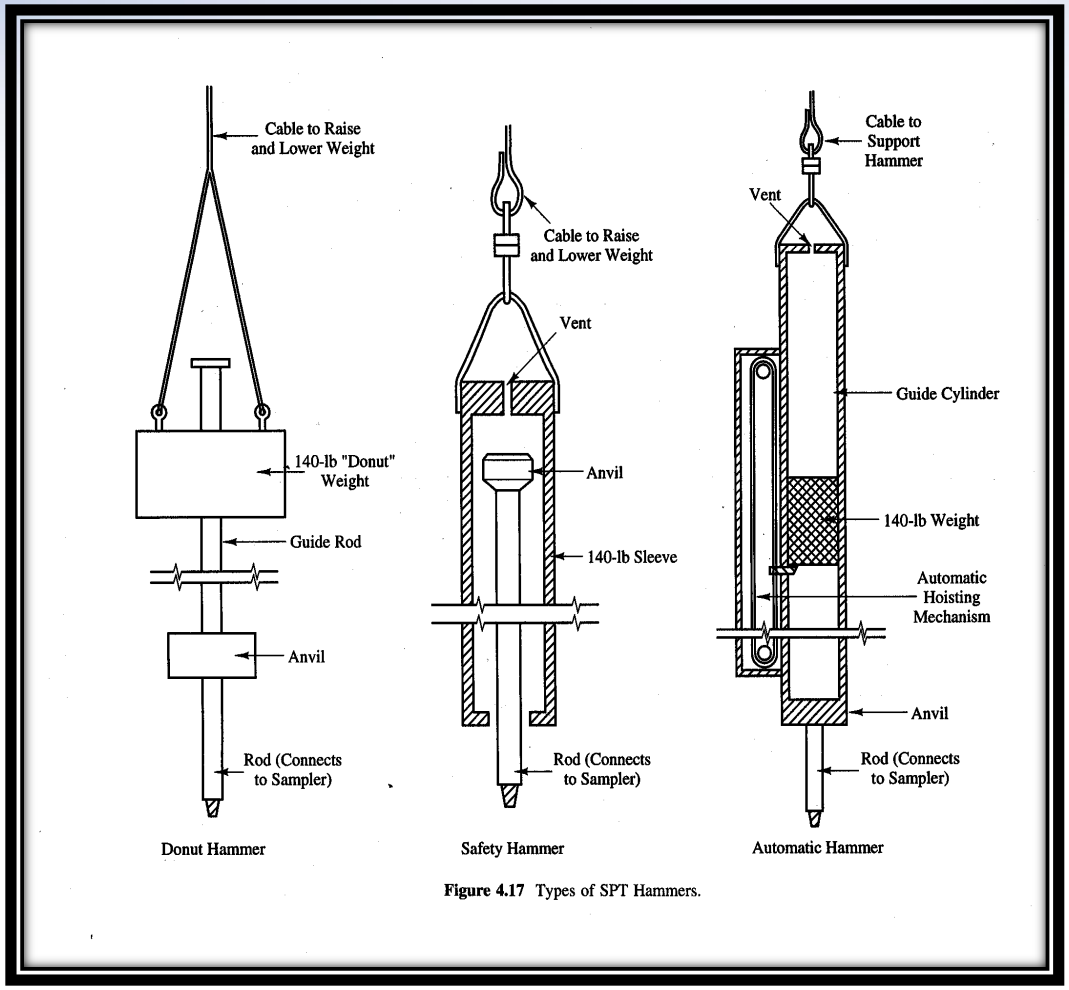

Figure 4.17 Types of SPT Hammers.

In-Situ Testing

In-Situ Testing

– SPT Split Spoon Sampler

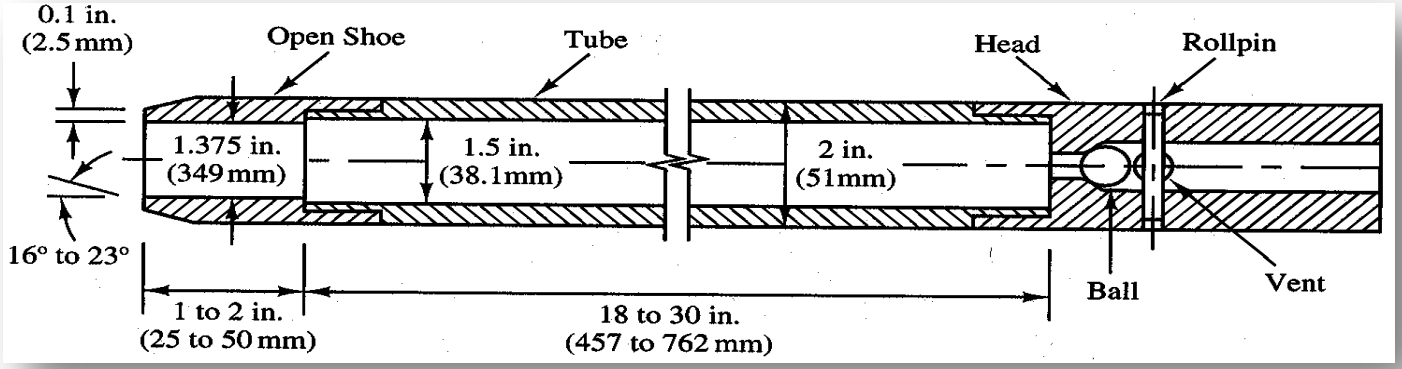

In-Situ Testing

- SPT Test procedure defined by ASTM D1586 (1999)
  - Record the number of blows required for each 6 in of penetration or fraction thereof:
    - The first 6 in is considered to be a seating drive
    - The “standard penetration resistance”, “blow count”, or “N-value” is the sum of the blows for the second and third 6-in increments and is expressed as “blows per foot (bpf)”
    - If the sampler is driven less than 18 in., the number of blows for each 6-in increment and fractions thereof should be recorded (e.g., 50/4 in.)

In-Situ Testing

- Theoretical free-fall energy of the SPT hammer

$$E_{theo} = W*h$$
$$= (140 \text{ lb.})(30 \text{ in.})$$
$$= 4200 \text{ in.-lb.}$$

  - Where W is the weight of the hammer
  - Where h is the height of the fall of the hammer

- Friction and eccentric loading cause losses

$$E_{actual} = ER_r \cdot E_{theo}$$

Country	Hammer	Release	Er_r (%)
USA	Safety Donut	2 turns of rope 2 turns of rope	55 45
Japan	Donut Donut	Tombi 2 turns of rope	78-85 65-67
China	Automatic Donut	Trip Manual	60 55
UK	Automatic	Trip	73

In-Situ Testing

- Standard rod energy ratio of 60%
  - Er_r obtained via calibration (ASTM D4633) or assumed based on typical values

$$N_{60} = \frac{ER_r}{60} \cdot N$$
$$= C_E \cdot N$$

In-Situ Testing

– It is common to normalize the standard penetration resistance to a vertical effective stress of 1 atmosphere

$$C_N=(p_a/\sigma_v)^{0.5} \leq 2$$

P_a=atmospheric pressure in same units as σ_v

e.g., pa =100 kPa or 2000 psf

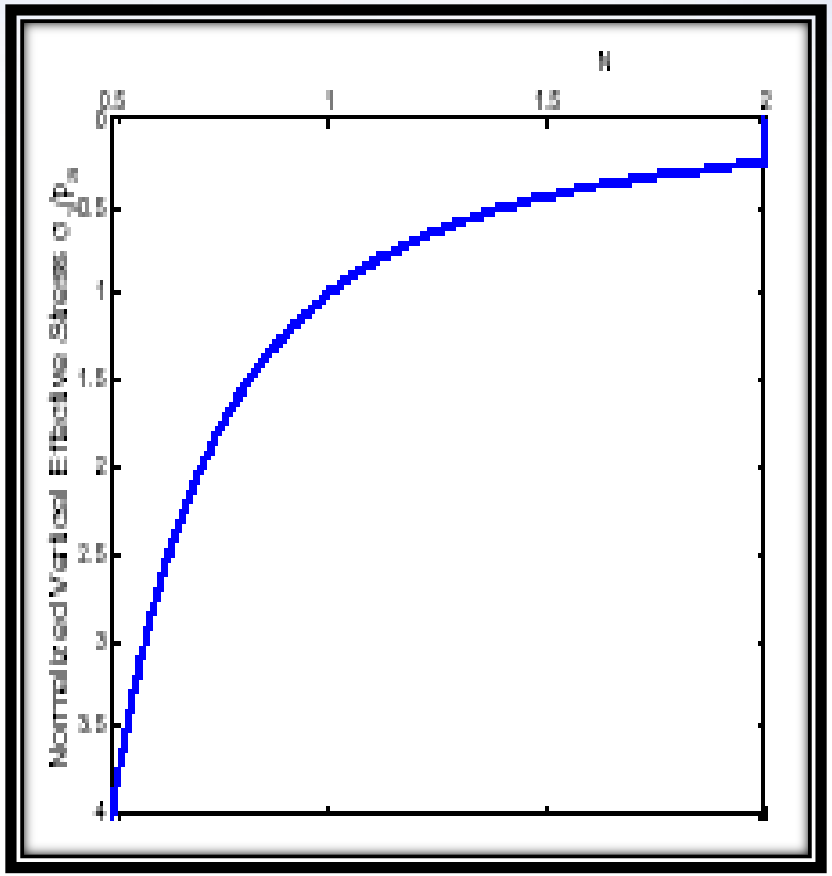

In-Situ Testing

- It is common to combine the energy and overburden corrections as follows:

$$(N_1)_{60} = C_N \cdot C_E \cdot N$$

- Be careful to use appropriate corrections when using N-values in engineering correlations. For example, some correlations may utilize N_{60}, not $(N_1)_{60}$
- Additional Corrections:

Factor	Equipment Variable	Value
Borehole Diameter (C_B)	65-115 mm 150 mm 200 mm	1.00 1.05 1.15
Sampling Method (C_S)	Standard sampler Sampler w/o liners	1.0 1.2
Rod Length (C_R)	3-4 m 4-6 m 6-10 m > 10 m	0.75 0.85 0.95 1.00

In-Situ Testing

$$(N_1)_{60} = C_N C_E C_B C_R C_S N_m$$

$(N_1)_{60}$ = Resistencia a la penetración corregido

C_N = Factor de corrección para esfuerzo efectivo

C_E = Factor de corrección para la razón energía del martillo

C_B = Factor de corrección para el diámetro del barreno

C_R = Factor de corrección para el largo de la barra

C_S = Factor de corrección para el toma muestra

N_m = Resistencia a la penetración medido

In-Situ Testing

SPT Interpretation

- Density
  - Relative density of coarse-grained soils

N Value	Classification	D_r (%)
0-4	Very Loose	0-15
4-10	Loose	15-35
10-30	Medium	35-65
30-50	Dense	65-85
>50	Very Dense	85-100

In-Situ Testing

- Relative density of un-cemented, un-aged normally consolidated quartz sands (Skempton, 1986; Mayne, 2001)

$$D_r^2 = ((N_1)_{60})/60$$

- Additional corrections for particle size, ageing, and over-consolidated

$$D_r^2 = ((N_1)_{60})/(C_P \cdot C_A \cdot C_{OCR})$$

In-Situ Testing

– Effective friction angle of coarse – grained soils

$$\bar{\phi} = \tan^{-1}\left(\frac{N}{12.2 + 20.3\frac{\bar{\sigma}_{v0}}{p_a}}\right)^{0.34}$$

$$\bar{\phi} = \sqrt{15.4\,(N_1)_{60}} + 20^\circ$$

after DeMello (1971), Schmertmann (1975), and Mayne (2001)

N assumed to be N_{60}

after Hatanaka and Uchida (1996) and Mayne (2001)

In-Situ Testing

- Standard Penetration Test (SPT)

Advantages	Disadvantages
– Obtain a sample and a number – Simple and rugged – Suitable in many soil types	– Obtain a sample and a number – Disturbed sample suitable for index tests only – Crude number for analysis

In-Situ Testing

- Cone Penetration Test (CPT)
  - Instrumented steel probe with a 60° apex tip and internal strain gages or load cells to measure tip stress (q_c) and sleeve friction resistance (f_s).
  - Hydraulically pushed at a rate of 2 cm/sec
  - No boring, no samples, no cuttings, no spoil
  - Continuous readings of q_c, f_s, and other parameters
  - ASTM D 5778

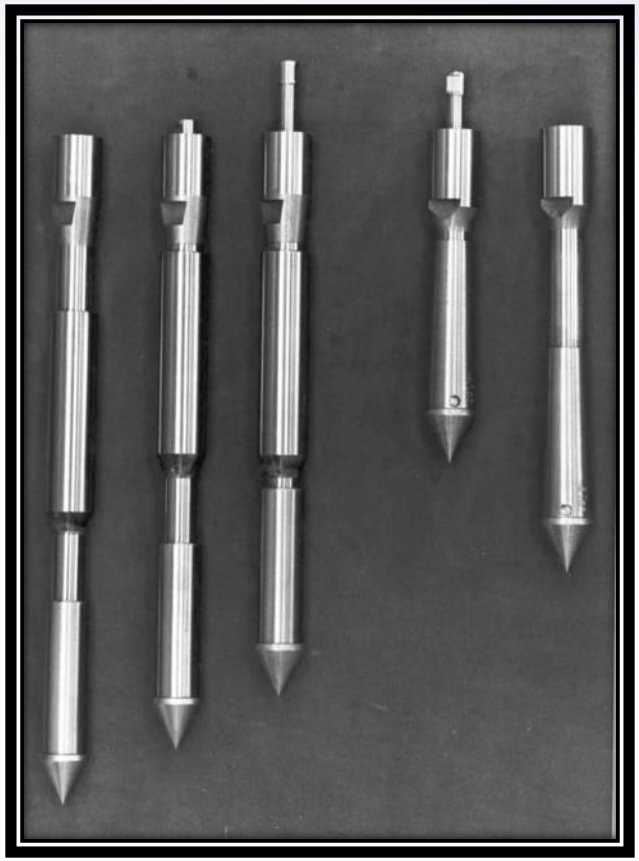

In-Situ Testing

Cone Penetration Test (CPT)

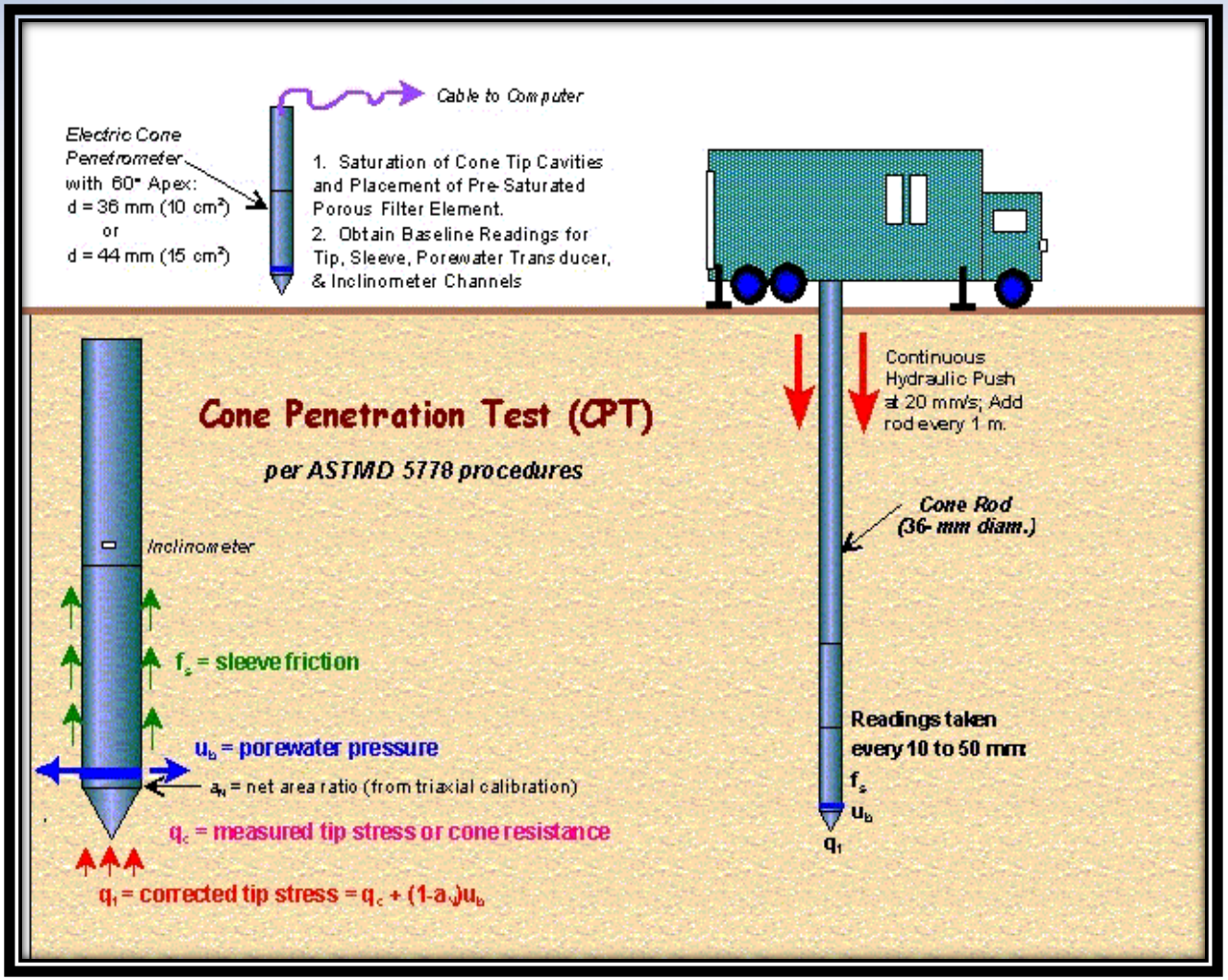

In-Situ Testing

Cone Penetration Test (CPT)

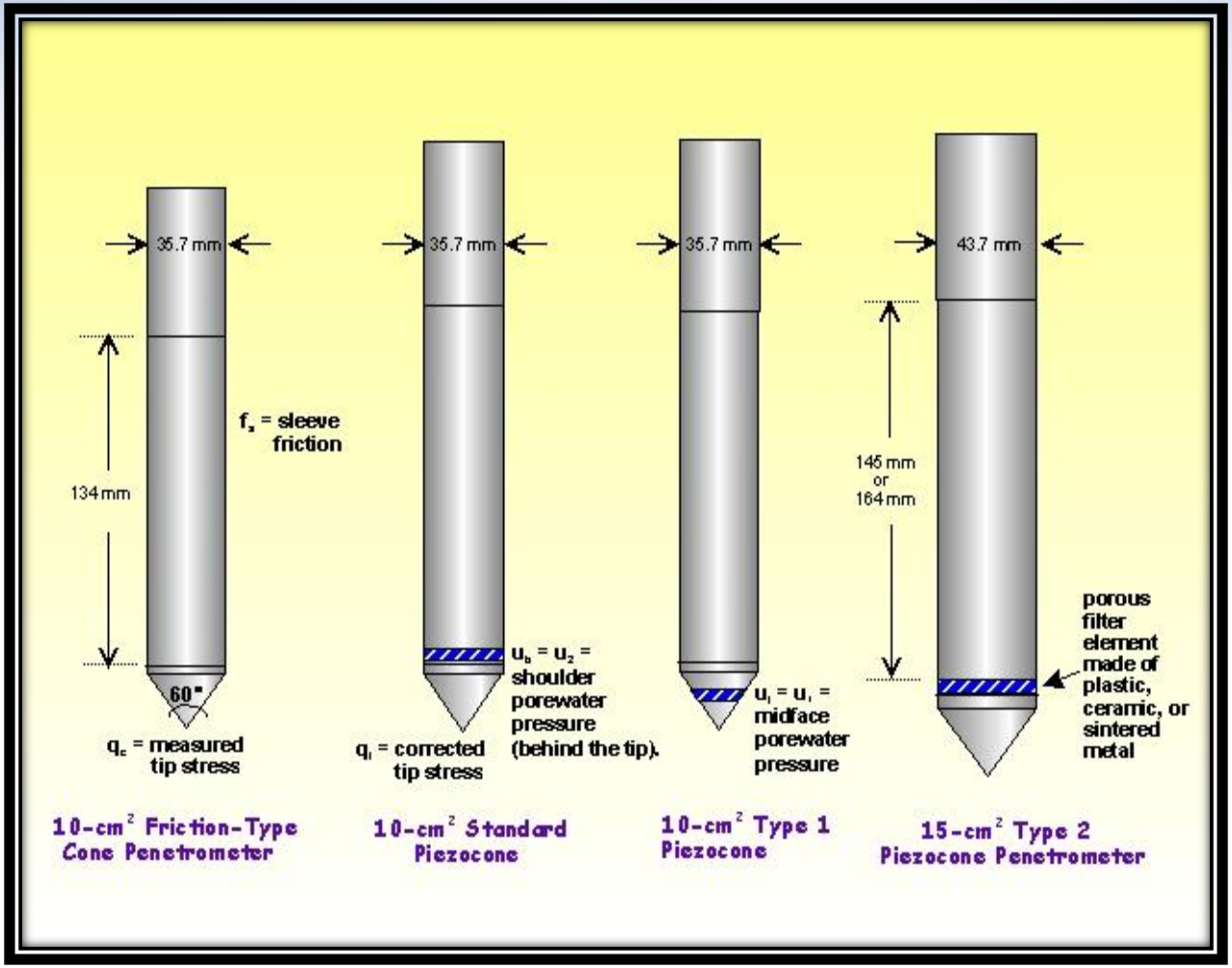

In-Situ Testing

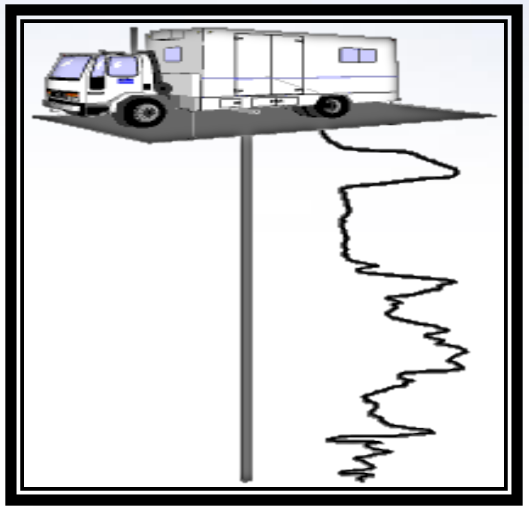

CPT Mobile 25-tonne rigs with enclosed cabins to allow testing under all weather conditions

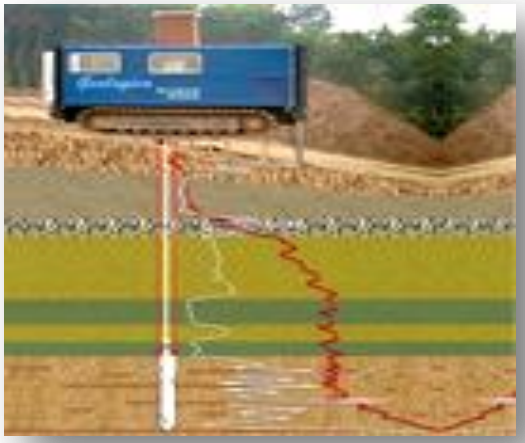

In-Situ Testing

- Corrections to CPT data
  - Tip Stress correction for pore water pressures on unequal areas; important for intact Clays & Silts: $q_T = q_c + (1-a_N)\, u_b$
  - Net area ratio (a_N) obtained by calibrating penetrometer in triaxial cell.
  - Sleeve Friction correction for pore water pressures
  - Use equal end areas on friction sleeve
  - Baseline Readings – Obtain before & after each sounding

In-Situ Testing

Cone Penetration Test (CPT)

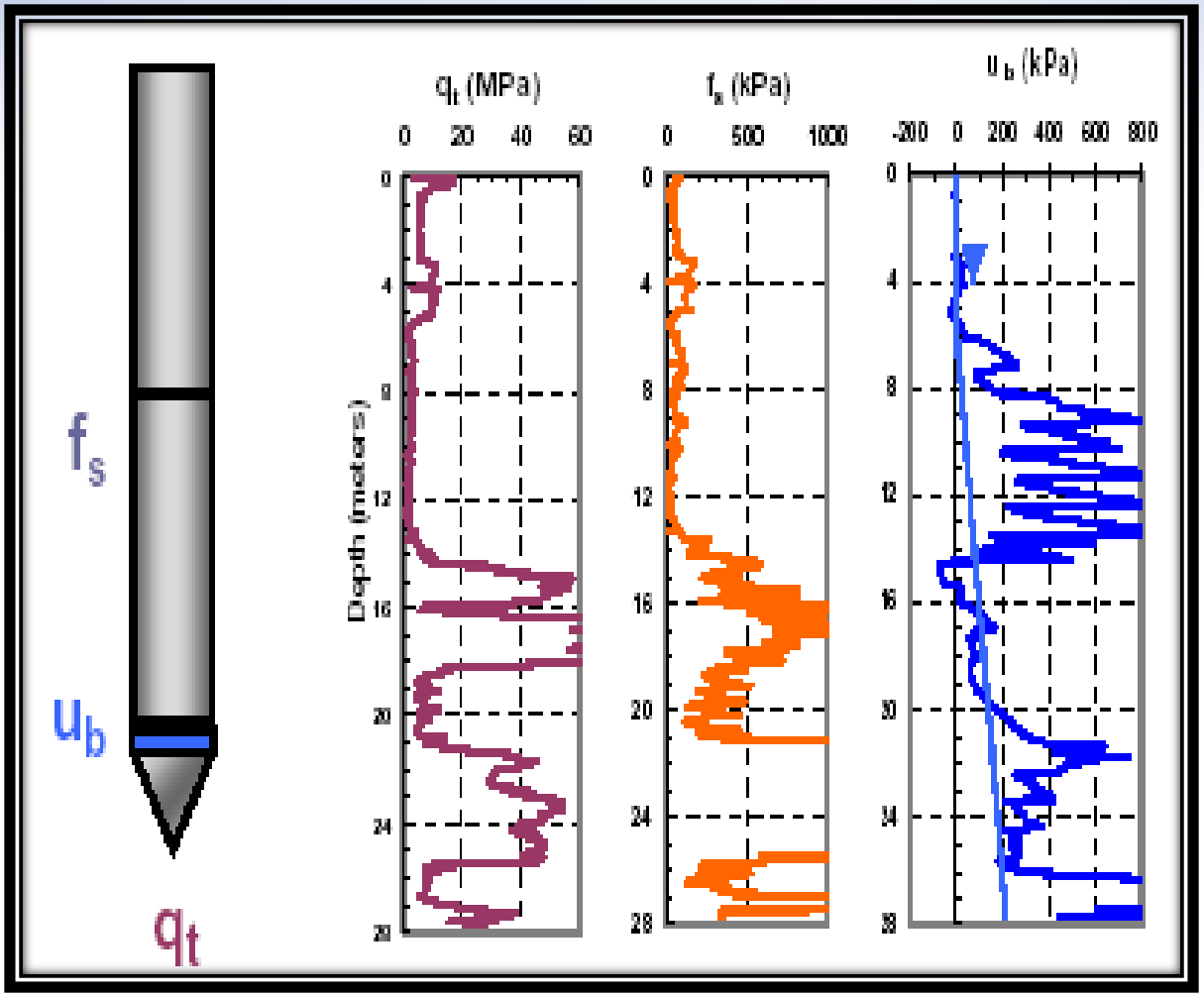

In-Situ Testing

Comparison of CPT and SPT test results

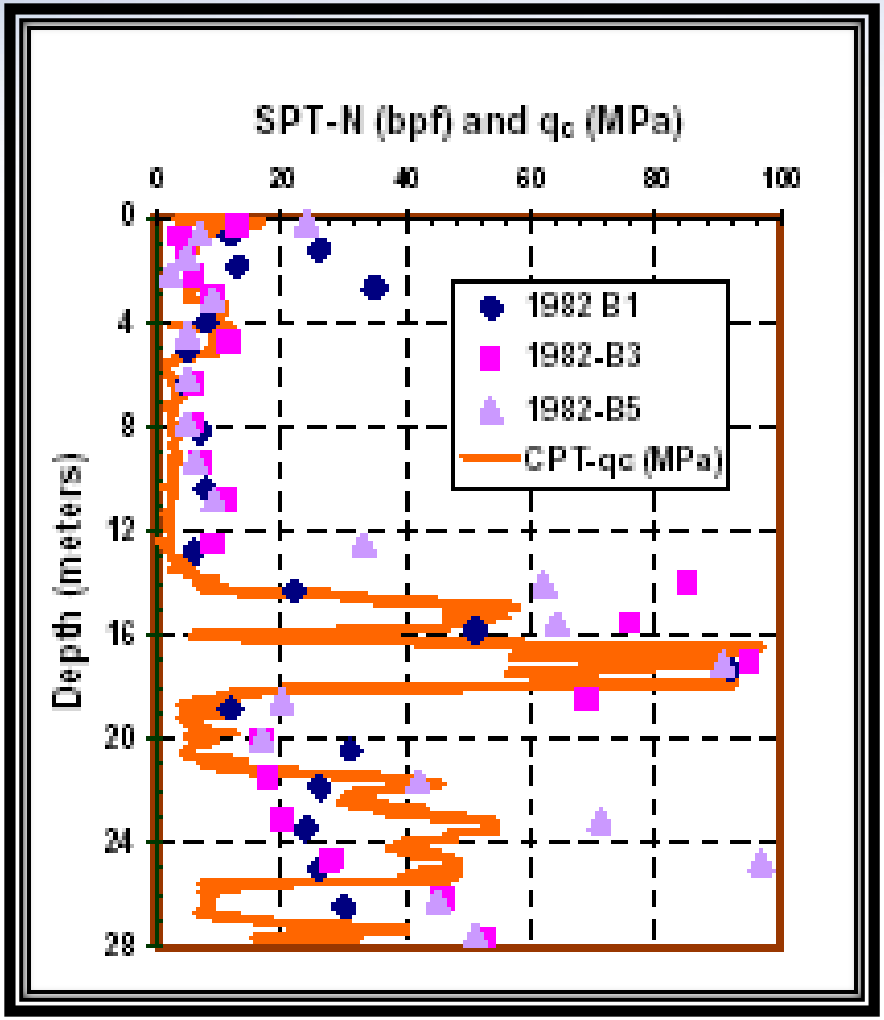

In-Situ Testing

- Seismic Cone Penetration Test (SCPT)
  - Anchoring System
  - Automated Source
  - Polarized Wave
  - Down hole V_s

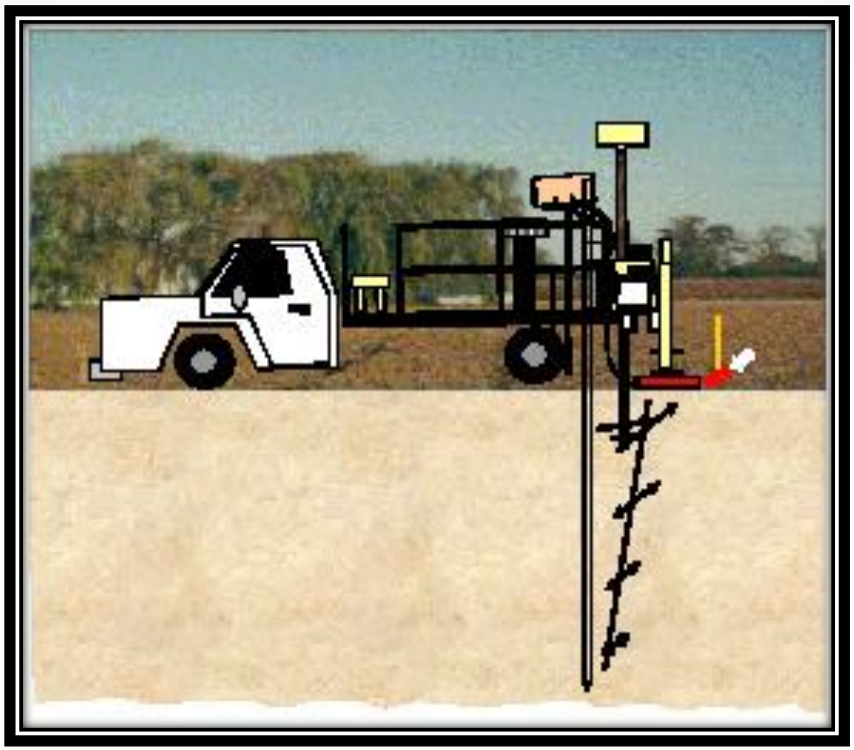

In-Situ Testing

- Seismic Cone Penetration Test Results

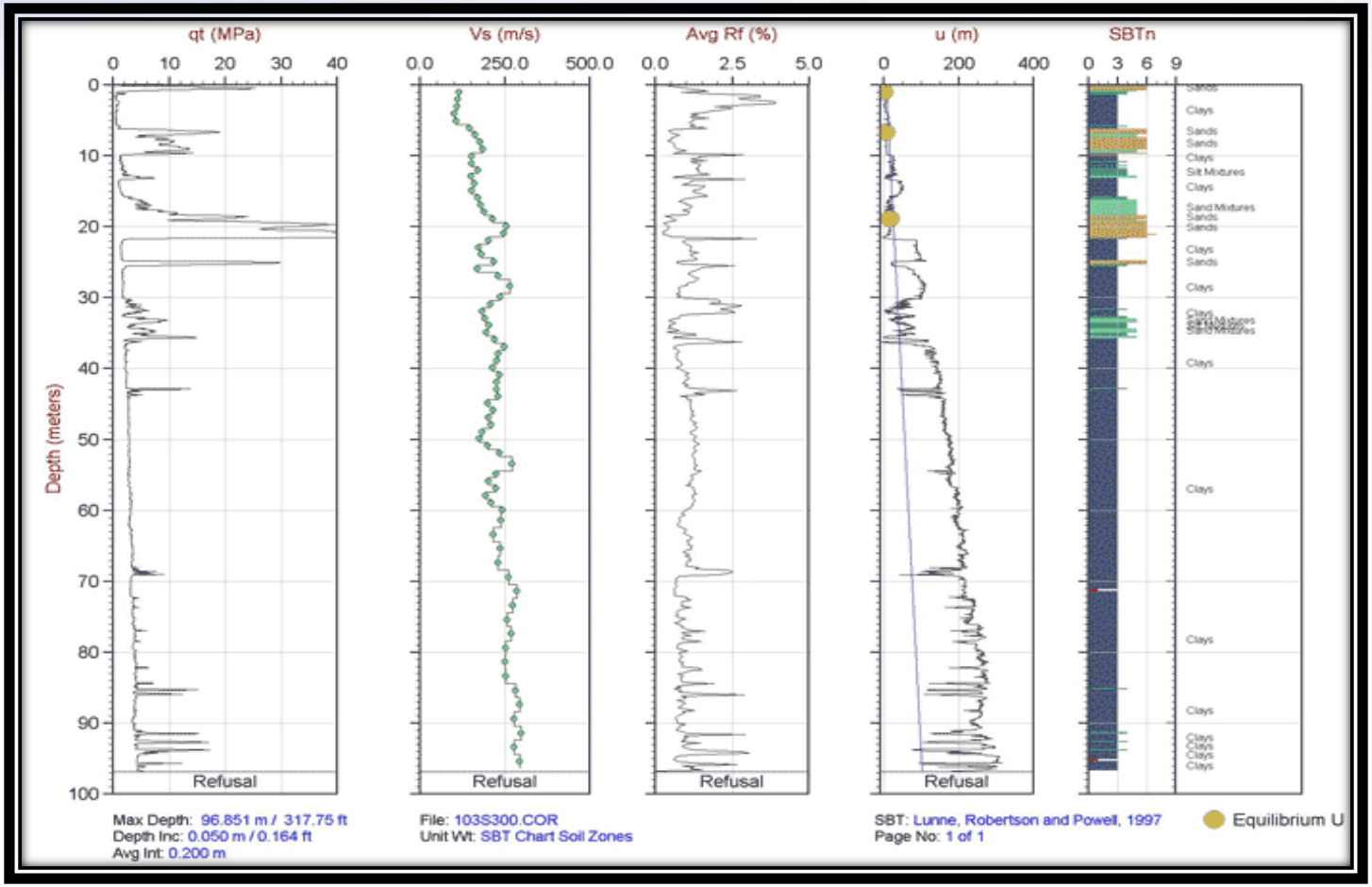

In-Situ Testing

CPT Interpretation

– Soil Type

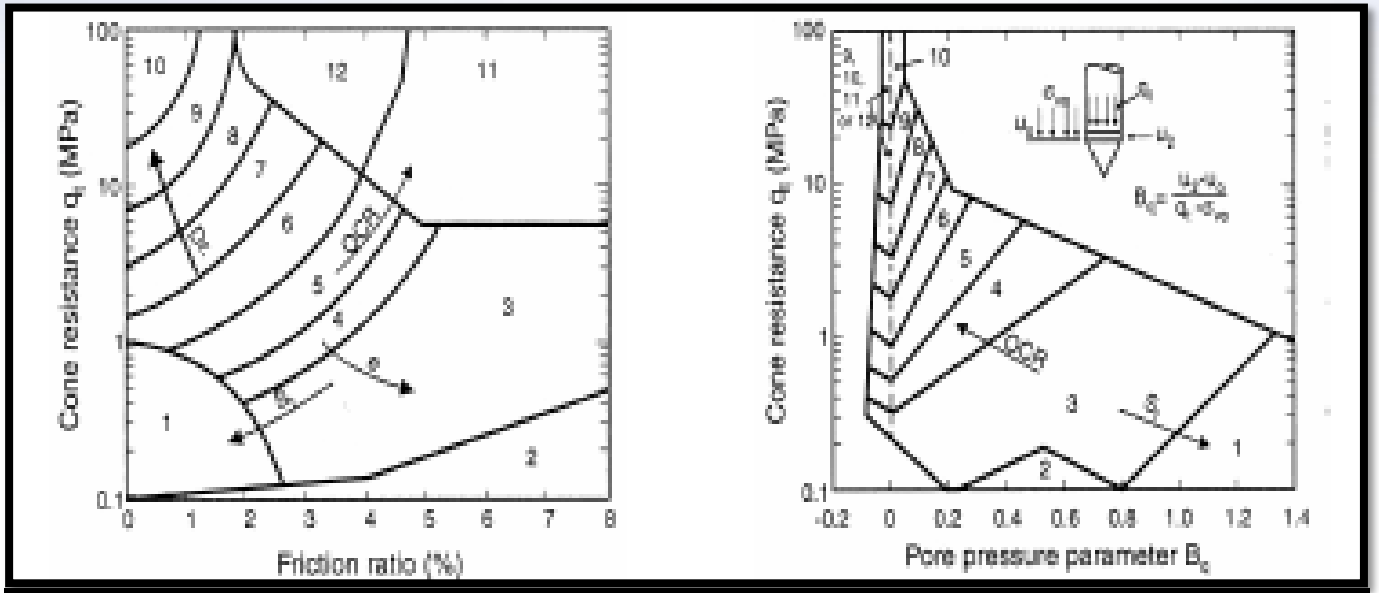

Soil Behavior Type (Robertson et al., 1986; Robertson & Campanella, 1988)

1-Sensitive fine grained	5-Clayey silt to silty clay	9-sand
2-Organic material	6-Sandy silt to silty sand	10-Gravelly sand to sand
3-Clay	7-Silty sand to sandy silt	11-Very stiff fine grained*
4-Silty clay to clay	8-Sand to silty sand	12-Sand to clayey sand *

*Note: Overconsolidated or cemented

In-Situ Testing

- Density
  - NC and OC Ticino Sand

$$D_r = \frac{1}{C_2} \ln\left[\frac{q_c}{C_0(\bar{\sigma}_m)^{C_1}}\right]$$

$C_0 = 205$

$C_1 = 0.51$

$C_2 = 2.93$

q_c and $\bar{\sigma}_m$ in kPa

Baldi et al. (1986)

In-Situ Testing

- Un-cemented, Un-aged Quartz Sands

$$D_r = -98 + 66 \log_{10}\left[\frac{q_c}{(\sigma_{vo})^{0.5}}\right]$$

q_c and σ_{vo} in t/m^2

Jamiolkowski et al. (1986)

- Clean NC Sands

$$D_r = 100\sqrt{\frac{q_{c1}}{305}}$$

$$q_{c1} = \frac{q_c}{\left(\frac{\sigma_{vo}}{p_a}\right)^{0.5}} \leq 305$$

Kulhawy and Mayne (1991)

In-Situ Testing

- Sands

$$\bar{\phi} = 17 + 11 \log\left[\frac{q_c}{(\sigma_{v0}\, p_a)^{0.5}}\right]$$ Ladd et al. (1977)

$$\bar{\phi} = 17.6 + 11.0 \log\left[\frac{q_c}{(\sigma_{v0}\, p_a)^{0.5}}\right]$$ Kulhawy and Mayne (1990)

$$\bar{\phi} = \tan^{-1}\left[0.1 + 0.38 \log\left(\frac{q_c}{\sigma_{v0}}\right)\right]$$ Robertson and Campanella (1990)

- Clays

$$s_u = \frac{q_c - \sigma_{v0}}{N_k}$$

$$N_k \cong 9 \text{ to } 20$$

$$N_{k,ave} \cong 15$$

Aas et al. (1986)
Konrad and Law (1986)
Jamiolkowski et al. (1988)
Houlsby and Wroth (1989)

In-Situ Testing

- Clays - OCR

$$OCR \cong \frac{0.75(q_T - u_1)}{\overline{\sigma}_{v0}}$$

Chen and Mayne (1996)

In-Situ Testing

Cone Penetration Test

Advantages	Disadvantages
– Fast and continuous profiling – Results not operator dependent	– No sample is obtained – High capital investment – Requires skilled operator and calibration – May not work in all soil types

In-Situ Testing

- Vane Shear Test (VST)

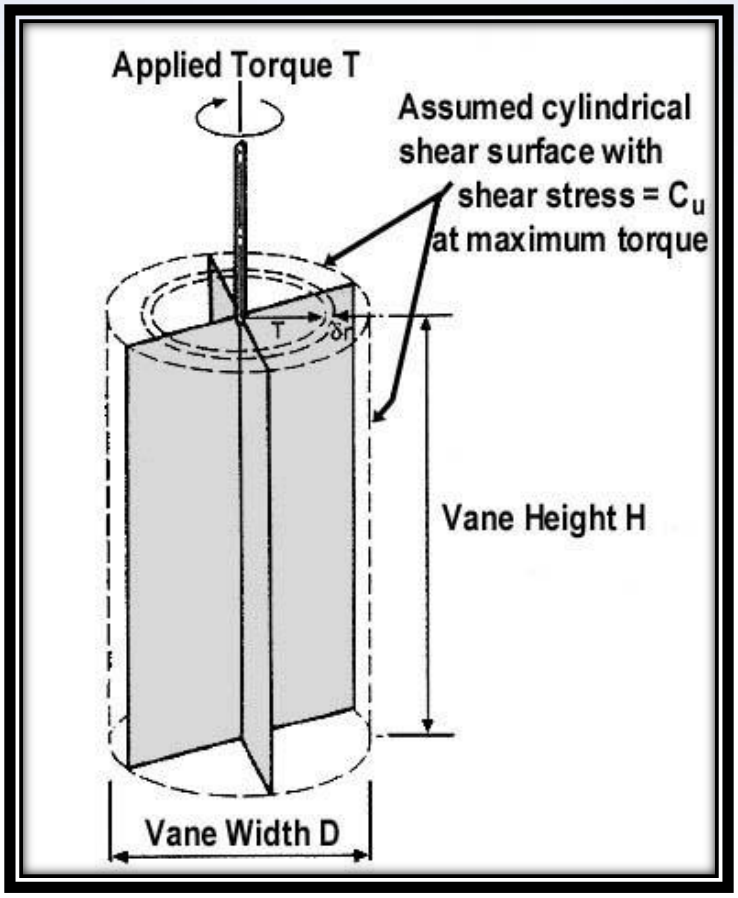

In-Situ Testing

– Vane Shear Test Process

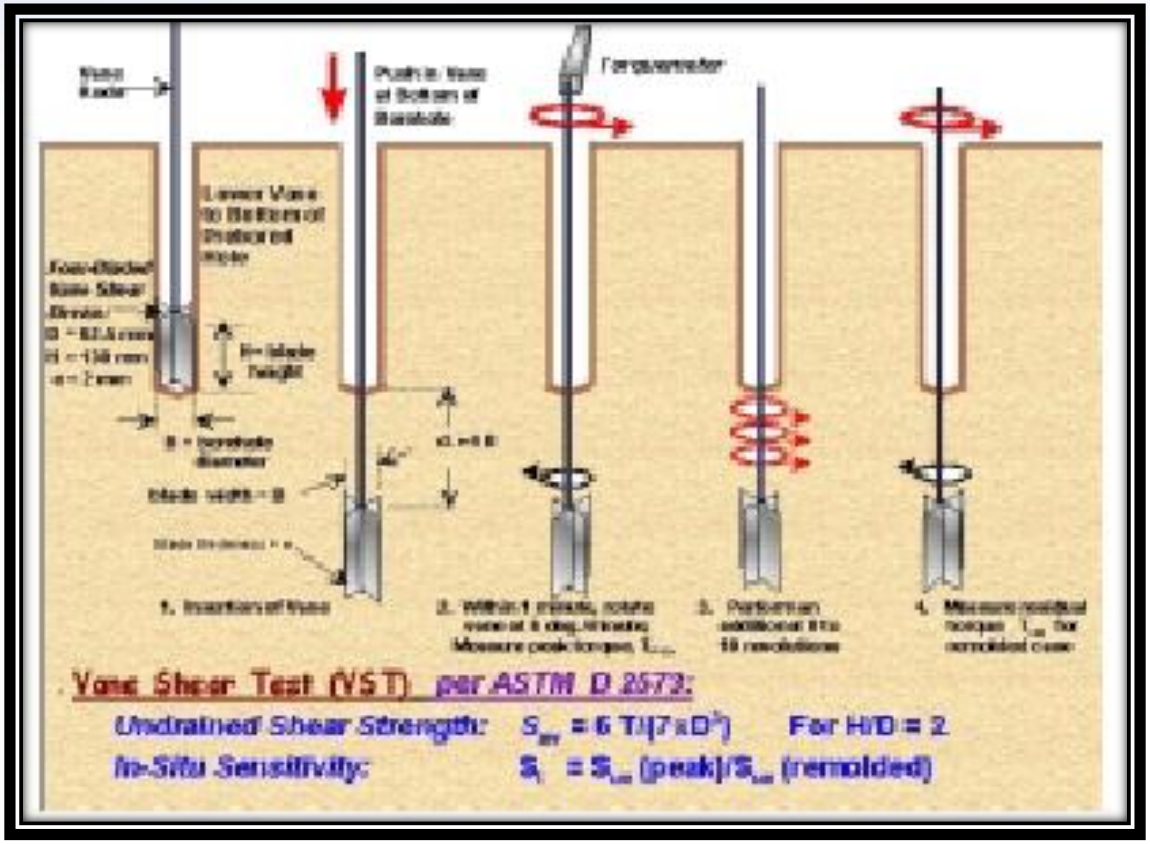

In-Situ Testing

– Vane Shear Testing Devices

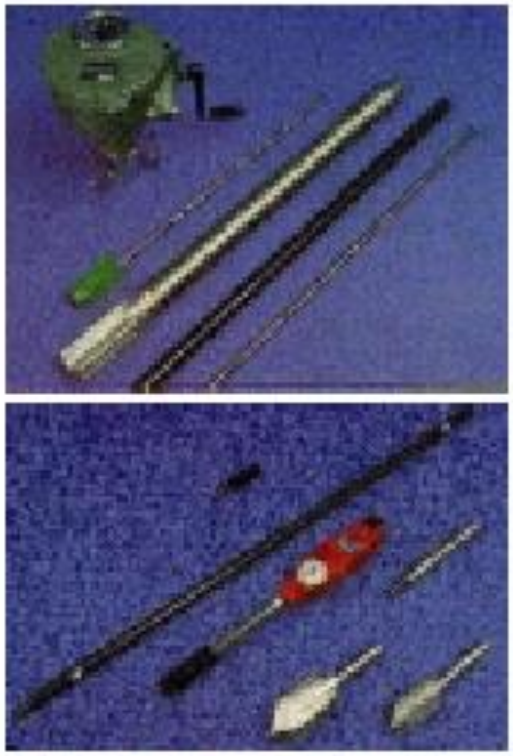

Scandinavian Vanes

McClelland Offshore Vane

In-Situ Testing

– Different Penetration Tests

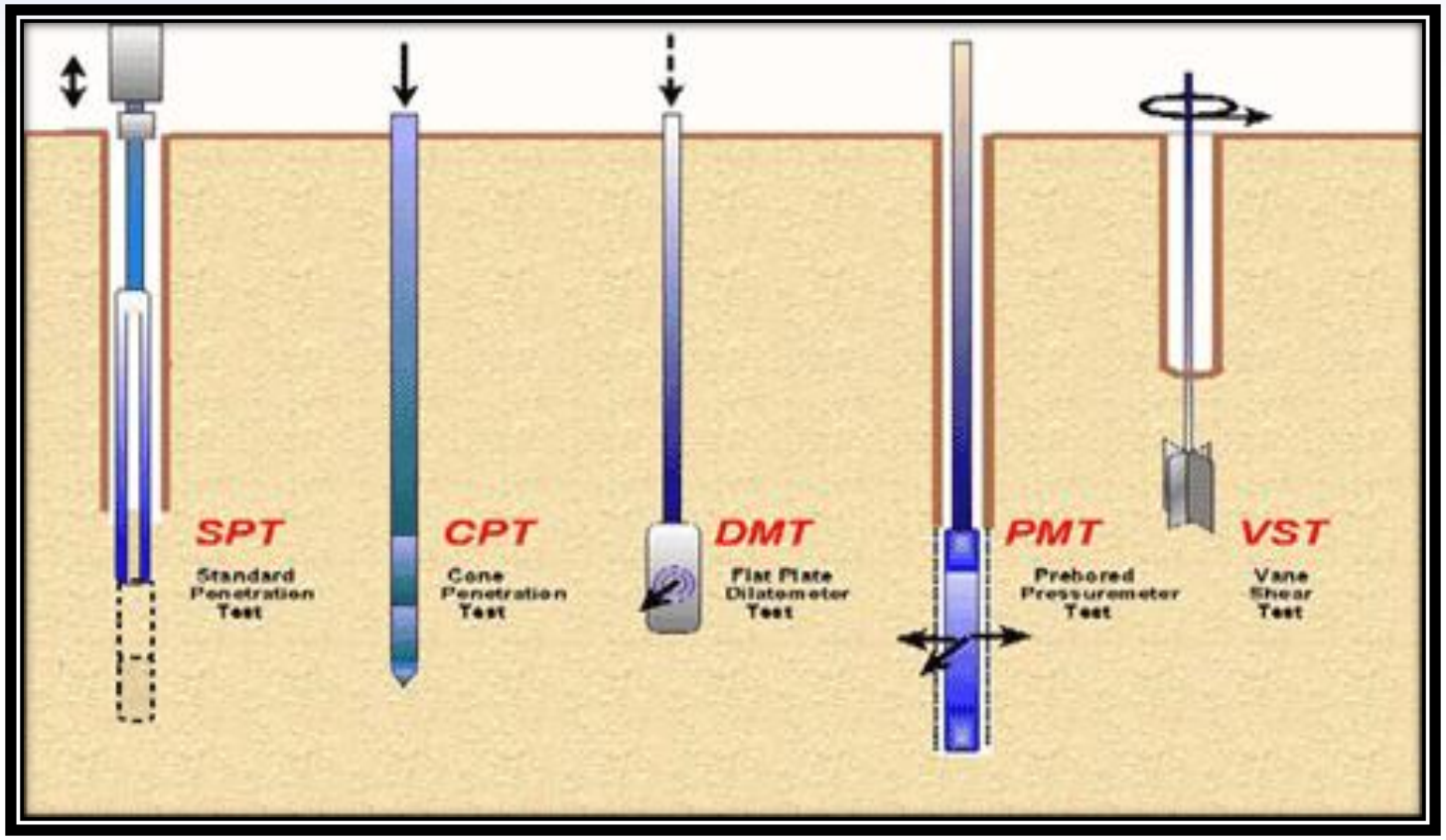

In-Situ Testing

- Flat Dilatometer Test (DMT)

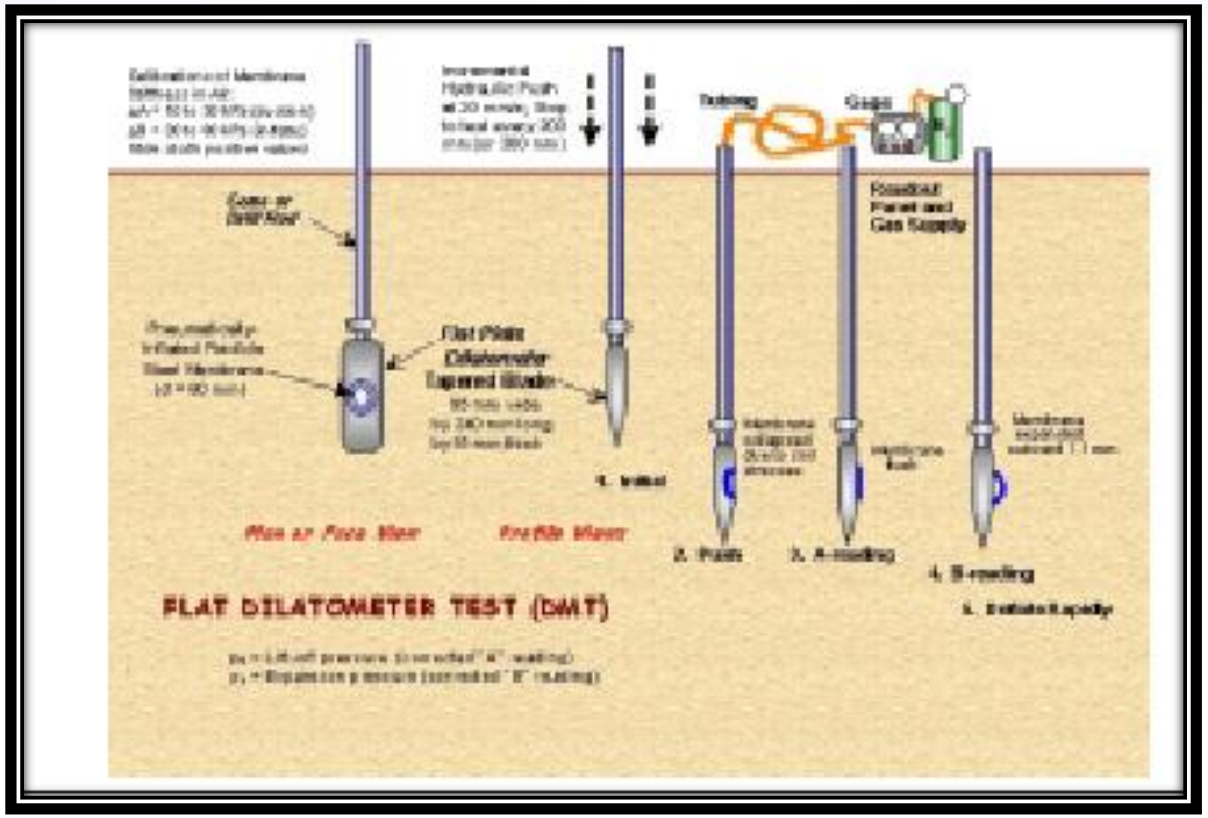

In-Situ Testing

In-Situ Testing

- Flat Dilatometer Test (DMT) Machine

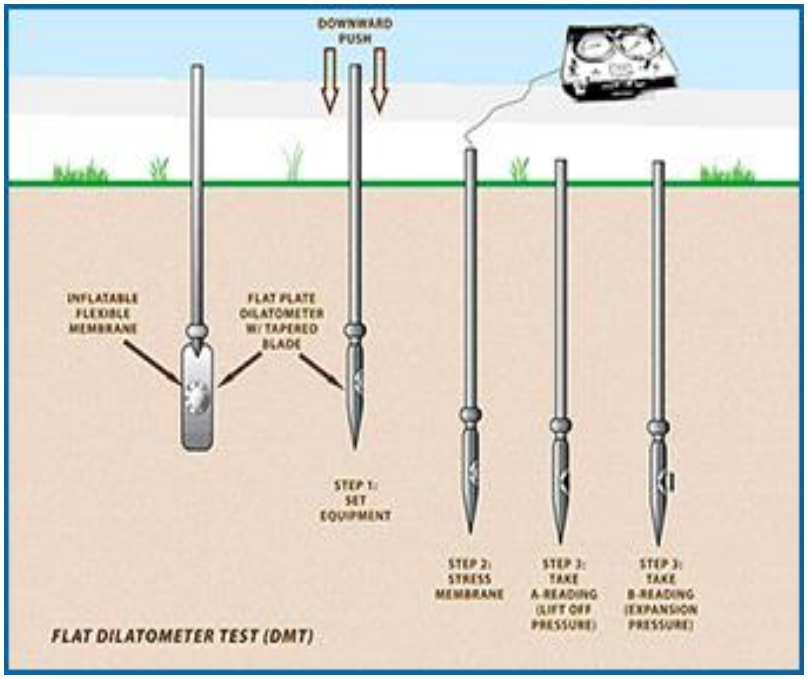

In-Situ Testing

- Two readings at each depth
  - Lift-off pressure (A)
  - Expansion pressure (B)
- Corrections for membrane stiffness (Schmertmann, 1986)

$$p_0 = 1.05(A + \Delta A - z_m) - 0.05(B + \Delta B - z_m)$$

$$p_1 = B - \Delta B - z_m$$

$\Delta A, \Delta B$ = calibration factors

z_m = gage offset zero reading

In-Situ Testing

DMT Interpretation

- Soil Type
  - DMT results have been correlated with the parameters that geotechnical engineers need the most :
    - soil shear strength and
    - deformation properties
  - The weaker the soils are, the more critical they are to the geotechnical engineering design.
  - We generally perform dilatometer tests at 20 centimeter (8 inch) depth intervals

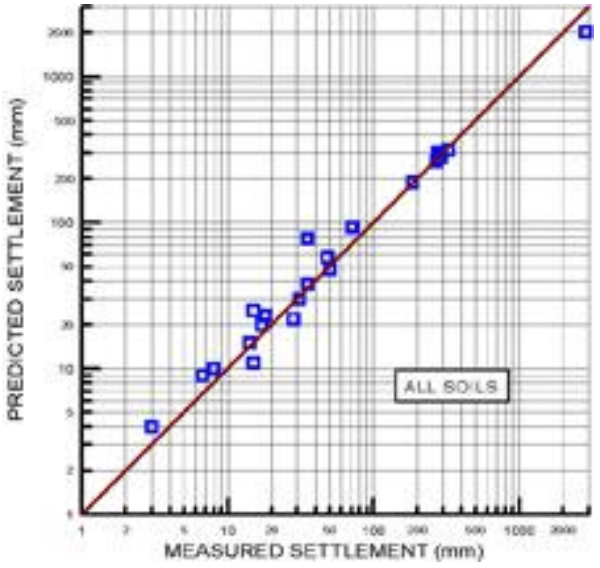

In-Situ Testing

- Material index

$$I_D = \frac{p_1 - p_0}{p_0 - u_0}$$

**u_0 = static pore water pressure

- Clay
  - $I_D < 0.6$
- Silt
  - $0.6 < I_D < 1.8$
- Sand
  - $I_D > 1.8$

- Dilatometer modulus

$$K_D = \frac{p_0 - u_0}{\overline{\sigma}_{v0}}$$

- Horizontal stress index

$$E_D = 34.7(p_1 - p_0)$$

In-Situ Testing

– Strength

Sand

$$\overline{\Phi} \cong 37.3\left[\frac{K_D - 0.8}{K_0 + 0.8}\right]^{0.082}$$ Campanella and Robertson (1991)

$$\overline{\Phi}_{\text{lower bound}} = 28 + 14.6 \log K_D - 2.1 \log^2 K_D$$ Marchetti (1997)

Clay

$$s_u = 0.22\sigma_{v0}\left(\frac{K_D}{2}\right)^{1.25}$$ Marchetti (1980)

$$s_u = d_s\sigma_{v0}\left(\frac{K_D}{2}\right)^{1.25}$$ Lacasse and Lunne (1988)

$$s_u = \frac{p_0 - u_0}{10}$$ Schmertmann (1981)

$$d_s = \begin{cases} 0.20\,TC \\ 0.19\ VST \\ 0.14\ DSS \end{cases}$$

In-Situ Testing

– K_0

$$K_0 = \left(\frac{K_D}{1.5}\right)^{0.47} - 0.6$$ Marchetti (1980)

$$K_0 = 0.27 K_D$$ Mayne and Kulhawy (1990)

$$K_0 = a K_D^m$$ Lunne et al. (1990)

In-Situ Testing

- Flat Plate Dilatometer Test (DMT)

• Advantages	• Disadvantages
– Simple and robust – Results not operator dependent	– No sample is obtained – E_D only theoretically derived parameter – Correlations generally applicable to insensitive, un-cemented, intact materials – May require “calibration” for local soil conditions

In-Situ Testing

- Pressuremeter Test (PMT)

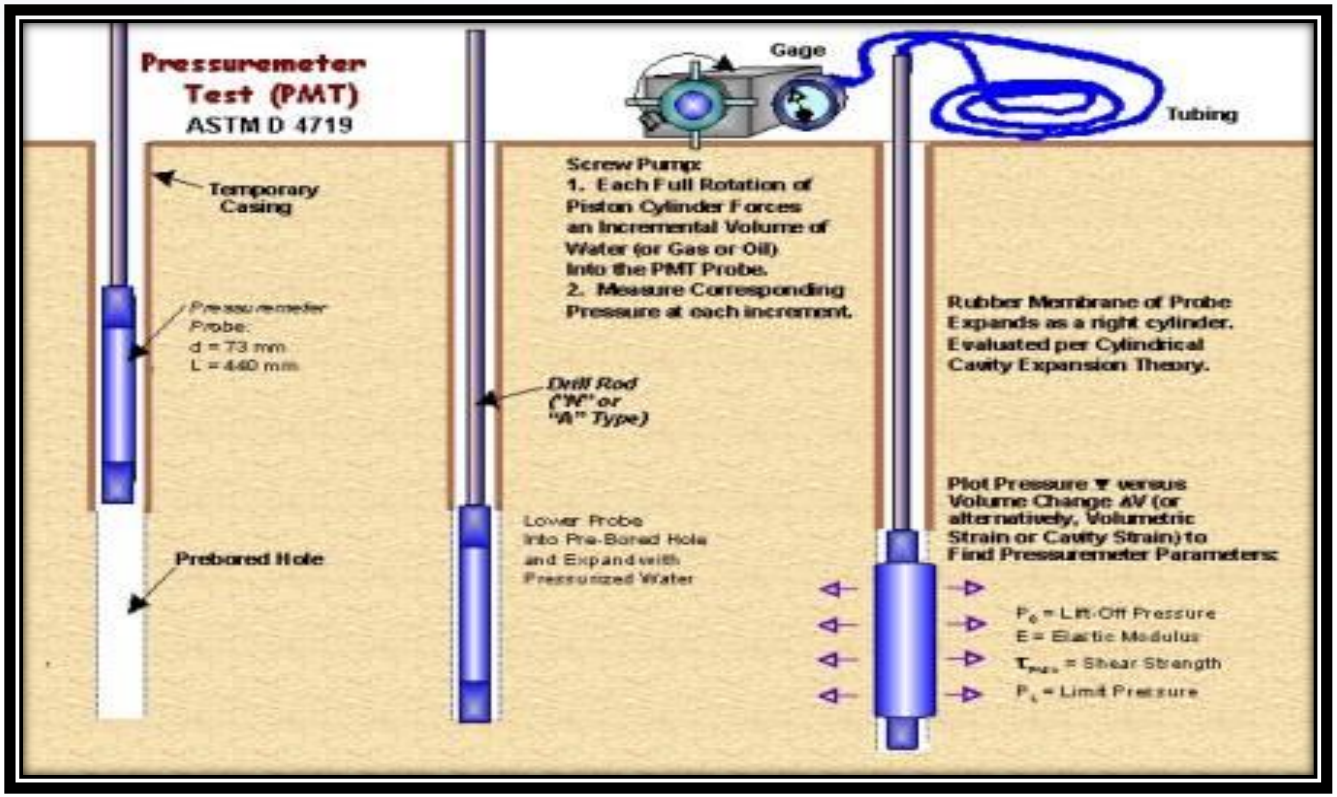

In-Situ Testing

– Pre-Bored Pressuremeter

Menard Pressure Panel

Texam Monocell Probe

In-Situ Testing

- In-Situ Methods

Advantages

- A larger, more representative volume of soil is tested that should include macroscopic features
- Many devices provide a continuous vertical profile
- In situ tests may be performed in soils that are difficult (or undesirable) to sample including coarse- grained soils, highly structured soils, and environmentally sensitive materials.
- Soils are tested in their natural environment that may not be preserved during sampling, handling, and laboratory testing.
- Site investigations based on in situ tests are often more economical and less time consuming than those based on laboratory tests.

after Jamiolkowski et al. (1985)

In-Situ Testing

– In-Situ Methods

Disadvantages

- For many in situ tests, boundary conditions in terms of stresses and/or strains are poorly defined and, thus, rational interpretation of the test results is very difficult.
- Drainage conditions during in situ tests are unknown and, thus, it is uncertain if the derived soil parameters represent drained, undrained or partially drained behavior.
- The degree of disturbance caused by advancing the testing device into the soil and its influence on the derived soil parameters is likely large, but its exact magnitude is unknown.
- Modes of deformation and failure associated with in situ tests is generally different than typical civil engineering structures
- The strain fields are non- uniform and strain rates are higher than those applied in laboratory tests and full- scale structures.
- With the exception of the SPT, the soil type is not directly identified.

after Jamiolkowski et al. (1985)

CAPITULO 11 SHEAR STRENGTH OF SOIL

INTRODUCTION

- The shear strength of a soil mass is the internal resistance per unit that the soil mass can offer to resist failure and sliding along any plane inside it. One must understand the nature of shearing resistance in order to analyze soil stability problems, such as bearing capacity, slope stability, and lateral pressure on earth retaining structures.

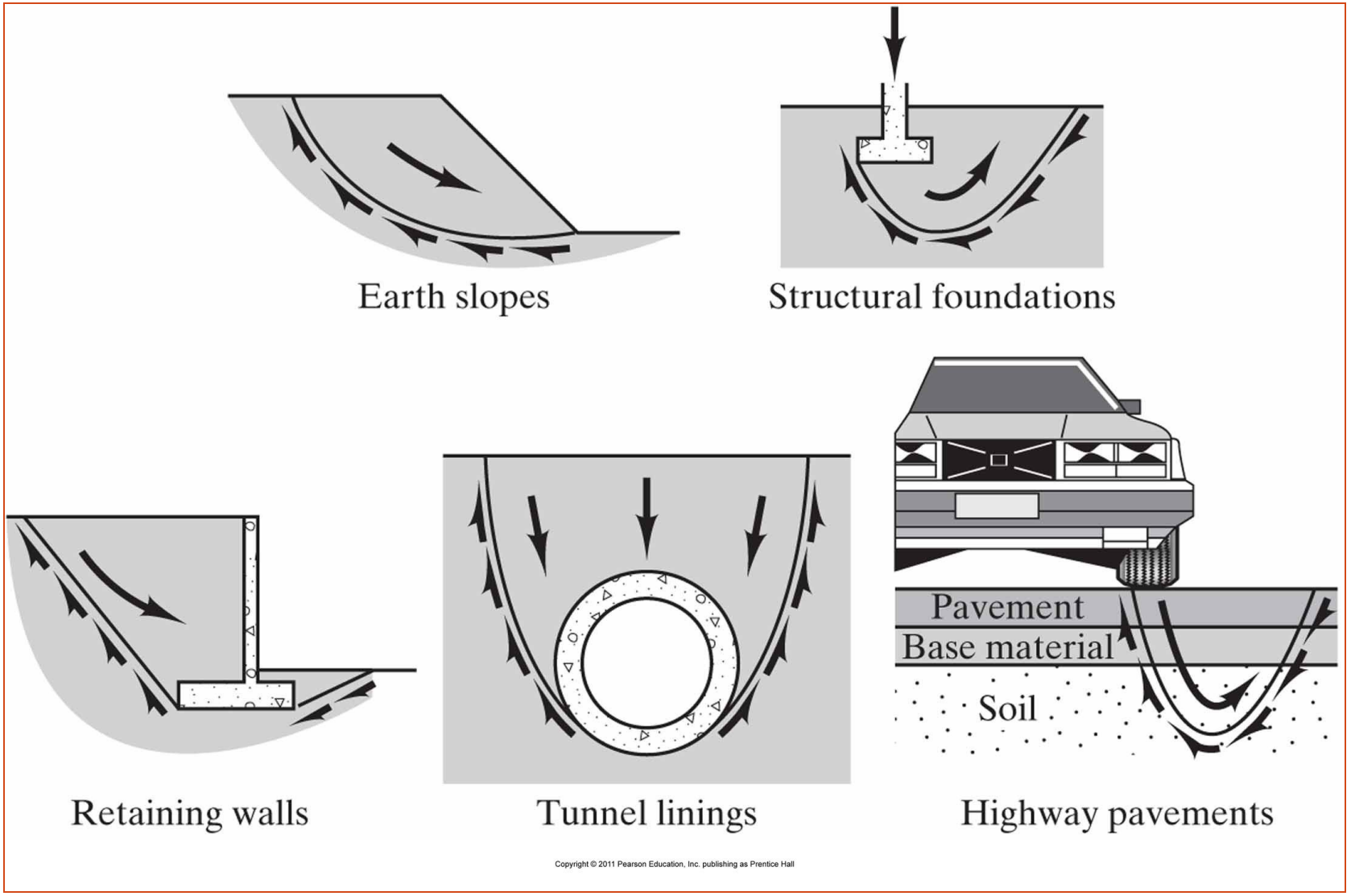

Figure Typical applications of strength analyses in soils.

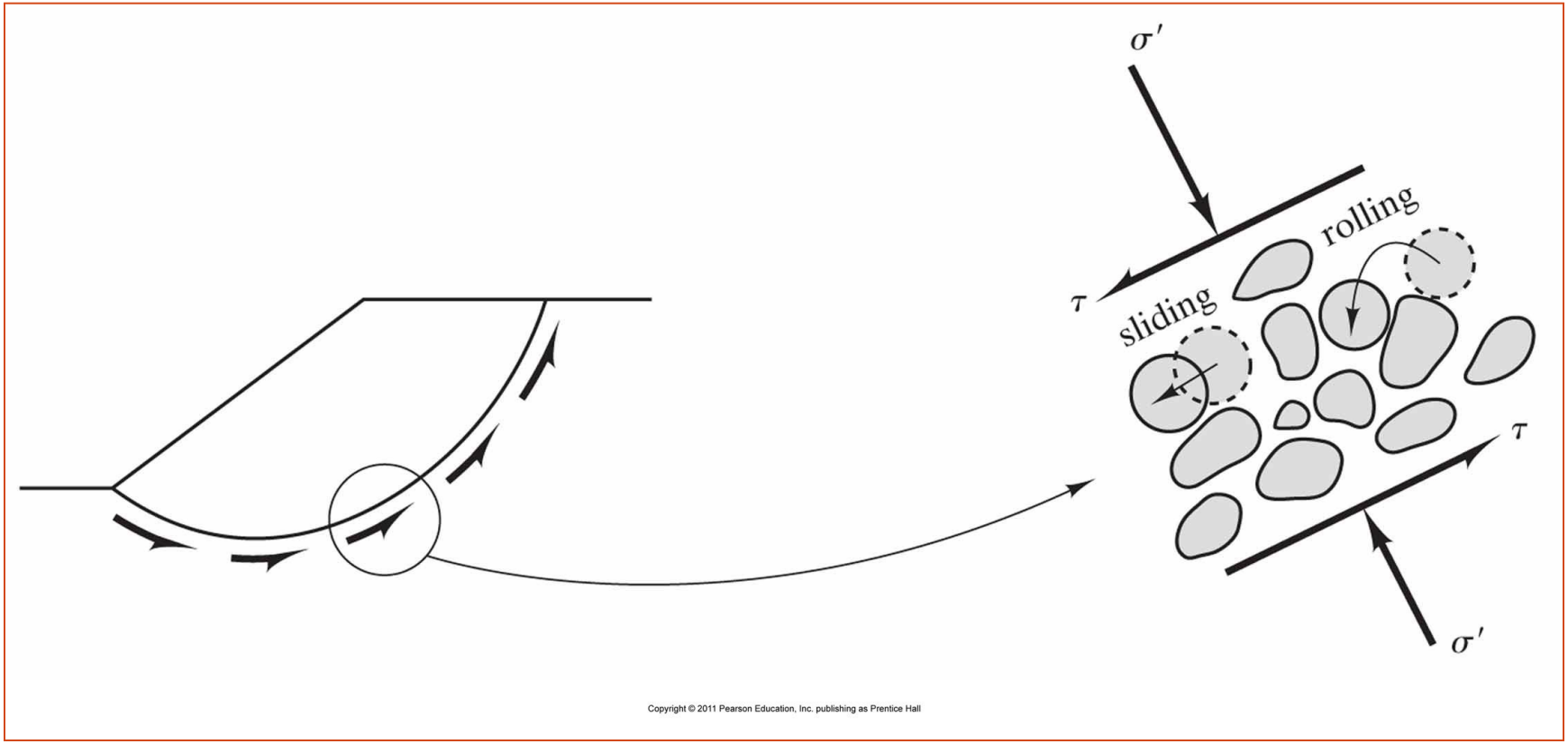

Figure 12.2 Shear failures occur in a soil when the shear stresses are large enough to make the particles roll and slide past each other.

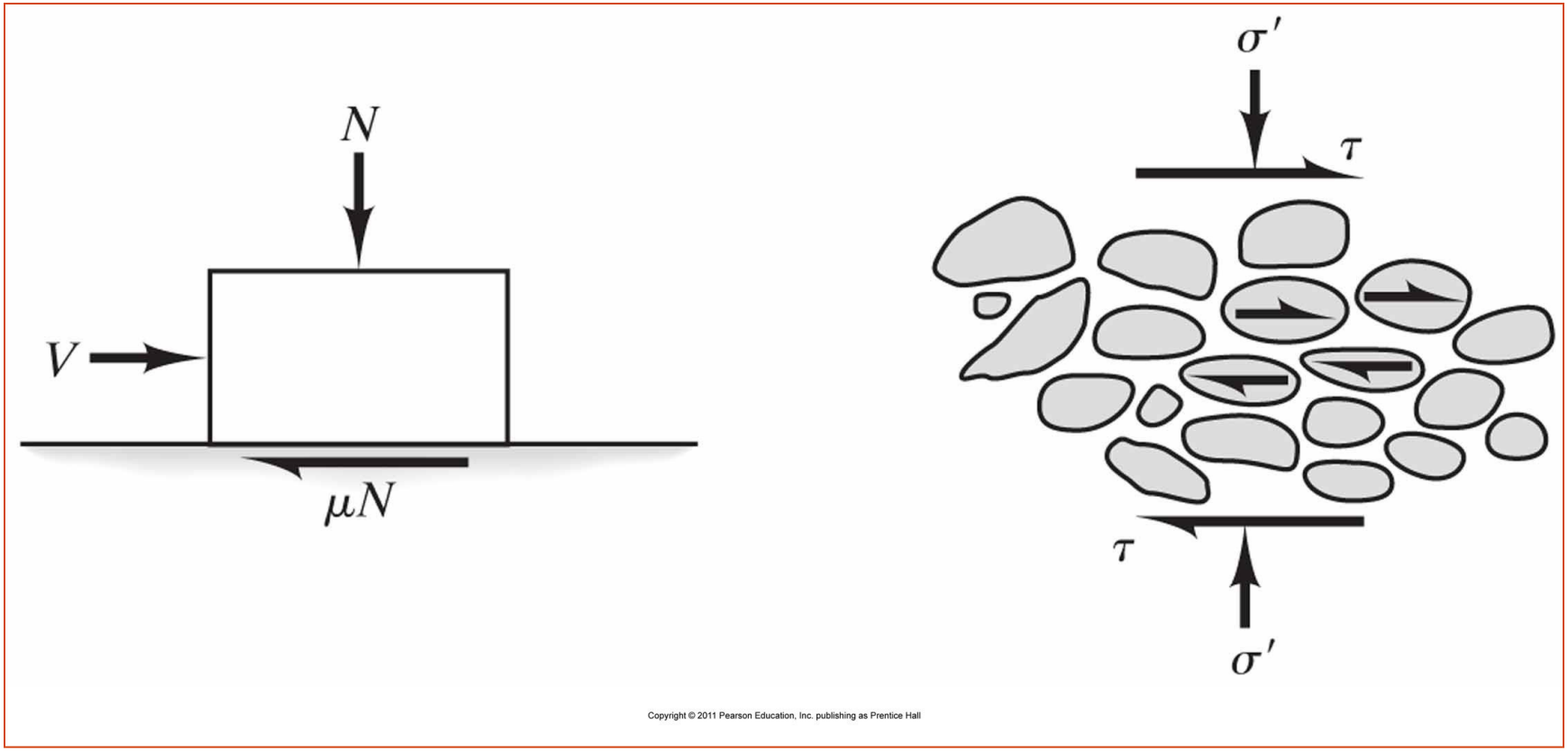

Figure Comparison between friction on a sliding block and frictional strength in soil.

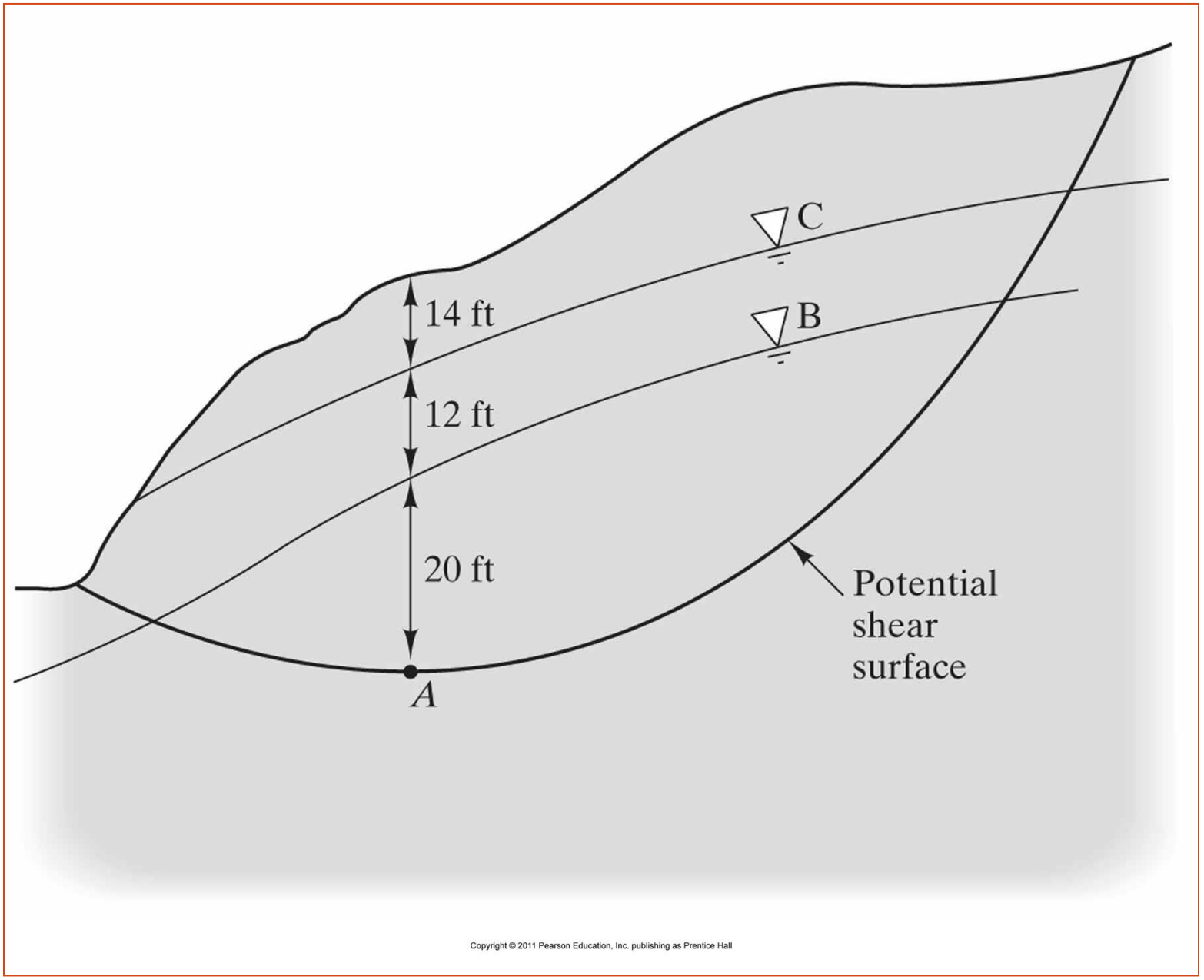

Figure Cross-section of a potential landslide.

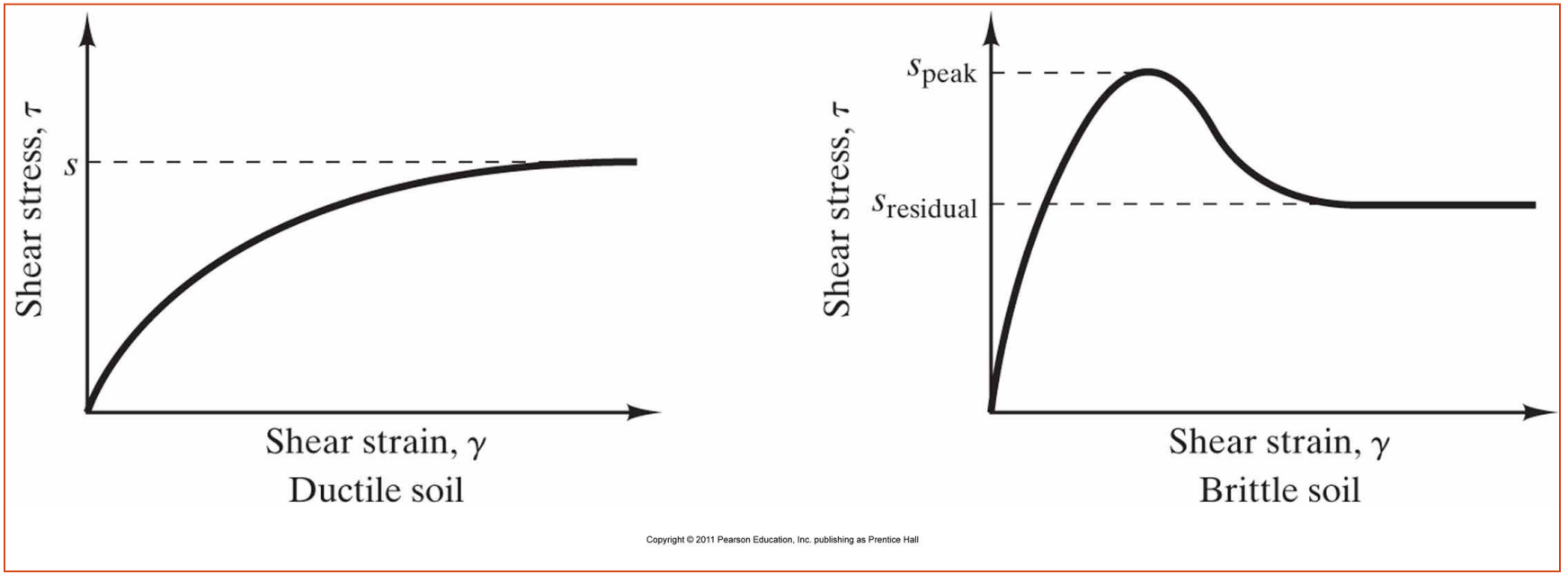

Figure Shear stress-strain curves of soil, and definitions of failure.

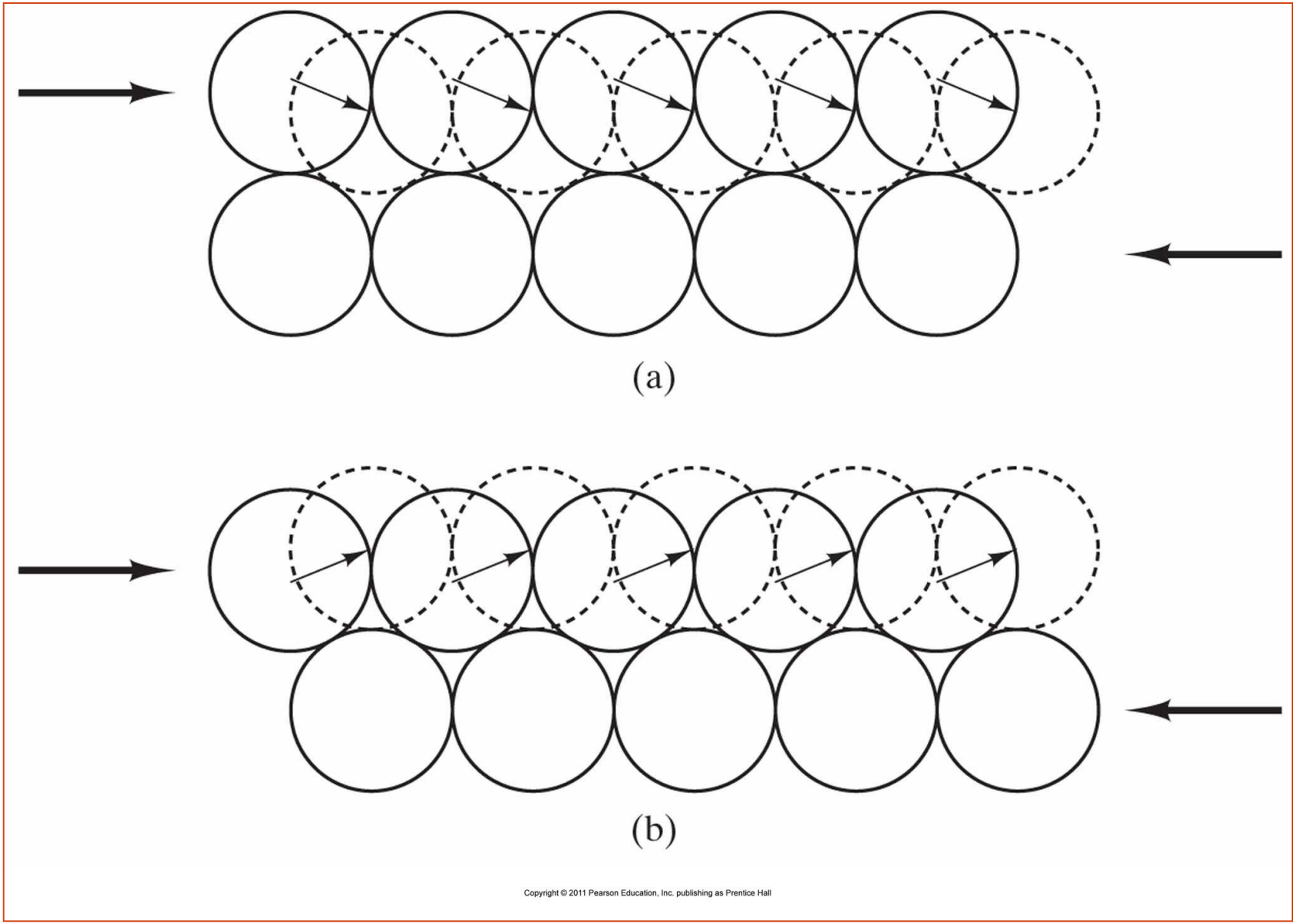

Figure Shear-induced volume change: (a) loose soil tends to contract during shear; (b) dense soil tends to dilate during shear.

11.1 MOHR COULOMB FAILURE CRITERION

MOHR COULOMB FAILURE CRITERION

- Mohr (1900) presented a theory for rupture in materials that contended that a material fail because of a critical combination of normal stress and shearing stress and not form either maximum normal or shear stress alone. Thus, the functional relationship between normal stress and shear stress on a failure plane can be expressed in the following form Eq. (11.1)

- $$\tau_f = f(\sigma) \qquad (11.1)$$

- The failure envelope defined by Eq. (11.1) is a curved line. For most soil mechanics problems, it is sufficient to approximate the shear stress on the failure plane as a line function of the normal stress (Coulomb, 1776). This linear function can be written as Eq. (11.2)

- $$\tau_f = c + \sigma \tan\phi \quad (11.2)$$

Where:

- c= cohesion
- Φ= angle of internal friction
- σ=normal stress on the failure plane
- τ_f=shear strength

- The preceding equation is called the Mohr Coulomb failure criterion.
- In saturated soil, the total normal stress at a point is the sum of the effective stress ($\boldsymbol{\sigma'}$) and pore water pressure ($\boldsymbol{u}$), or:

- $\sigma = \sigma' + u$

- The effective stress ***σ'*** is carried by the soil solids. The Mohr-Coulomb failure criterion, expressed in terms of effective stress, will be of the form Eq. (11.3)

- $$\tau_f = c' + \sigma' \tan \phi' \quad (11.3)$$

Where:

- *c'*=cohesion
- ϕ'=friction angle, based on effective stress.

- Thus Eqs. (11.2) and (11.3) are expressions of shear strength based on total stress and effective stress. The value of ***c'*** for sand and inorganic silt is "0". For normally consolidated clays, ***c'*** can be approximated to "0". Overconsolidated clays have values of ***c'*** that are greater than "0". The angle of friction,**ϕ'**, is sometimes referred to as the drained angle of friction.

- Typical values of for some granular soil are given in ***table 11.1.***

- The significance of Eq. (11.3) can be explained by referring to ***Figure 11.1***, which shows an elemental soil mass. Let the effective normal stress and the shear stress on the plane ***ab*** be ***σ'*** and ***τ***, respectively. ***Figure 11.1b*** shows the plot of the failure envelope define by Eq. (11.3).

- If the magnitudes of ***σ'*** and ***τ*** on plane ***ab*** are such that the plot as point ***A*** in ***Figure 11.b***, shear stress on plane ***ab*** plot as point ***B*** (which falls on the failure envelope), shear failure will occur along that plane. A state of stress on a plane represented by point ***C*** cannot exist, because it plots above the failure envelope, and shear failure in a soil would have occurred already.

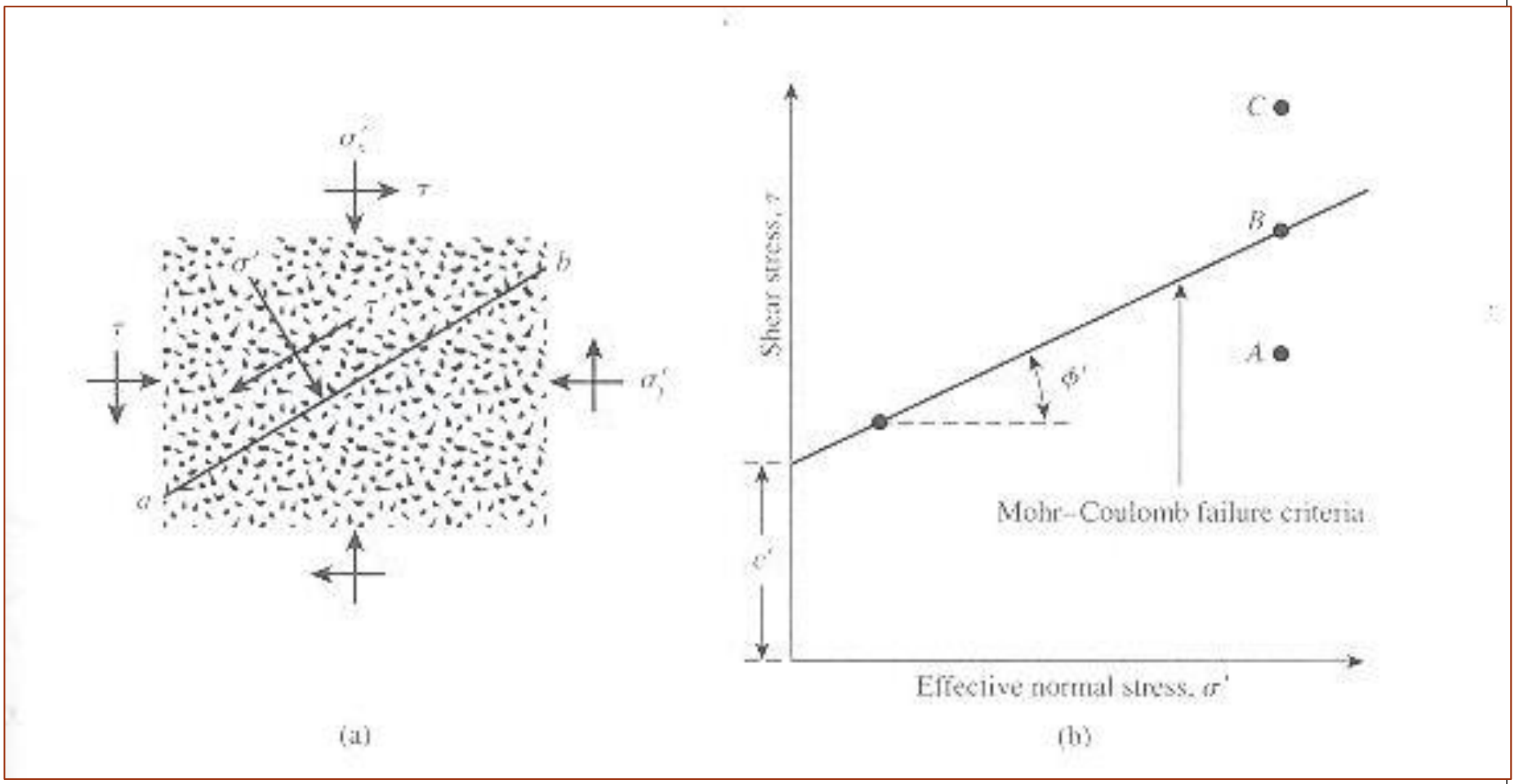

Figure 11.1 Mohr- Coulomb failure criterion

11.2 INCLINATION OF THE PLANE OF FAILURE CAUSED BY SHEAR

INCLINATION OF THE PLANE OF FAILURE CAUSED BY SHEAR

- As stated by the Mohr Coulomb failure criterion, failure from shear will occur when the shear stress on a plane reaches a value given by Eq. (11.3). To determine the inclination of the failure plane with the major principal plane, refer to ***Figure 11.2***, where σ'_1 σ'_3 are, respectively, the major and minor effective principal stresses. The failure plane ***EF*** makes an angle **θ** with the major principal plane.

- To determine the angle θ and the relationship between σ'_1 and σ'_3, refer to ***Figure 11.3***, which is a plot of Mohr's circle for the state of stress shown in ***Figure 11.2,*** and the radial line ***ad*** defines the failure envelope defined by the relationship .

$$\tau_f = c' + \sigma' \tan \phi'$$

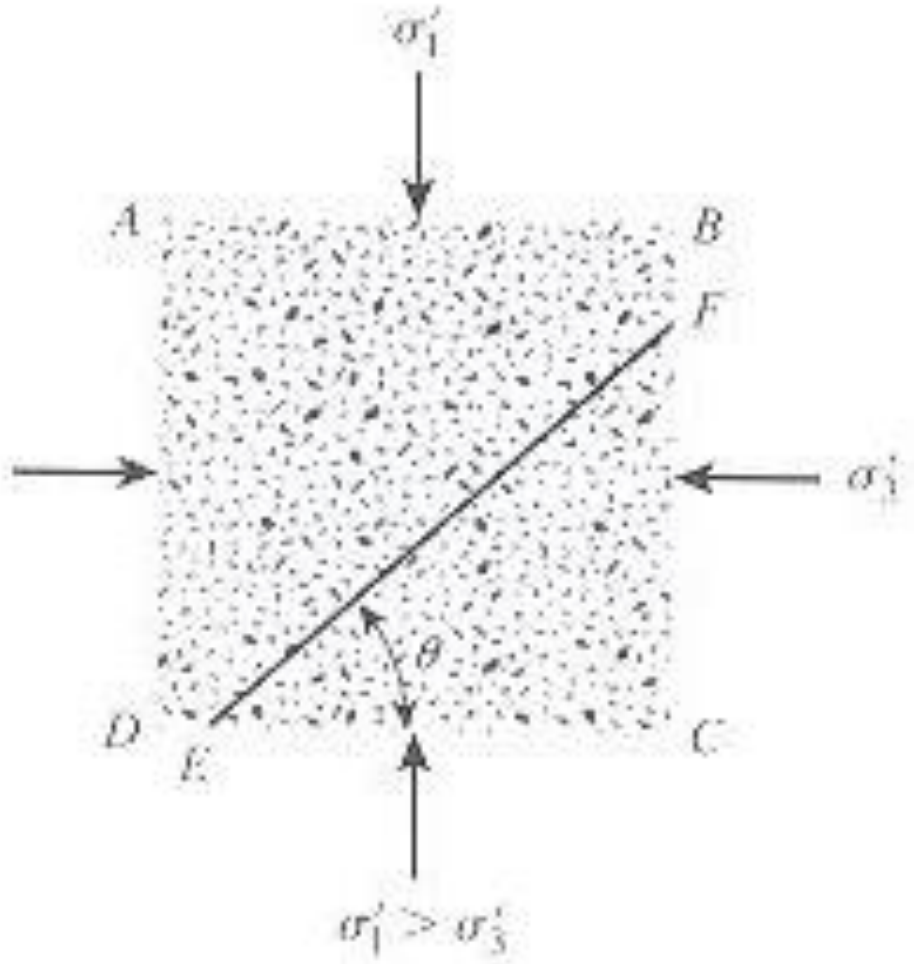

Figure 11.2 Inclination of failure plane in soil with major principal plane

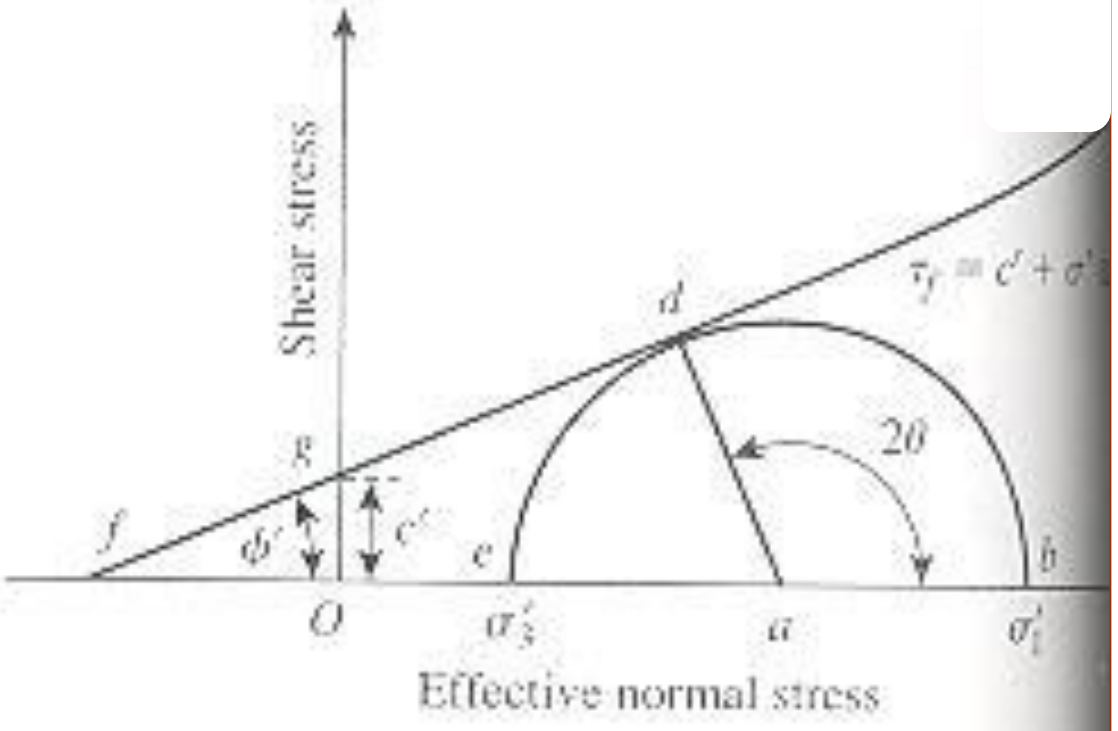

Figure 11.3 Mohr's circle and failure envelope

- The radial line ***ab*** defines the major principal plane (***CD*** in ***figure 11.2***), and the radial line ***ad*** defines the failure plane (***EF*** in ***Figure 11.2***). It can be shown that

$$\angle bad = 2\theta = 90 + \phi'$$

- Or Eq. 11.4

$$\theta = 45 + \frac{\phi'}{2} \qquad (11.4)$$

- Again, from figure 11.3, Eq. 11.5

$$\frac{\overline{ad}}{\overline{fa}} = \sin\phi' \qquad (11.5)$$

- Eq. 11.6a

$$\overline{fa} = fO + Oa = c'\cot\phi' + \frac{\sigma'_1 + \sigma'_2}{2} \qquad (11.6a)$$

- Also Eq. 11.6 b

$$\overline{ad} = \frac{\sigma'_1 - \sigma'_3}{2} \qquad (11.6b)$$

- Substituting Eqs. (11.6a) and (11.6b) into Eq. (11.5), we obtain

$$\sin\phi' = \frac{\frac{\sigma'_1 - \sigma'_2}{2}}{c'\cot\phi' + \frac{\sigma'_1 + \sigma'_3}{2}}$$

- Or, Eq. (11.7)
- $$\sigma'_1 = \sigma'_3\left(\frac{1+\sin\phi'}{1-\sin\phi'}\right) + 2c\left(\frac{\cos\phi'}{1-\sin\phi'}\right) \qquad (11.7)$$

- However,
- $$\frac{1+\sin\phi'}{1-\sin\phi'} = \tan^2\left(45 + \frac{\phi'}{2}\right)$$

- And

$$\frac{\cos\phi'}{1-\sin\phi'} = \tan\left(45 + \frac{\phi'}{2}\right)$$

- Thus Eq. (11.8)

$$\sigma'_1 = \sigma'_3 \tan^2\left(45 + \frac{\phi'}{2}\right) + 2c' \tan\left(45 + \frac{\phi'}{2}\right) \qquad (11.8)$$

- An expression similar to Eq. (11.8) could be derived using Eq. 11.2 (that is, total stress parameters ***c*** and **ϕ**),or Eq. (11.9)

$$\sigma_1 = \sigma_3 \tan^2\left(45 + \frac{\phi}{2}\right) + 2c \tan\left(45 + \frac{\phi}{2}\right) \qquad (11.9)$$

11.3 LABORATORY TEST FOR DETERMINATION OF SHEAR STRENGTH PARAMETERS

LABORATORY TEST FOR DETERMINATION OF SHEAR STRENGTH PARAMETERS

- There are several laboratory methods now available to determine the shear strength parameters (i.e.,c,ϕ,c', ϕ')of various soil specimens in the laboratory. They are as follows:

  - Direct shear test
  - Triaxial test
  - Direct simple shear test
  - Plane strain triaxial test
  - Torsional ring shear test

- The direct shear test and the triaxial test are the two commonly used techniques for determining the shear strength parameters.

TABLE Shear Strength Evaluation for Static Sability Analysis

Scenario	Soil Type	Drainage Condition	Analysis Type	Shear Strength Parameters	Lab Test Method
Short-term (End-of-construction)	Sands and gravels	Drained	Effective stress	c' and ϕ'	• Drained direct shear • CU with pore pressure measurements • CD
	Clays	Undrained	Total stress	$c_T = s_u$ $\phi_T = 0$	• Undrained direct shear • UU • CU
Long-term	Sands and gravels	Drained	Effective stress	c' and ϕ'	• Drained direct shear • CU with pore pressure measurements • CD
	Clays	Drained	Effective stress	c' and ϕ'	• Drained direct shear • CU with pore pressure measurements • CD

11.4 DIRECT SHEAR TEST

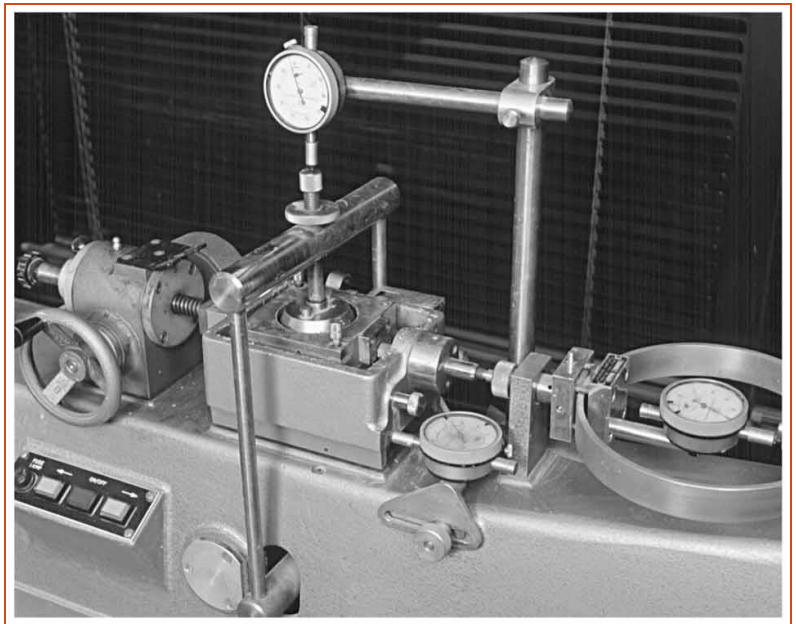

(a)

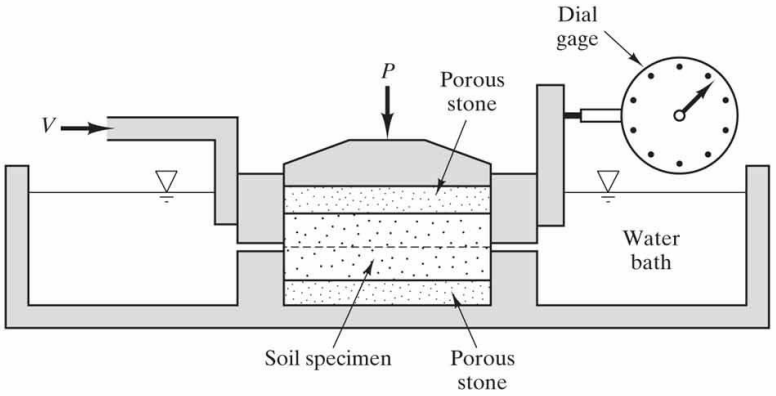

(b)

Figure (a) A direct shear machine. The specimen is inside the shear box, directly below the upper dial gage; (b) cross-section through shear box showing the specimen and shearing action.

DIRECT SHEAR TEST

- The direct shear test is the oldest and simplest form of shear test arrangement. A diagram of the direct shear test apparatus is shown in ***Figure 11.4***.

- The test equipment consists of a metal shear box in which the soil specimen is placed. The soil specimen may be square or circular in plan. The size of the specimens generally used is about 51 *mm* x 51 *mm* or 102 *mm* x 102*mm* across and about *25 mm* high.

- The box is split horizontally into halves. Normal force on the specimen is applied form the top of the shear box. The normal stress on the specimens can be as great as 1050 *kN/m^2.*

- Shear force is applied by moving one half of the box relative to the other to cause failure in the soil specimen.

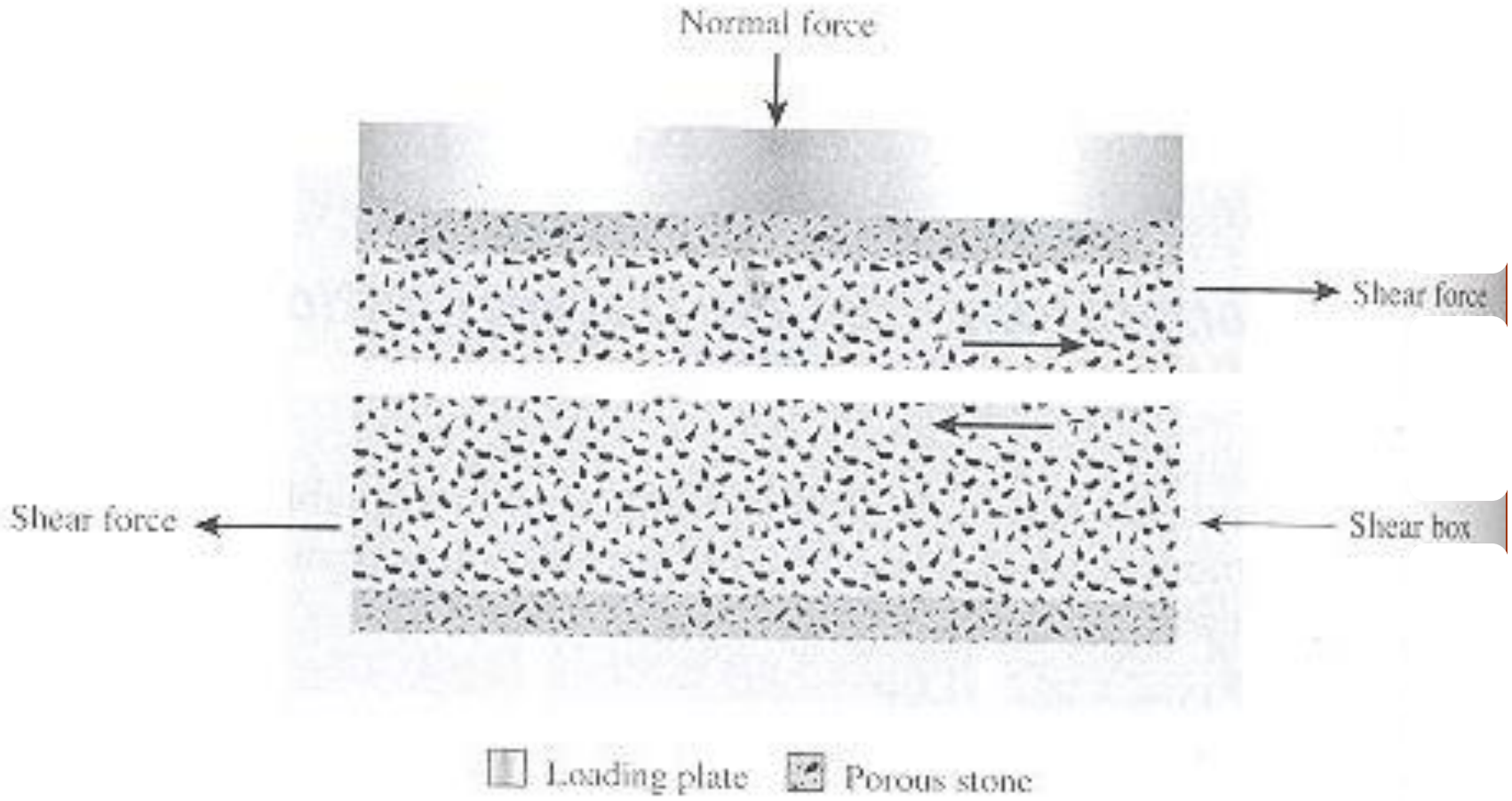

Figure 11.4 Diagram of direct shear test arrangement

- Depending on the equipment, the shear test can be either stress controlled or strain controlled. In stress-controlled test, the shear force is applied in equal increments until the specimen fails. The failure occurs along the plane of split of the shear box. After the application of each incremental load, the shear displacement of the top half of the box is measured by a horizontal dial gauge. The change in the height of the specimen (and thus the volume change of the specimen) during the test can be obtained from the readings of a dial gauge that measures the vertical movement of the upper loading plate.

- In strain controlled tests, a constant rate of shear displacement is applied to one half of the box by a motor that acts through gears. The constant rate of shear displacement is measured by a horizontal dial gauge.

- The resisting shear force of the soil corresponding to any shear displacement can be measured by a horizontal proving ring or load cell. The volume change of the specimen during the test is obtained in a manner similar to that in the stress controlled tests.

- ***Figure 11.5*** shows a photograph of strain controlled direct shear test equipment.

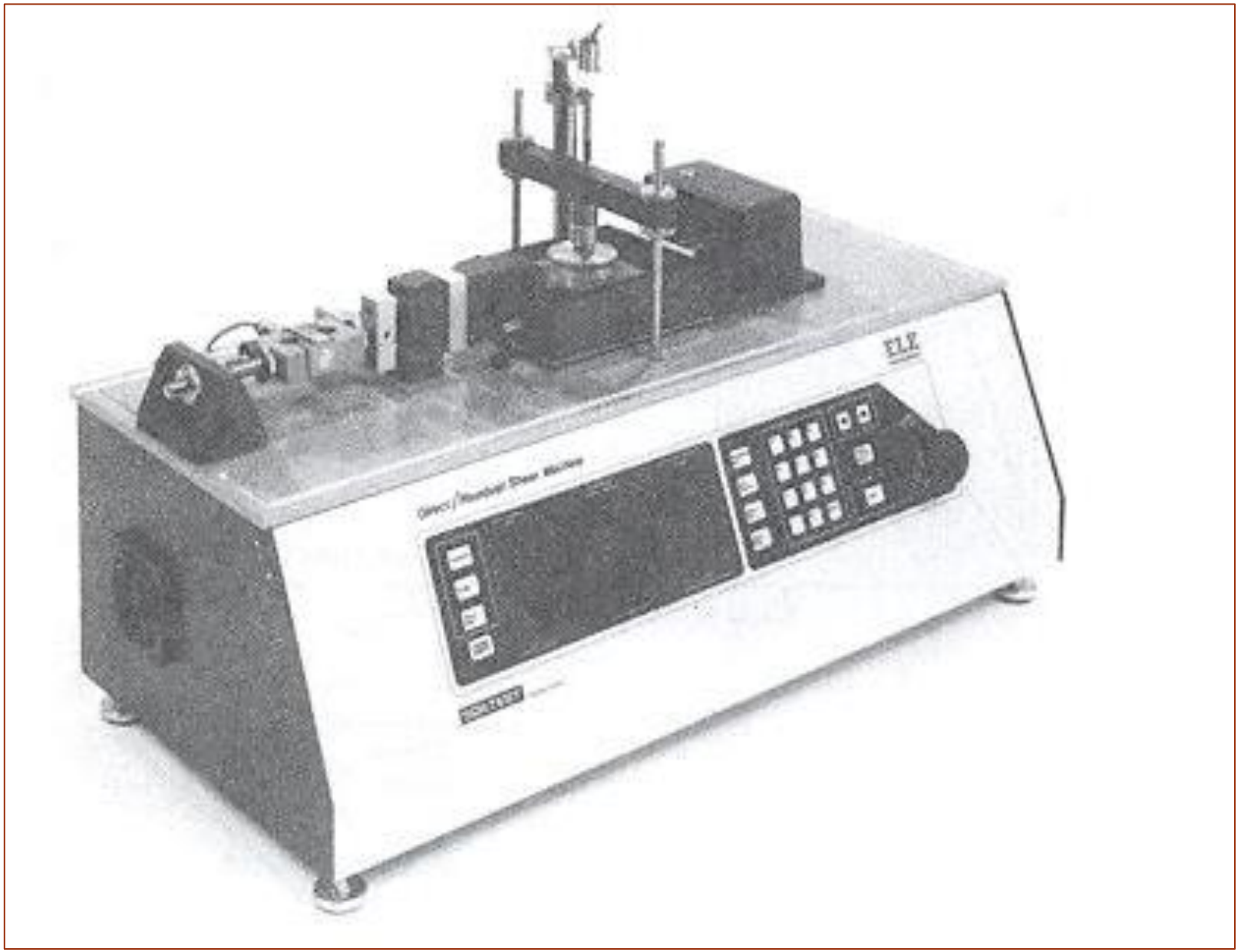

Figure 11.5 Strain-controlled direct shear test equipment (Courtesy of Soiltest, Inc., Lake Bluff, Illinois)

- The advantage of the strain controlled test is that in the case of dense sand, peak shear resistance (that is, at failure) as well as lesser shear resistance (that is, at a point after failure called ultimate strength) can be observed and plotted.

- In stress controlled tests, only the peak shear resistance can be observed and plotted. Note that the peak shear resistance in stress controlled test can be only approximated because failure occurs at a stress level some where between the prefailure load increment and the failure load increment.

- Nevertheless, compared with strain controlled tests, stress controlled tests probably model real field situations better.

- For a given test, the normal stress can be calculated as Eq. (11.10)

- ***Figure 11.6*** shows a typical plot of shear stress and change in the height of the specimen against shear displacement for dry loose and dense sands. These observations were obtained from a strain controlled test. The following generalizations can be developed from ***Figure 11.6*** regarding the variation of resisting shear stress with shear displacement:

1. In loose sand, the resisting shear stress increases with shear displacement until a failure shear stress of τ_f is reached. After that, the shear resistance remains approximately constant for any further increase in the shear displacement.

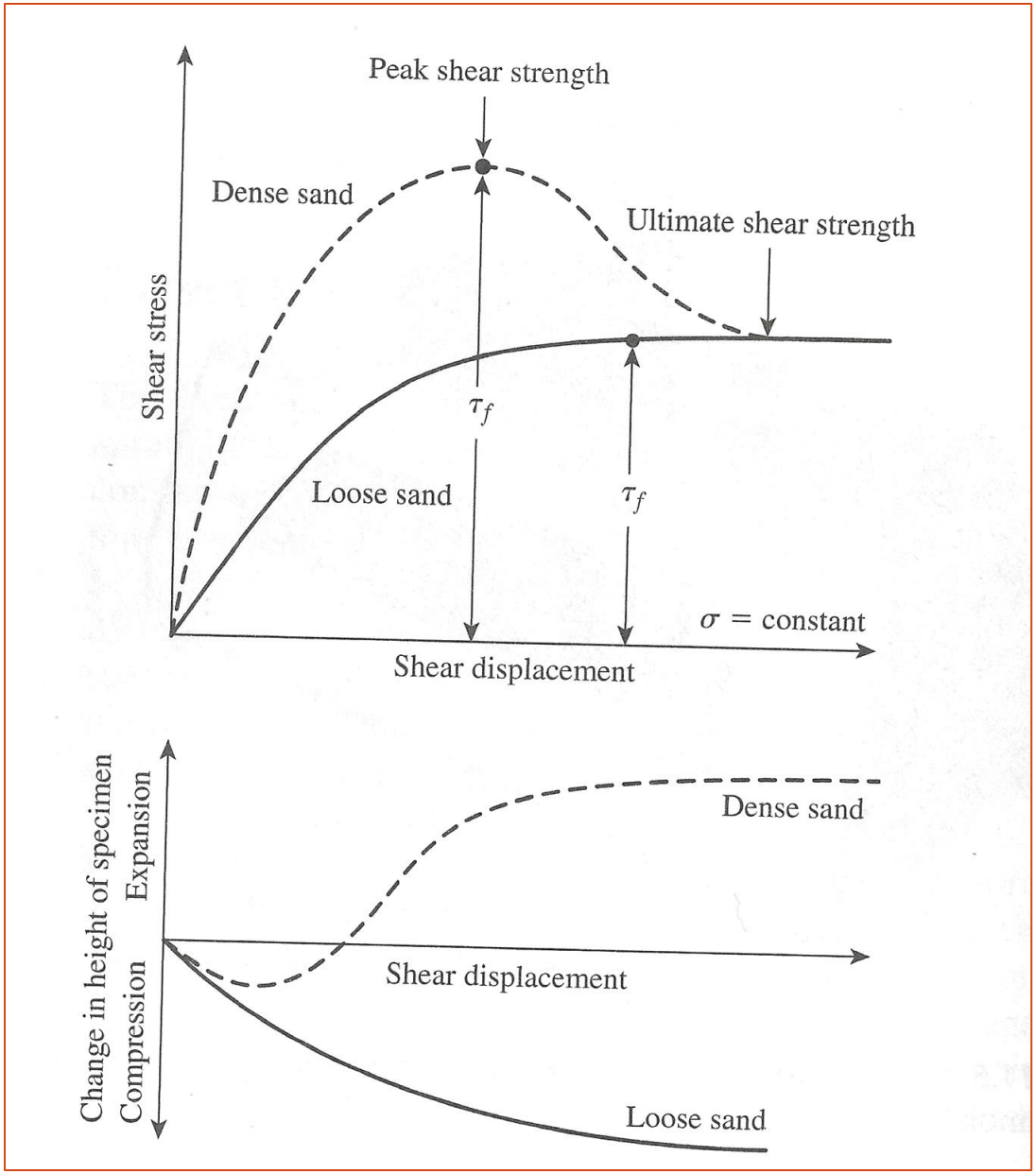

Figure 11.6 Plot of shear stress and change in height of specimen against shear displacement for loose and dense dry sand (direct shear test)

2. In dense sand, the resisting shear stress increases with shear displacement until it reaches a failure stress of τ_f . This τ_f is called the peak shear strength. After failure stress is attained, the resisting shear stress gradually decreases as shear displacement increases until it finally reaches a constant value called the ultimate shear strength.

It is important to note that, in dry sand,

- $\sigma = \sigma'$
- And
- $c' = 0$

3. Direct shear test are repeated on similar specimens at various normal stresses. The normal stresses and the corresponding values of τ_f obtained from a number of test are plotted on a graph form which the shear strength parameters are determined.

- ***Figure 11.7*** shows such a plot for tests on a dry sand. The equation for the average line obtained from experimental results is Eq. (11.12)

- $$\tau_f = \sigma' \tan \phi' \qquad (11.12)$$

- So, the friction angle can be determined as follows:

- $$\phi' = \tan^{-1}\left(\frac{\tau_f}{\sigma'}\right)$$

- It is important to note that in situ cemented sands may show a ***c'*** intercept.

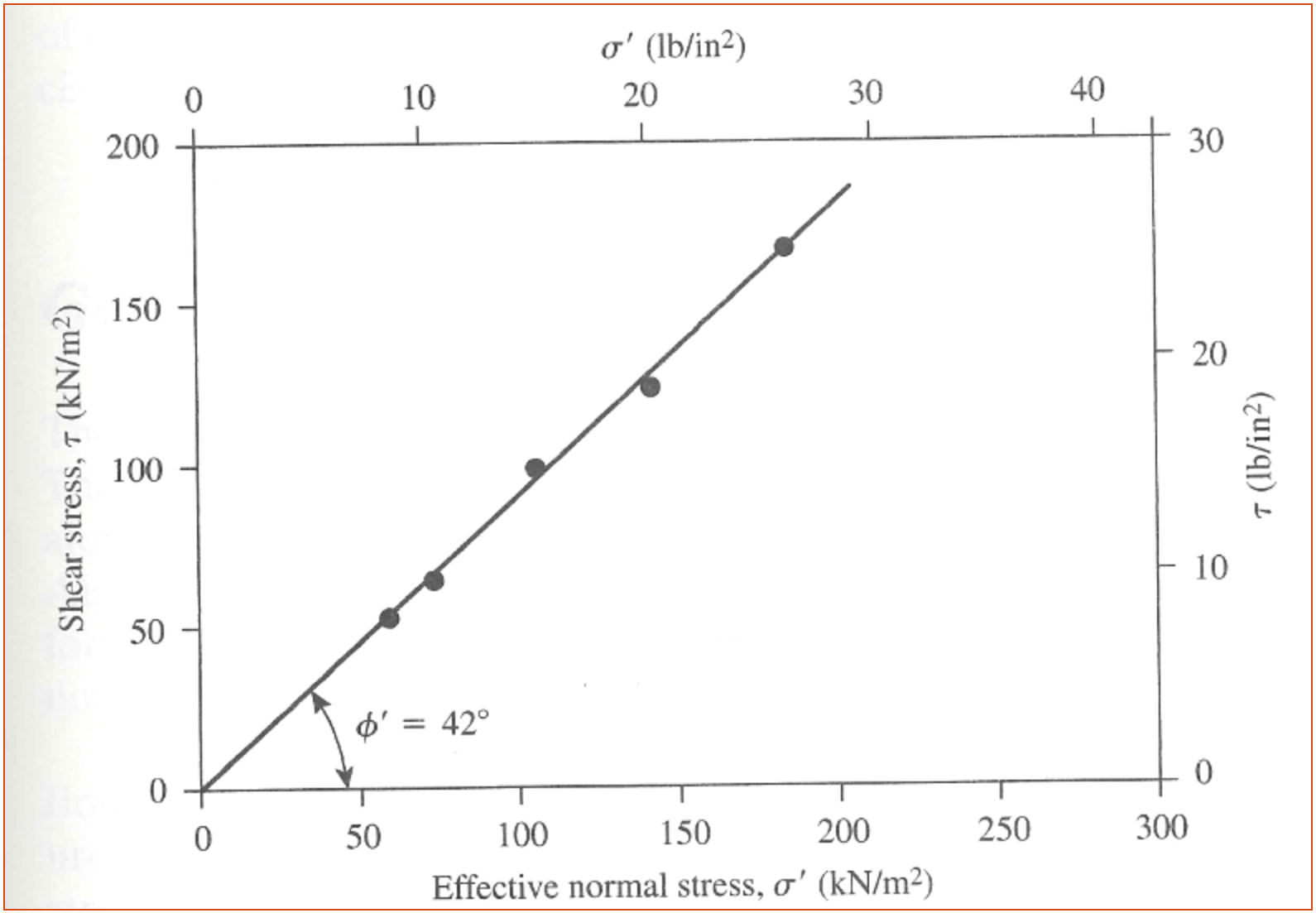

Figure 11.7 Determination of shear strength parameters for a dry sand using the results of direct shear test

11.5 DRAINED DIRECT SHEAR TEST ON SATURATED SAND AND CLAY

DRAINED DIRECT SHEAR TEST ON SATURATED SAND AND CLAY

- In the direct shear test arrangement, the shear box that contains the soil specimen is generally kept inside a container that can be filled with water to saturate the specimen.

- A drained test is made on a saturated soil specimen by keeping the rate of loading slow enough so that the excess pore water pressure generated in the soil is dissipated completely by drainage. Pore water from the specimen is drained through two porous stones. (see ***Figure 11.4***)

- Because the hydraulic conductivity of sand is high, the excess pore water pressure generated due to loading (normal and shear) is dissipated quickly. Hence, for an ordinary loading rate, essentially full drainage conditions exist.
- The friction angle, ϕ' , obtained form a drained from a drained direct shear test of saturated sand will be the same as that for a similar specimen of dry sand.

- The hydraulic conductivity of clay is very small compared with. When a normal load is applied to a clay soil specimen, as sufficient length of time must elapse for full load consolidation that is , for dissipation of excess pore water pressure. For this reason, the shearing load must be applied very slowly. The test may last form two to five days.

- ***Figure 11.8*** shows the results of a drained direct shear test on an overconsolidated clay.

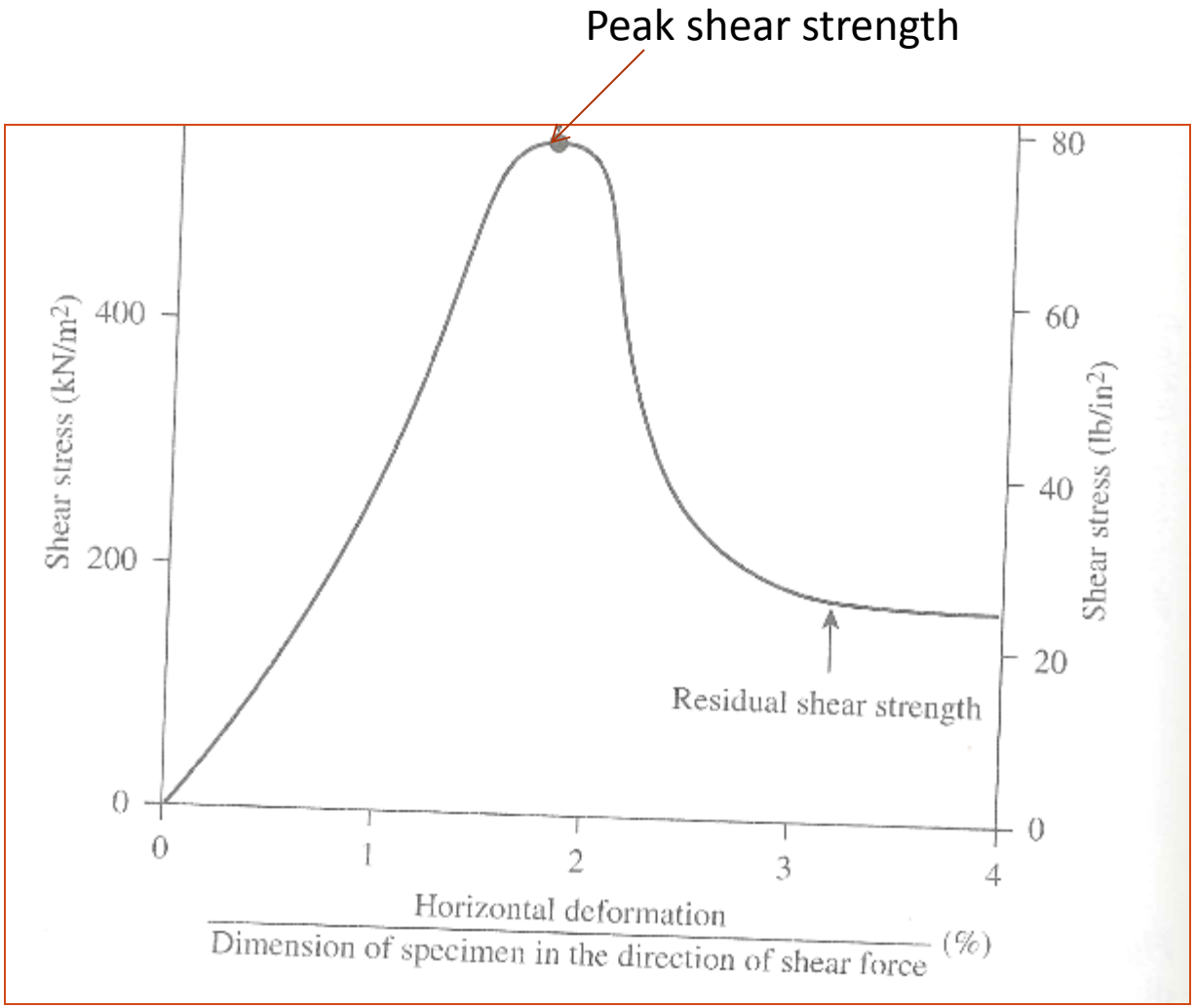

Figure 11.8 Results of a drained direct shear test on an overconsolidated clay (Note: Residual shear strength in clay is similar to ultimate shear strength in sand (see *figure 11.6)*

- ***Figure 11.9*** shows the plot of τ_f against ***σ'*** obtained form a number of drained direct shear tests on a normally consolidated clay and an overconsolidated. Note that the value ***c'=0*** for a consolidated clay.

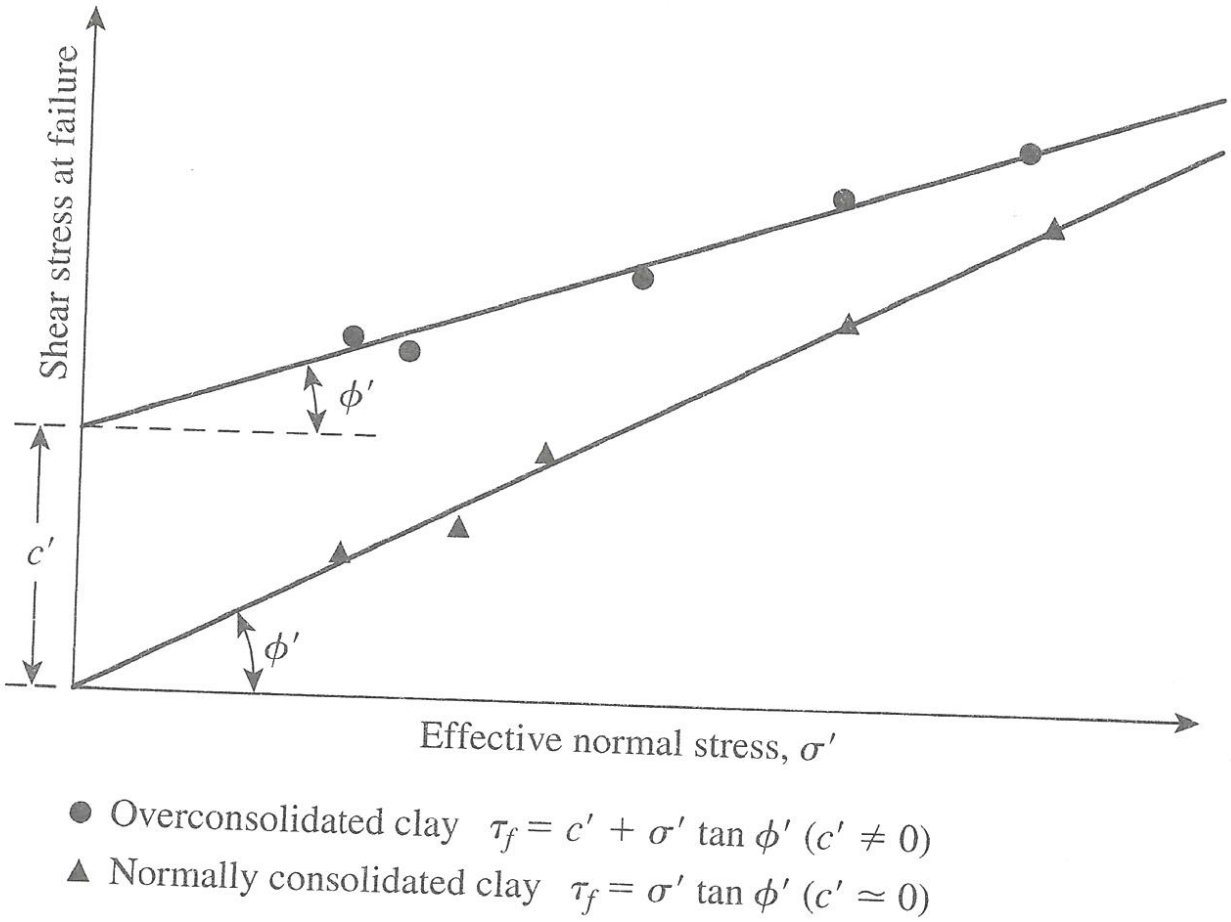

Figure 11.9 Failure envelope for clay obtained from drained direct shear test

11.7 CRITICAL VOID RATIO

CRITICAL VOID RATIO

- It has been shown in ***Figure 11.6*** that, during a shear test in dense sand, there is the tendency for the specimen to dilate as the test progresses. Similarly, in sand, the volume gradually decreases. An increase of decrease in volume means a change in the void ratio of the soil.

- The nature of the change of void ratio with shear displacement for loose and dense sand is shown in ***Figure 11.15***. The void ratio for which the change in volume remains constant during shearing is called the critical void ratio. The concept of critical void ratio was first introduced in 1938 by A. Casagrande.

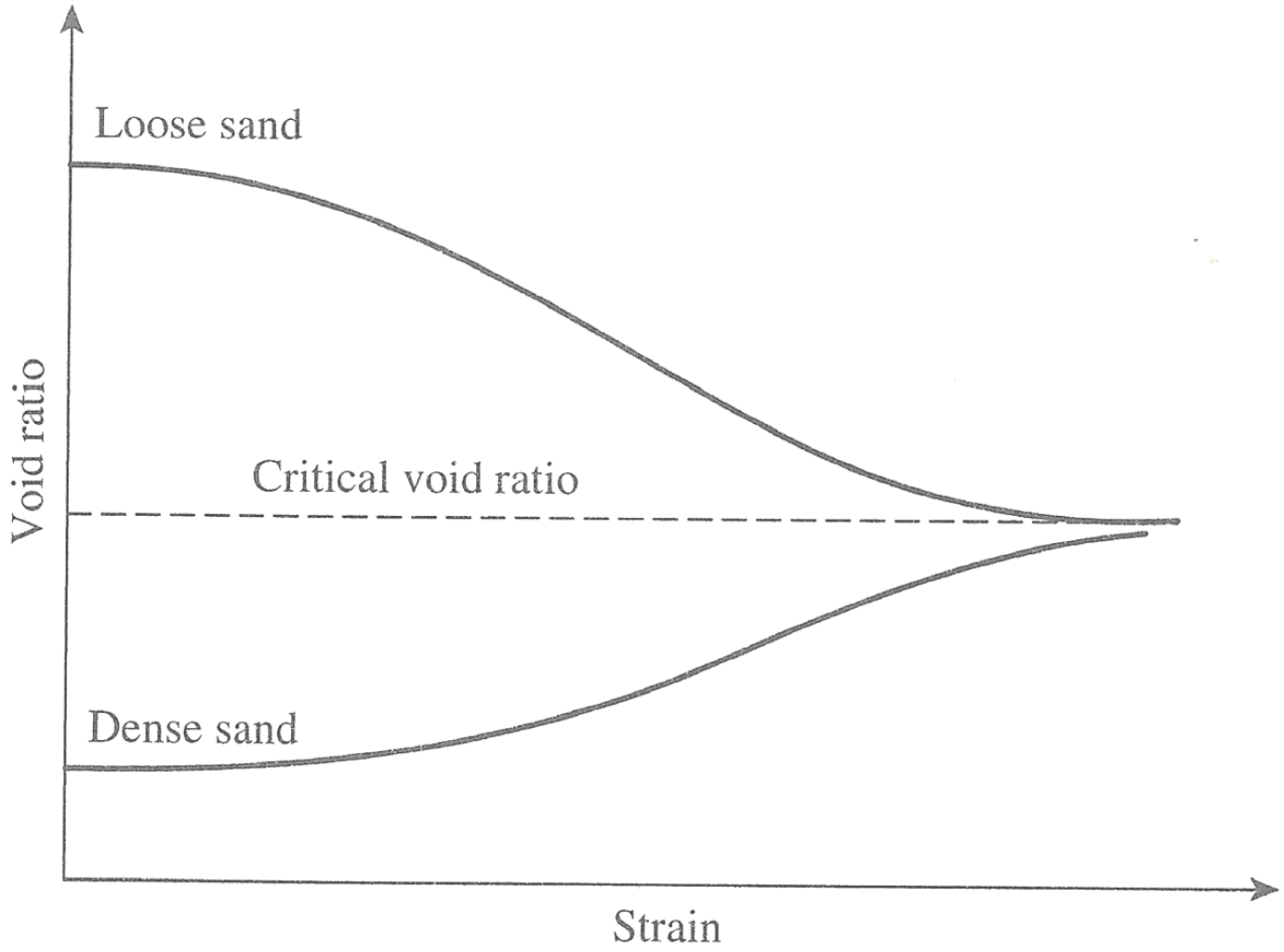

Figure 11.15 Definition of critical void ratio

EXAMPLE 11.1

- Direct shear test were performed on a dry, sandy soil. The size of the specimen was 2 *in* x2 *in* x 0.75 *in*.
- Test results are as follows:

Test no.	Normal force (lb)	Normal[a] stress $\sigma = \sigma'$ (lb/ft^2)	Shear force at failure (lb)	Shear stress[b] at failure τ_f (lb/ft^2)
1	20	720	12.0	432.0
2	30	1080	18.3	658.8
3	70	2520	42.1	1515.6
4	100	3600	60.1	2163.6

- Find the shear stress parameters.

SOLUTION

- The shear stresses, τf, obtained from the test are plotted against the normal stresses in ***figure 11.16***. From which $c'=0$, $\phi'=32°$.

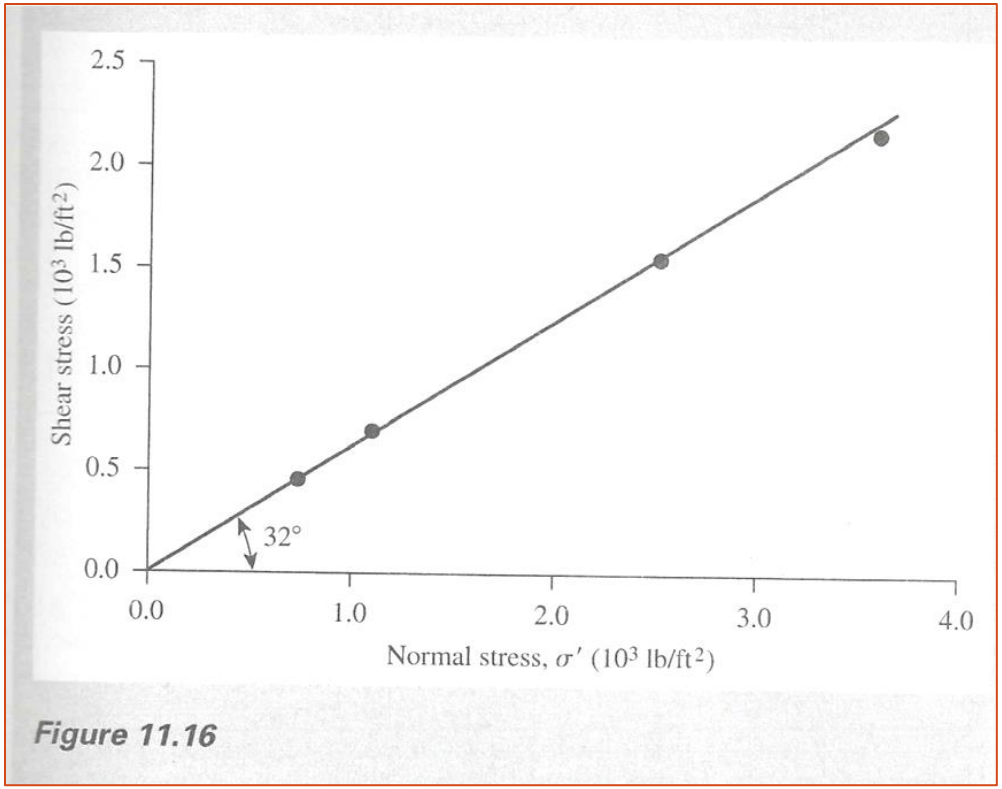

Figure 11.16

EXAMPLE 11.2

- Following are the results of fourdrained direct shear test on an overconsolidated clay:

  - Diameter of specimen=50*mm*
  - Height of specimen=25*mm*
  - Determine the relationships for peak shear strength (τ_f) and residual shear strength (τ_r).

Test no.	Normal force, N (N)	Shear force at failure, S_{peak} (N)	Residual shear force, $S_{residual}$ (N)[a]
1	150	157.5	44.2
2	250	199.9	56.6
3	350	257.6	102.9
4	550	363.4	144.5

[a] See Figure 11.8

SOLUTION

- Ares of the specimen (***A***)

- $A = \frac{\pi}{4}\left(\frac{50}{1000}\right)^2 = 0.0019634 m^2$

- Now the following table can be prepared:

Test no.	Normal force, N (N)	Normal stress, σ' (kN/m²)	Peak shear force, S_{peak} (N)	$\tau_f = \frac{S_{peak}}{A}$ (kN/m²)	Residual shear force, $S_{residual}$ (N)
1	150	76.4	157.5	80.2	44.2
2	250	127.3	199.9	101.8	56.6
3	350	178.3	257.6	131.2	102.9
4	550	280.1	363.4	185.1	144.5

- The variations of τ_f and τ_r with σ' are plotted in ***figure 11.17***. from the plots we find that

- $peak\_strength: \tau_f\,(KN/m\text{^}2) = 40 + \sigma' \tan 27$

  $residual\_strength: \tau_r\,(KN/m\text{^}2) = \sigma' \tan 14.6$

- (Note: for all overconsolidated clays, the residual shear strength can be expressed as:

- $\tau_r = \sigma' \tan \sigma'_r$

- Where ϕ'_r =effective residual friction angle)

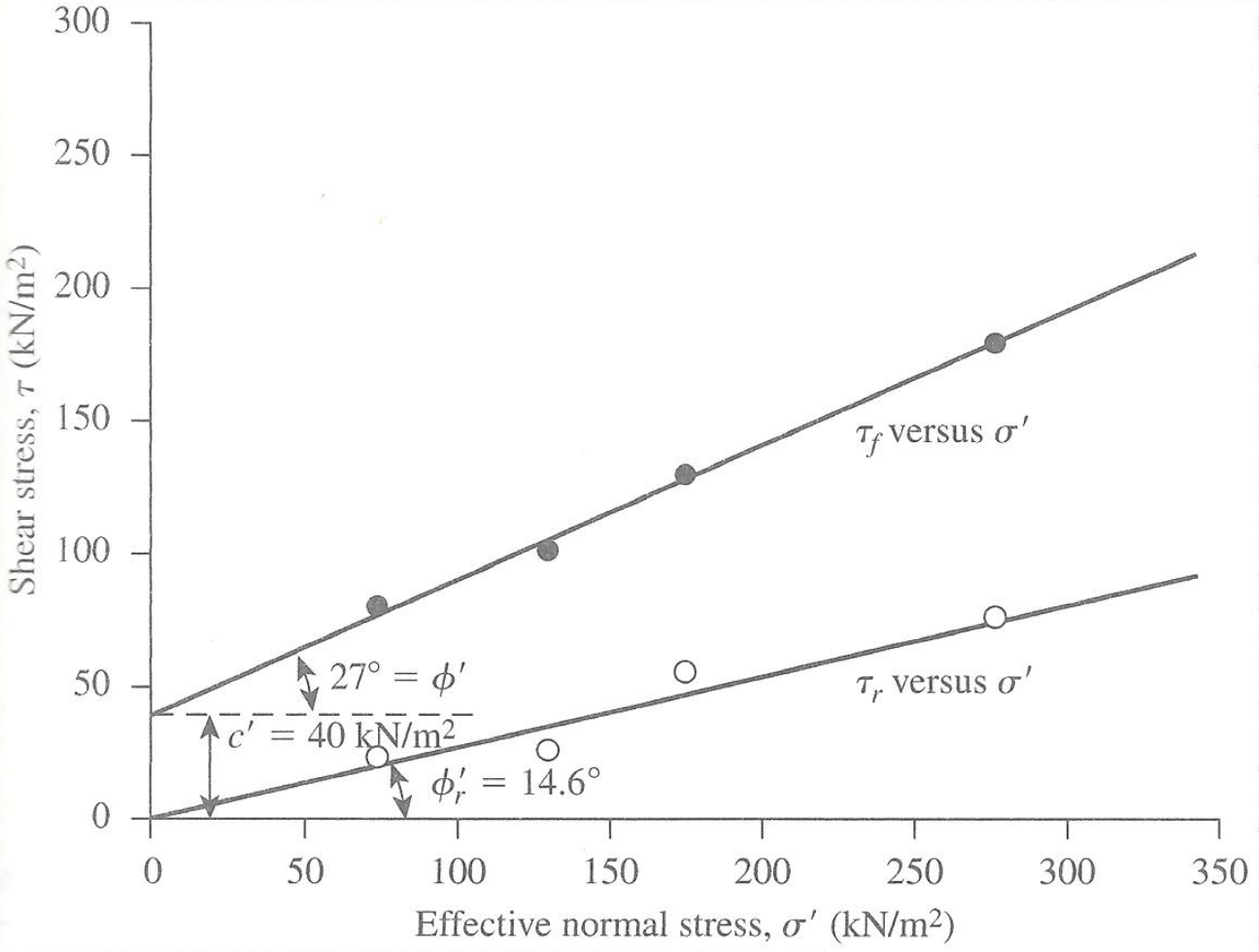

Figure 11.17 Variations of τ_f and τ_r with σ'

11.8 TRIAXIAL SHEAR TEST

TRIAXIAL SHEAR TEST

- The triaxial shear test is one the most reliable methods available for determining shear strength parameters. It is used widely for research and conventional testing. A diagram of the triaxial test layout is shown in ***Figure 11.18***.

- In this test, as soil specimen about 36mm in diameter and 76 mm long generally is used. The specimen is encased by a thin rubber membrane and placed inside a plastic cylindrical chamber that usually is filled with water or glycerine.

- The specimen is subjected to a confining pressure by compression of the fluid in the chamber. (Note: air is sometimes used as a compression medium). To cause shear failure in the specimen, one must apply axial stress through a vertical loading ram (some times called deviator stress). This stress can be applied in one of two ways:

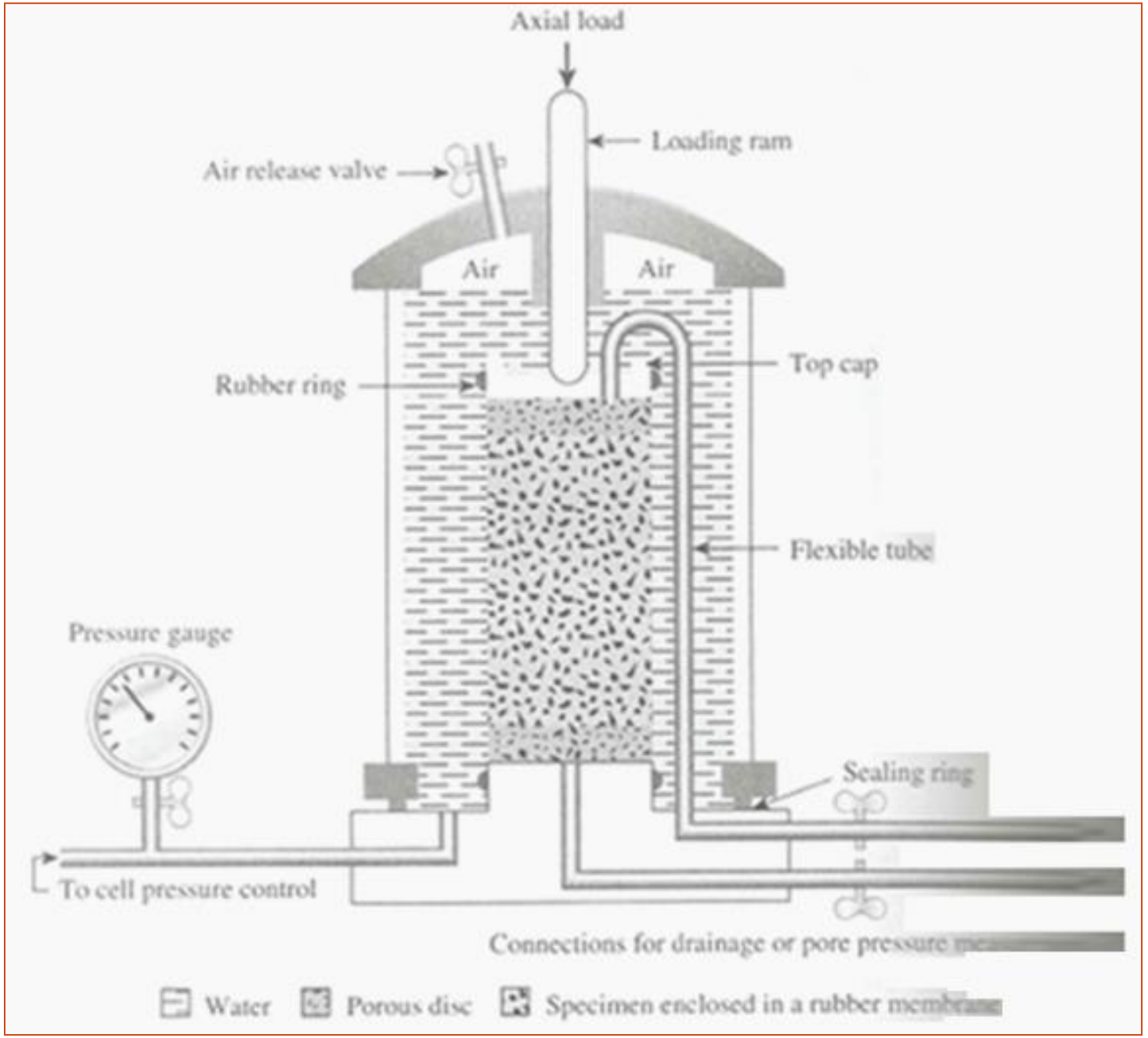

Figure 11.18 Diagram of triaxial equipment (After Bishop and Bjerrum, 1960)

Figure Photograph of a typical triaxial test system. (Courtesy of Geocomp Corp.)

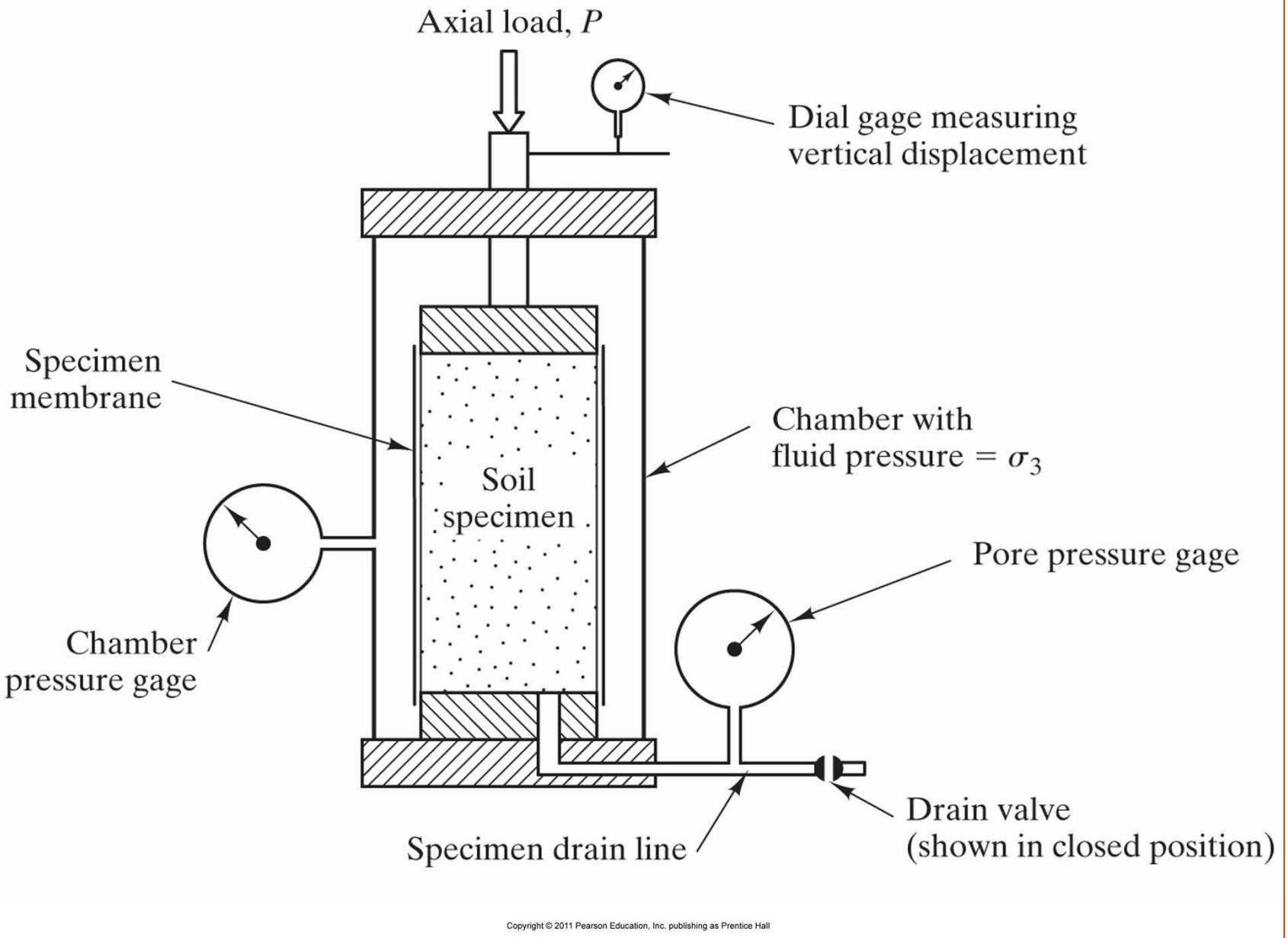

Figure Schematic of a triaxial cell.

1. Application of dead weights or hydraulic pressure in equal increments until the specimen fails. (Axial deformation of the specimen resulting from the load applied through the ram is measured by a dial gauge)

2. Application of axial deformation at a constant rate by means of a geared or hydraulic loading press. This is a strain controlled test.

- The axial load applied by the loading ram corresponding to a given axial deformation is measured by a proving ring or load cell attached to the ram.

- Connections to measure drainage into or out of the specimen, or to measure pressure in the pore water (as per the test conditions), also are provided. The following three standard types of triaxial test generally are conducted:

1. Consolidated drained test or drained tes (CD test)
2. Consolidated undrained test (CU test)
3. Unconsolidted undrained test or undreined test (UU test)

- The general procedures and implications for each of the tests in saturated soils are described in the following sections.

11.9 CONSOLIDATED DRAINED TRIAXIAL TEST

CONSOLIDATED DRAINED TRIAXIAL TEST

- In the CD test, the saturated specimen first is subjected to an all around confining pressure,, by compression of the chamber fluid (***Figure 11.19a***). As confining pressure is applied, the pore water pressure of the specimen increases by u_c (if drainage is prevented). This increase in the pore water pressure can be expressed as a nondimensional parameter in the form Eq. (11.14)

- $$B = \frac{u_c}{\sigma_3} \qquad (11.4)$$

Where:

- *B*= Skempton's pore pressure parameter (Skempton, 1954).

- For saturated soft soils, ***B*** is approximately **equal to 1**; however, for saturated stiff soils, the magnitude of ***B*** can be **less than 1**. Black and Lee (1973) gave the theoretical values of ***B*** for various soils at compete saturation. These values are listed in ***table 11.2***.

- Now, if the connection to drainage is opened, dissipation of the excess pore water pressure, and thus consolidation, will occur. With time, u_c will become equal to “0”. In saturated soil, the change in the volume of the specimen () that takes place during consolidation can be obtained from the volume of pore water drained (***Figure 11.20a***).

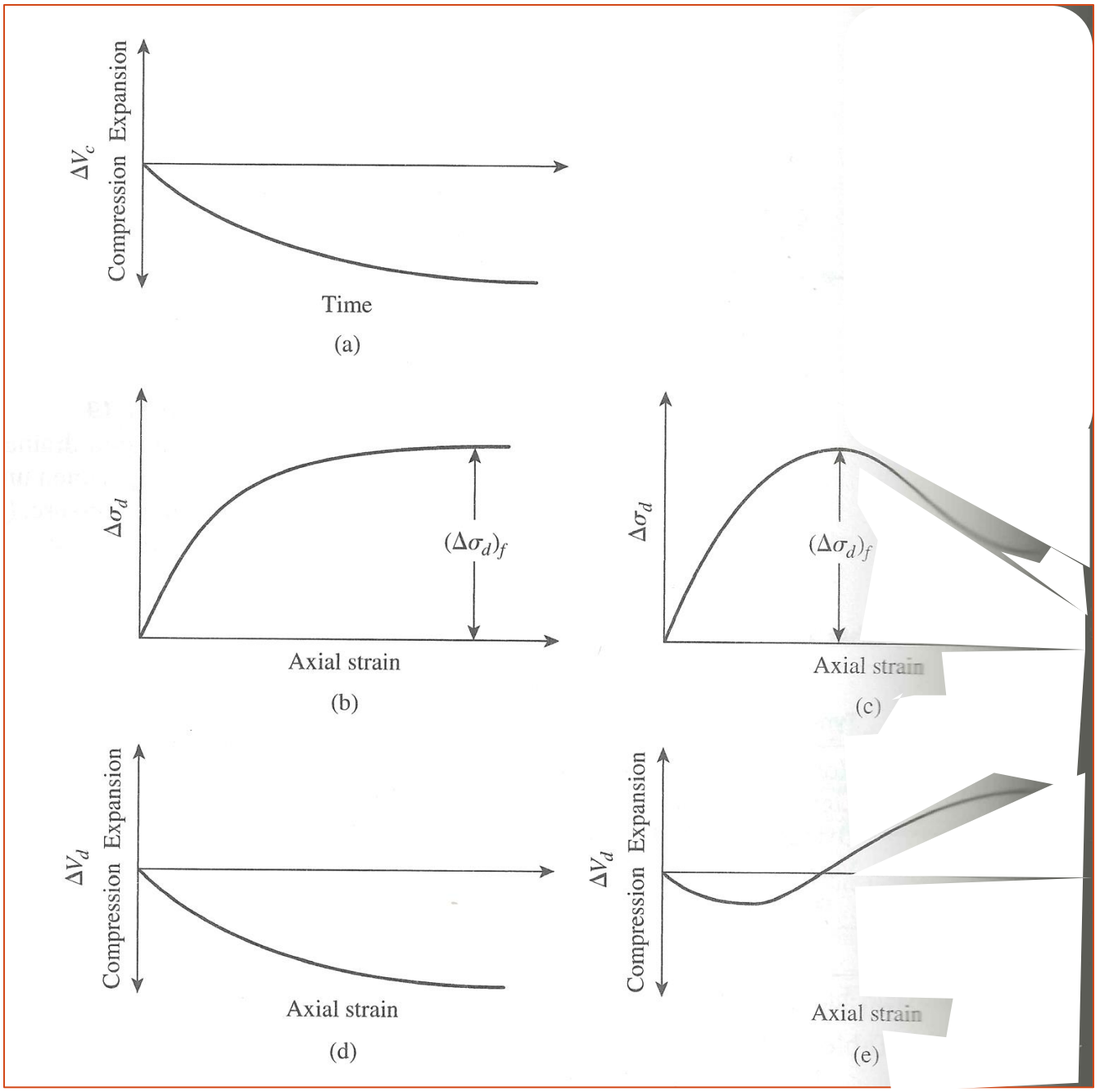
ΔV_c
Compression Expansion
Time
(a)
$\Delta\sigma_d$
$(\Delta\sigma_d)_f$
Axial strain
(b)
$\Delta\sigma_d$
$(\Delta\sigma_d)_f$
Axial strain
(c)
ΔV_d
Compression Expansion
Axial strain
(d)
ΔV_d
Compression Expansion
Axial strain
(e)

Figure 11.20

- Next, the deviation stress, $\Delta\sigma_d$, on the specimen is increased very slowly (***Figure 11.19b***). The drainage connection is kept open, and the slow rate or deviator stress application allows complete dissipation of any pore water pressure that developed as a result (Δu_d).

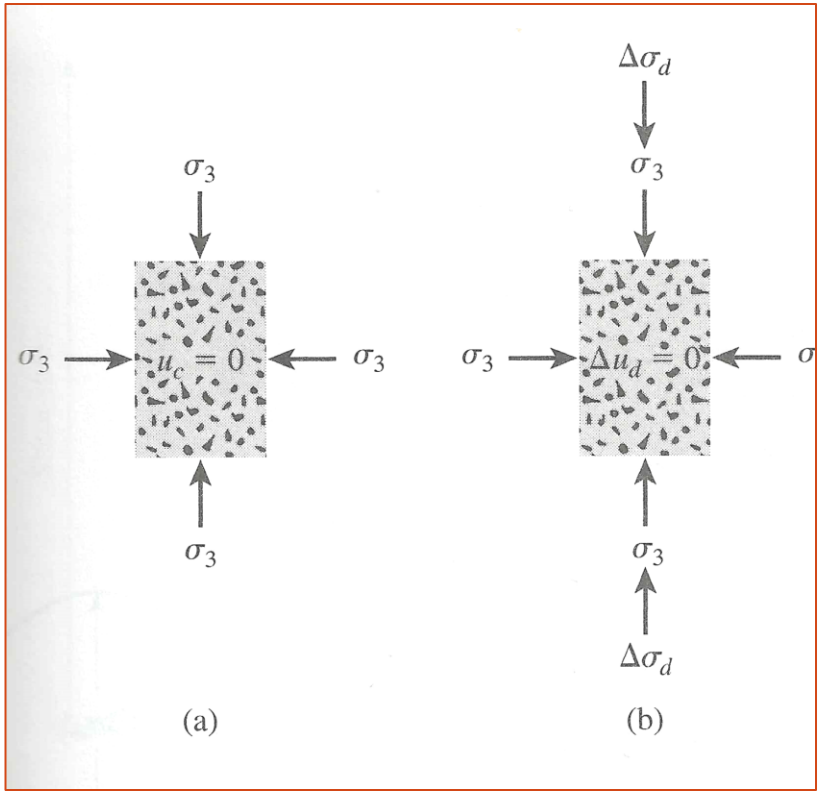

Figure 11.19 Consolidated drained triaxial test: (a) specimen under chamber-confining pressure; (b) deviator stress application

Table 11.2 Theoretical Values of B at Complete Saturation

Type of soil	Theoretical value
Normally consolidated soft clay	0.9998
Lightly overconsolidated soft clays and silts	0.9988
Overconsolidated stiff clays and sands	0.9877
Very dense sands and very stiff clays at high confining pressures	0.9130

- A typical plot of the variation of deviator stress against strain in loose sand and normally consolidated clay is shown in ***Figure 11.20b***. ***Figure 11.20c*** shows a similar plot for dense sand and overconsolidated clay. The volume change,, of specimens that occurs because of the application of deviator stress in various soils is also shown in ***Figures 11.20d and 11.20*** .

- Because the pore water pressure developed during the test is completely dissipated, we have:
- Total and effective confining stress=$\sigma_3 = \sigma'_3$
- And
- Total and effective axial stress at failure= $\sigma_3 + (\Delta\sigma_d)_f = \sigma_1 = \sigma'_1$

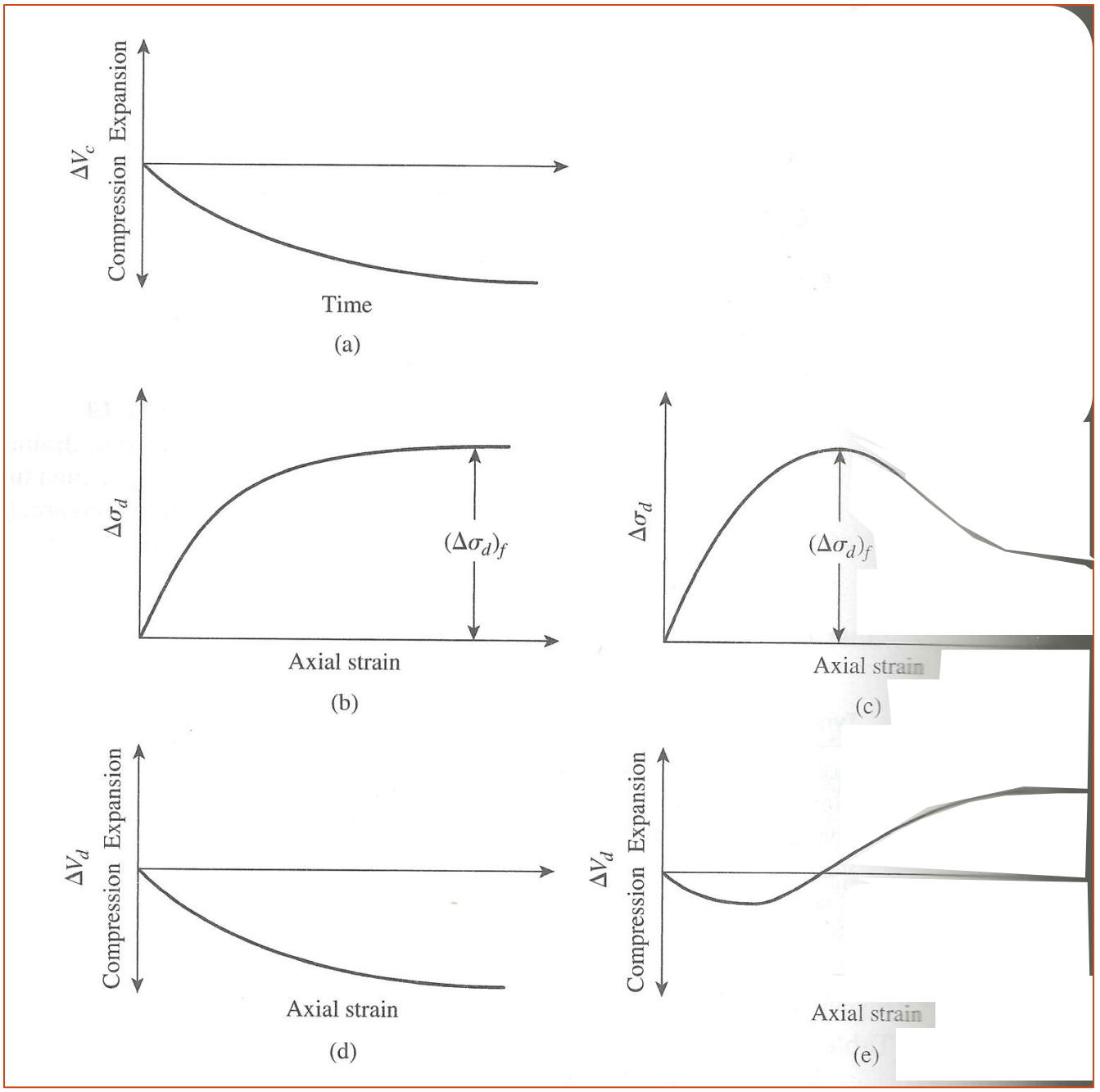
ΔV_c
Compression Expansion
Time
(a)
$\Delta\sigma_d$
$(\Delta\sigma_d)_f$
Axial strain
(b)
$\Delta\sigma_d$
$(\Delta\sigma_d)_f$
Axial strain
(c)
ΔV_d
Compression Expansion
Axial strain
(d)
ΔV_d
Compression Expansion
Axial strain
(e)

Figure 11.20

- In a triaxial test, σ'_1 is the major principal effective stress at failure and σ'_3 is the minor principal effective stress at failure.

- Several test on similar specimens can be conduced by varying the confining pressure. With the major and minor principal stresses at failure for each test the Mohr's circles can be drawn and the failure envelopes can be obtained. ***Figure 11.21*** shows the type of effective stress failure envelope obtained for test on sand and normally consolidated clay.

- The coordinates of the point of tangency of the failure envelope with a Mohr's circle (that is, point ***a***) give the stresses (normal and shear) on the failure plane of that test specimen.

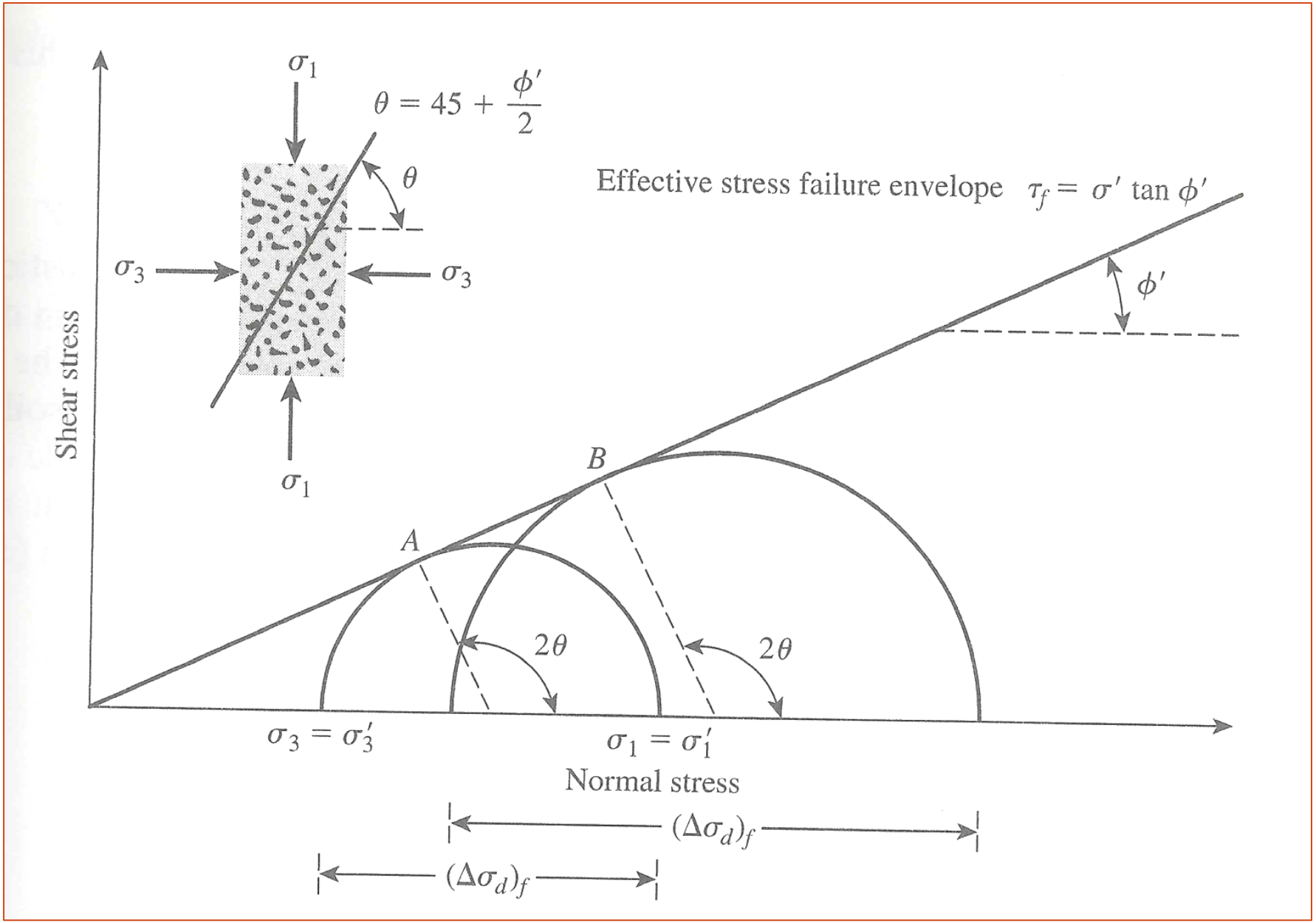

Figure 11.21 Effective stress failure envelope from drained test on sand and normally consolidated clay

- Overconsolidation results when a clay initially is consolidated under an all around chamber pressure of $\sigma_c = (\sigma'_c)$ and is allowed to swell by reducing the chamber pressure to $\sigma_3 = (\sigma'_3)$.
- The failure envelope obtained from drained triaxial test of such overconsolidated clay specimens shows two distinct branches (***ab*** and ***bc*** in ***figure 11.22***). The portion ***ab*** has a flatter slope with a cohesion intercept, and the shear strength equation for this branch can be written as Eq. (11.15)

- $$\tau_f = c' + \sigma' \tan \phi'_1 \quad (11.15)$$

- The portion ***bc*** of the failure envelope represents a normally consolidated stage of soil and follows the equation

- $$\tau_f = \sigma' \tan \phi'_1$$

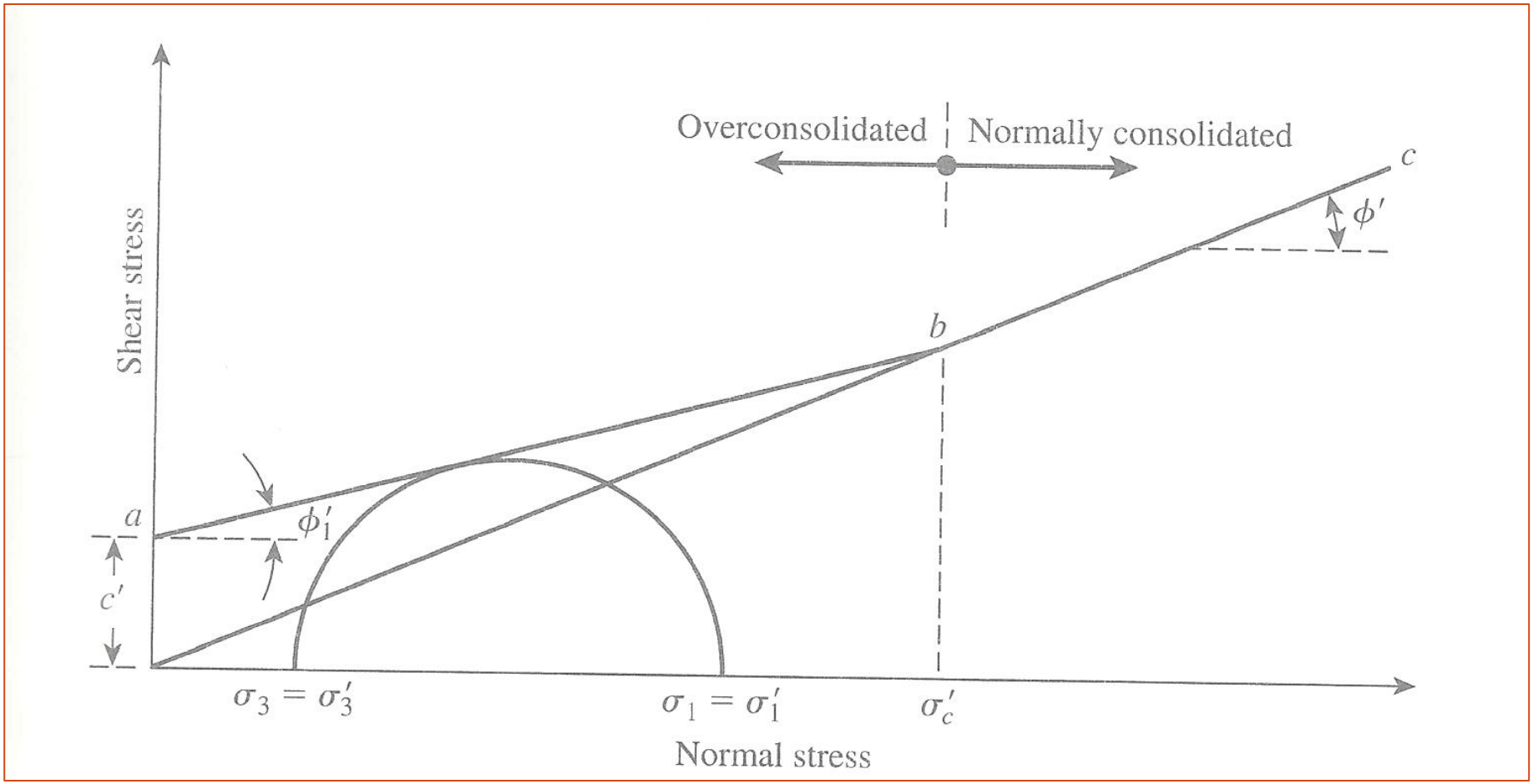

Figure 11.22 Effective stress failure envelope for overconsolidated clay

- A consolidated drained triaxial test on a clayey soil may take several days to complete. This amount of time is required because deviator stress must be applied very slowly to ensure full drainage from the soil specimen. For this reason, the ***CD*** type of triaxial test is uncommon.

Comments on drained and residual friction angles of clay

- The drained angle of friction, ϕ', generally decreases with the plasticity index of soil. This fact is illustrated in ***Figure 11.23*** for a number of clays from data reported by Kenney (1959).
- Although the data are scattered considerably, the general pattern seems to hold. In ***Figure 11.8***, the residual shear strength of clay soil is defined. Also in ***example 11.2***, the procedure to calculate residual friction angle, ϕ'_r, is shown.

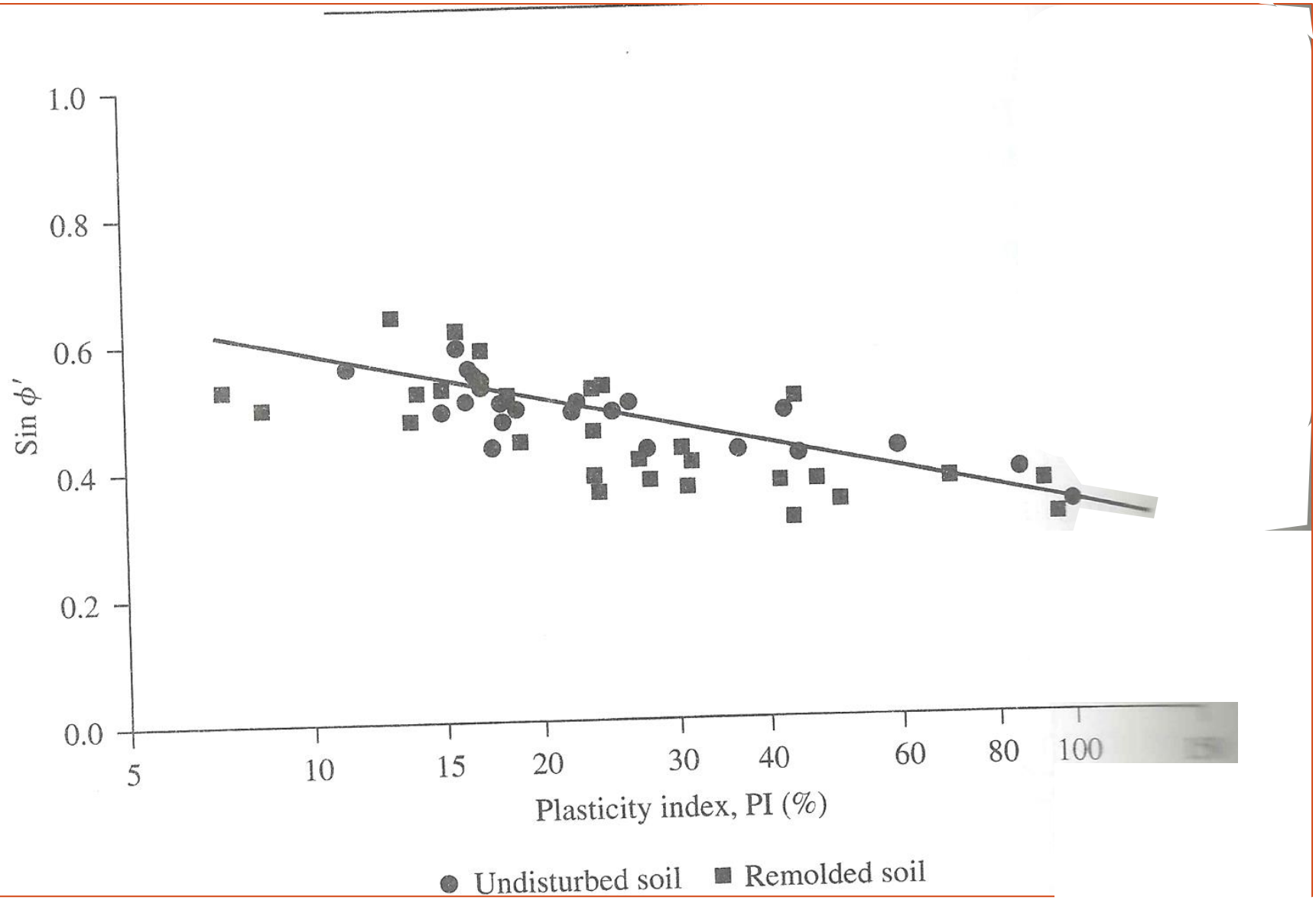

Figure 11.23 Variation of *sin* ϕ with plasticity index for a number of soils (After Kenney 1959)

- Skempton 1964 provided the results of the variation of the residual angle of friction, ϕ'_r, of a number of clayey soils with the clay size fraction (< 2μm) present.

- The following table shows a summary of these results:

Soil	Clay-size fraction (%)	Residual friction angle, ϕ_r (deg)
Selset	17.7	29.8
Wiener Tegel	22.8	25.1
Jackfield	35.4	19.1
Oxford clay	41.9	16.3
Jari	46.5	18.6
London clay	54.9	16.3
Walton's Wood	67	13.2
Weser-Elbe	63.2	9.3
Little Belt	77.2	11.2
Biotite	100	7.5

- At a very high clay content, ϕ'_r, approaches the value of the angle of sliding friction for sheet minerals. For highly plastic sodium montmorillonites, the magnitude of , ϕ'_r, may be as low as 3 to 4^o.

EXAMPLE 11.3

- A consolidated drained triaxial test was conducted on a normally consolidated clay. The results are as follows:

- $\sigma_3 = 276KN/m\text{^}2$

  $(\Delta\sigma_d)_f = 276KN/m\text{^}2$

- Determine
  - Angle of friction ϕ'
  - Angle θ that the failure plane makes with the major principal plane
  - Normal stress σ' and shear stress, τ_f on the failure plane

- For normally consolidated soil, the failure envelope equation is

- $$\tau_f = \sigma' \tan \phi' \_(Because\_c = 0)$$

- For the triaxial test, the effective major and minor principal stresses at failure are as follows:

- $$\sigma'_1 = \sigma_1 = \sigma_3 + (\Delta\sigma_d)_f = 276 + 276 = 552\_KN/m\text{^}2$$
  $$and$$
  $$\sigma'_3 = \sigma_3 = 276\_KN/m\text{^}2$$

Part a

- The Mohr's circle and the failure envelope are shown in figure 11.24 from a which we find that

- $$\sin\phi' = \frac{AB}{OA} = \frac{\left(\frac{\sigma'_1 - \sigma'_3}{2}\right)}{\left(\frac{\sigma'_1 + \sigma'_3}{2}\right)}$$

- Or

- $$\sin\phi' = \frac{\sigma'_1 - \sigma'_3}{\sigma'_1 + \sigma'_3} = \frac{552 - 276}{552 + 276} = 0.333$$

  or

  $$\phi' = 19.45^o$$

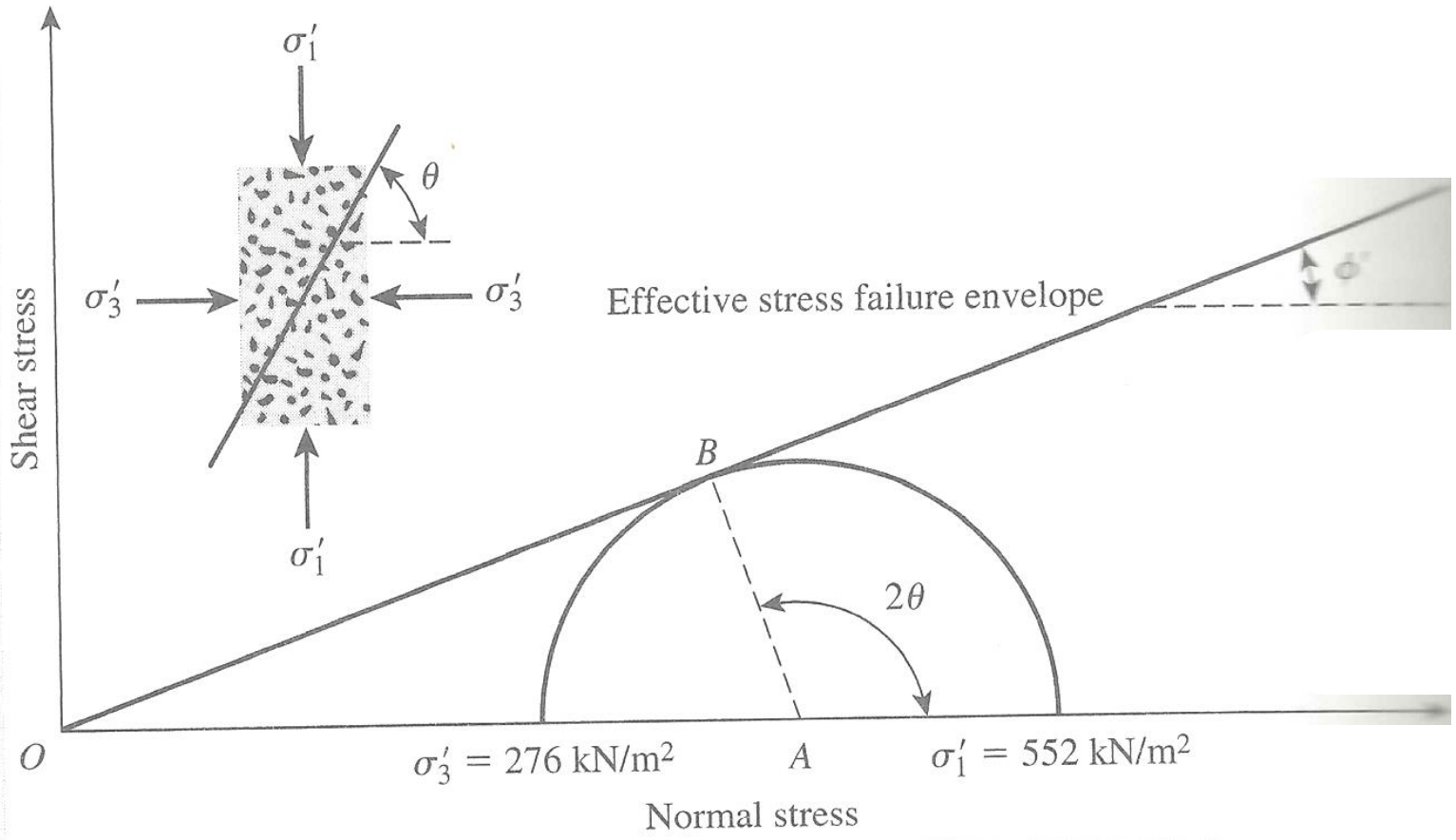

Figure 11.24 Mohr's circle and failure envelope for a normally consolidated

Part b

- From eq.(11.4)

$$\theta = 45 + \frac{\phi'}{2} = 45^{o} + \frac{19.45^{0}}{2} = 54.73^{0}$$

Part c

- Using eq.(9.8) and (9.9) we get

- $$\sigma'(on\_the\_failure\_plane) = \frac{\sigma'_1 + \sigma'_3}{2} + \frac{\sigma'_1 - \sigma'_3}{2}\cos 2\theta$$

- And
- $$\tau_f = \frac{\sigma'_1 - \sigma'_3}{2}\sin 2\theta$$
- Substituting the values of σ'_1=552 *KN/m^2*, σ'_3=276 *KN/m^2*, and θ=54.73° into the preceding equations, we get
- $$\sigma' = \frac{552+276}{2} + \frac{552-276}{2}\cos(2x54.73) = 368.03 KN/m^2$$

  and

  $$\tau_f = \frac{552-276}{2}\sin(2x54.73) = 130.12 KN/m^2$$

EXAMPLE 11.4

- For the triaxial test described in example 11.3,
- Determine the effective normal stress on the plane of maximum shear stress.
- Explain why the shear failure occurred along a plane with θ=54.73° and not along the plane of maximum shear stress

SOLUTION

Part a

- From eq. (9.9) we can see that the maximum shear stress will occur on the plane with θ=45°, from eq(9.8)

- $$\sigma' = \frac{\sigma'_1 + \sigma'_3}{2} + \frac{\sigma'_1 - \sigma'_3}{2}\cos 2\theta$$

- Substituting θ=45° into the preceding equation we get

- $$\sigma' = \frac{552 + 276}{2} + \frac{552 - 276}{2}\cos 90 = 414\_KN/m\text{^}2$$

Part b

- The shear stress that will cause failure along the plane with θ=45° is

- $$\tau_f = \sigma' \tan\phi' = 414 \tan(19.45) = 146.2\_KN/m\text{^}2$$

- However the shear stress induced on that plane is

- $$\tau_f = \frac{\sigma'_1 - \sigma'_3}{2} \sin 2\theta = \frac{552 - 276}{2} \sin 90 = 138\_KN/m\text{^}2$$

- Because τ=138 *KN/m^2*<146.2 *KN/m^2*=τ_f, the specimen did not fail along the plane of maximum shear stress.

EXAMPLE 11.5

- The equation of the effective stress failure envelope for normally consolidated clayey soil is $\tau_f = \sigma' \tan 30^\circ$. A drained triaxial test was conducted with the same soil at a chamber confining pressure of 10 *lb/in^2*. Calculate the deviator stress at failure.

SOLUTION

- For normally consolidated clay ***c'***=0. Thus, from eq(11.8).

- $$\sigma'_1 = \sigma'_3 \tan^2(45 + \frac{\phi'}{2})$$

  $$\phi' = 30^0$$

  $$\sigma'_1 = 10 \tan^2(45 + \frac{30}{2}) = 30\_lb/in\text{^}2$$

  so

  $$(\Delta\sigma_d)_f = \sigma'_1 - \sigma'_3 = 30 - 10 = 20\_lb/in\text{^}2$$

EXAMPLE 11.6

- The results of two drained triaxial test on a saturated clay follow:
- Specimem I:

- $\sigma_3 = 10\_lb/in\text{^}2$
  $(\Delta\sigma_d)_f = 24.7\_lb/in\text{^}2$
- Specimem II:

- $\sigma_3 = 15\_lb/in\text{^}2$
  $(\Delta\sigma_d)_f = 33.5\_lb/in\text{^}2$
- Determine the shear strength parameters.

SOLUTION

- Refer to ***figure 11.25***. for specimen I, the principal stresses at failure are

- $\sigma'_3 = \sigma_3 = 10\_lb/in\text{^}2$

  and

  $\sigma'_1 = \sigma_1 = \sigma_3 + (\Delta\sigma_d)_f = 10 + 24.7 = 34.7\_lb/in\text{^}2$

- Similarly, the principal stresses at failure for specimen II are

  $\sigma'_3 = \sigma_3 = 15\_lb/in\text{^}2$

- *and*

  $\sigma'_1 = \sigma_1 = \sigma_3 + (\Delta\sigma_d)_f = 15 + 33.5 = 48.5\_lb/in\text{^}2$

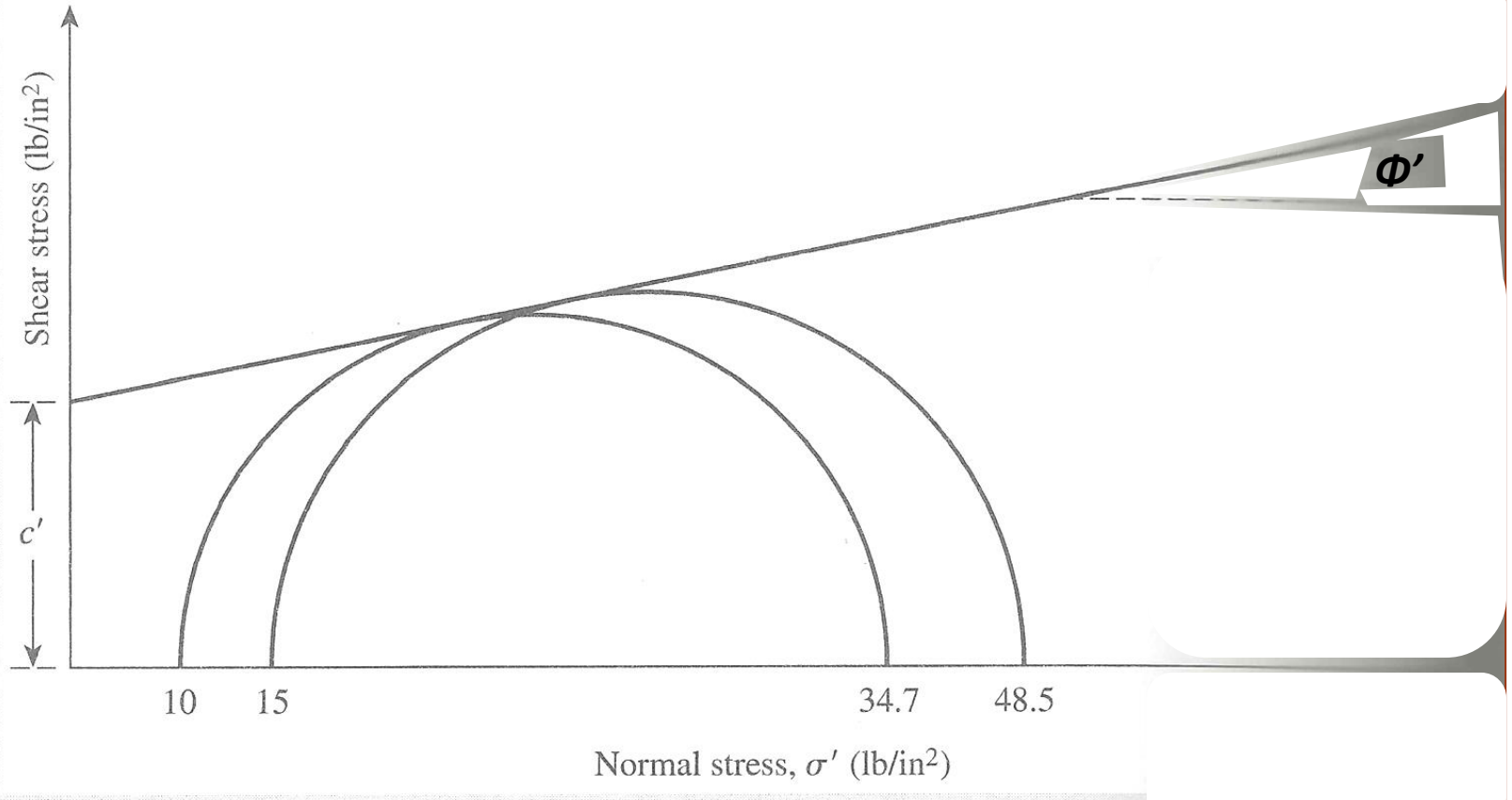

Figure 11.25 Effective stress failure envelope and Mohr's circles for Specimens

- Using the relationship given by eq(11.8), we have

- $$\sigma'_1 = \sigma'_3 \tan^2(45 + \frac{\phi'}{2}) + 2c' \tan(45 + \frac{\phi'}{2})$$

- Thus for specimen I,

- $$34.7 = 10 \tan^2(45 + \frac{\phi'}{2}) + 2c' \tan(45 + \frac{\phi'}{2})$$

- And for specimen II

- $48.5 = 15\tan^2(45 + \frac{\phi'}{2}) + 2c'\tan(45 + \frac{\phi'}{2})$

- Solving the two preceding equations, we obtain

- $\phi' = 28^0$

  $c' = 2.1\_lb/in\text{^}2$

11.10 CONSOLIDATED UNDRAINED TRIAXIAL TEST

CONSOLIDATED UNDRAINED TRIAXIAL TEST

- Is the most common type of triaxial test. In this test, the saturated soil specimen is first consolidated by an all around chamber fluid pressure,σ_3, that results in drainage (***Figure 11.26a and 11.26b***).

- After the pore water pressure generated by the application of confining pressure is dissipated, the deviator stress, $\Delta\sigma_d$, on the specimen is increased to cause the shear failure (***Figure 11.26c***).

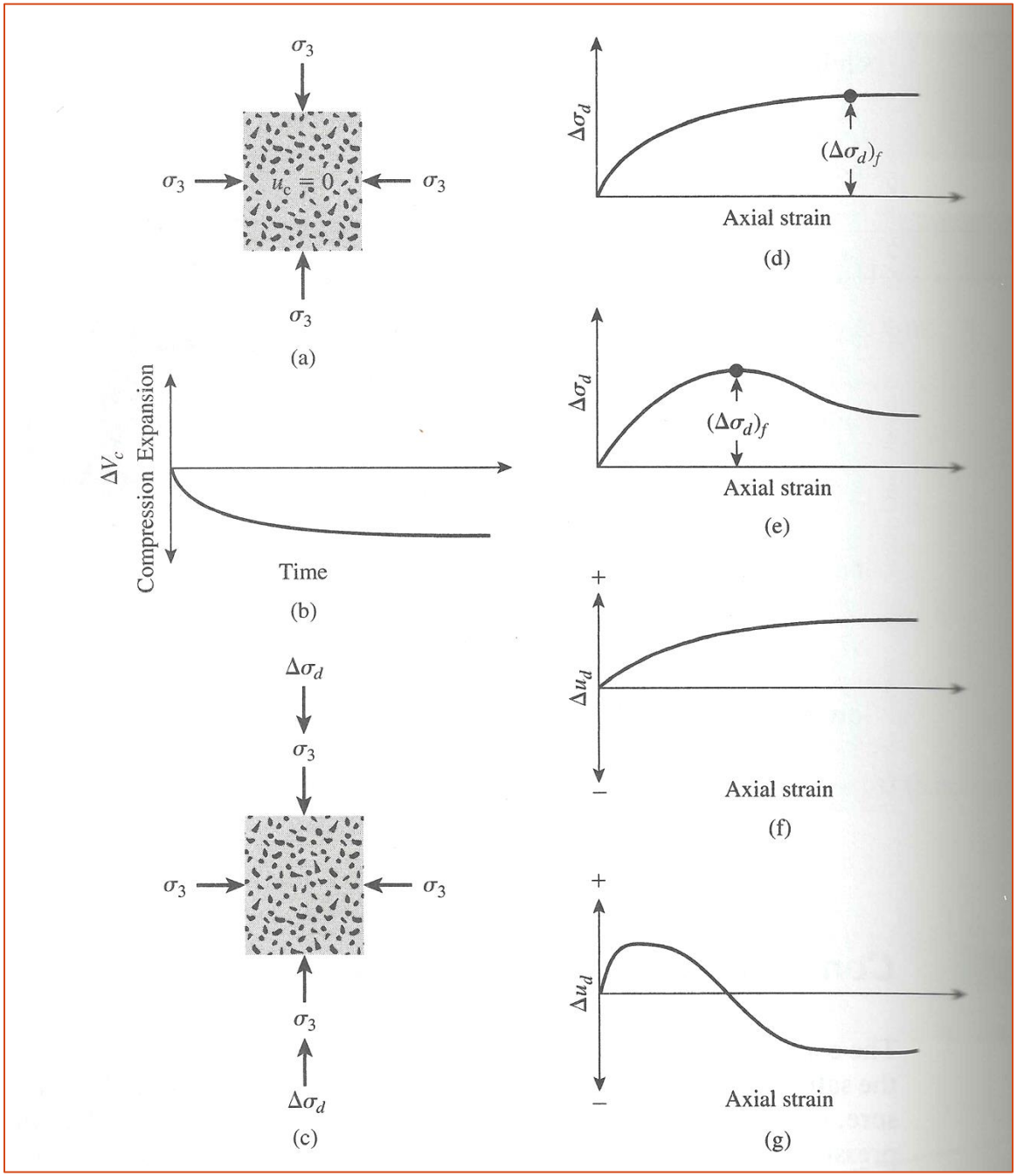
σ_3
σ_3
$u_c = 0$
σ_3
σ_3
(a)
ΔV_c
Compression Expansion
Time
(b)
$\Delta\sigma_d$
σ_3
σ_3
σ_3
σ_3
$\Delta\sigma_d$
(c)
$\Delta\sigma_d$
$(\Delta\sigma_d)_f$
Axial strain
(d)
$\Delta\sigma_d$
$(\Delta\sigma_d)_f$
Axial strain
(e)
+
Δu_d
−
Axial strain
(f)
+
Δu_d
−
Axial strain
(g)

Figure 11.26

- During this phase of the test, the drainage line form the specimen is kept closed. Because drainage is not permitted, the pore water pressure, Δu_d, will increase. During the test, simultaneous measurements of $\Delta\sigma_d$ and Δu_d are made.
- The increase in the pore water pressure, Δu_d, can be expressed in a nondimensional form as Eq. (11.16)

$$\overline{A} = \frac{\Delta u_d}{\Delta \sigma_d} \qquad (11.16)$$

Where:

- $\overline{A}$ = Skempton's pore pressure parameter (1954)

- The general patterns of variation of and with axial strain for sand and clay soils are shown in ***Figure 11.26d*** through ***11.26g***. In loose sand and normally consolidated clay, the pore water pressure increases with strain.

- In dense sand overconsolidated clay, the pore water pressure increases with strain to a certain limit beyond which it decreases and becomes negative (with respect to the atmospheric pressure). This decrease is because of a tendency of the soil to dilate.

- Unlike the consolidated drained test, the total and effective and principal stresses are not the same in the consolidated undrained test. Because the pore water pressure at failure is measured in this test, the principal stresses may be analyzed as follows:

- Major principal stress at failure (total):
- Major principal stress at failure (effective):
- Minor principal stress at failure (total):
- Minor principal stress at failure (effective):

- In these equations, $(\Delta u_d)_f$ = pore water pressure at failure. The preceding derivation show that:

$$\sigma_1 - \sigma_3 = \sigma'_1 - \sigma'_3$$

- Test on several similar specimens with varying confining pressures may be conducted to determine the shear strength parameters. ***Figure 11.27*** shows the total effective stress Mohr's circle obtained form consolidated undrained triaxial test in sand and normally consolidated clay.

- Note that ***A*** and ***B*** are two total stress Mohr's circles obtained from two tests. ***C*** and ***D*** are the effective stress Mohr's circles corresponding to total stress circles ***A*** and ***B*** , respectively. The diameters of circles ***A*** and ***C*** are the same; similarly, the diameters of circles ***B*** and ***D*** are the same.

- In ***Figure 11.27***, the total stress envelope can be obtained by drawing a line that touches all the total stress Mohr's circles. For sand and normally consolidated clays, this will be approximately a straight line passing through the origin and may be expressed by the equation:

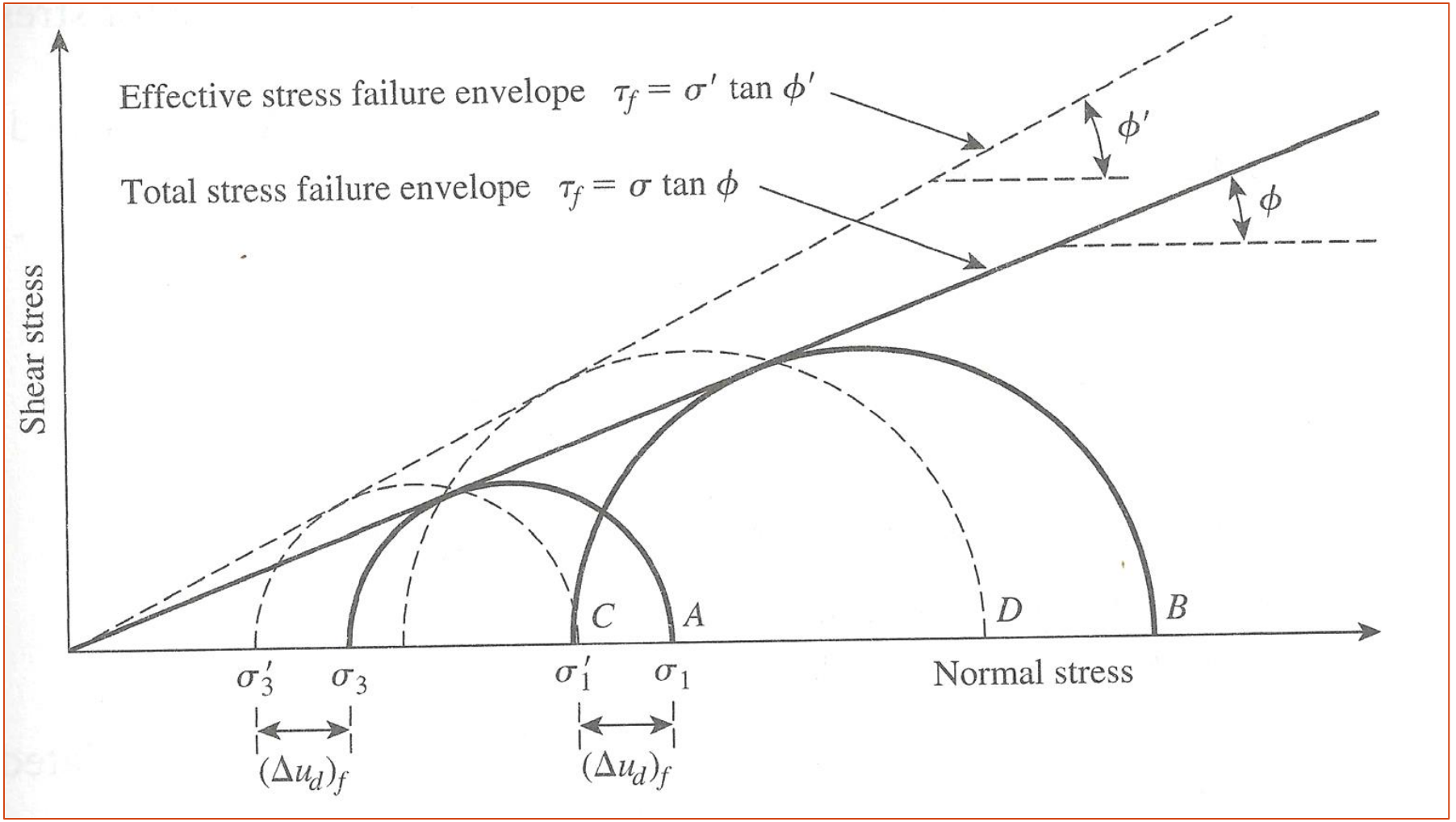

Figure 11.27 Total and effective stress failure envelopes for consolidated undrained triaxial test. (Note: The figure assumes that no back pressure is applied)

- $\tau_f = \sigma \tan \phi$ (11.17)

Where:

- σ=total stress
- ϕ= the angle that the total stress failure envelope makes with the normal stress axis, also known as the consolidated undrained angle of shearing resistance
- Equation (11.17) is seldom used for practical considerations

- Test on several similar specimens with varying confining pressures may be conducted to determin =e the shear strength parameters.

- ***Figure 11.27*** shows the total and effective stress Mohr's circles at failure obtained from consolidated undrained triaxial test in sand and normally consolidated clay. Note that a and ***B*** are two total stress Mohr's circles obtained form two tests. ***C*** and ***D*** are the effective stress Mohr's circles ***A*** and ***C*** are the same; similarly, the diameters of circles ***B*** and ***D*** are the same.

- In ***Figure 11.27***, the total stress failure envelope can be obtained by drawing a line that touches all the total stress Mohr's circles. For sand and normally consolidated clays, this will be approximately a straight line passing through the origin and may be expressed by the equation (11.17)

- Again referring to ***Figure 11.27***, we see that the failure envelope that is tangent to all the effective stress Mohr's circles can be represented by the equation , which is the same as that obtained from consolidated drained test (see ***Figure 11.21***)

- $\tau_f = \sigma' \tan \phi'$

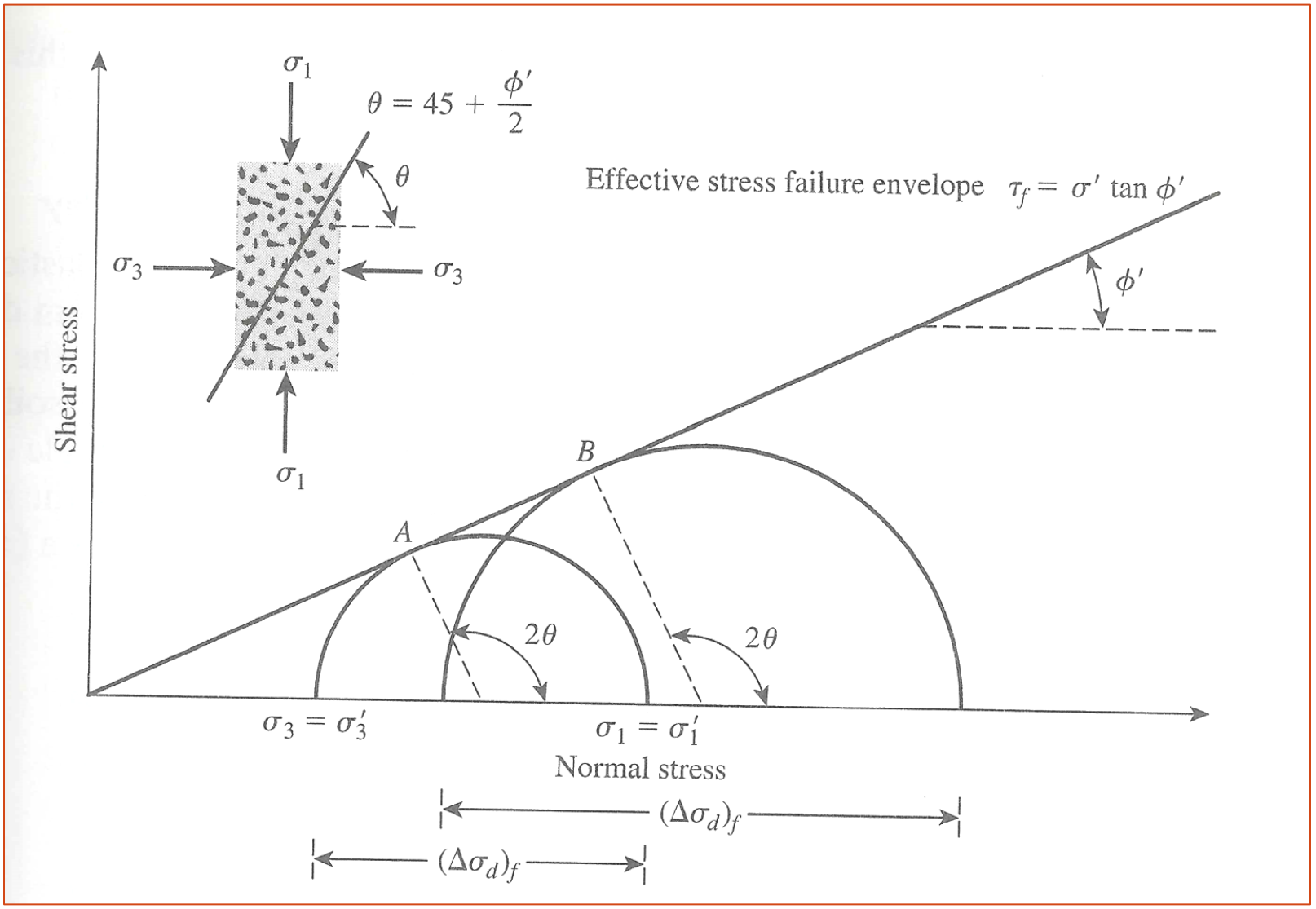

Figure 11.21 Effective stress failure envelope from drained test on sand and normally consolidated clay

- In overconsolidated clays, the total stress failure envelope obtained from consolidated undrained test will take the shape shown in ***Figure 11.28***. The straight line ***a'b'*** is represented by the equation (11.18)

- $$\tau_f = c + \sigma \tan \phi_1 \qquad (11.18)$$

- And the straight line ***b'c'*** follows the relationship given by Eq. (11.17). The effective stress failure envelope drawn from the effective stress Mohr's circles will be similar to that shown in ***Figure 11.28***.

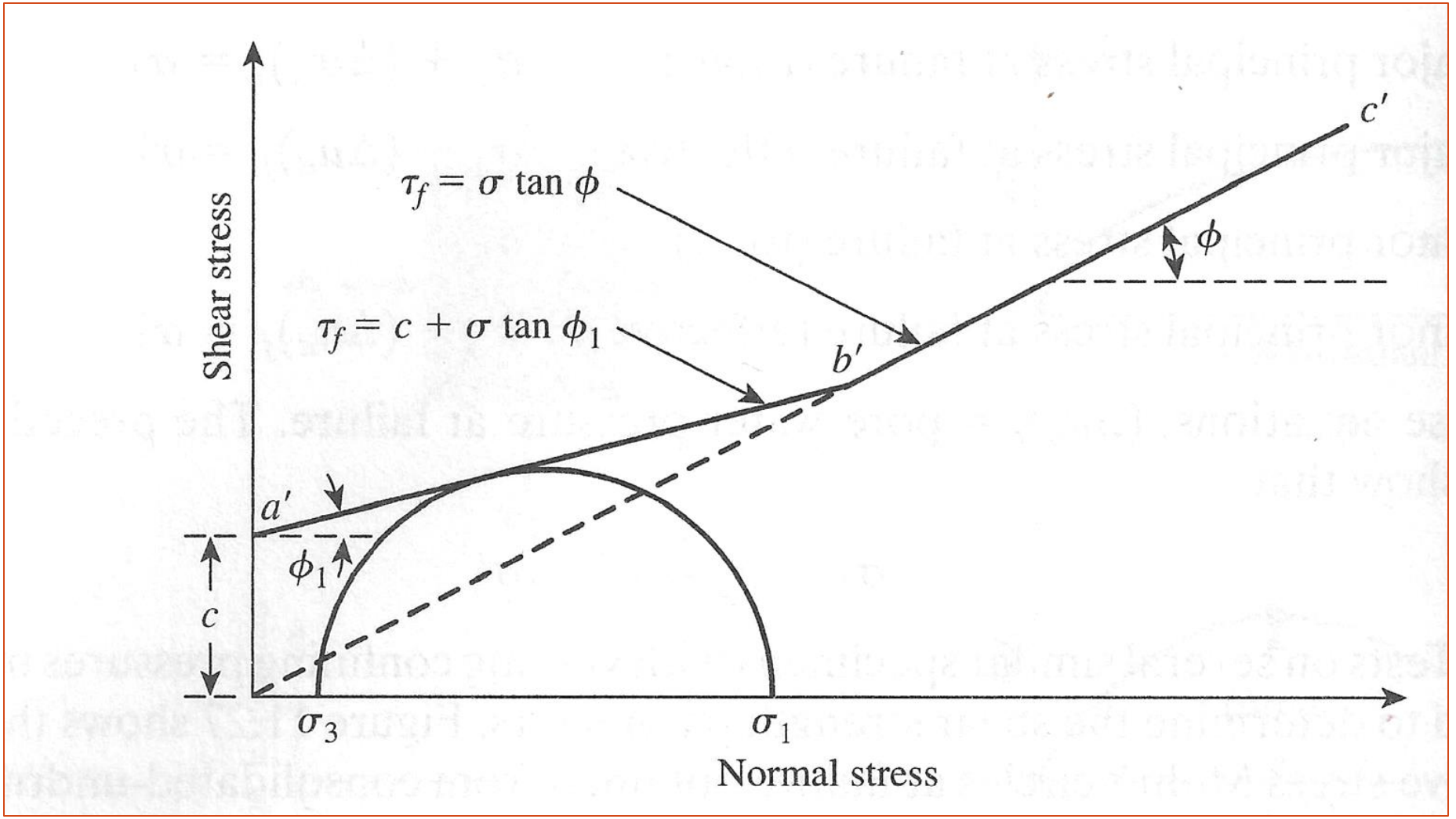

Figure 11.28 Total stress failure envelope obtained from consolidated undrained tests in over consolidated clay

- Consolidated drained test on clay soils take considerable time. For this reason, consolidated undrained test can be conducted on such soils with pore pressure measurements to obtain the drainage shear strength parameters.
- Because drainage is allowed in these test during the application of deviator stress, they can be performed quickly.

- Skempton's pore water pressure parameter $\overline{A}$ was defined in Eq. (11.16). At a failure, the parameter $\overline{A}$ can be written as Eq. (11.19)

- $$\overline{A} = \overline{A_f} = \frac{(\Delta u_d)_f}{(\Delta \sigma_d)_f} \qquad (11.19)$$

- The general range of $\overline{A_f}$ values in most clay soils is as follow:
- Normally consolidated clays:0.5 to 1
- Overconsolidated clays: -0.5 to 0

- ***Table 11.3*** gives the values $\overline{A_f}$ of for some normally consolidated clays as obtained by the Norwegian Geothechnical Institute.

- Laboratory triaxial test of Simons 1960 on Oslo clay, Weald clay, and London clay showed that $\overline{A_f}$ becomes approximately zero at an overconsolidation value of about 3 or 4 (***Figure 11.29***)

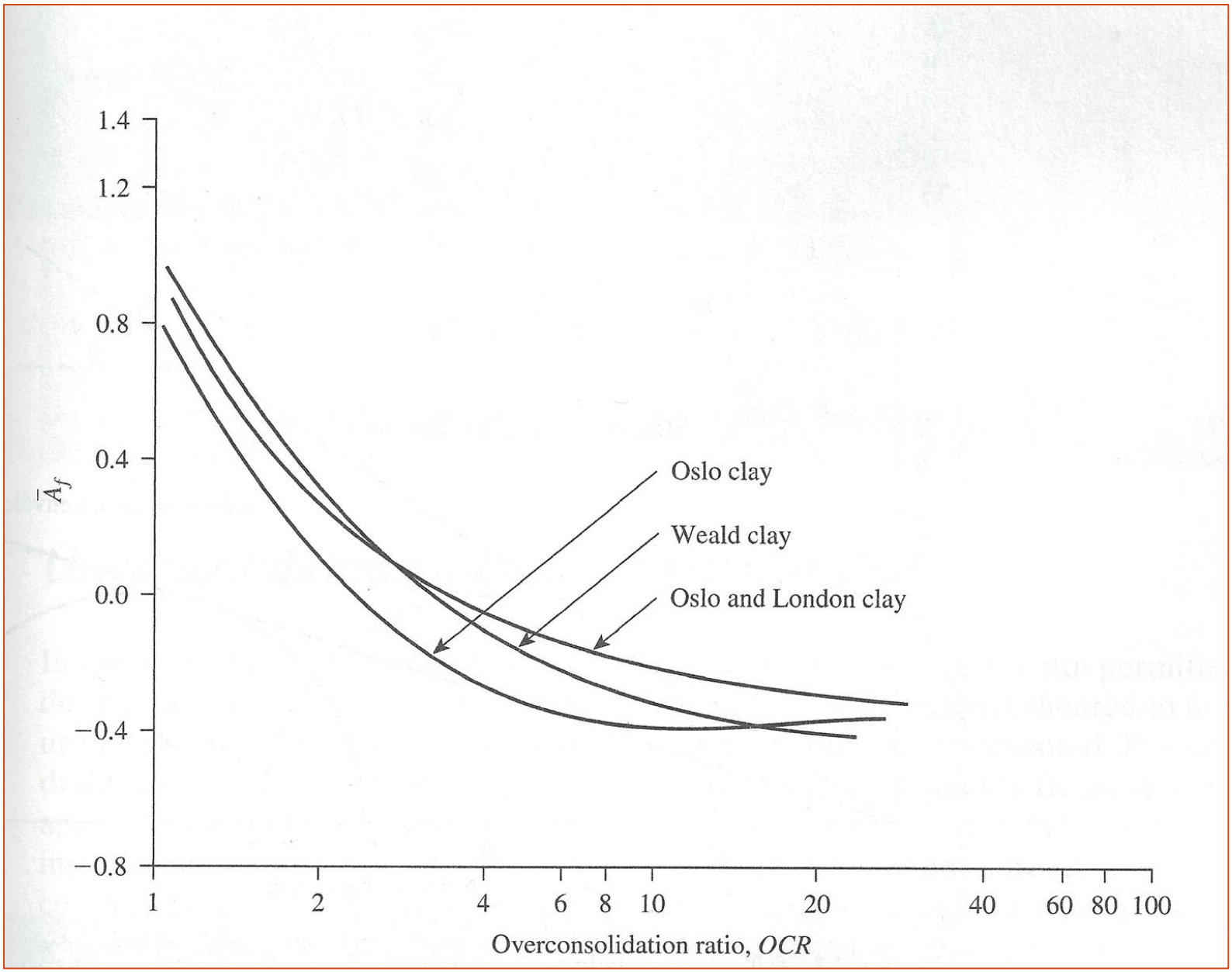

Figure 11.29 Variation of A_f with overconsolidation ratio for three clays (Based on Simon, 1960)

Triaxial Test Results for Some Normally Consolidated Clays
the Norwegian Geotechnical Institute*

	Liquid limit	Plastic limit	Liquidity index	Sensitivity[a]	Drained friction angle, ϕ' (deg)	$\bar{A}_f$
Sisters, Canada	127	35	0.28		19	0.72
	69	28	0.68	5	25.5	1.03
Edet, Sweden	68	30	1.32	50	26	1.10
	59	22	0.58	5	28.5	0.87
	57	22	0.63	6	27	1.00
Edet, Sweden	63	30	1.58	50	23	1.02
River, Sweden	60	27	1.30	12	28.5	1.05
River, Sweden	60	30	1.50	40	24	1.05
	48	25	0.87	4	31.5	1.00
	36	20	0.50	2	34	0.75
	33	18	1.08	8	28	1.18

Bjerrum and Simons (1960)
11.14 for the definition of sensitivity.

EXAMPLE 11.7

- A specimen of saturated sand was consolidated under an all around pressure of 60 *lb/in^2.* The axial stress was then increased and drainage was prevented. The specimen failed when the axial deviator stress reached 50 *lb/in^2*. The pore water pressure at failure was 41.35 *lb/in^2*. Determine

a. Consolidated undrained angle of shearing resistance, ϕ
b. Drained friction angle, ϕ'

SOLUTION

Part a

- At failure σ3=60 lb/in^2
- $\sigma_1 = \sigma_3 + (\Delta\sigma_d)_f = 60 + 50 = 110\_lb/in\text{^}2$
- From ***figure 11.30***
- $$\sin\phi = \frac{AB}{OA} = \frac{\sigma_1 - \sigma_3}{\sigma_1 + \sigma_3} = \frac{110 - 60}{110 + 60} = \frac{50}{170} = 0.294$$

  or

  $$\phi = 17.1^0$$

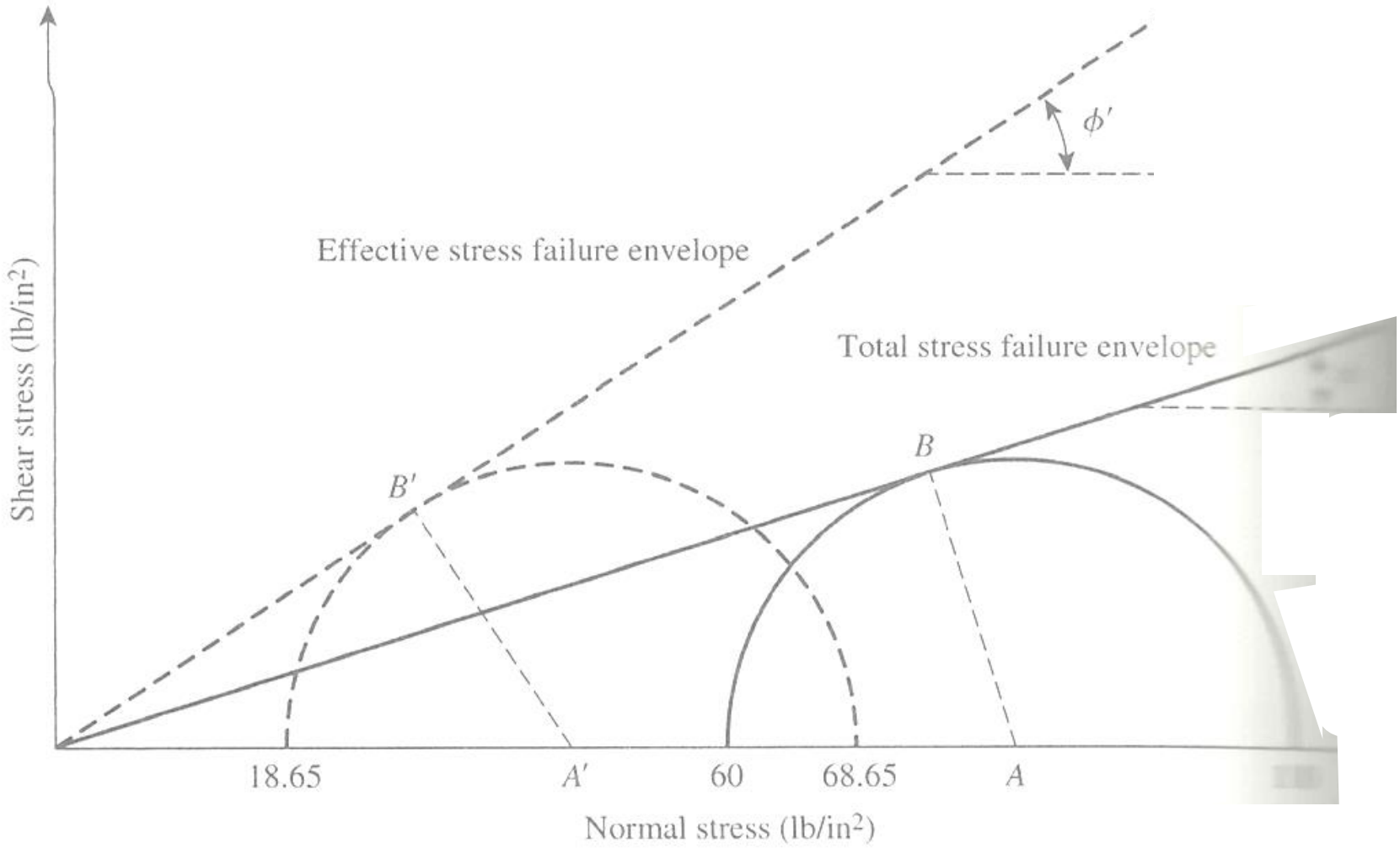

Figure 11.30 Failure envelopes and Mohr's circles for a saturated sand

Part b

- $\sigma'_3 = \sigma_3 - (\Delta u_d)_f = 60 - 41.35 = 18.65\_lb/in\text{^}2$

  $\sigma'_1 = \sigma_1 - (\Delta u_d)_f = 110 - 41.35 = 68.65\_lb/in\text{^}2$

  $$\sin\phi' = \frac{A'B'}{OA'} = \frac{\sigma'_1 - \sigma'_3}{\sigma'_1 + \sigma'_3} = \frac{68.65 - 18.65}{68.65 + 18.65} = \frac{50}{87.3} = 0.5727$$

  or

  $\phi = 34.94^0$

EXAMPLE 11.8

- Refer to the soil specimen described in example 11.7. what would be the deviator stress at failure, $(\Delta\sigma_d)_f$,

  If a drained test was conducted with the same chamber all around pressure (that is 60 *lb/in^2*)

SOLUTION

- From eq(11.8) (with ***c'***=0)

- $$\sigma'_1 = \sigma'_3 \tan^2\left(45 + \frac{\phi'}{2}\right)$$

  $$\sigma'_3 = 60\_lb/in\text{^}2, and\_\sigma' = 34.94^0 \left(from\_example\_11.7\right)\_so$$

- $$\sigma'_1 = 60\tan^2\left(45 + \frac{34.94}{2}\right) = 220.85\_lb/in\text{^}2$$

  $$\left(\Delta\sigma_d\right)_f = \sigma'_1 - \sigma'_3 = 220.85 - 60 = 160.85\_lb/in\text{^}2$$

11.11 UNCONSOLIDATED UNDRAINED TRIAXIAL TEST

UNCONSOLIDATED UNDRAINED TRIAXIAL TEST

- In unconsolidated undrained tests, drainage form the soil specimen is not permitted during the application of chamber pressure σ_3 .
- The test specimen is sheared to failure by the application of deviator stress, $\Delta\sigma_d$, and drainage is prevent. Because drainage is not allowed at any stage, the test can be performed quickly. Because of the application of chamber confining pressure, σ_3 the pore water pressure will increase by u_c .
- A further increase in the pore water pressure Δu_d will occur because of the deviator stress application. Hence, the total pore water pressure u in the specimen at any stage of deviator stress application can be given as Eq. (11.20)

$$u = u_c + \Delta u_d \qquad (11.20)$$

- From Eqs. (11.14) and (11.16), $u_c = B\sigma_3$ and $\Delta u_d = \overline{A}\Delta\sigma_d$,so Eq. (11.21)

- $$u = B\sigma_3 + \overline{A}\Delta\sigma_d = B\sigma_3 + \overline{A}(\sigma_1 - \sigma_3) \quad (11.21)$$

- This test usually is conducted on clay specimens and depends on a very important strength concept for cohesive soils if the soil is fully saturated.
- The added axial stress at failure () is practically the same regardless of the chamber confining pressure. This property is shown in ***Figure 11.31***. The failure envelope for the total stress Mohr's circles becomes a horizontal line and hence is called as ϕ=0 condition.

- From eq. (11.9) with ϕ =0 we get Eq. (11.22)
- $$\tau_f = c = c_u \quad (11.22)$$

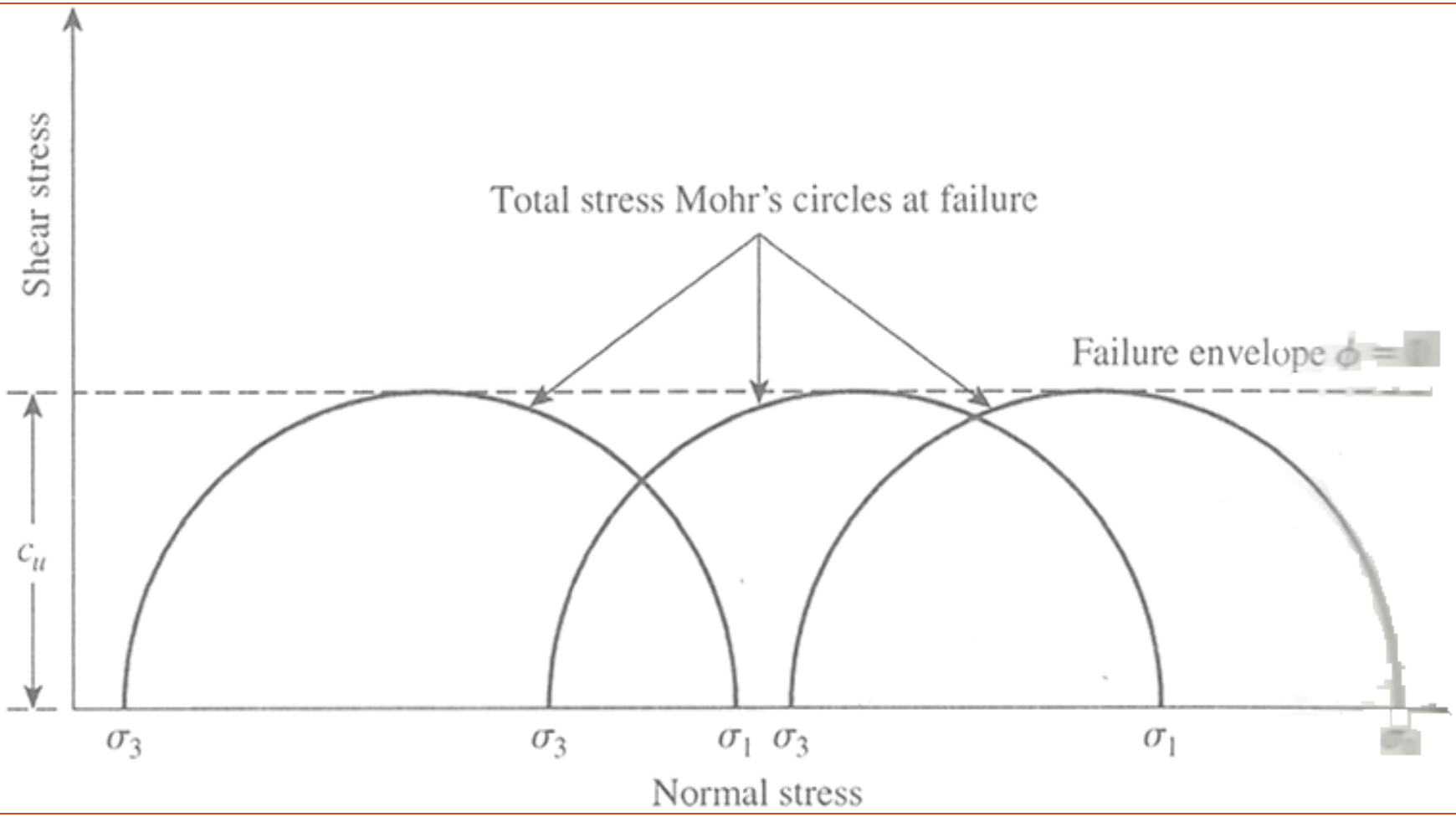

Figure 11.31 Total stress Mohr's circles and failure envelope (ϕ=0) obtained from unconsolidated-undrained triaxial test on fully saturated cohesive soil

- Where c_u is the undrained shear strength and is equal to the radius of the Mohr's circles. Note that ϕ=0 concept is applicable to only saturated clays and silts.

- The reason for obtaining the same added axial stress $(\Delta\sigma_d)_f$ regardless of the confining pressure can be explained as follows. If a clay specimen (No. I) is consolidated at a chamber pressure σ_3, and then sheared to failure without drainage, the total stress conditions at failure can be represented by the Mohr's circle ***P*** in ***Figure 11.32***. The pore pressure developed in the specimen at failure is equal to $(\Delta u_d)_f$. Thus, the major and minor principal effective stresses at failure are, respectively,

$$\sigma'_1 = \left[\sigma_3 + (\Delta\sigma_d)_f\right] - (\Delta u_d)_f$$

- and

$$\sigma'_3 = \sigma_3 - (\Delta u_d)_f$$

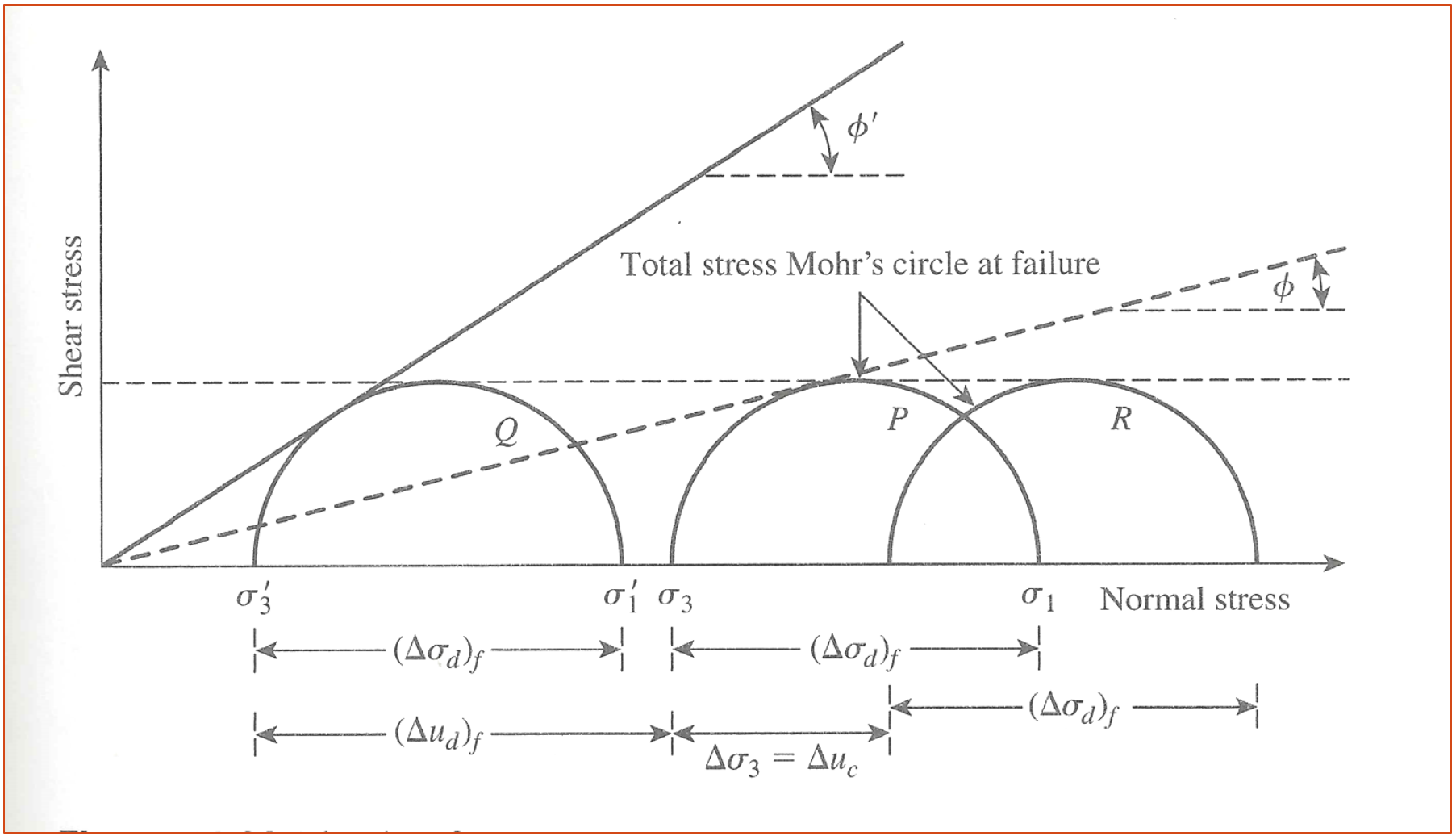

Figure 11.32 The ϕ=0 concept

- ***Q*** is the effective stress Mohr's circle drawn with the preceding principal stresses. Note that the diameters of circles ***P*** and ***Q*** are the same. Now let us consider another similar clay specimen (No. II) that has been consolidated under a chamber pressure σ_3 with initial pore pressure equal to "zero". If the chamber pressure is increase by $\Delta\sigma_3$ without drainage, the pore water pressure will increase by an amount Δu_c.

- For saturated soils under isotropic stresses, the pore water pressure increase is equal to the total stress increase, so $\Delta u_c = \Delta\sigma_3$ (***B=1***). At this time, the effective confining pressure is equal to

$$\sigma_3 + \Delta\sigma_3 - \Delta u_c = \sigma_3 + \Delta\sigma_3 - \Delta\sigma_3 = \sigma_3$$

- This is the same as the effective confining pressure of specimen No. I before the application of deviator stress. Hence, if specimen II is sheared to failure by increasing the axial stress, it should fail at the same deviator stress $(\Delta\sigma_d)_f$ that was obtained for specimen I. The total stress Mohr's circle at failure will be ***R*** (see ***Figure 11.32***). The added pore pressure increase caused by the application of $(\Delta\sigma_d)_f$ will be $(\Delta u_d)_f$.

- At failure, the minor principal effective stress is

$$\left[\left(\sigma_3 + \Delta\sigma_3\right)\right] - \left[\Delta u_c + \left(\Delta u_d\right)_f\right] = \sigma_3 - \left(\Delta u_d\right)_f = \sigma'_3$$

- And the major principal effective stress is

$$\left[\sigma_3 + \Delta\sigma_3 + (\Delta\sigma_d)_f\right] - \left[\Delta u_c + (\Delta u_d)_f\right] = \left[\sigma_3 + (\Delta\sigma_d)_f\right] - (\Delta u_d)_f$$
$$= \sigma_1 - (\Delta u_d)_f = \sigma'_1$$

- Thus the effective stress Mohr's circle will still be ***Q*** because strength is a function of effective stress. Note that the diameters of circles ***P, Q*** and ***R*** are all the same. Any value of $\Delta\sigma_3$ could have been chosen for testing specimen II. In any case the deviator stress $(\Delta\sigma_d)_f$ to cause failure would have been the same as long as the soil was fully saturated and fully undrained during both stages of the test.

11.12 UNCONFINED COMPRESSION TEST ON SATURATED CLAY

UNCONFINED COMPRESSION TEST ON SATURATED CLAY

- The unconfined compression test is a special type of unconsolidated undrained test that is commonly used for clay specimens. In this test, the confining pressure σ_3 is "0". An axial load is rapidly applied to the specimen to cause failure.
- At failure, the total minor principal stress is zero and the total major principal stress is σ_1 (***Figure 11.33***). Because the undrained shear strength is independent of the confining pressure as long as the soil is fully saturated and fully undrained, we have Eq. (11.23)

- $$\tau_f = \frac{\sigma_1}{2} = \frac{q_u}{2} = c_u \qquad (11.23)$$

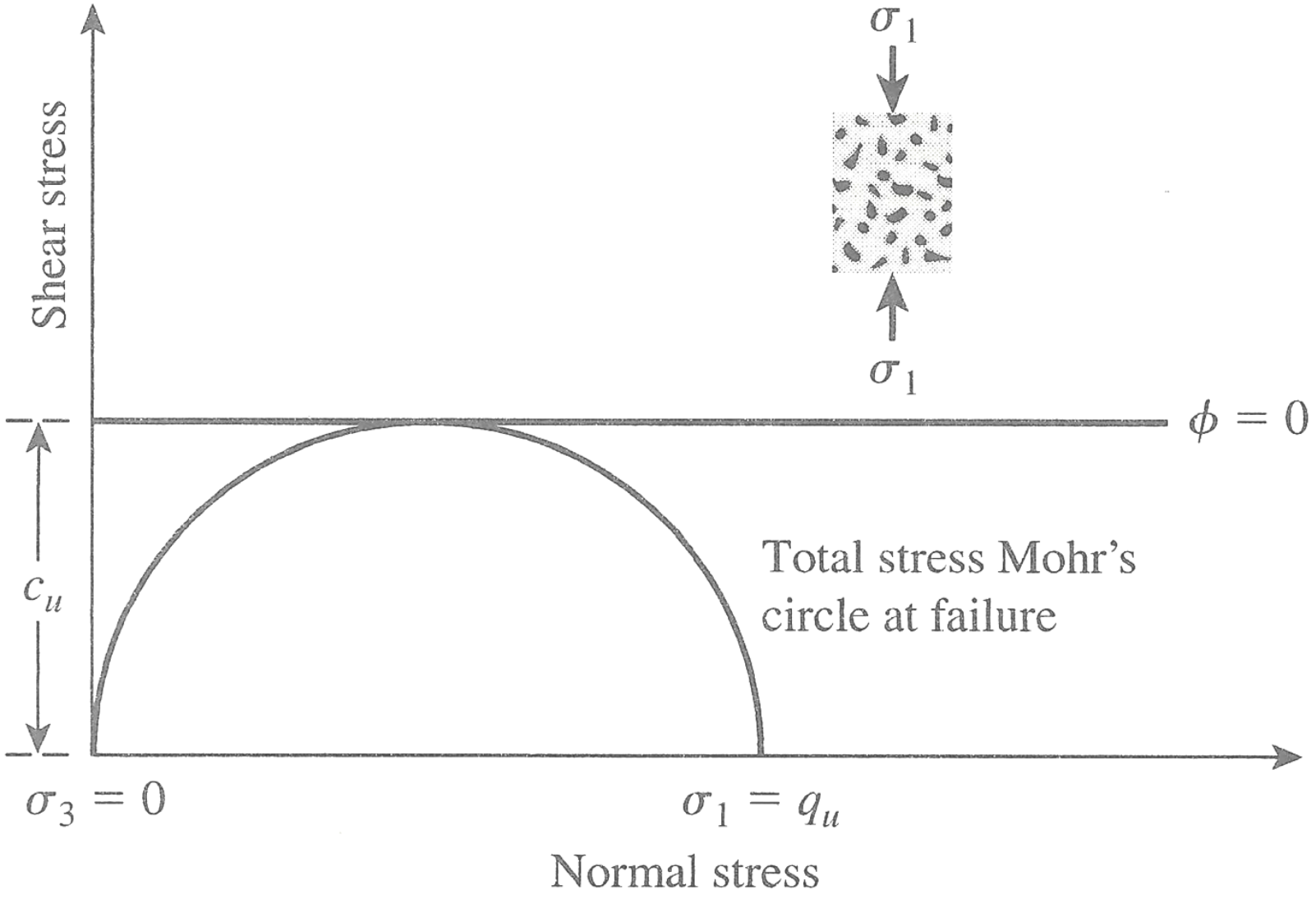

Figure 11.33 Unconfined compression test

- Where q_u is the unconfined compression strength. ***Table 11.4*** unconfined gives the approximate consistencies of clays on the basis of their unconfined compression test equipment is shown in ***Figure 11.34***.

- Theoretically, for similar saturated clay specimens, the unconfined compression test and the unconsolidted undrained triaxial test should yield the same values of c_u. In practice, however, unconfined compression test on saturated clays yield slightly lower values of cu than those obtained from unconsolidated undrained test.

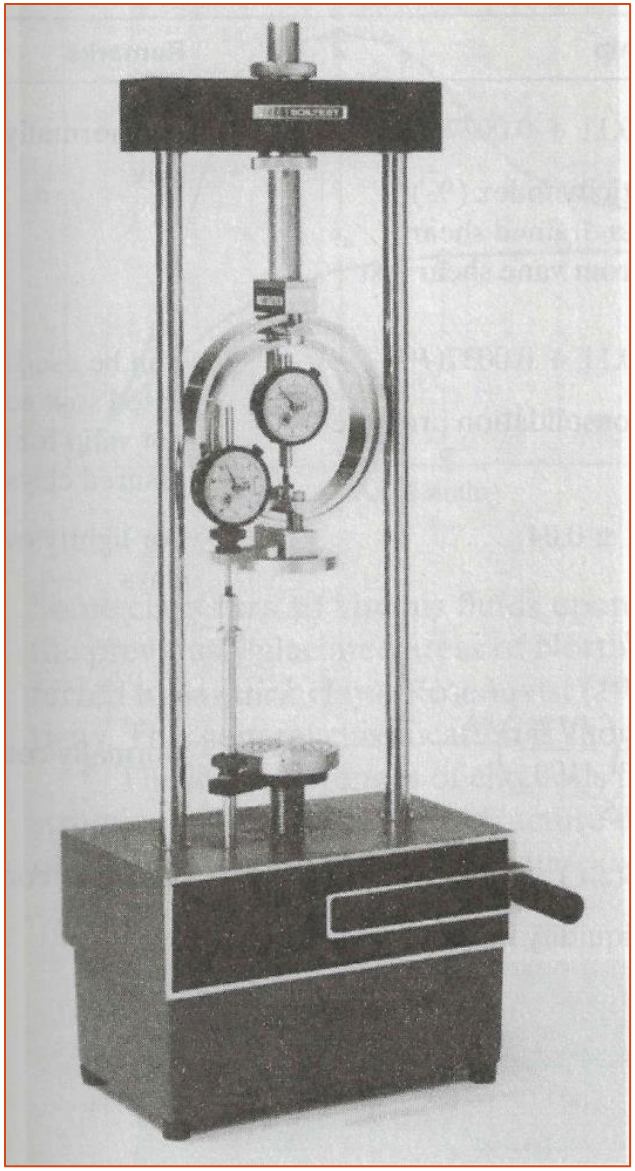

Figure 11.34 Unconfined compression test equipement (Curtesy of Soiltes, Inc., Lake Bluff, Illinois)

Figure Conducting an unconfined compression test.

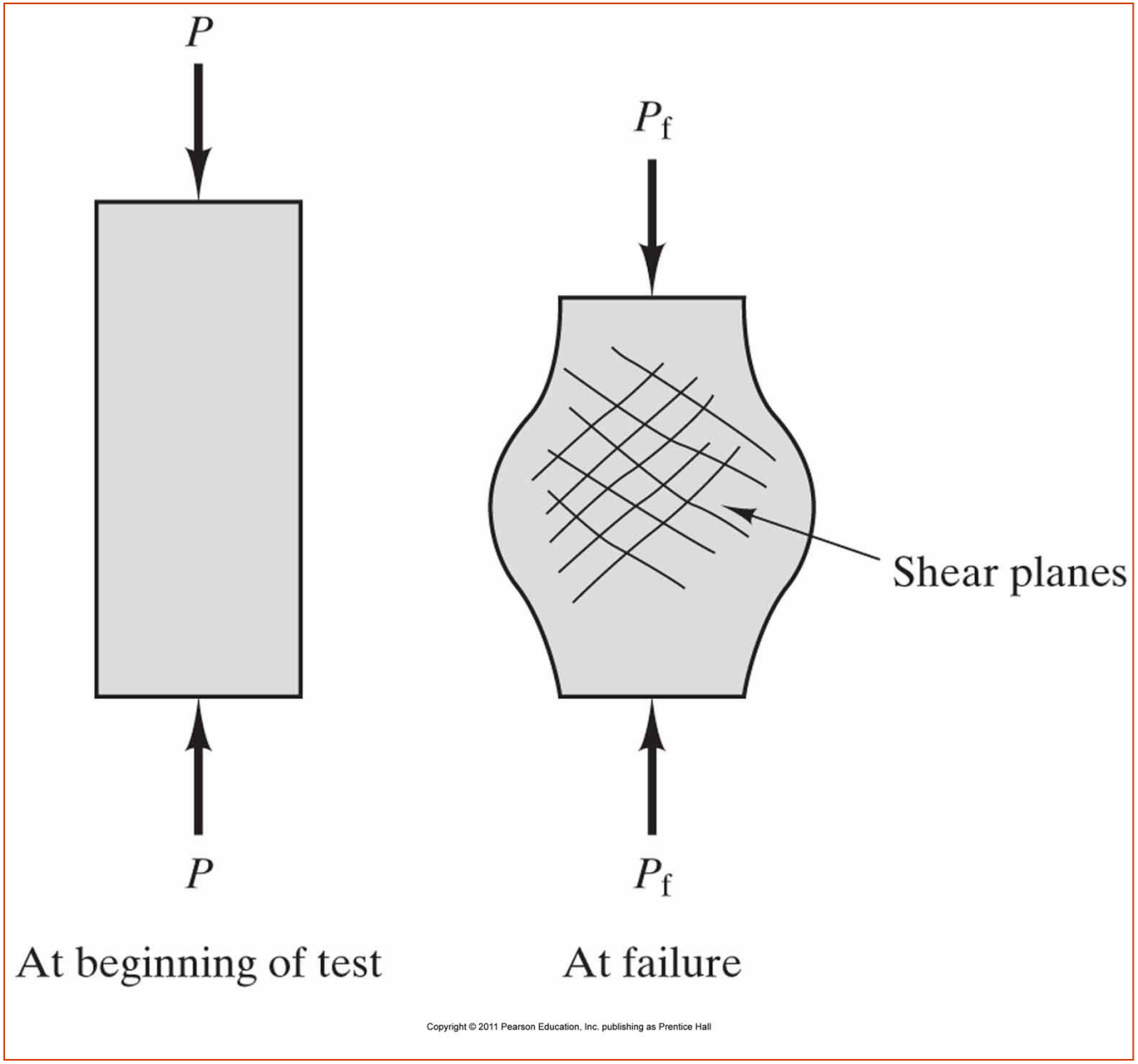

Figure Loading and failure mode in an unconfined compression test.

Table 11.4 General Relationship of Consistency and Unconfined Compression Strength of Clays

Consistency	q_u kN/m^2	q_u ton/ft^2
Very soft	0–25	0–0.25
Soft	25–50	0.25–0.5
Medium	50–100	0.5–1
Stiff	100–200	1–2
Very stiff	200–400	2–4
Hard	>400	>4

11.13 EMPIRICAL RELATIONSHIPS BETWEEN UNDRAINED COHESION AND EFFECTIVE OVERBURDEN PRESSURE

EMPIRICAL RELATIONSHIPS BETWEEN UNDRAINED COHESION AND EFFECTIVE OVERBURDEN PRESSURE

- Several empirical relationships can be observed between cu and the effective overburden pressure (σ'_o) in the field. Some of these relationships are summarized in ***Table 11.5***.

- The overconsolidation ratio was defined as:

- $$OCR = \frac{\sigma'_c}{\sigma'_o}$$

- Where:
  - σ_c=preconsolidation pressure

Table 11.5 Empirical Equations Related to c_u and σ'_O

Reference	Relationship	Remarks
Skempton (1957)	$\frac{c_{u(\text{VST})}}{\sigma'_O} = 0.11 + 0.0037(PI)$ PI = plasticity index (%) $c_{u(\text{VST})}$ = undrained shear strength from vane shear test	For normally consolidated clay
Chandler (1988)	$\frac{c_{u(\text{VST})}}{\sigma'_c} = 0.11 + 0.0037(PI)$ σ'_c = preconsolidation pressure	Can be used in overconsolidated soil; accuracy ±25%; not valid for sensitive and fissured clays
Jamiolkowski, *et al.* (1985)	$\frac{c_u}{\sigma'_c} = 0.23 \pm 0.04$	For lightly overconsolidated clays
Mesri (1989)	$\frac{c_u}{\sigma'_O} = 0.22$	
Bjerrum and Simons (1960)	$\frac{c_u}{\sigma'_O} = 0.45\left(\frac{PI\,\%}{100}\right)^{0.5}$ for $PI > 0.5$	Normally consolidated clay
	$\frac{c_u}{\sigma'_O} = 0.18(LI)^{0.15}$ for LI = liquidity index > 0.5	Normally consolidated clay
Ladd, *et al.* (1977)	$\frac{\left(\frac{c_u}{\sigma'_O}\right)_{\text{overconsolidated}}}{\left(\frac{c_u}{\sigma'_O}\right)_{\text{normally consolidated}}} = (OCR)^{0.8}$ OCR = overconsolidation ratio	

11.14 SENSITIVITY AND THIXOTROPY OF CLAY

SENSITIVITY AND THIXOTROPY OF CLAY

- For many naturally deposited clay soils, the unconfined compression strength is reduced greatly when the soils are tested after remolding without any change in the moisture content, as shown in ***Figure 11.35***. this property of clay soils is called sensitivity. The degree of sensitivity may be defined as the ratio of the unconfined compression strength in an undisturbed state to that in a remolded state, or Eq. (11.25)

$$S_t = \frac{q_{u(undisturbed)}}{q_{u(remolded)}}$$

- The sensitivity ratio of most clays ranges from about 1 to 8; however, highly floculent marine clay deposits may have sensitivity ratios ranging from about 10 to 80.

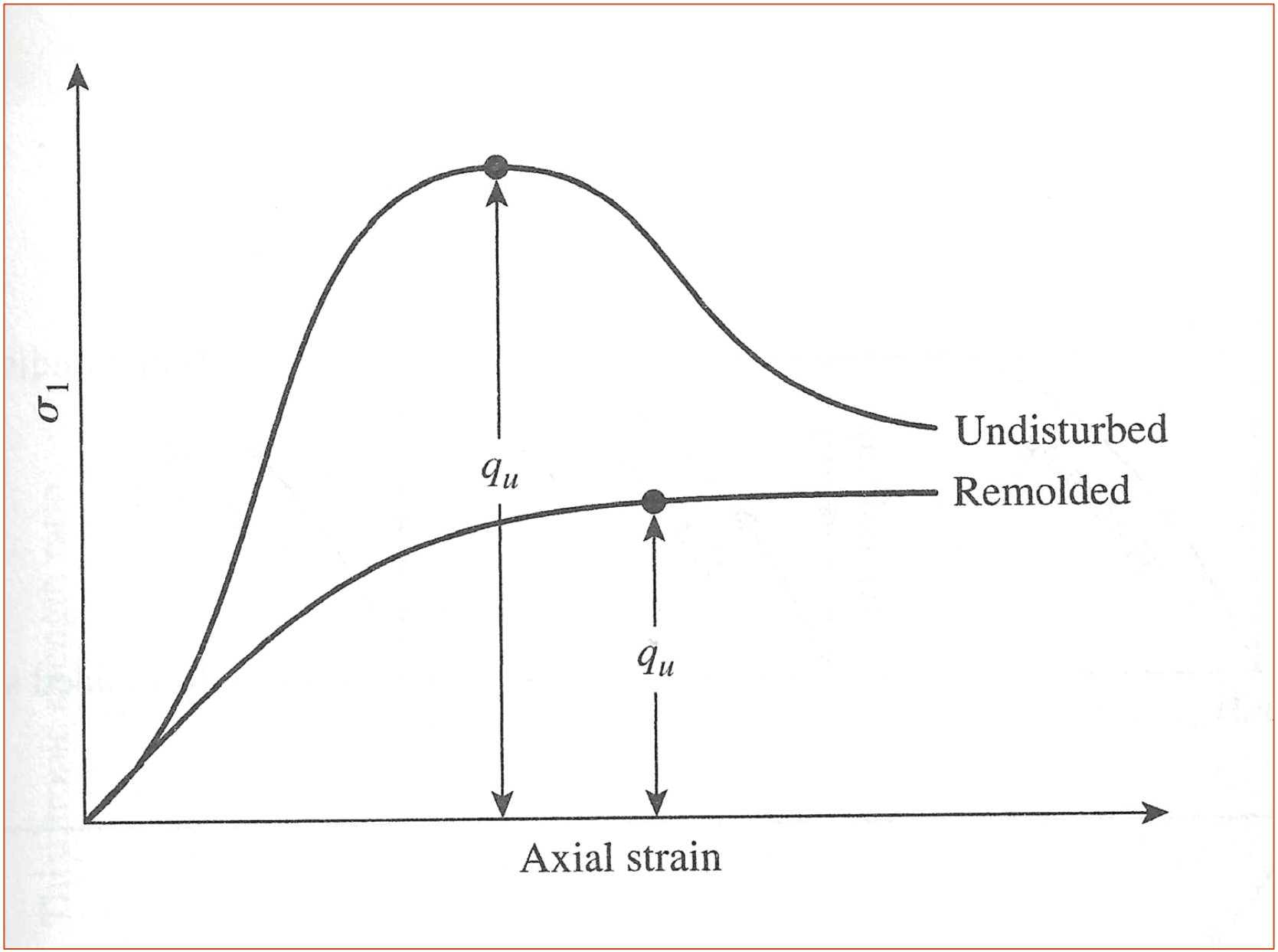

Figure 11.35 Unconfined compression strength for undisturbed and remolded clay

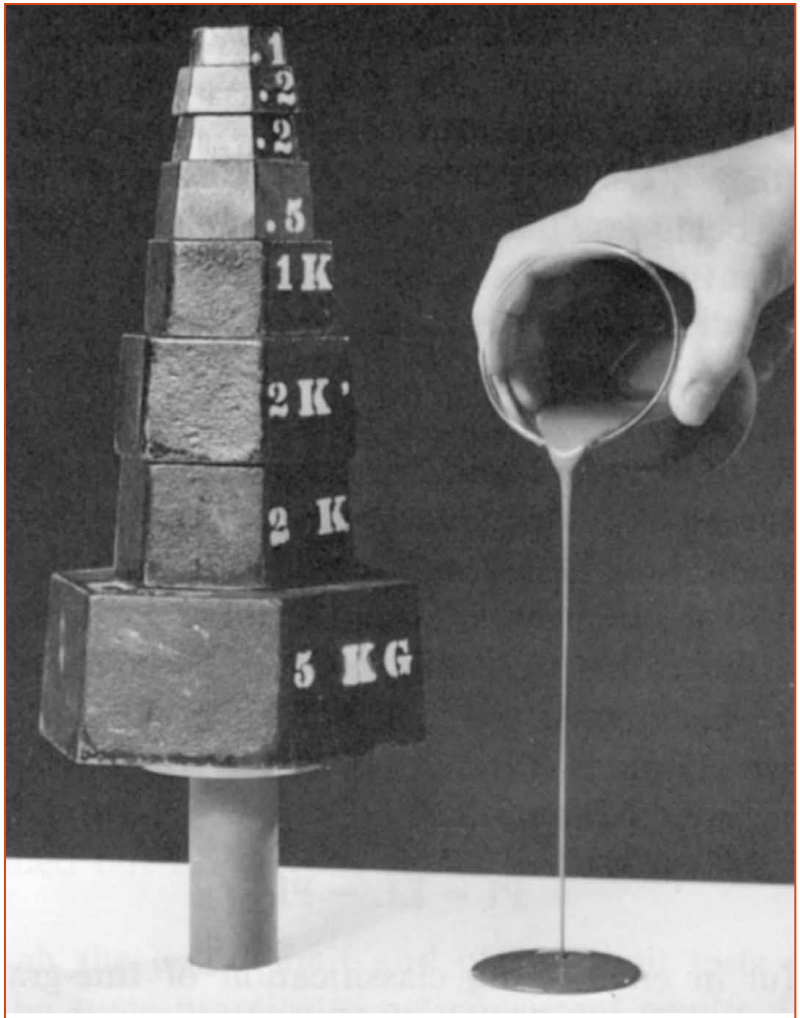

Figure Undisturbed and remolded samples of Leda clay from Ottawa, Ontario. Both samples are at the same moisture content; the only difference is the remolding. This is an extreme example of a sensitive clay, with an S_t of about 1500. (National Research Council of Canada.)

TABLE Typical Classification of Sensitivity[a]

Classification	Sensitivity, S_t	
	United States	Sweden
Low sensitivity	2–4	< 10
Medium sensitivity	4–8	10–30
High sensitivity	8–16	30–50
Quick	> 16	50–100
Extra quick	—	> 100

[a] Adapted from Holtz and Kovacs, 1981.

- Some clays turn to viscous fluids upon remolding. These clays are found mostly in the previously glaciated areas of North America and Scandinavia. Such clays are referred to as quick clays. Rosenqvist (1953) classified clays on the basis of their sensitivity. This general classification is shown in ***Figure 11.36***.

- The loss of strength of clay particle structure that was developed during the original process of sedimentation.

- If, however, after remolding, a soil specimen is kept in an undisturbed state (that is, without any change in the moisture content), it will continue to gain strength with time. This phenomenon is referred to as thixotropy.

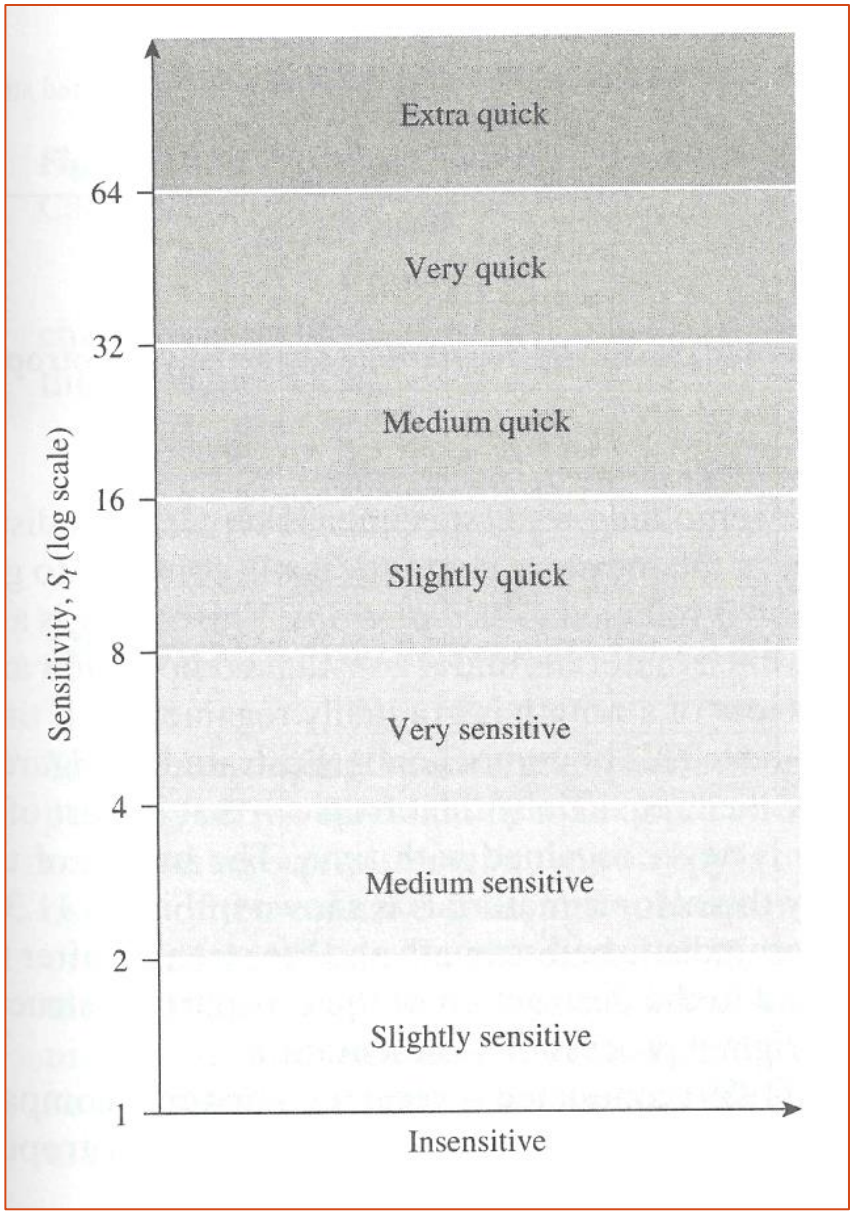

Figure 11.36 Classification of clays based on sensitivity

- Thixotropy is a time dependent, reversible process in which material under constant composition and volume soften when remolded.

- This loss of strength is gradually regained with time when the materials are allowed to rest. This phenomenon is illustrated in ***Figure 11.37a***.

- Most soils, however, are partially thixotropic that is, part of strength loss caused by remolding is never regained. The nature of the strength time variation for partially thixotropic materials is shown in ***Figure 11.37 b***.

- For soils, the difference between the undisturbed strength and the strength after thixotropic hardening can be attributed to the destruction of the clay particle structure that was developed during the original process of sedimentation.

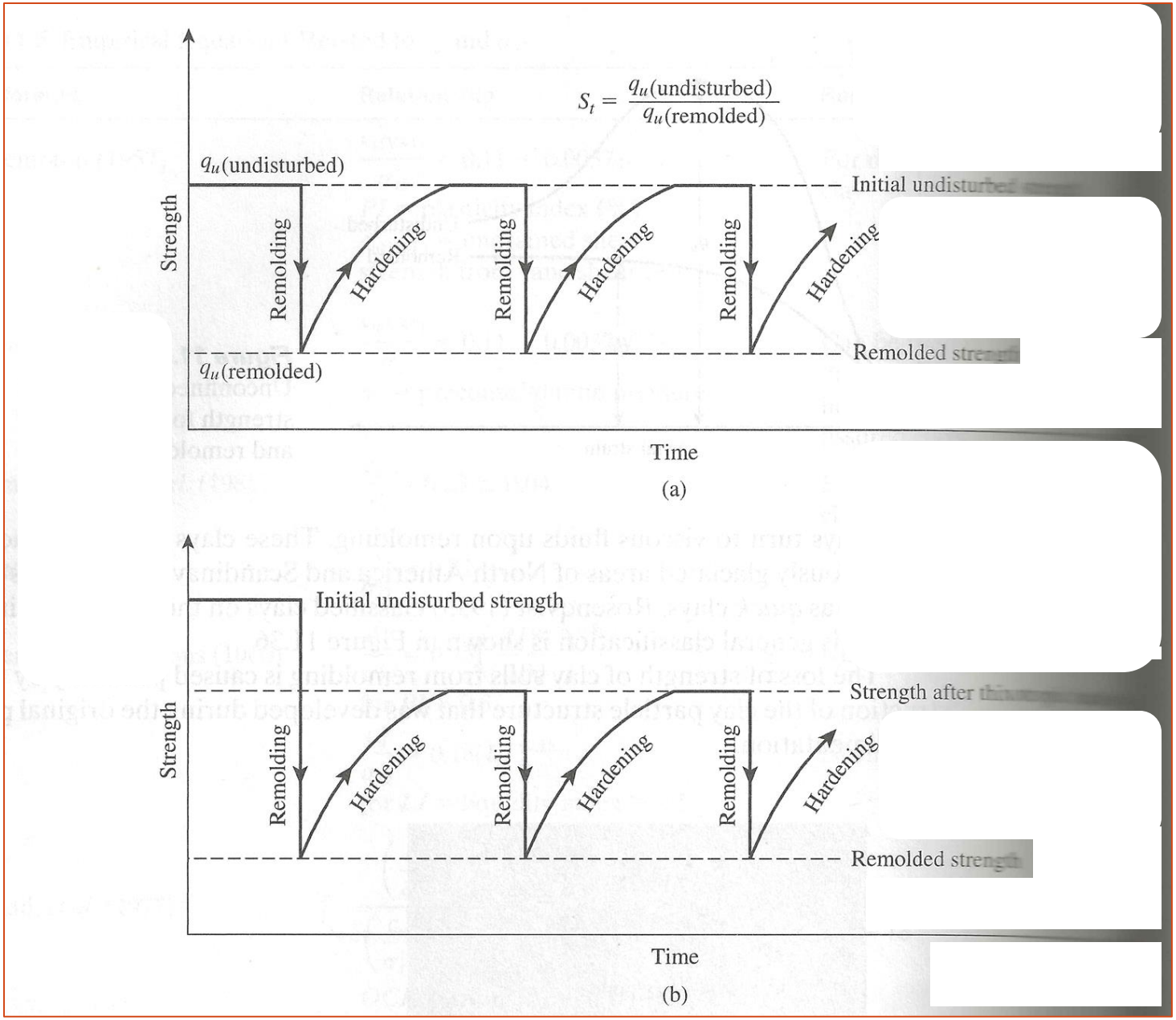

Figure 11.37 Behavior of (a) thixotropic material: (b) partially thixotropic material

- Seed and Chan (1959) conducted several test on three compacted clays with a water content near or below the plastic limit to study the thixotropic strength regain characteristics of the clays. The results of these test are shown in ***Figure 11.38***. Note that in ***Figure 11.38*** Eq. (11.26)

- Thixotropic strength ratio= $\frac{c_u(\text{at time } t \text{ after compaction})}{c_u(\text{at time } t=0 \text{ after compaction})}$

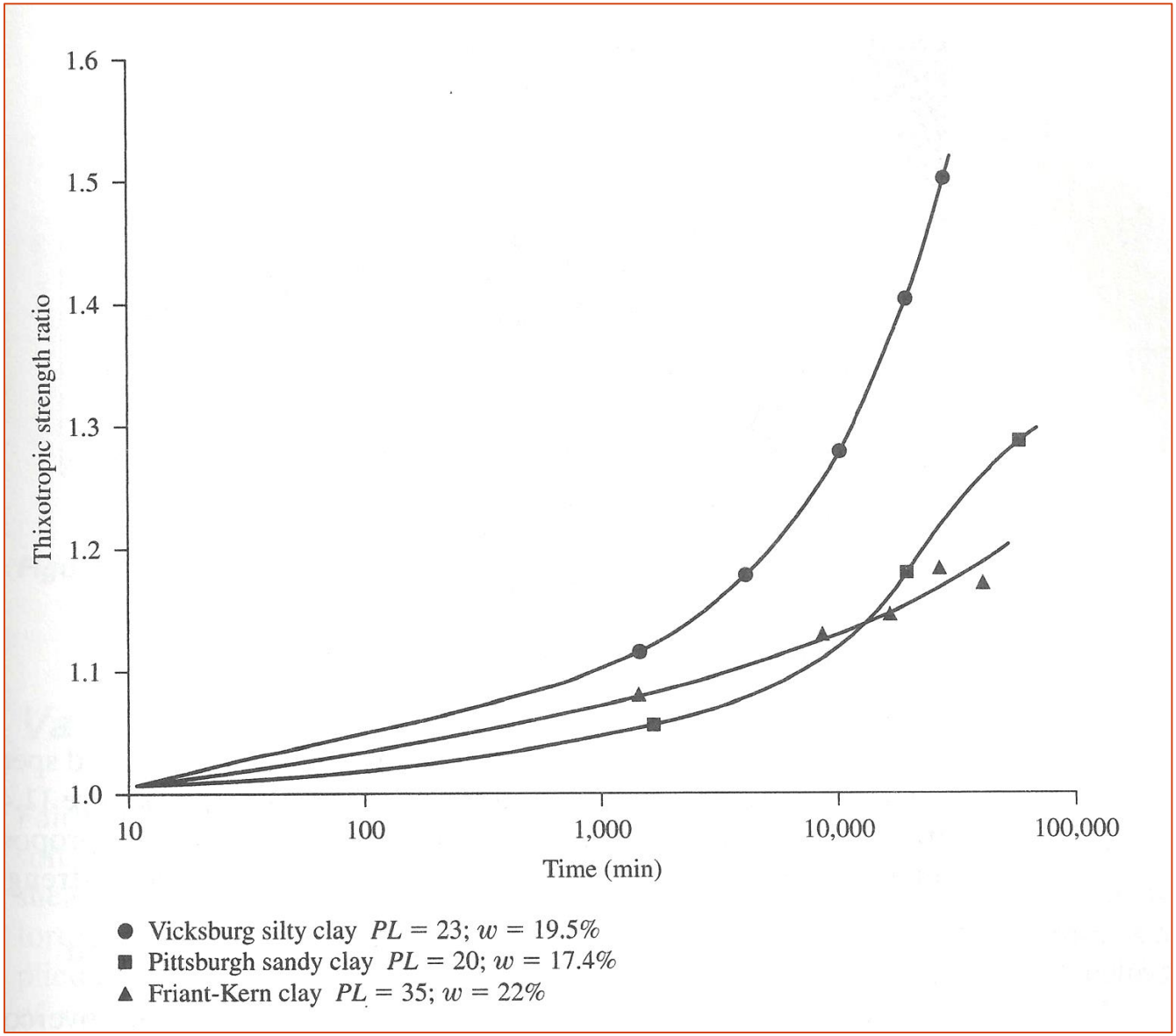

Figure 11.38 Thixotropic strength increase with time for three days (Based on Seed and Chen, 1959)

11.16 VANE SHEAR TEST

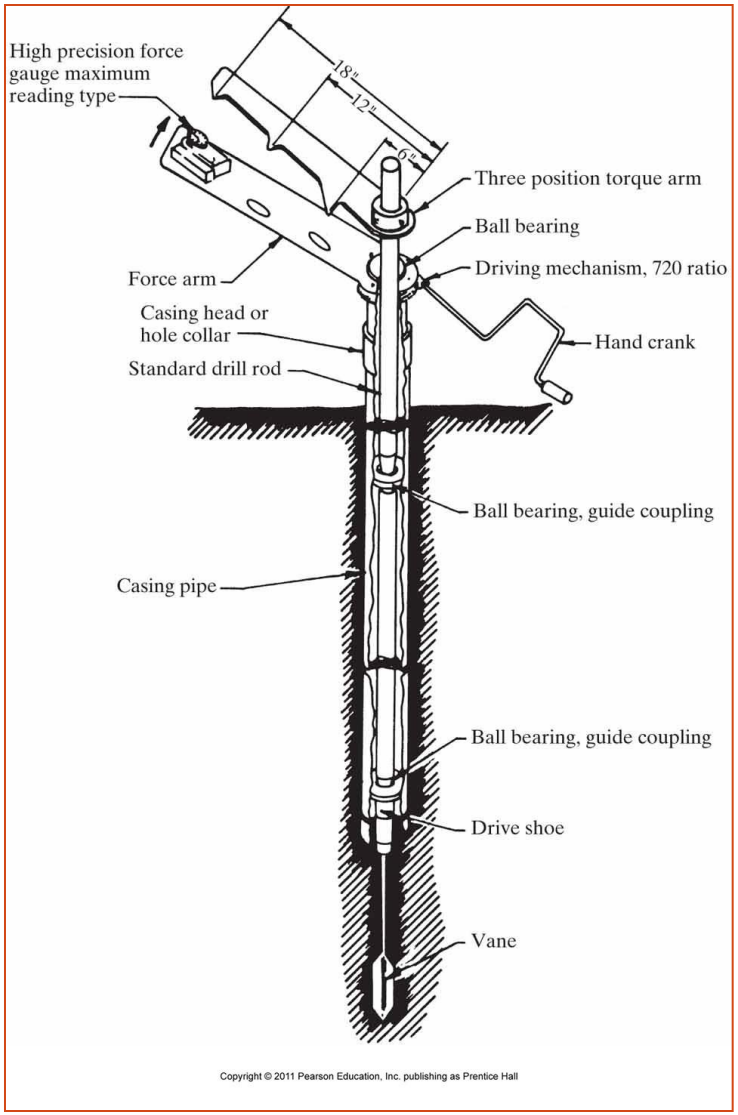

Figure Vane shear test. (U.S. Navy, 1982.)

VANE SHEAR TEST

- Fairly reliable results for the undrained shear strength, ***cu*** (**ϕ**= 0 concept), of very soft to medium cohesive soils may be obtained directly form vane shear tests.

- The shear vane usually consists of four thin, equal sized steel plates welded to a steel torque rod (***Figure 11.42***). First, the vane is pushed into the soil. Then toque is applied at the top of the torque rod to rotate the vane at a uniform speed. A cylinder of soil of height h and diameter d will resist the torque until the soil fails. The undrained shear strength of the soil can bee calculated as follow.

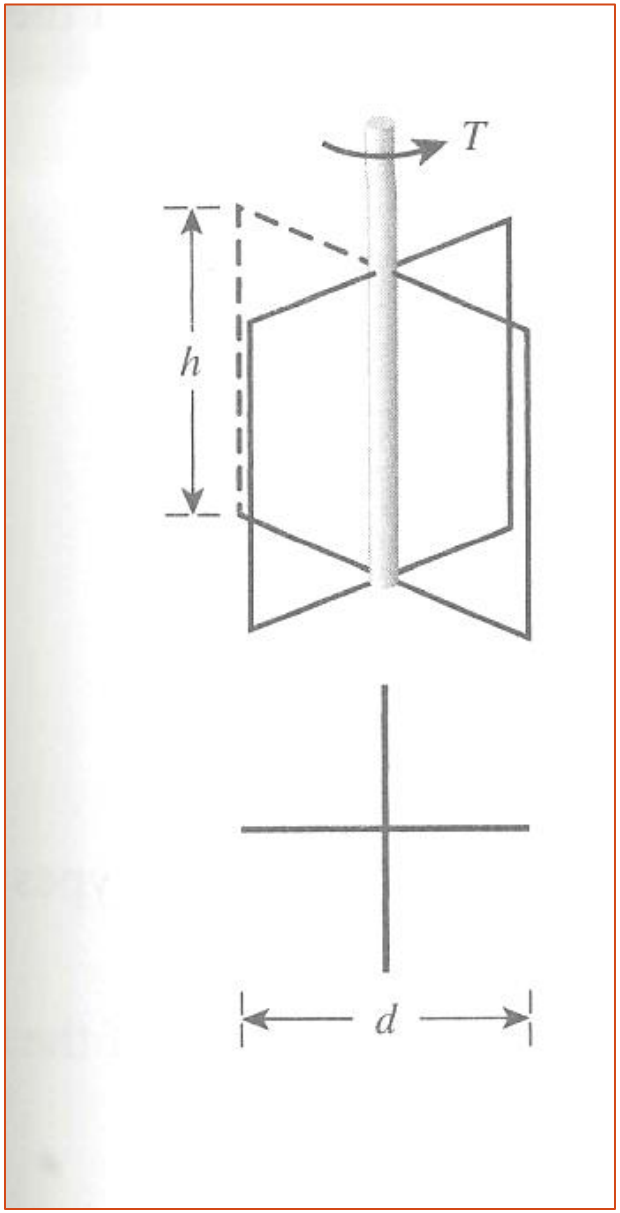

Figure 11.42 Diagram of vane shear test equipment

- If T is the maximum torque applied at the head of the torque rod to cause failure, it should be equal to the sum of the resisting moment of the shear force along the side surface of the soil cylinder (***M_s***) and the resisting moment of the shear force at each end (***M_e***) (***Figure 11.43***):

- $$T = M_s + M_e + M_e$$

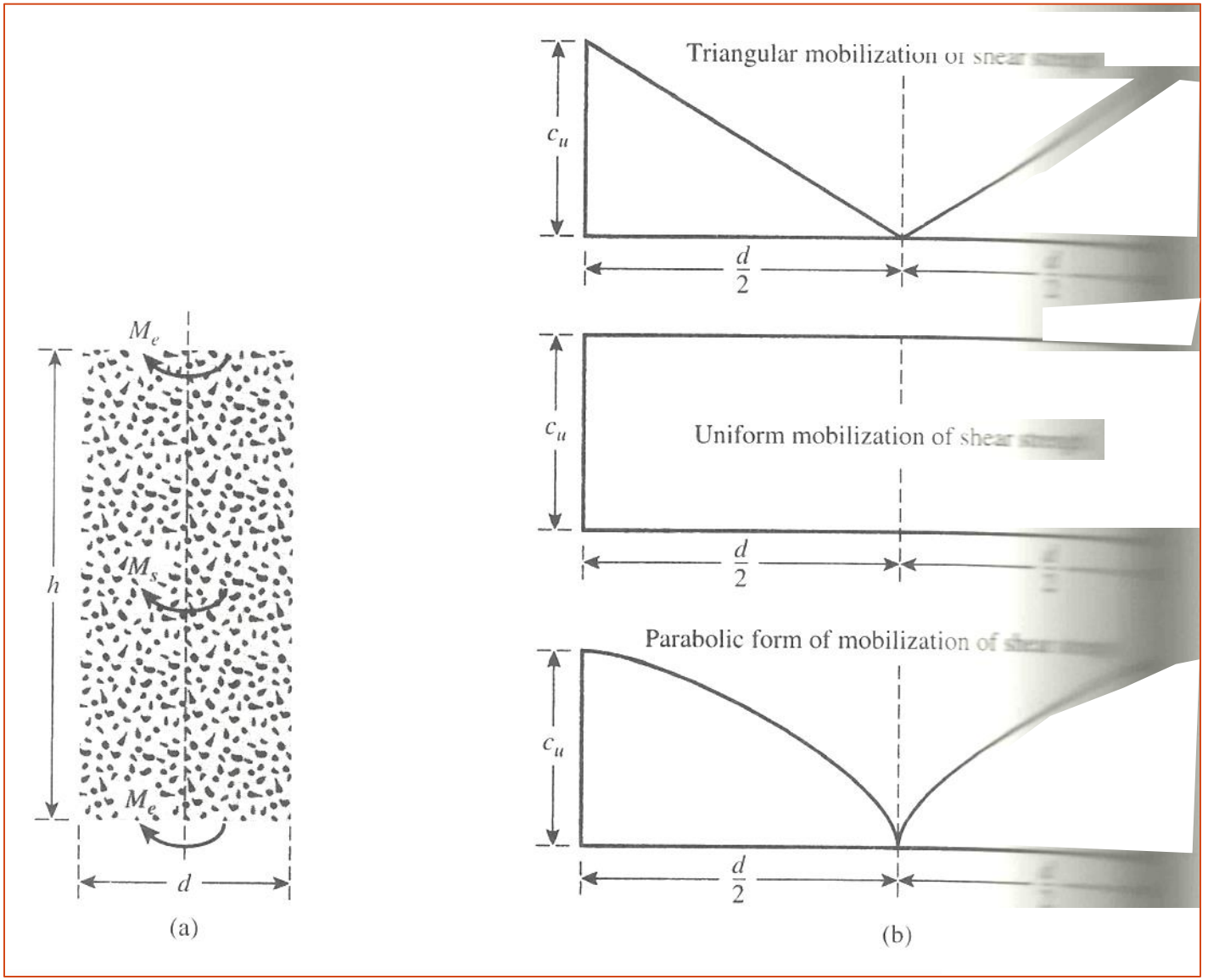

Figure 11.43 Derivation of Eq. (11.31): (a) resisting moment of shear force, (b) variations in shear strength- mobilization

- The resisting moment can be given as Eq. (11.29)

- $$M_s = (\pi dh)c_u(d/2) \qquad (11.29)$$

Where:

- d= diameter of the shear vane
- h= height of the shear vane

- For the calculation of Me, investigators have assumed several types of distribution of shear strength mobilization at the ends of the soil cylinder:

1. Triangular. Shear strength mobilization cu at the periphery of the soil cylinder and decreases linearly to zero at the center.

2. Uniform. Shear strength mobilization is constant (that is, cu) from the periphery to the center of the soil cylinder.

3. Parabolic. Shear strength mobilization is cu at the periphery of the soil cylinder and decreases parabolically to zero at the center.

- These variations in shear strength mobilization are shown in ***Figure 11.43b***. In general, the torque, ***T***, at failure can be expressed as Eq. (11.30)

- $$T = \pi c_u \left[\frac{d^2 h}{2} + \beta \frac{d^3}{4} \right] \qquad (11.30)$$

Or Eq. 11.31

- $$c_u = \frac{T}{\pi \left[\frac{d^2 h}{2} + \beta \frac{d^3}{4} \right]} \qquad (11.31)$$

Where:

- β=1/2 for triangular mobilization of undrained shear strength
- β =2/3 for uniform mobilization of undrained shear strength
- β =3/5 for parabolic mobilization of undrained shear strength

- Note that Eq. (11.31) usually is referred to as Calding's equation

- Vane shear test can be conducted in the laboratory and in the field during soil exploration. The laboratory shear vane has dimensions of about 13 *mm*. in diameter and 25 *mm* in height. ***Figure 11.44*** shows a photograph of laboratory vane shear test equipment. ***Figure 11.45*** shows the field vanes recommended by ASTM 2004. ***Table 11.6*** gives the ASTM recommended dimensions of field vanes.

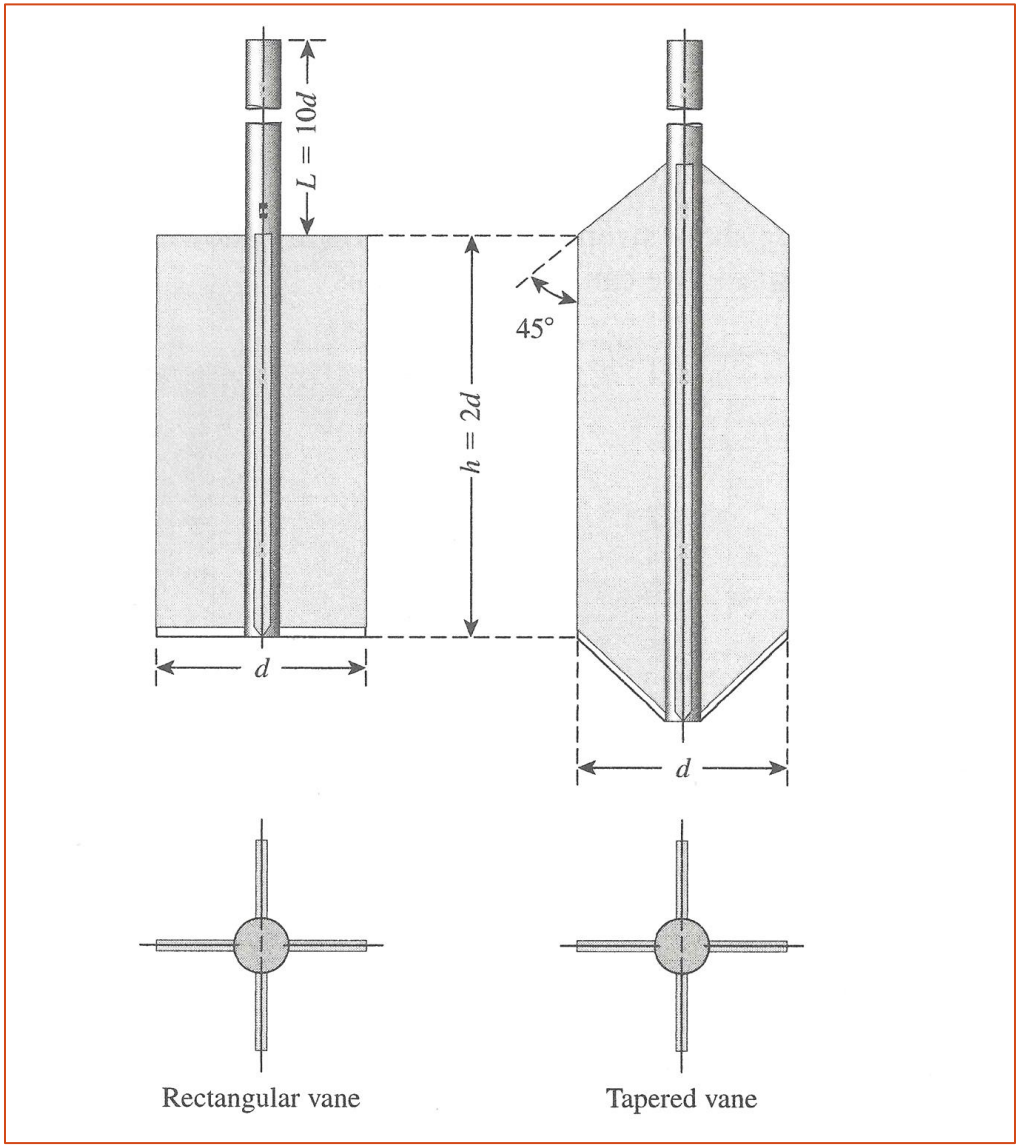

Figure 11.45 Geometry field vanes (Source: From Annual Book of ASTM Standards, 04.08, p.346. Copyright 2004 American Society for Testing Materials. Reprinted with permission)

- Eq. (11.32)

- $$c_u\left(kN/m^2\right)=\frac{T(N.m)}{\left(366\times10^{-8}\right)d^3} \qquad (11.32)$$

- And Eq. (11.33)

- $$c_u\left(lb/\ ft^2\right)=\frac{T\left(lb.ft\right)}{0.00211d^3} \qquad (11.33)$$

- In the field, where considerable variation in the undrained shear strength can be found with depth, vane shear test are extremely useful. In a short period, one can establish a reasonable pattern of the change of c_u with depth.
- However, if the clay deposit at a given site is more or less uniform, a few unconsolidted undrained triaxial tests on undisturbed specimens will allow a reasonable estimation of soil parameters for design work. Vane shear test also are limited by the strength of soils in which they can be used.
- The undrained shear strength obtained from a vane shear test also depends on the rate of application of torque T.

- ***Figure 11.46*** shows a comparison of the variation of c_u with the depth obtained from field vane shear test, unconfined compression tests, and unconsolidated undrained triaxial tests for Morgan City recent alluvium (Arman, et al., 1975). It can be seen that the vane shear test values are higher compared to the others.

- Bjerrum (1974) also showed that, as the plasticity of soil increases, cu obtained from vane shear test may give results that are unsafe for foundation design. For this reason, he suggested the correction

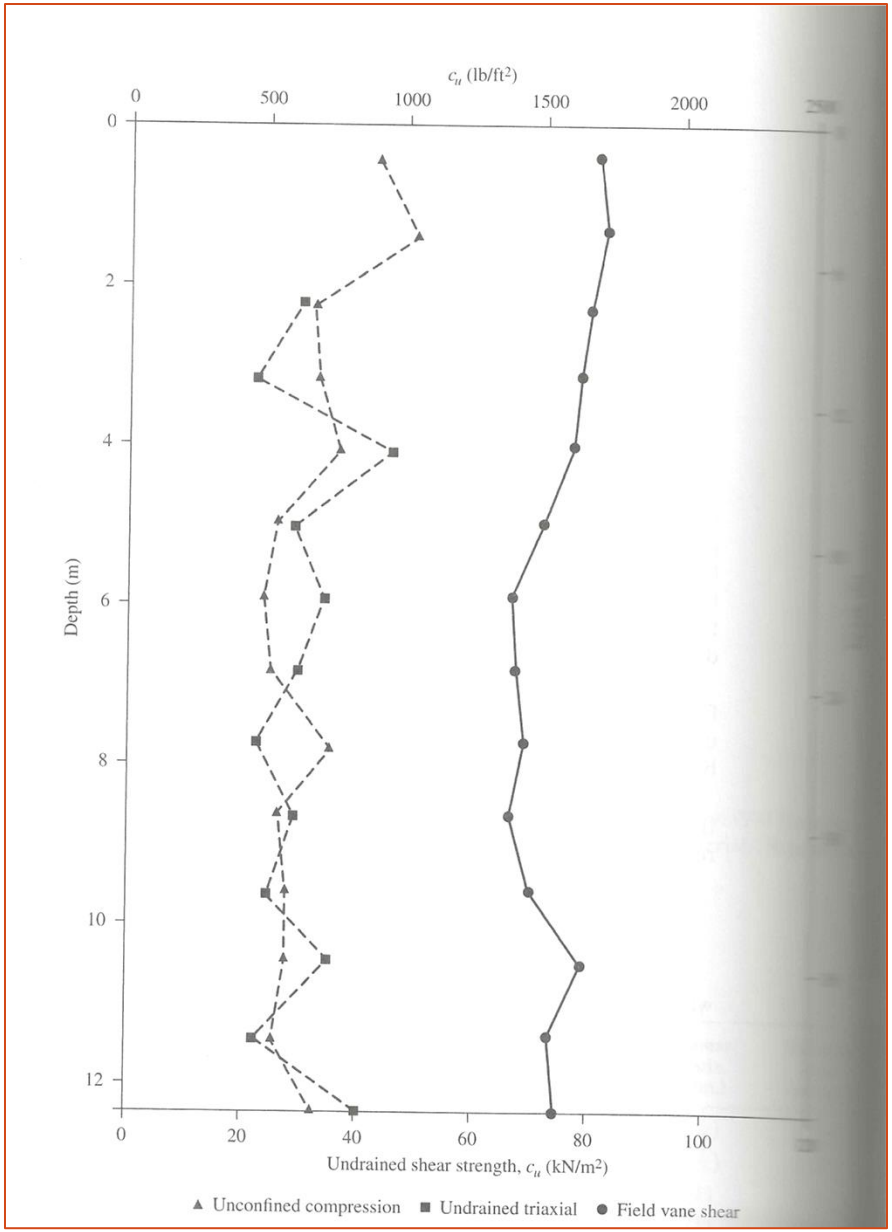

Figure 11.46 Variation of cu with depth obtained form various test for Morgan City recent alluvium Drawn form the test results of Arman, *et al., 1975)*

- $$c_{u(design)} = \lambda c_{u(vane-shear)}$$ (11.34)

Where

- λ=correction factor=1.7 -0.54 log (PI) (11.35)
- *PI*=Plasticity index

- More recently, Morris and Williams 1994 gave the correlations of λ as Eq (11.36)

$$\lambda = 1.18e^{-0.08(PI)} + 0.57(\ for - PI > 5)$$

- (11.36)

- and Eq. (11.37)

- $$\lambda = 7.01e^{-0.08(LL)} + 0.57(\ for - LL > 20) \quad (11.37)$$

Where:

  - LL=liquid limit (%)

EXAMPLE 11.9

- A soil profile is shown in ***figure 11.47***. the clay is normally consolidated. Its liquid limit is 60 and its plastic limit is 25. Estimate the unconfined compression strength of the clay at a depth of 10 m measured from the ground surface. Use skemptons relationship from table 11.5 and eqs. (11.34) and (11.35).

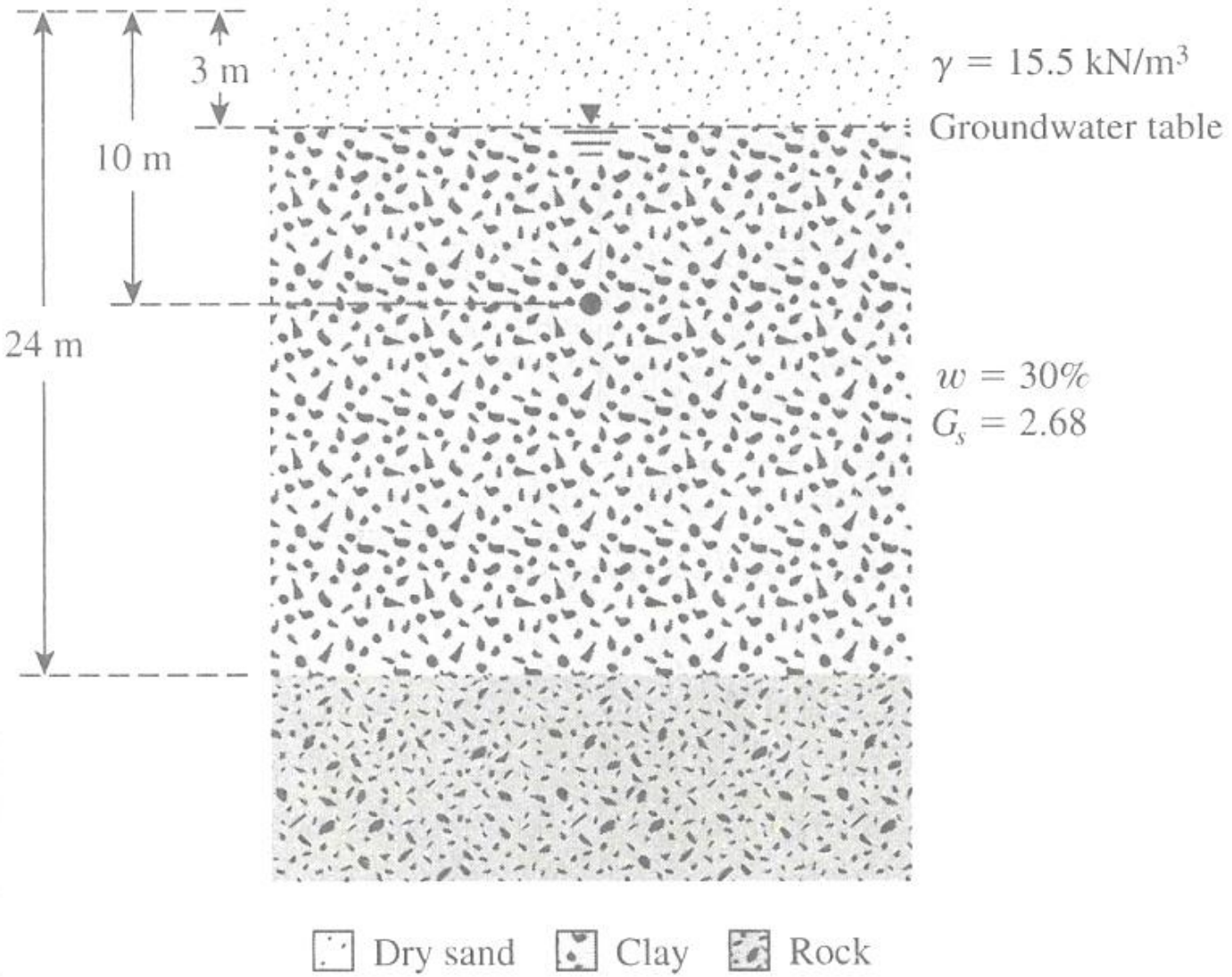
3 m
10 m
24 m
γ = 15.5 kN/m³
Groundwater table
w = 30%
G_s = 2.68
Dry sand
Clay
Rock

Figure 11.47

SOLUTION

- For the saturated clay layer, the void ratio is
- $$e = wG_s = (2.68)(0.3) = 0.8$$
- The effective unit weight is
- $$\gamma'_{clay} = \left(\frac{G_s - 1}{1+e}\right)\gamma_w = \frac{(2.68-1)(9.81)}{1+0.8} = 9.16\_KN/m\text{^}3$$
- The effective stress at a depth of 10m from the ground surface is
- $$\sigma'_0 = 3\gamma_{sand} + 7\gamma'_{clay} = (3)(15.5) + (7)(9.16) = 110.62\_KN/m\text{^}2$$

11.17 OTHER METHODS FOR DETERMINING UNDRAINED SHEAR STRENGTH

OTHER METHODS FOR DETERMINING UNDRAINED SHEAR STRENGTH

- A modified form of the vane shear test apparatus is the Torvane (***Figure 11.48***), which is a handheld device with a calibrated spring. This instrument can be used for determining c_u for tube specimens collected from the field. The torvane is pushed into the soil and then rotated until the soil fails. The undrained shear strength can be read at the top of the calibrated dial.

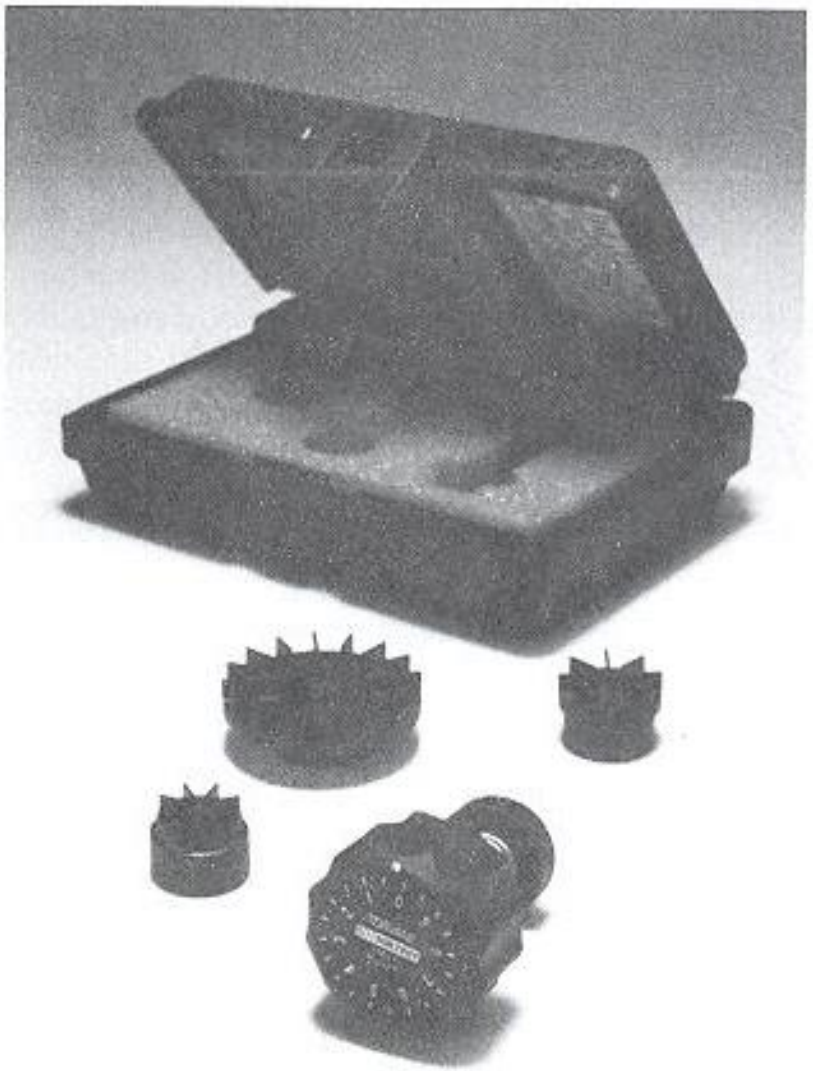

Figure 11.48
Torvane (*Courtesy* of Soiltest, Inc., Lake Bluff, Illinois)

- ***Figure 11.49*** shows a pocket penetrometer, which is pushed directly into the soil. The unconfined compression strength (q_u) is measured by a calibrated spring. This device can be used both in the laboratory and in the field.

Figure 11.49
Pocket penetrometer (*Courtesy* of Soiltest, Inc., Lake Bluff, Illinois)

- From table 11.5

- $$\frac{c_{u(VST)}}{\sigma'_0} = 0.11 + 0.0037(PI)$$

  $$\frac{c_{u(VST)}}{110.62} = 0.11 + 0.0037(60 - 25)$$

  and

  $$c_{u(VST)} = 26.49\_KN/m\text{^}2$$

- From eqs(11.34) and (11.35) we get

- $$c_u = \lambda c_{u(VST)}$$

  $$= [1.7 - 0.54\log(PI)]c_{u(VST)}$$

  $$= [1.7 - 0.54\log(60 - 25)]26.49 = 22.95\_KN/m\text{^}2$$

- So the unconfined compression strength is

- $q_u = 2c_u = (2)(22.95) = 45.9\_KN/m\text{^}2$

11.20 SUMMARY

SUMMARY

- In this chapter, the shear strengths of granular and cohesive soils were examined. Laboratory procedures for determining the shear strength parameters were described. In textbooks, determination of the shear strength parameters of cohesive soils appear to be fairly simple. However, in practice , the proper choice of these parameters for design and stability checks of various earth, earth retaining, and earth supported structures is very difficult and requires experience and an appropriate theoretical background in geotechnical engineering.

FIGURES

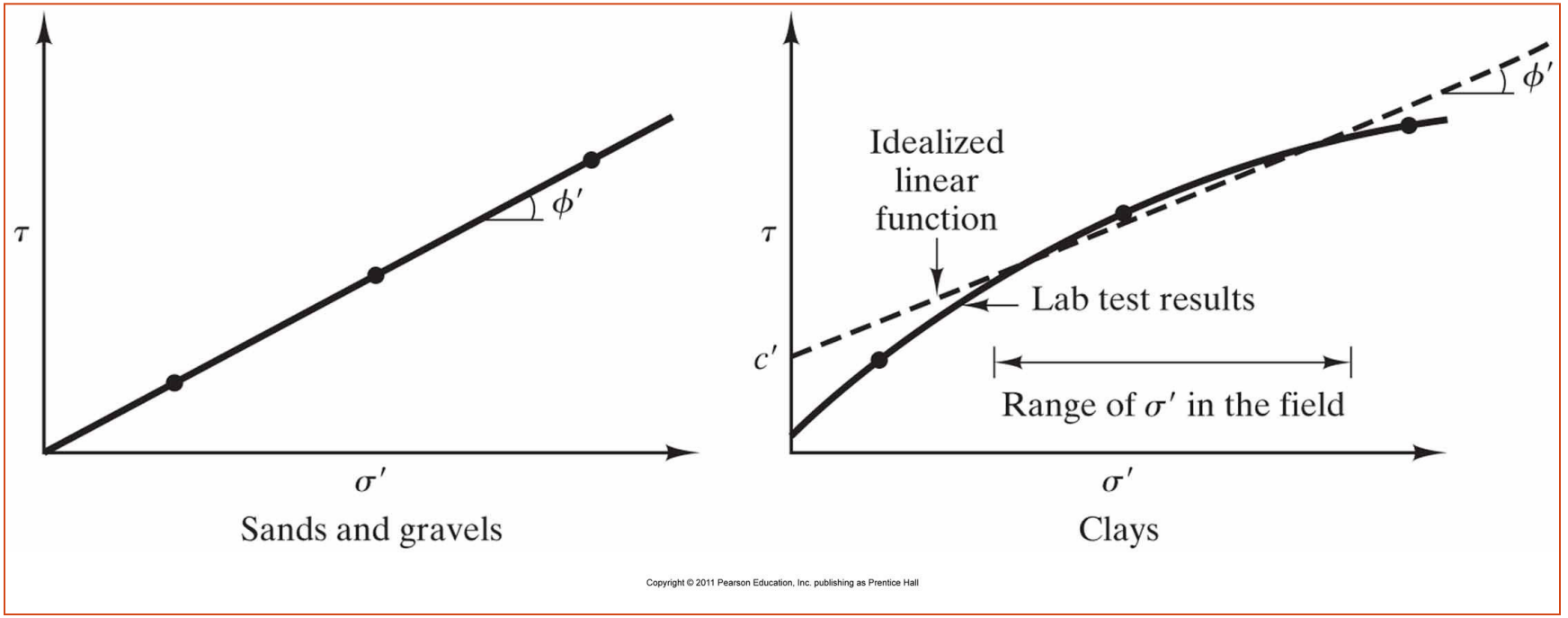

Figure Shear strength as a function of effective stress. Each data point represents the results of a laboratory test.

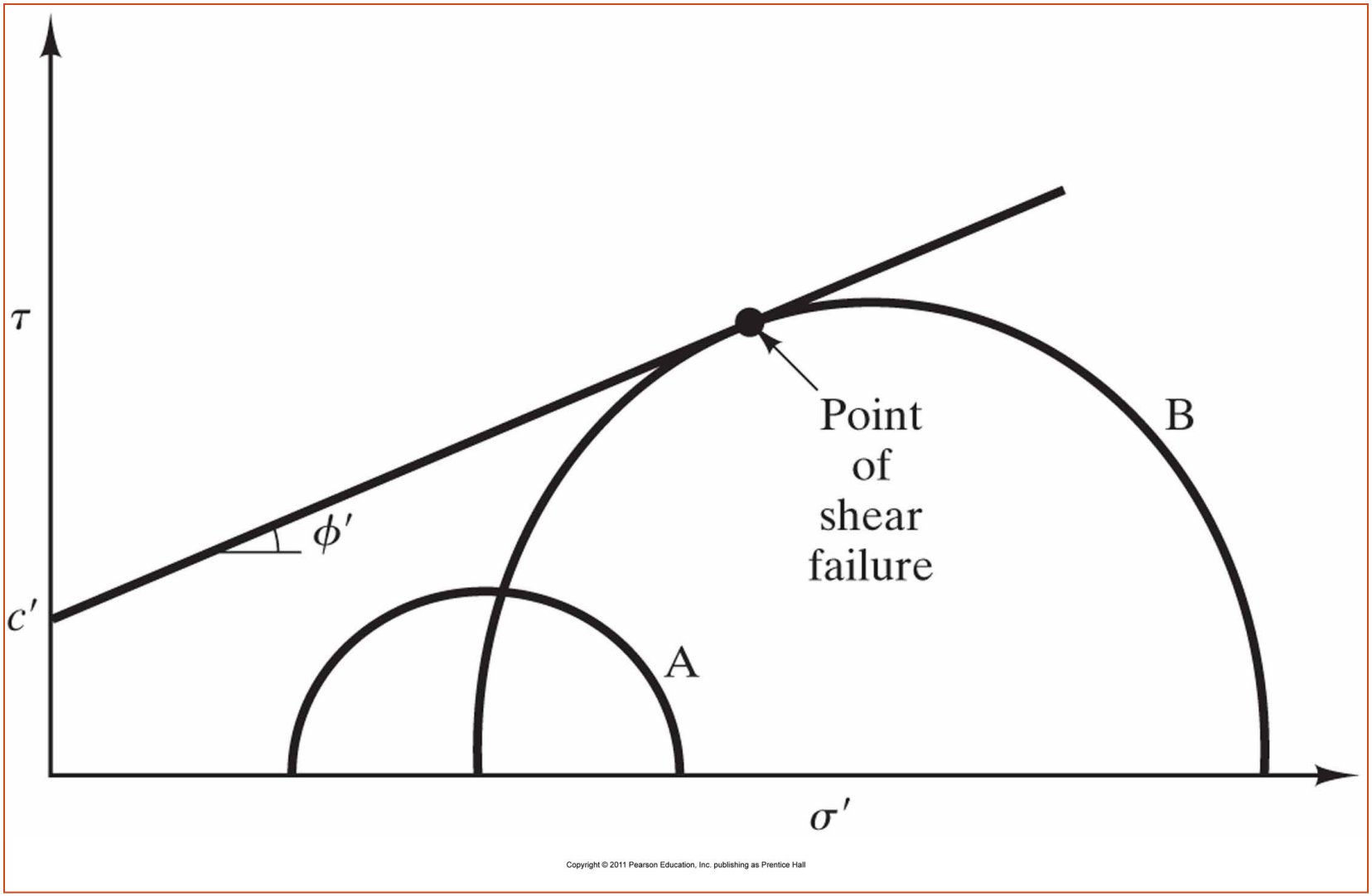

Figure Shear failure occurs when the Mohr circle is large enough to touch the failure envelope. Thus, no failure will occur at the point represented by Circle A, but failure will occur at the point represented by Circle B.

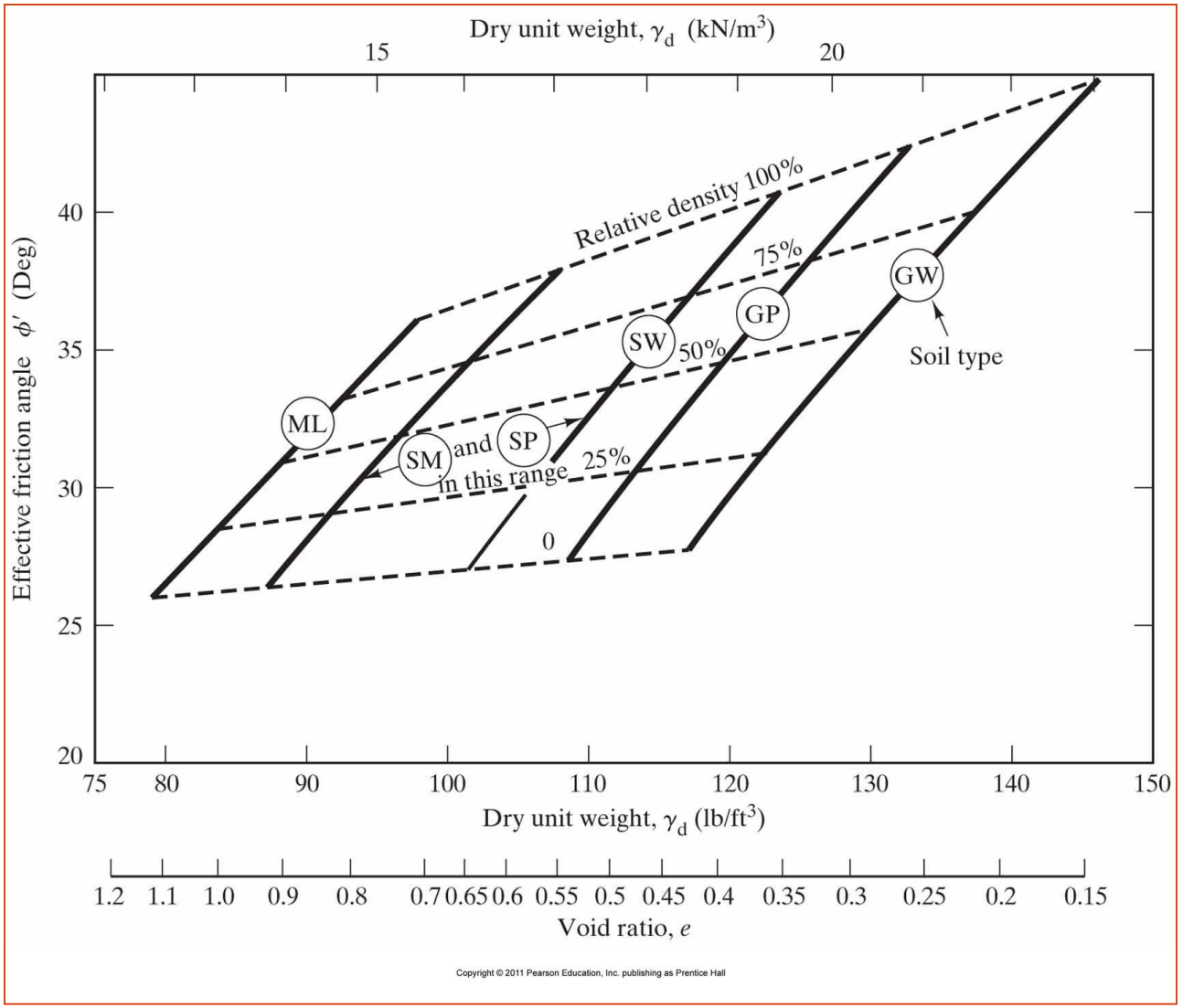

Figure Typical ϕ′ values for cohesionless soils without clay or cementing agents. (Adapted from U.S. Navy, 1982.)

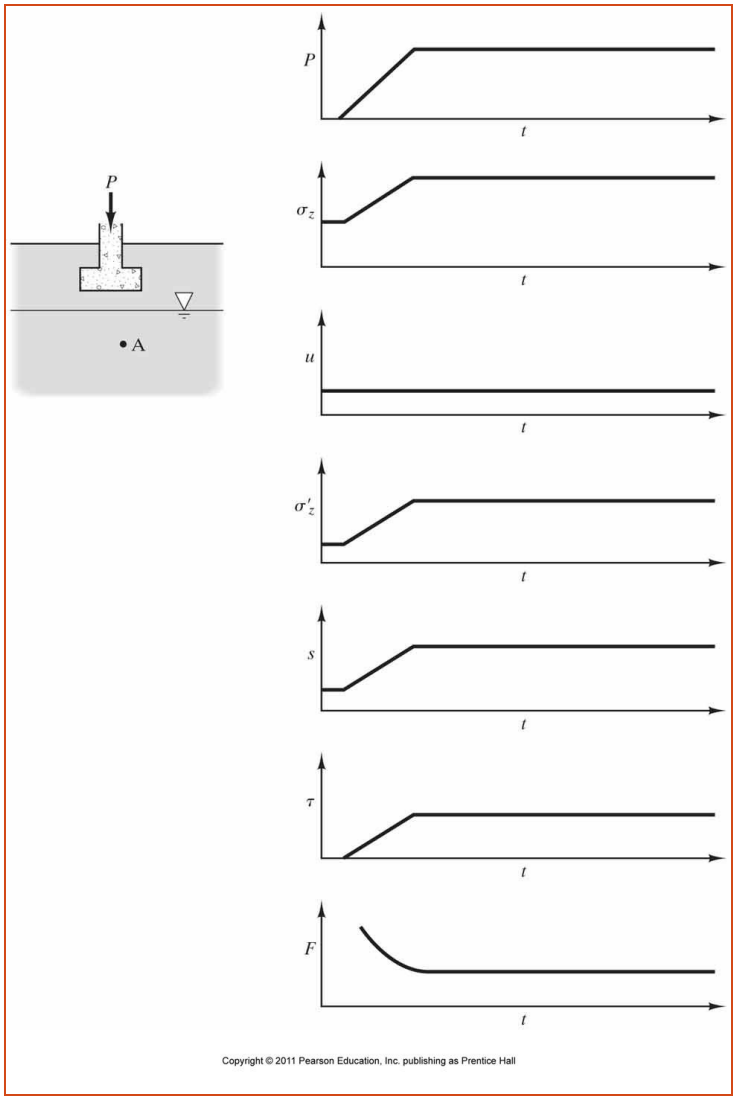

Figure Changes in normal and shear stresses, shear strength, and factor of safety with time at Point A in a saturated sand below a structural foundation.

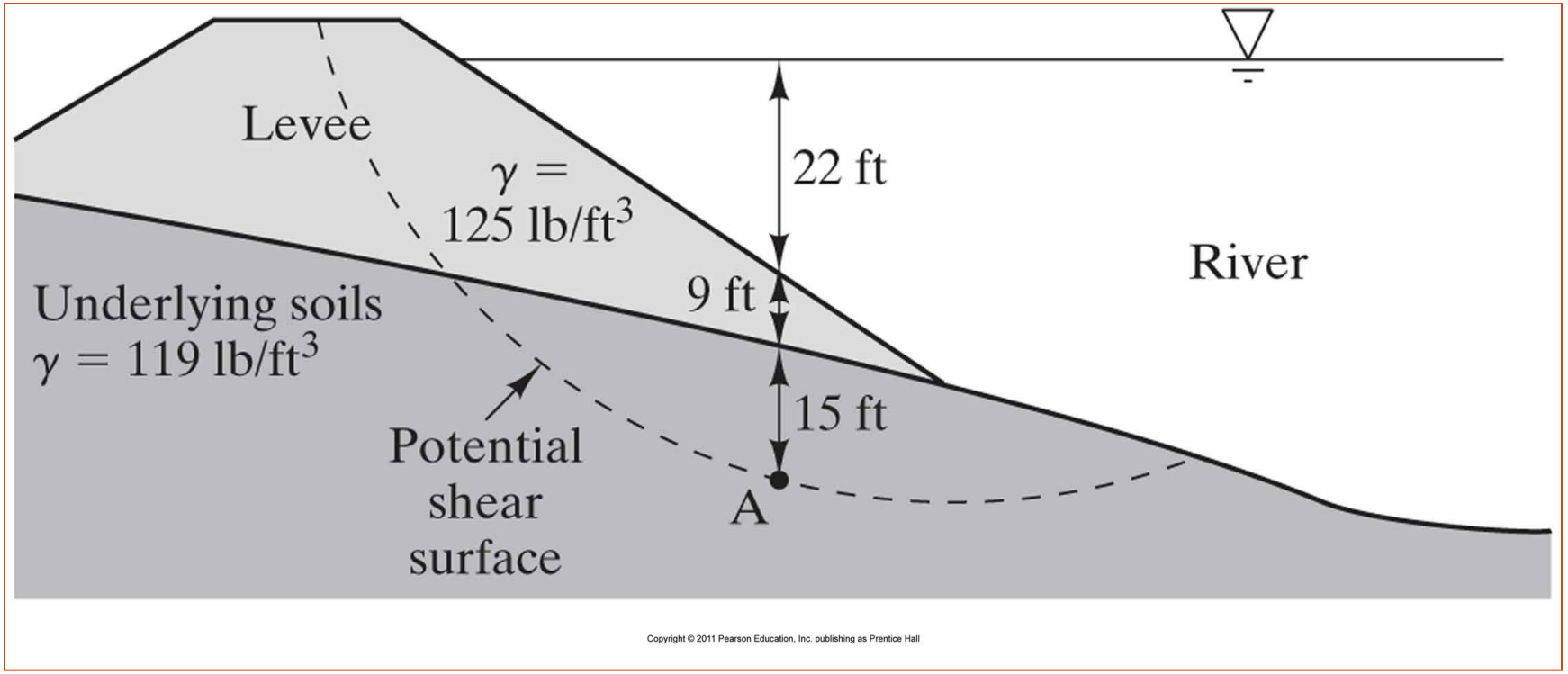

Figure Proposed levee.

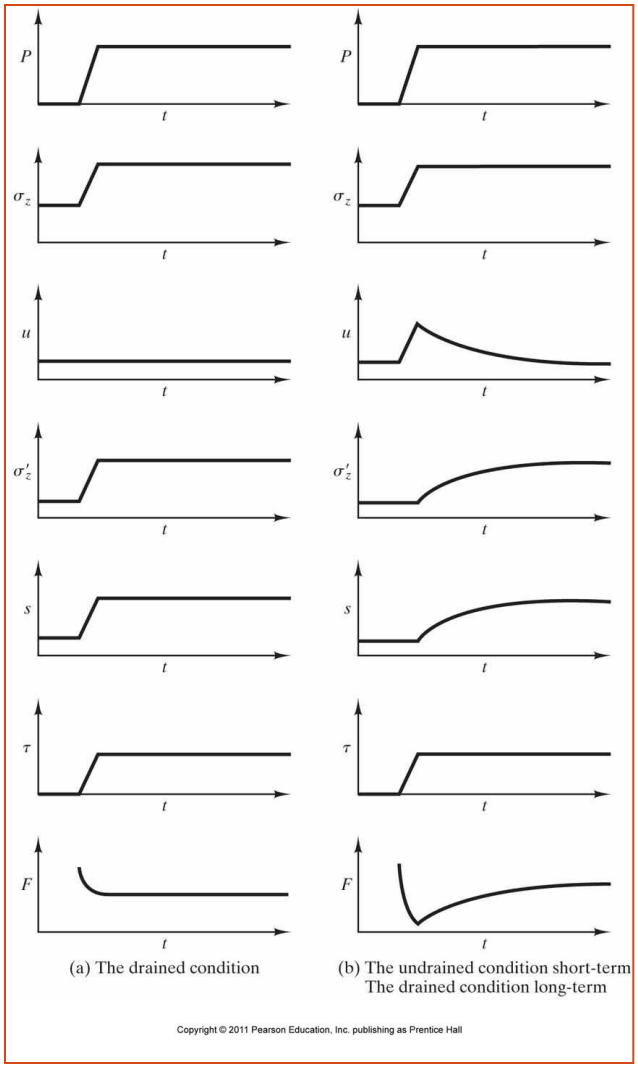

Figure Changes in normal and shear stresses, shear strength, and factor of safety with time at a point in a saturated clay below a fill or structural foundation: (a) extremely low rate of loading (the drained condition); (b) normal rate of loading (the undrained condition in short term and the drained condition in long term).

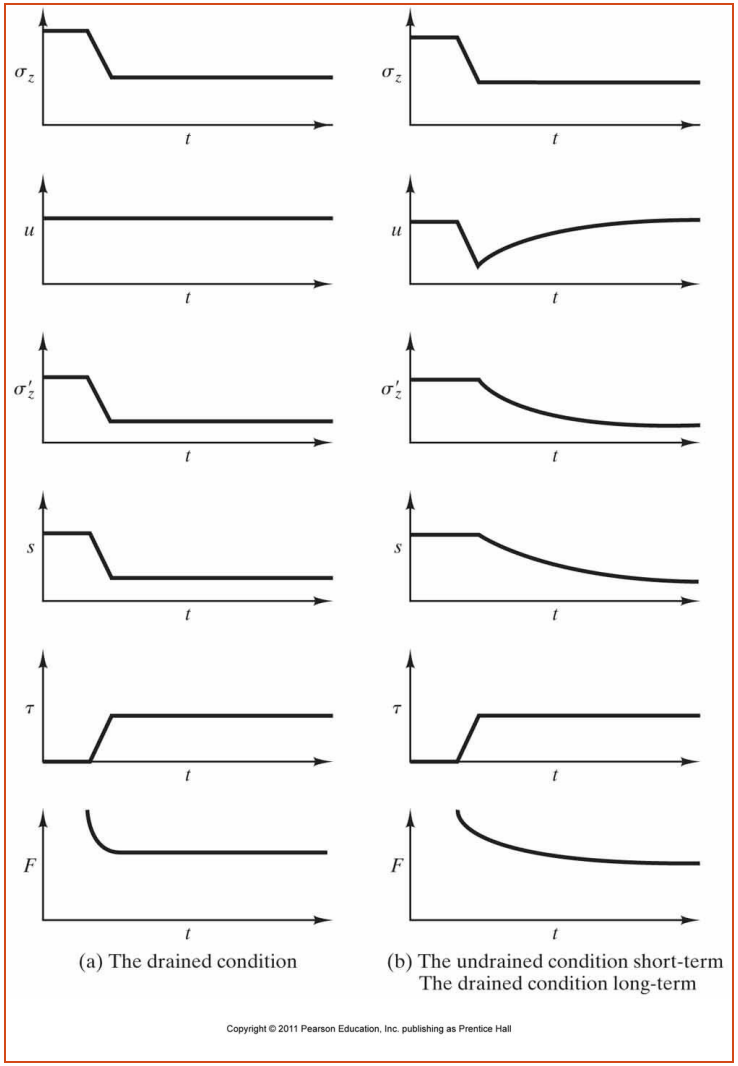

Figure Changes in normal and shear stresses, shear strength, and factor of safety with time at a point in a saturated clay below an excavation: (a) extremely low rate of loading (the drained condition); (b) normal rate of loading (the undrained condition in short term and the drained condition in long term).

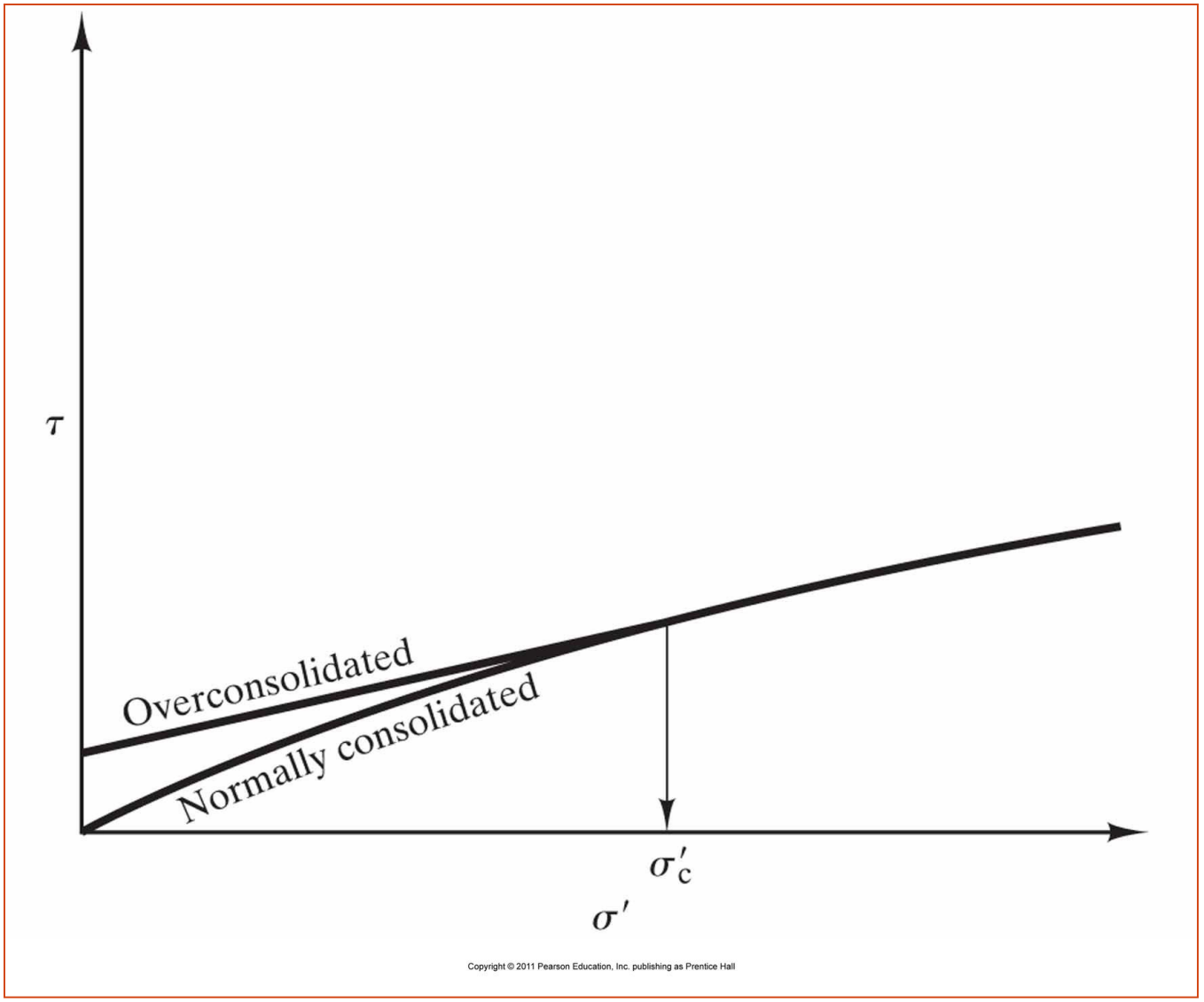

Figure Mohr-Coulomb failure envelopes for saturated, uncemented clays and silts under the drained condition.

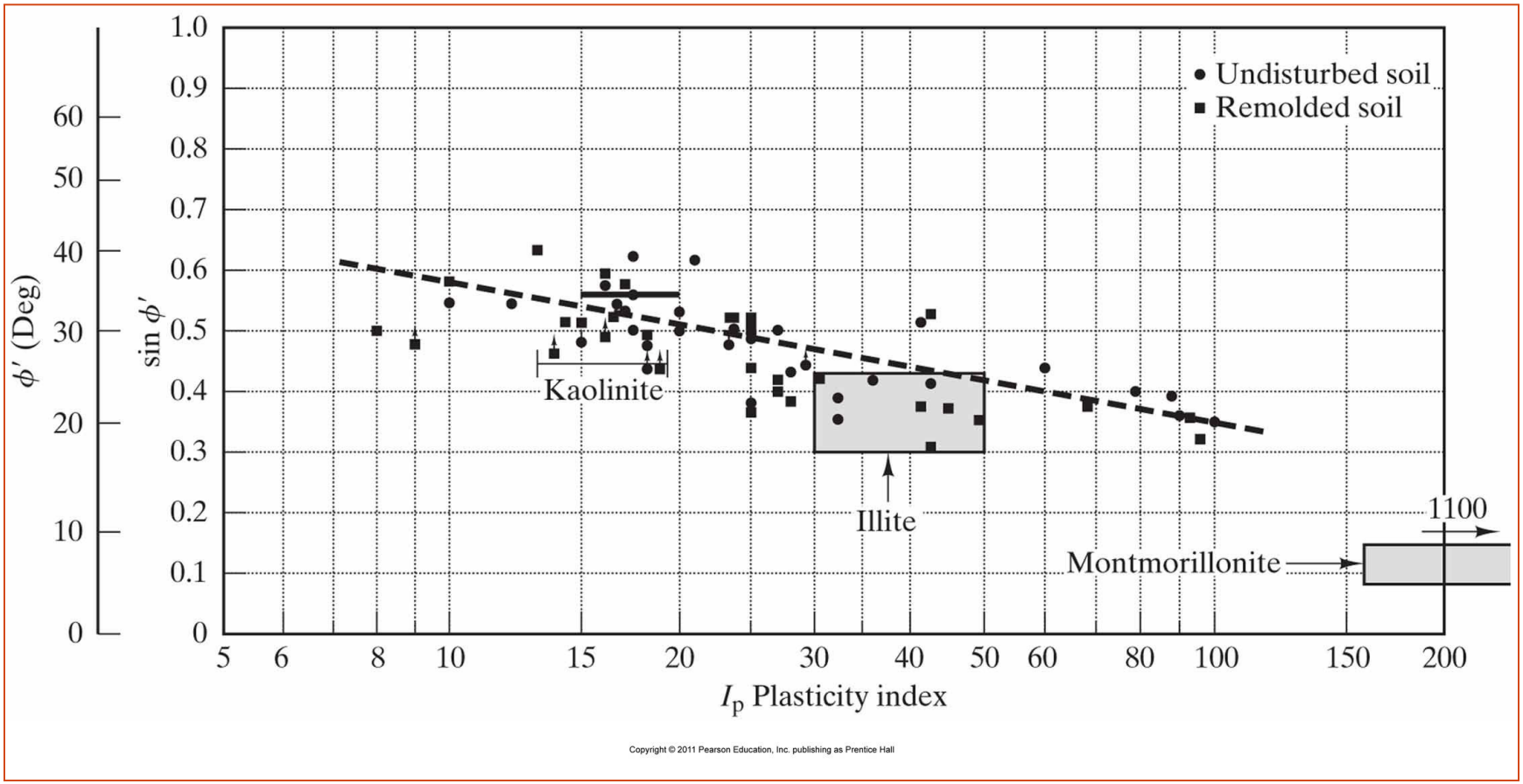

Figure Typical effective friction angles for normally consolidated, saturated clays and silts. (From Fundamentals
of Soil Behavior, 2nd ed. by J.K. Mitchell, Copyright © 1993; used by permission of John Wiley & Sons.)

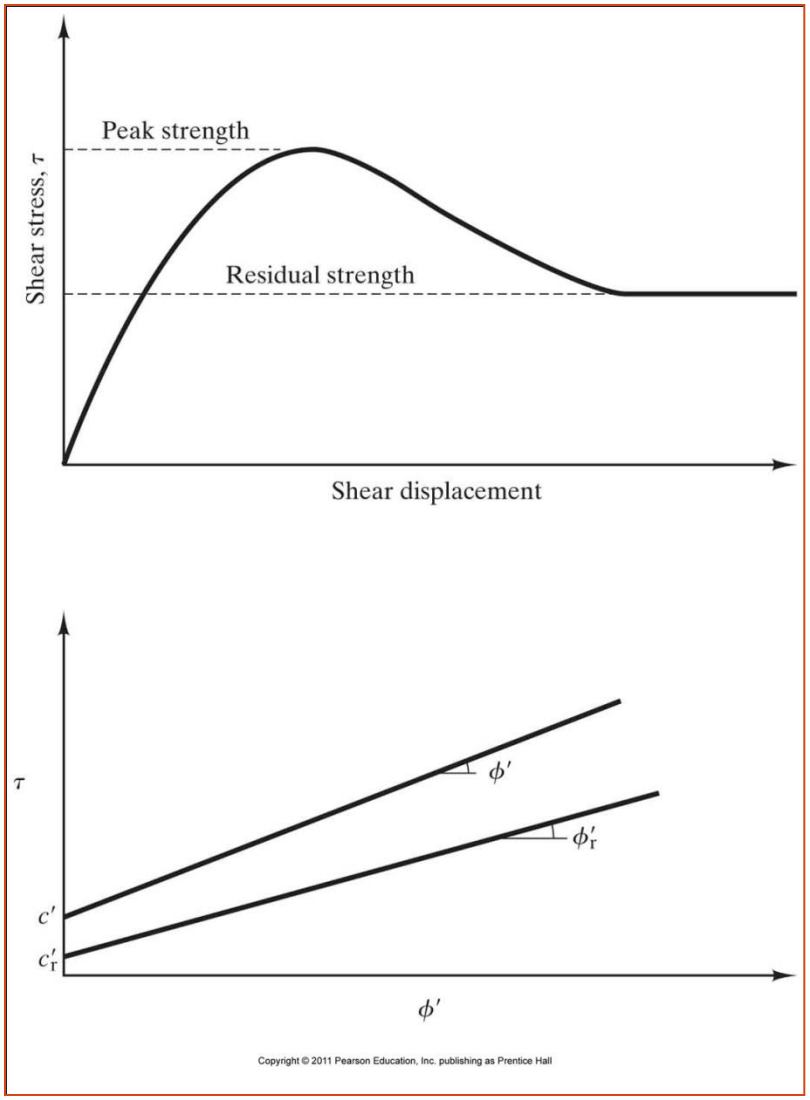

Figure The peak strength envelope is obtained from the shear strengths at the highest points of the stress-stain curves, while the residual strength envelope is obtained from the strengths at large strain.

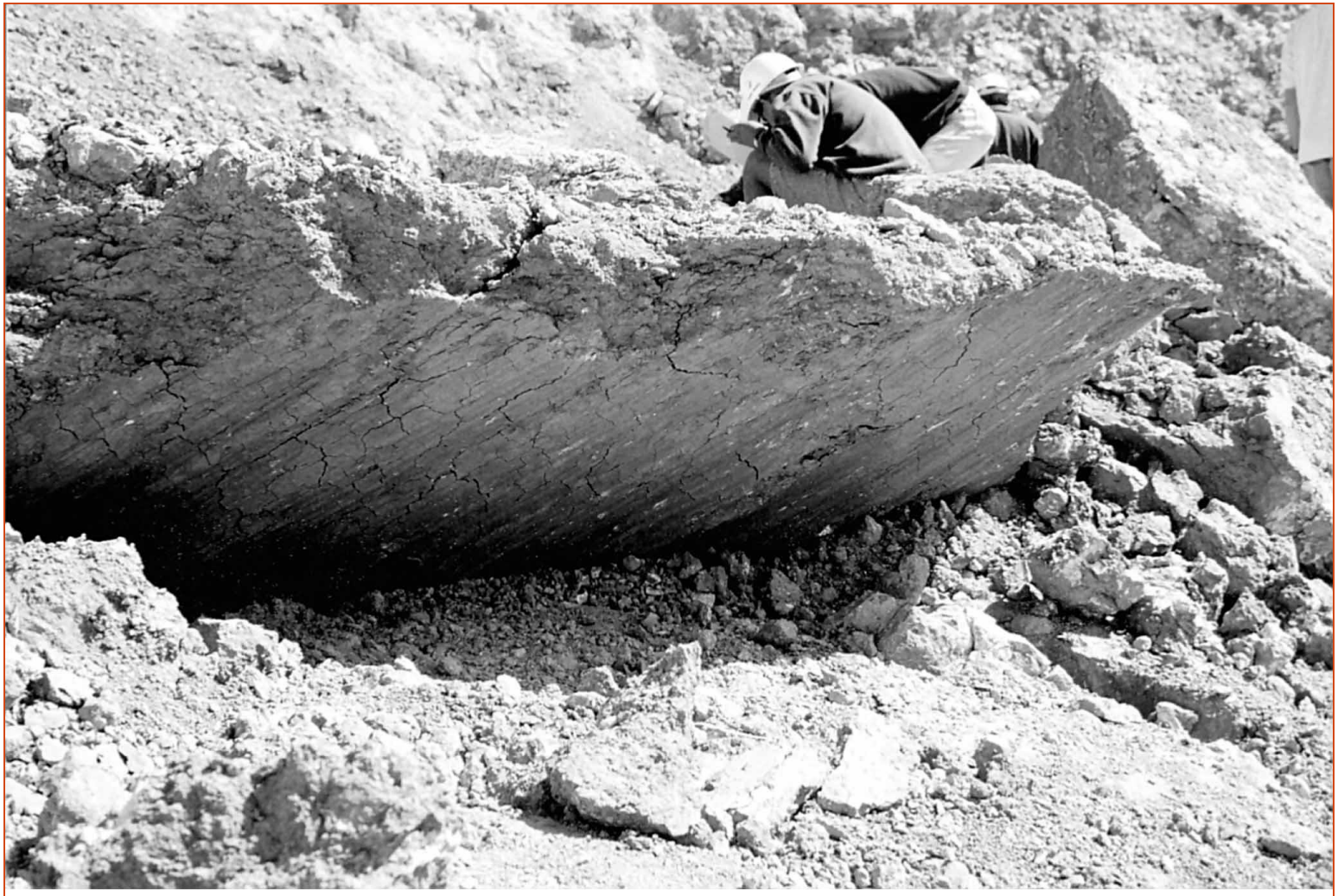

Figure This slickenside was formed by a landslide in a clay. The shear strength along this surface has been reduced to the residual value.

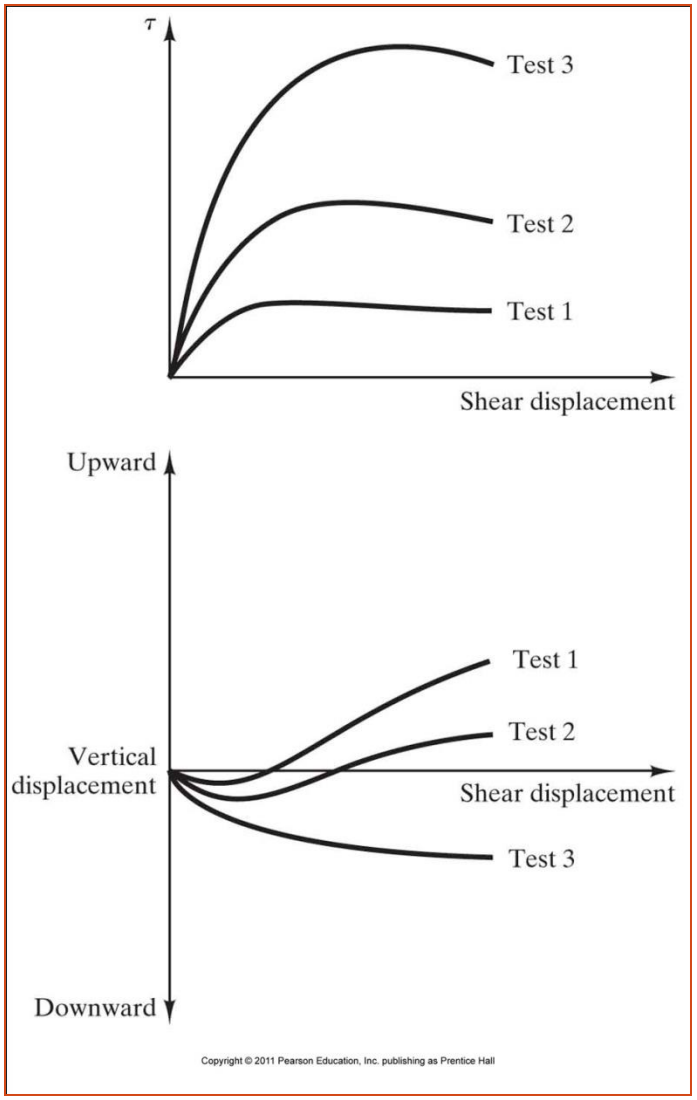

Figure Plots of typical test data from three drained direct shear tests on identical sand specimens, with σ'_z in the test increasing in the following order: Test 1, Test 2, and Test 3.

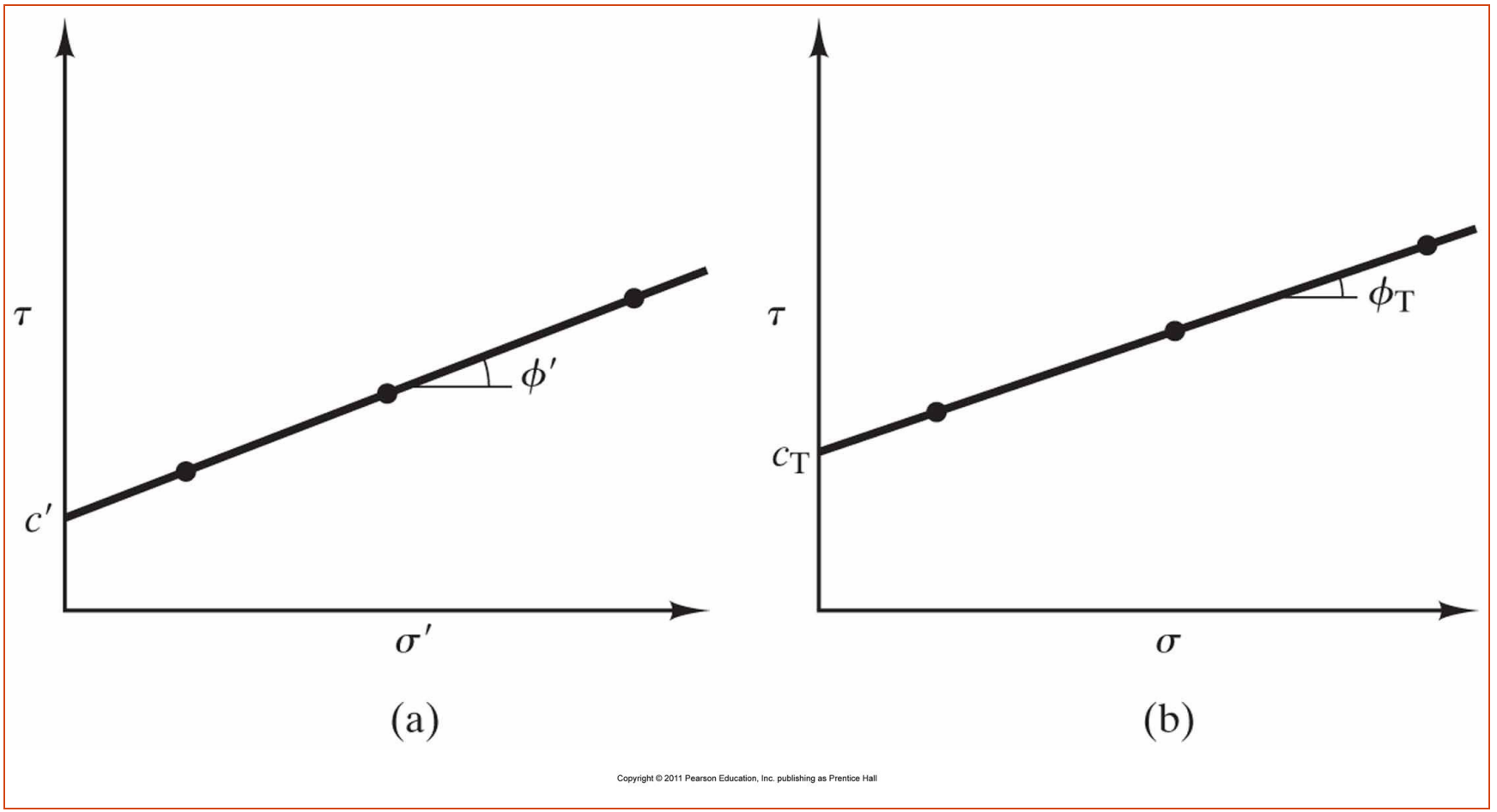

Figure Results from a series of direct shear tests: (a) results from drained tests plotted using effective stresses; (b) results from undrained tests plotted using total stresses.

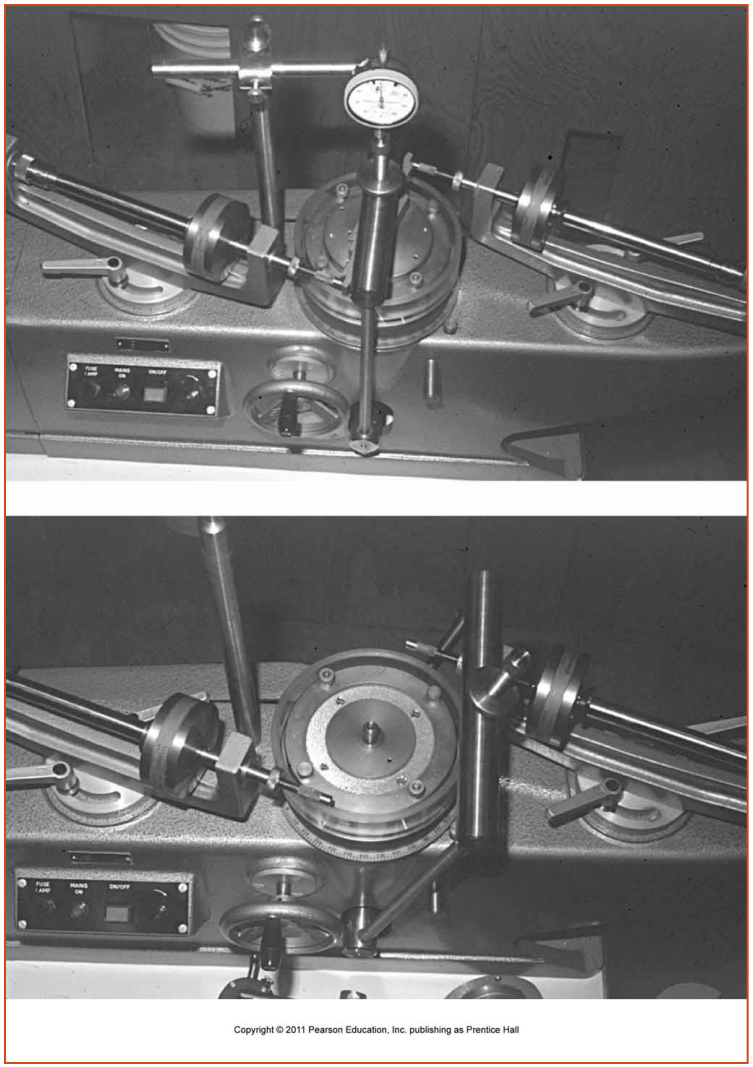

Figure Ring shear machine. The soil specimen is placed inside the annular space shown in the photograph on the top. Then the load cap is installed and the normal load is applied. Once the soil has consolidated, a torque is applied from below, and this torque is resisted by the rods shown in the photograph on the bottom.

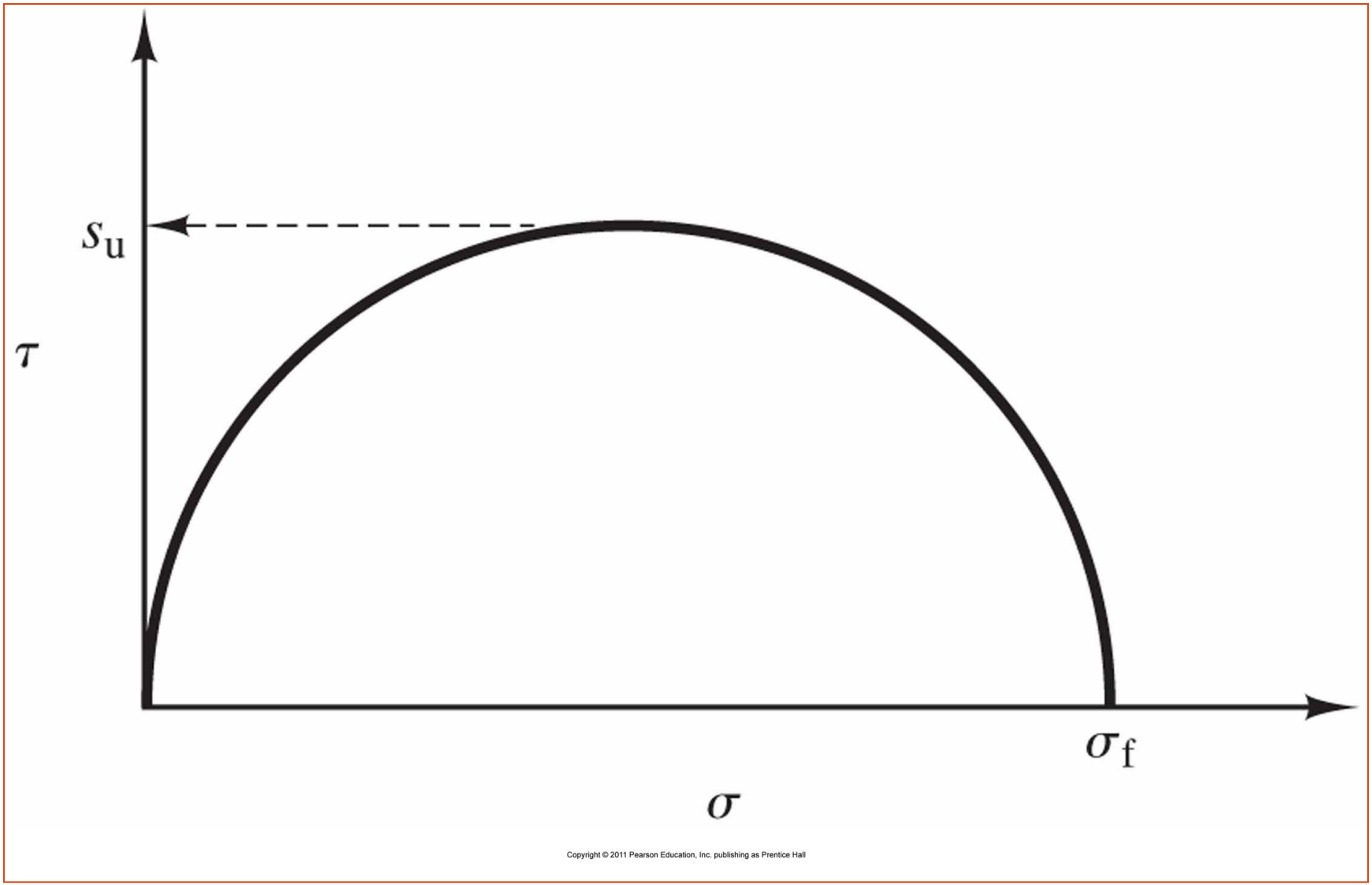

Figure Mohr circle at failure in an unconfined compression test.

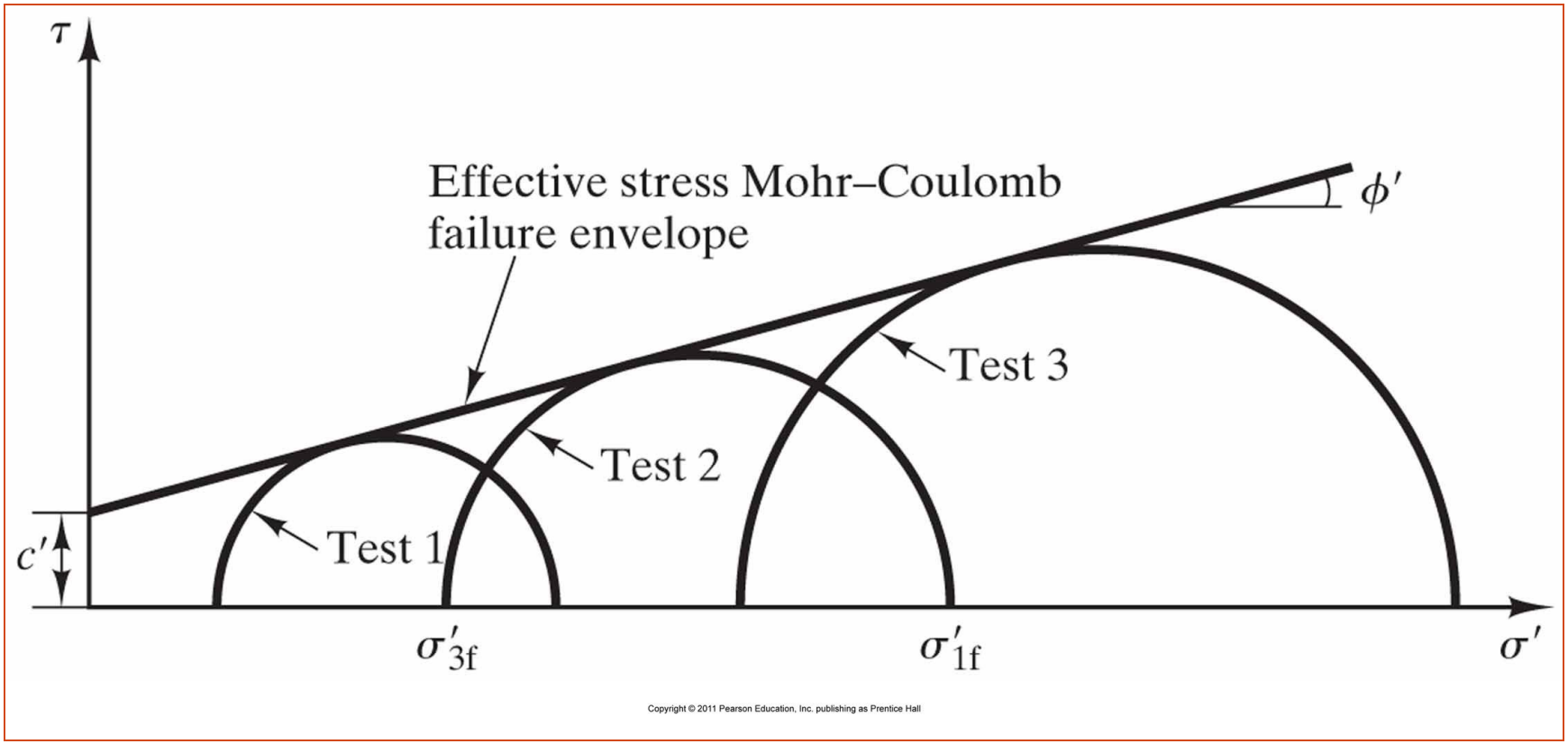

Figure Interpretation of data from a series of CD triaxial tests.

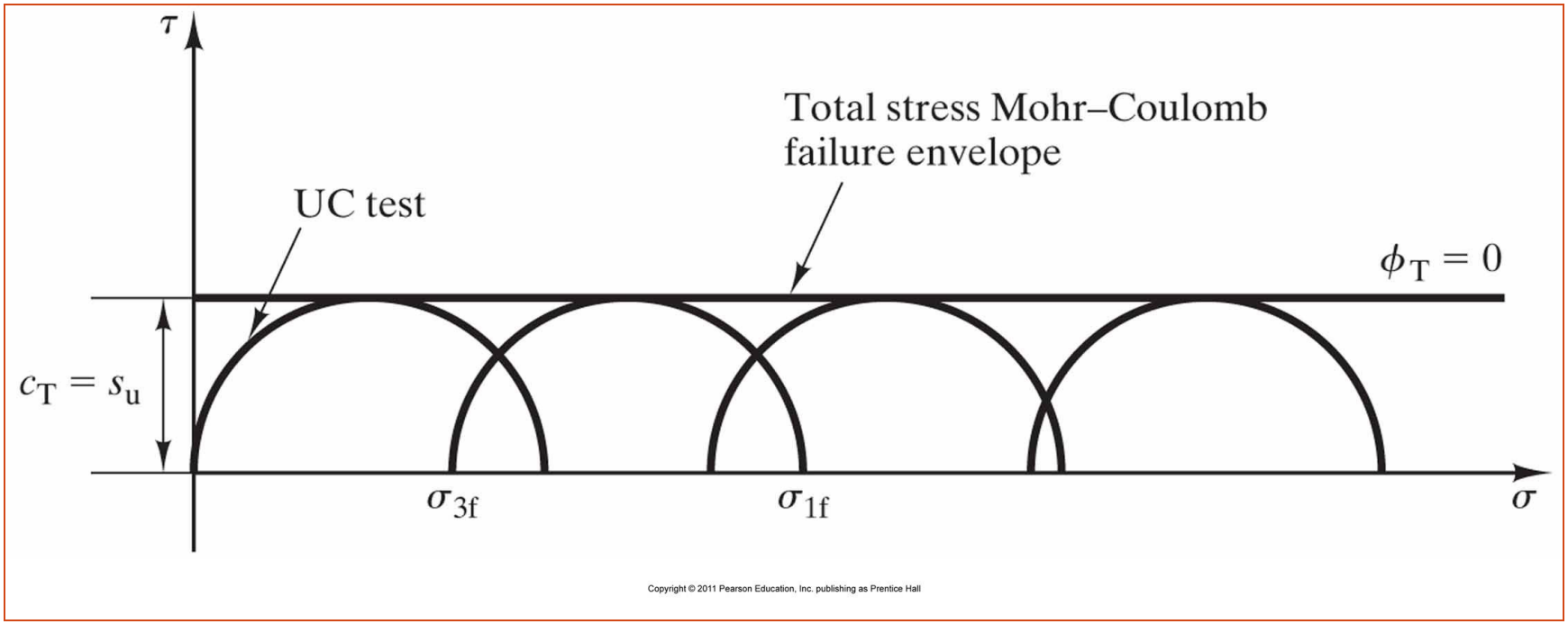

Figure Interpretation of data from a series of UU triaxial tests.

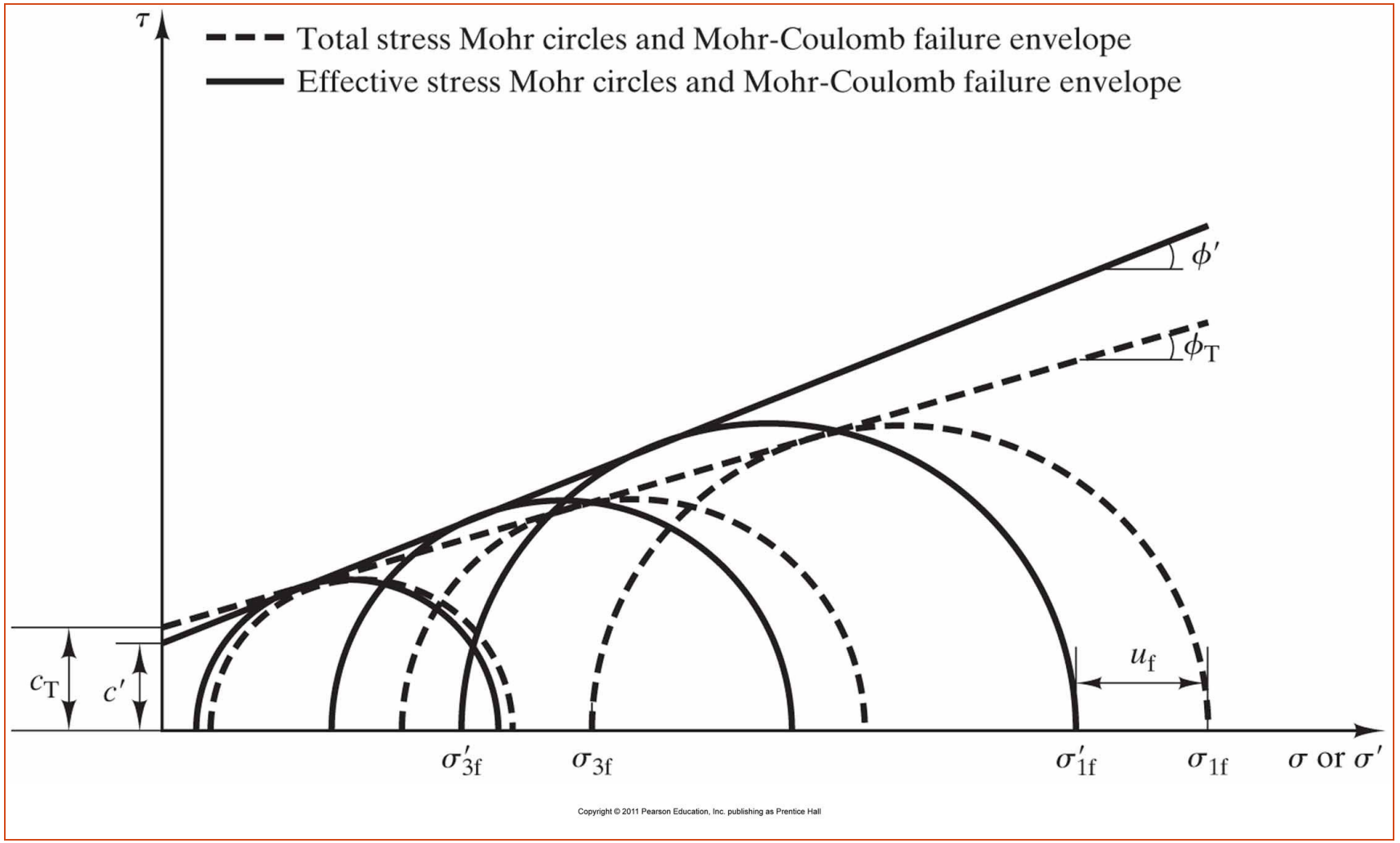

Figure Interpretation of data from a series of CU triaxial tests with pore pressure measurements.

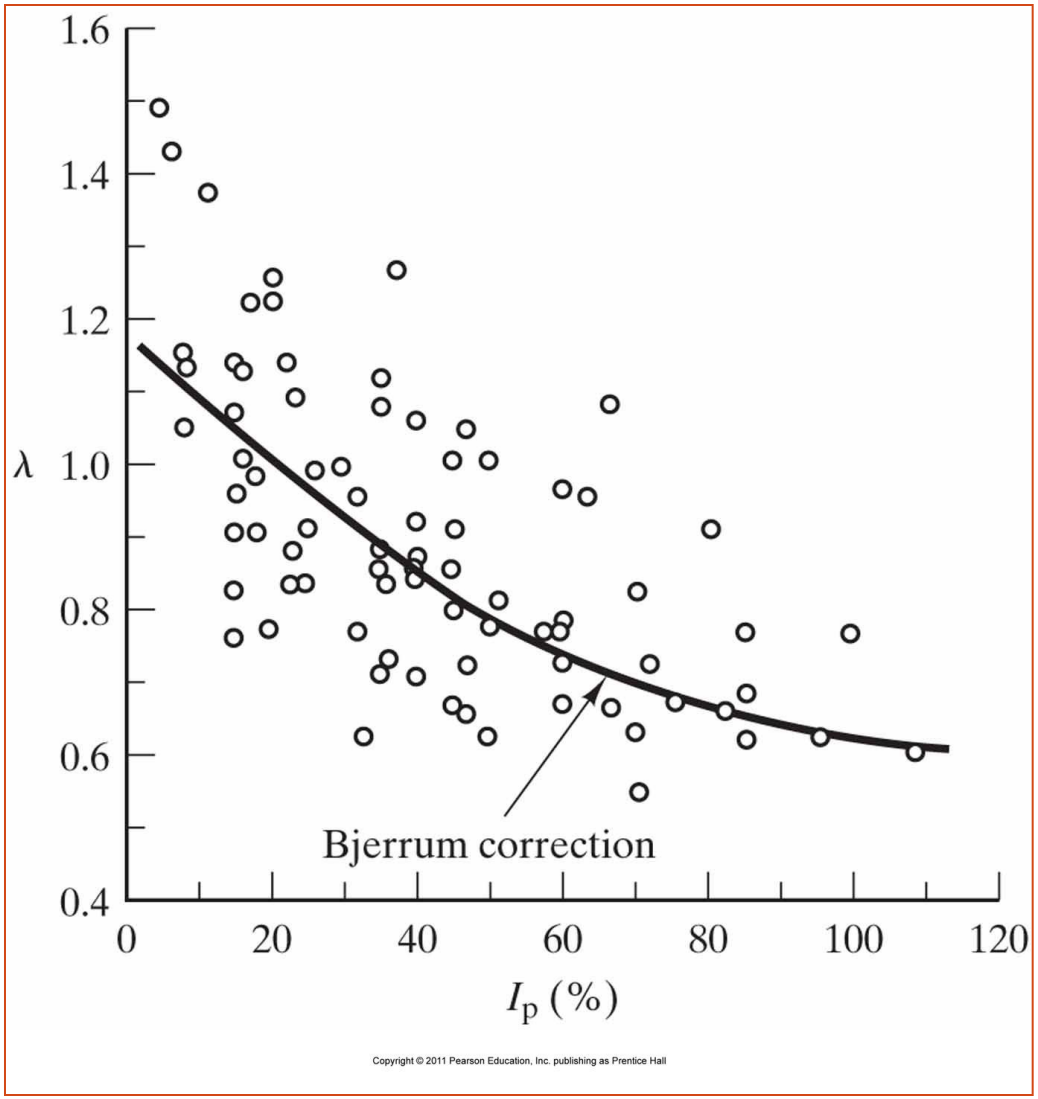

Figure Vane shear correction factor, . (From Soil Mechanics in Engineering Practice. 3rd ed. By Terzaghi, Peck, and Mesri Copyright © 1996. Used by permission of John Wiley & Sons, Inc.)

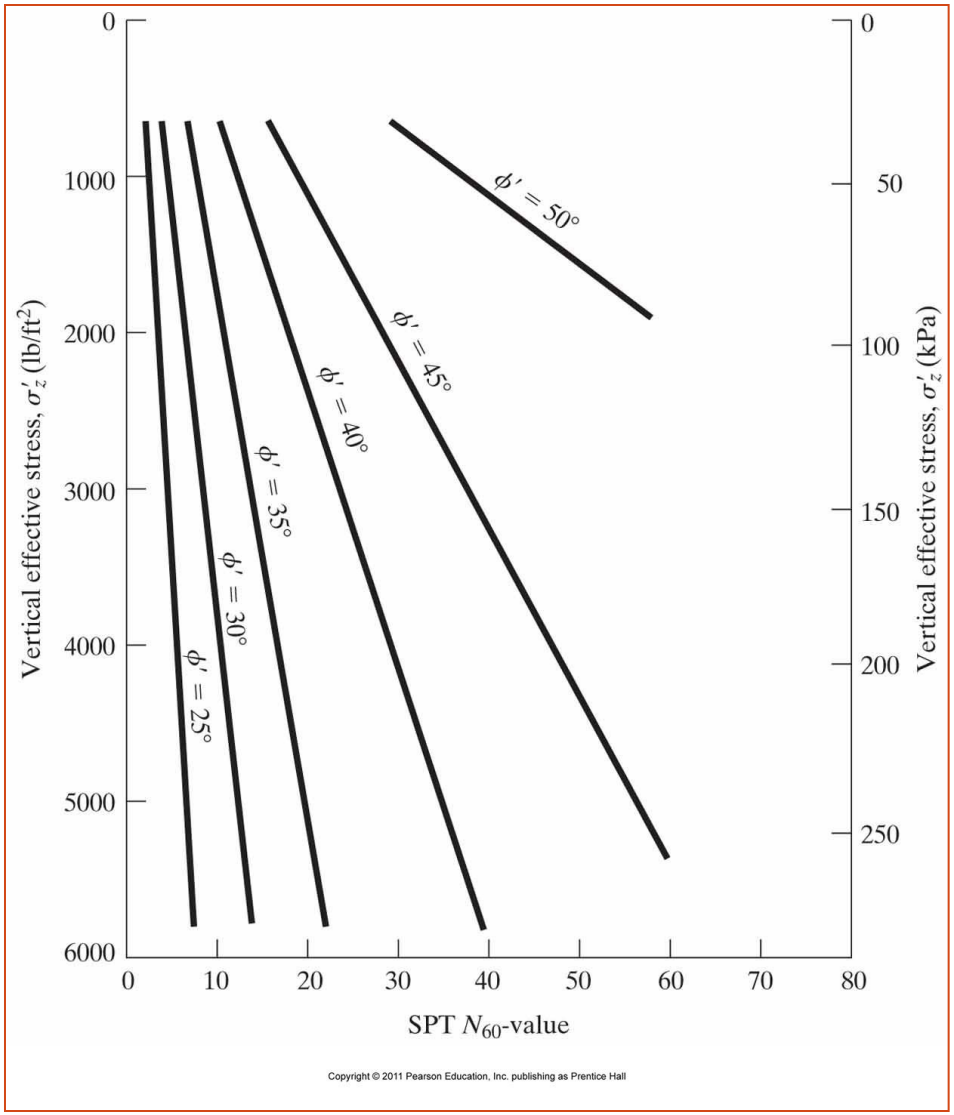

Figure Empirical correlation between N_{60} and ϕ′ for uncemented sands. (Adapted from DeMello, 1971.)

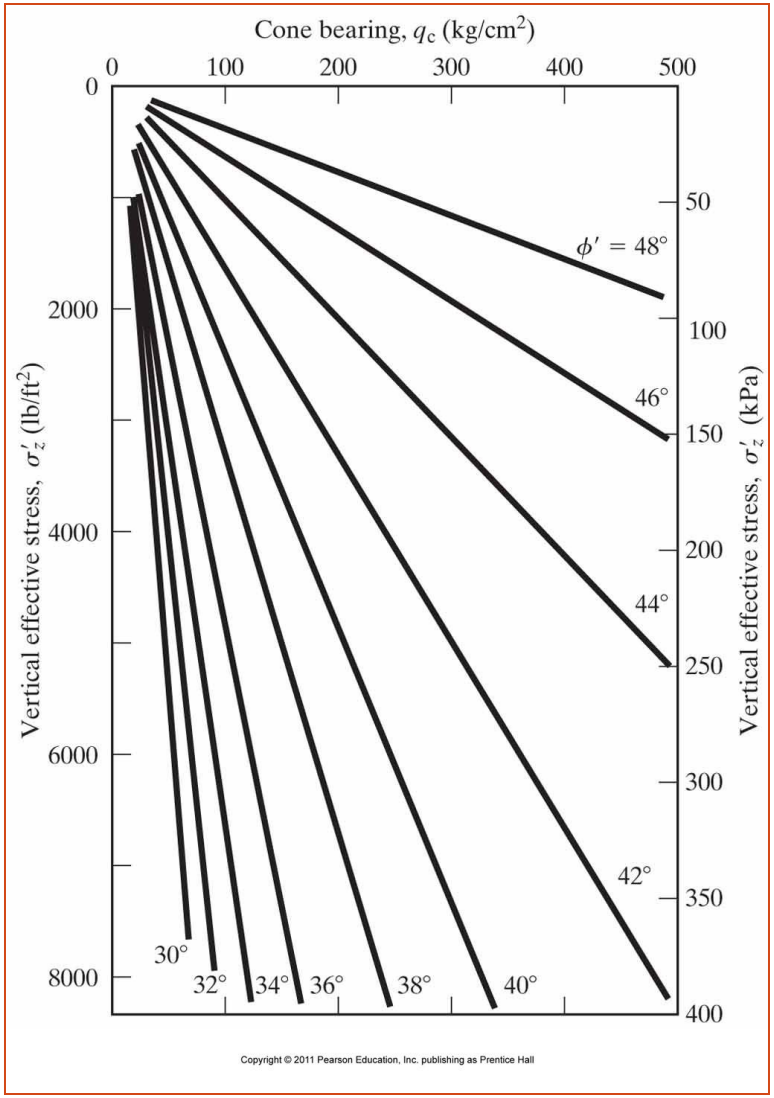

Figure Empirical correlation between q_c and ϕ′ for uncemented, normally consolidated quartz sands. (Adapted from Robertson and Campanella, 1983.)

Estructuras de Retención

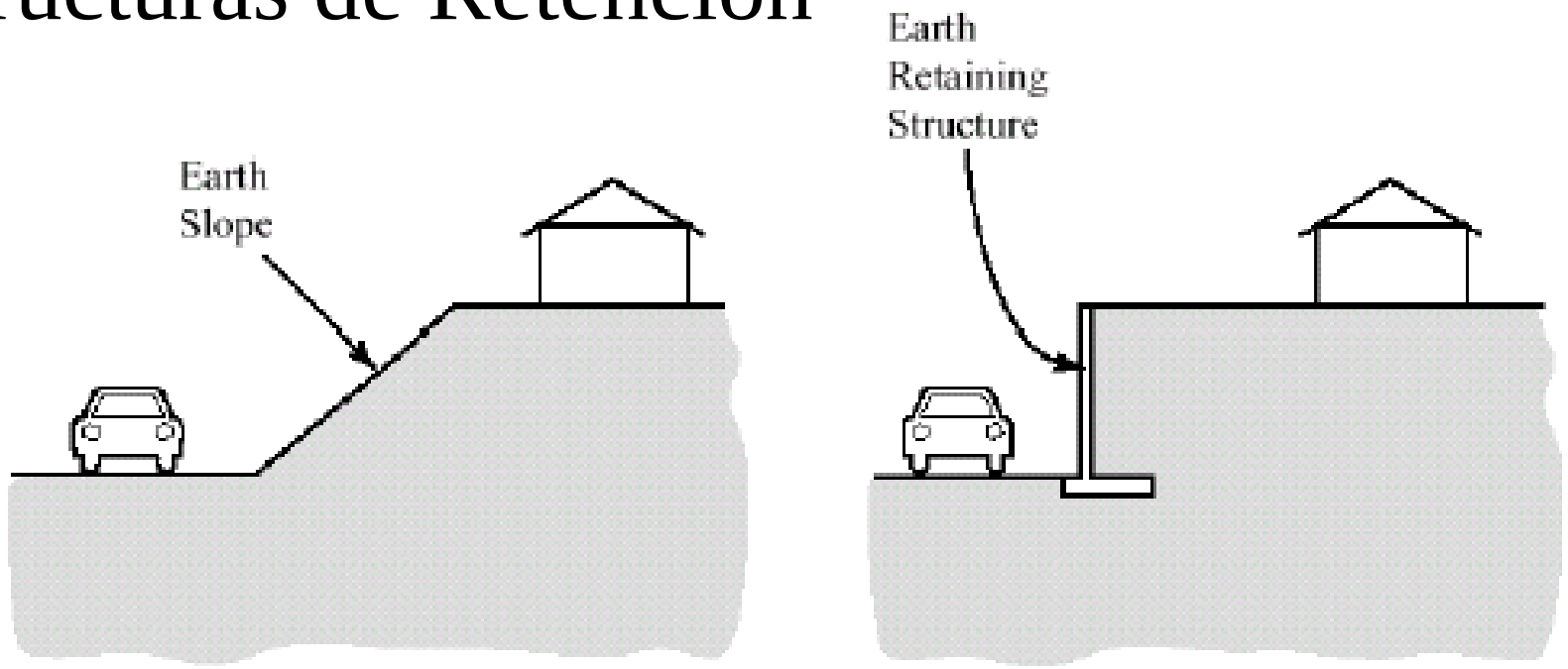

- Necesarias en situaciones donde una transición gradual ocuparía demasiado espacio
- Estructuras de retención son analizadas con respecto a la estabilidad del muro (vuelco, deslizamiento, capacidad portante y falla global) y a su integridad estructural
- Los muros de gaviones caen dentro del la categoría principal de estructuras de retención conocida como *Muros de Gravedad* (“Gabions, Massonry, Stones”)

Etapas en situación típica

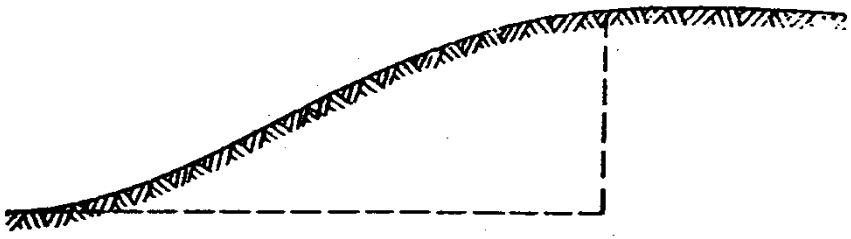

(a) Corte propuesto

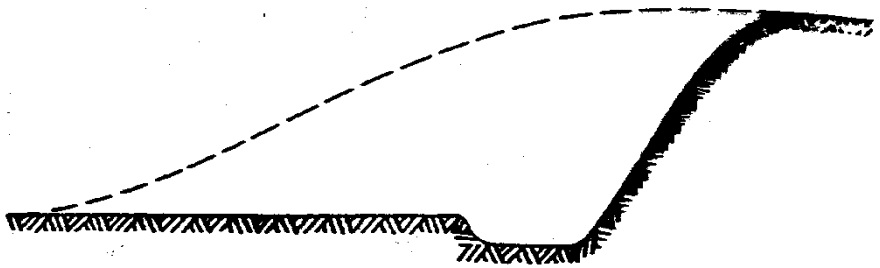

(b) Excavación

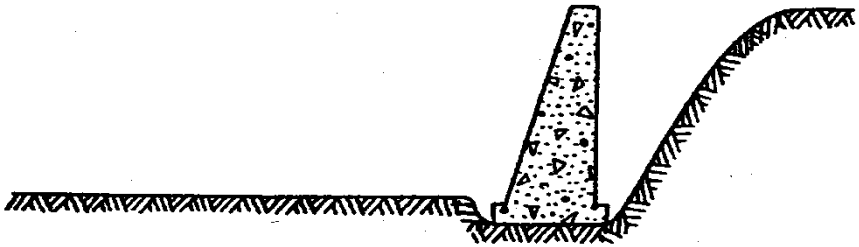

(c) Construcción muro gaviones (otro)

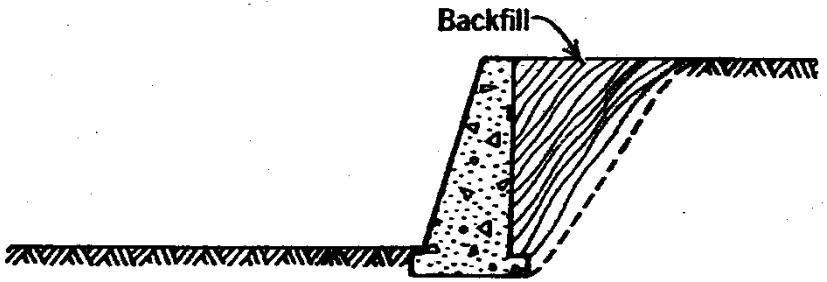

(d) Relleno compactado

- Muros de gravedad (incluyendo gaviones) son sistemas estabilizados externamente para resistir las cargas generadas por el empuje lateral del suelo valiéndose de su propio peso y de su rigidez.

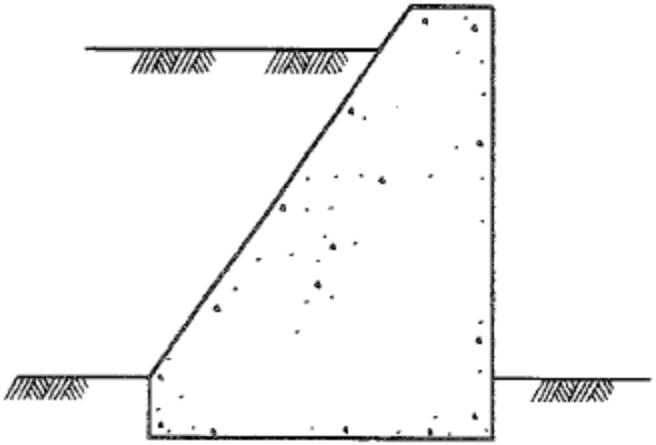

GRAVEDAD

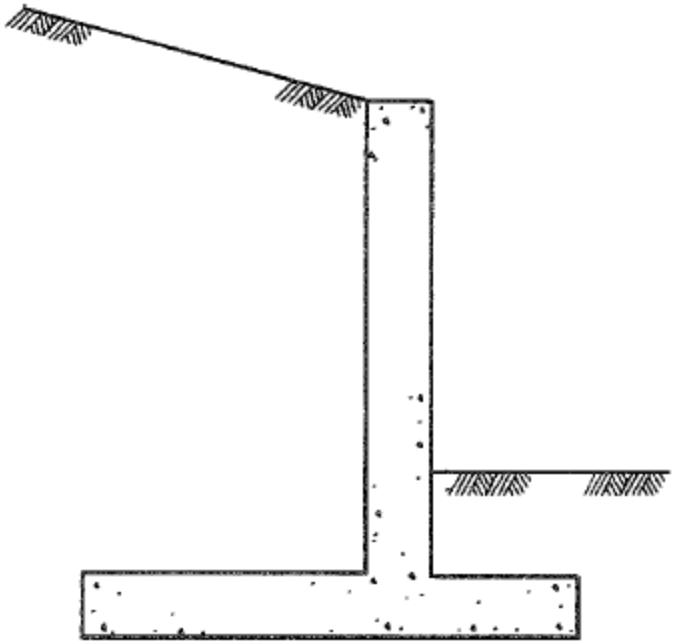

AL VOLADIZO DE CONCRETO REFORZADO

Fuerzas que resiste un muro de gravedad

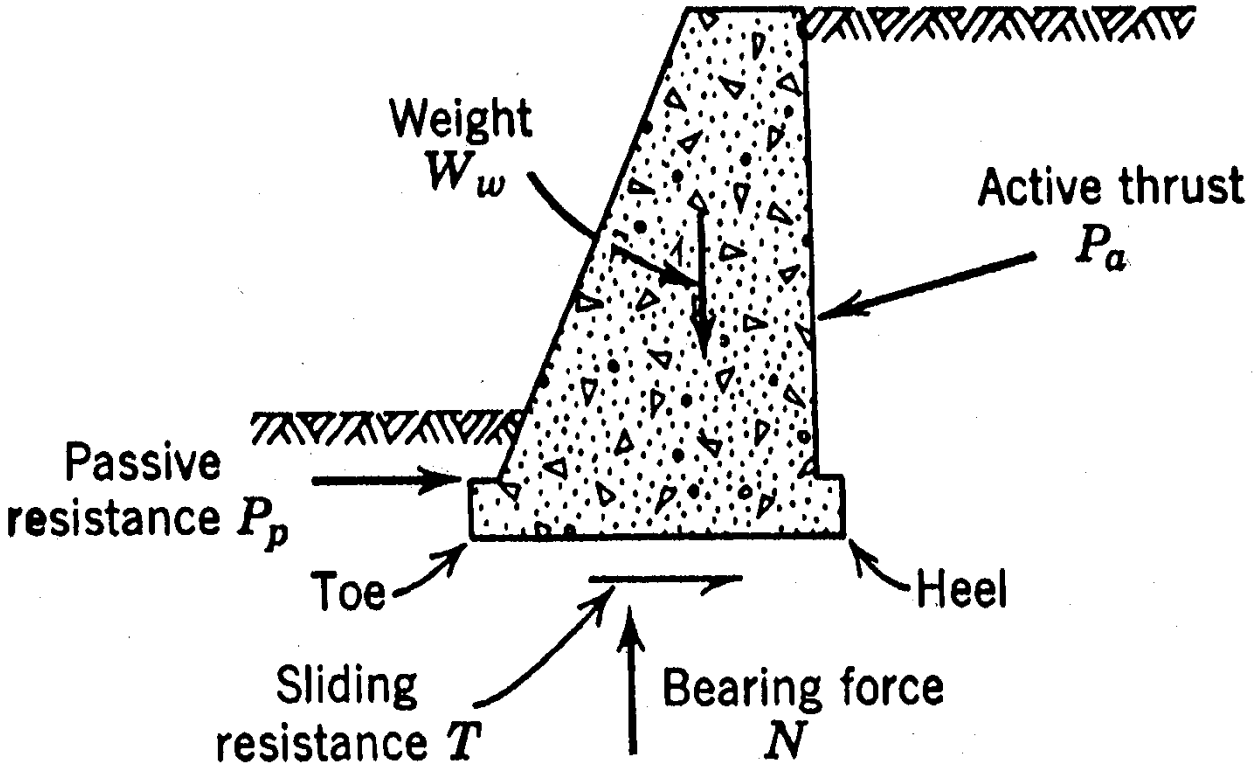

GRAVEDAD

Fuerzas que resiste un muro de gravedad

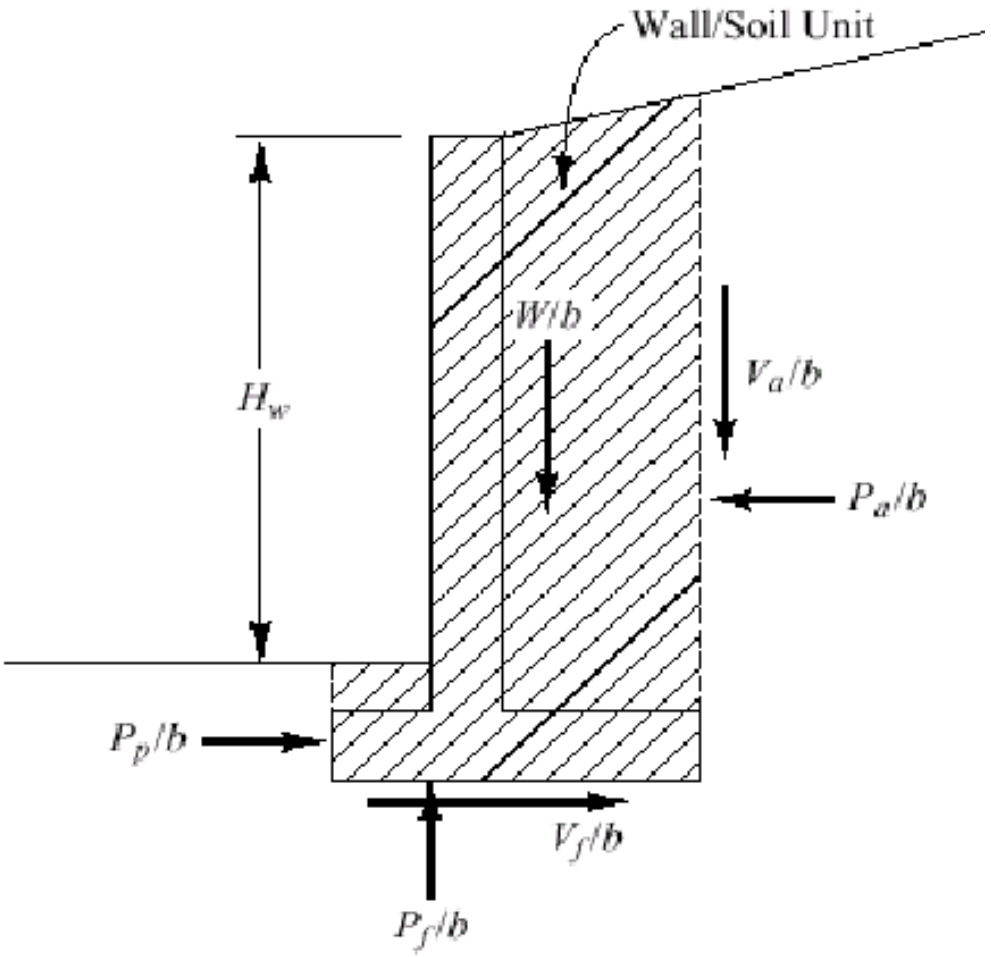

AL VOLADIZO

Coeficientes de empuje de tierra (presión lateral)

$$K=\sigma'_h/\ \sigma'_v$$

Donde:

K = coeficiente de presión lateral

σ'_v= esfuerzo vertical efectivo

σ'_h= esfuerzo horizontal efectivo

También vimos;

K_a = activo (hacia fuera) valores 0.25-0.33

K_o = reposo (no movimiento) valores 0.4-0.5

K_p = pasivo (hacia adentro) valores 3-4

Diferentes condiciones para los coeficientes de empuje de tierra lateral

- Condición en Reposo (At-Rest Condition)
  - Condición donde el movimiento del muro es cero o “mínimo”
  - Es la condición ideal para la pared, pero muy pocas veces ocurre en realidad
- Condición Activa (Active Condition)
  - Condición donde la pared se aleja del relleno
  - Genera la presión de empuje lateral de tierra mas bajo
- Condición Pasiva (Passive Condition)
  - Condición donde la pared se mueve hacia el relleno
  - Genera la presión de empuje lateral de tierra mas alto

Condición de reposo (At-rest)

- Presiones generadas en un muro que no experimenta movimiento lateral “unyielding wall”.
- Ejemplos donde aplica esta condición:
  - Muros de sótanos
  - Algunos tanques de agua rígidos soterrados
- No suele aplicar al caso de gaviones

Como estimar el coeficiente (K_0)

- Para arena

$$K_0 = 1 - \sin\phi \text{ (Jaky, 1944)}$$

- Para arcillas normalmente consolidadas (NC)

$$K_0 = 0.19 + 0.233\log(PI)$$

Donde: PI=índice de plasticidad

Como estimar el coeficiente (K_0)

- Para arcillas sobre-consolidadas (OC)
- OCR = σ'_p/σ'_v

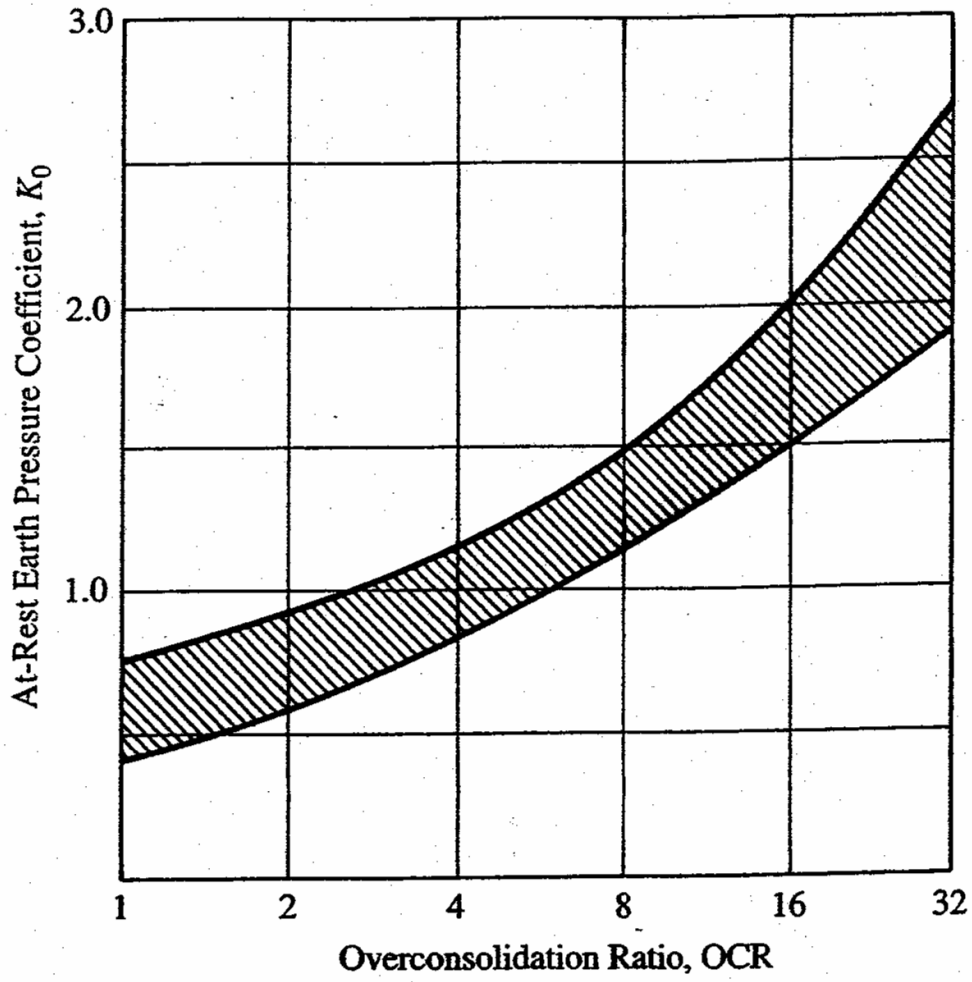

FIGURE 12–5 Relationship between K_0 and OCR [3].

Como estimar el coeficiente (K_0) (cont…)

- Para todo tipo de suelo

$$K_0 = (1 - \sin\phi')OCR^{\sin\phi'}$$

Donde: K_0 = coeficiente de presión lateral en reposo
ϕ' = ángulo de fricción efectiva del suelo
OCR = razón de sobreconsolidación del suelo

Nota:
-Esta ecuación esta basada en pruebas de laboratorio realizadas en 170 suelos, variando entre arcillas y gravas.
-Esta ecuación aplica únicamente cuando la superficie del relleno es horizontal.

Fuerza en reposo

$$P_0 = \frac{1}{2}\gamma H^2 K_0$$

Donde:

P_0 = Fuerza en reposo por longitud de pared unitaria

γ = peso unitario del suelo

H = altura de la pared

K_0 = coeficiente de presión lateral en reposo

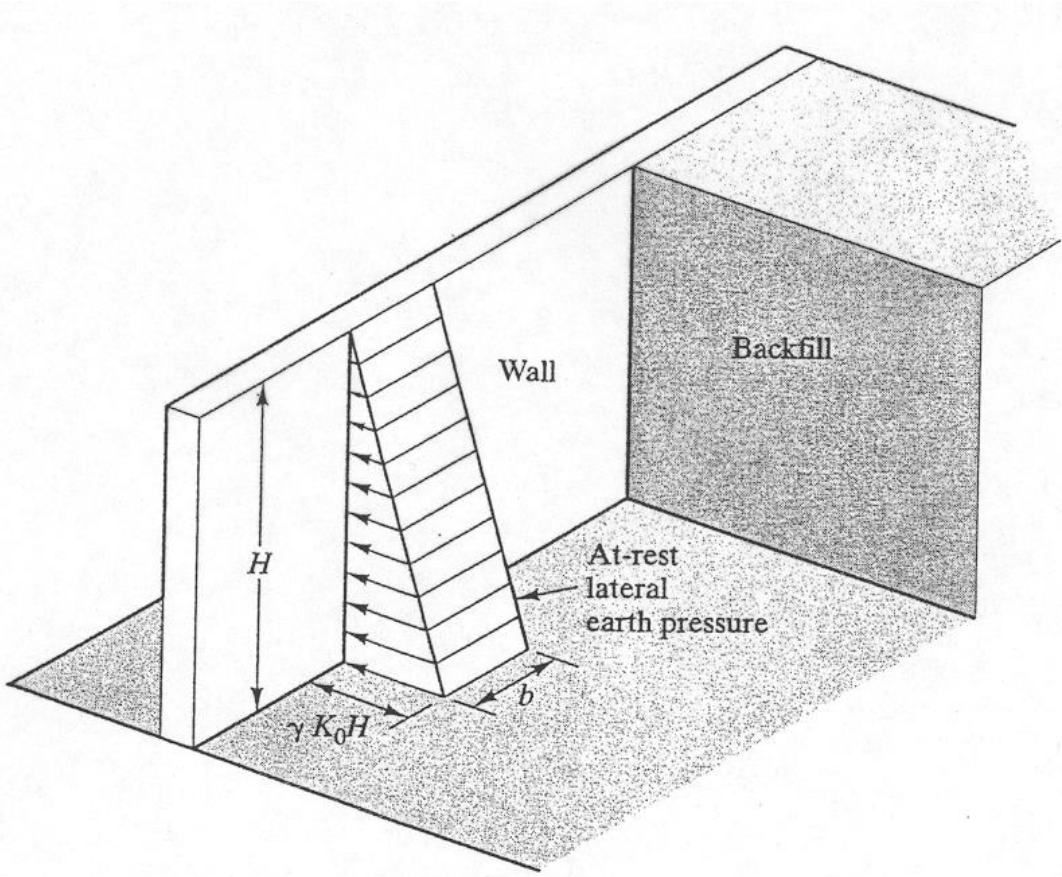

Figure 23.2 At-rest pressure acting on a retaining wall.

Teoría de Rankine para suelos con $c = 0$ y $\phi \geq 0$

- Suposiciones
  - El suelo es homogéneo e isotrópico
  - La superficie mas critica es un plano
  - La superficie del terreno es un plano (no tiene que ser horizontal)
  - El movimiento de la pared es suficiente para desarrollar la condición activa o pasiva.
  - La fuerza lateral resultante esta inclinada a un ángulo paralelo a la superficie del relleno
  - La teoría de Rankine se limita a paredes verticales
  - No existe fricción entre el suelo y la pared

Figure 23.4 Development of shear failure planes in the soil behind a wall as it transitions from the at-rest condition to the active conditon.

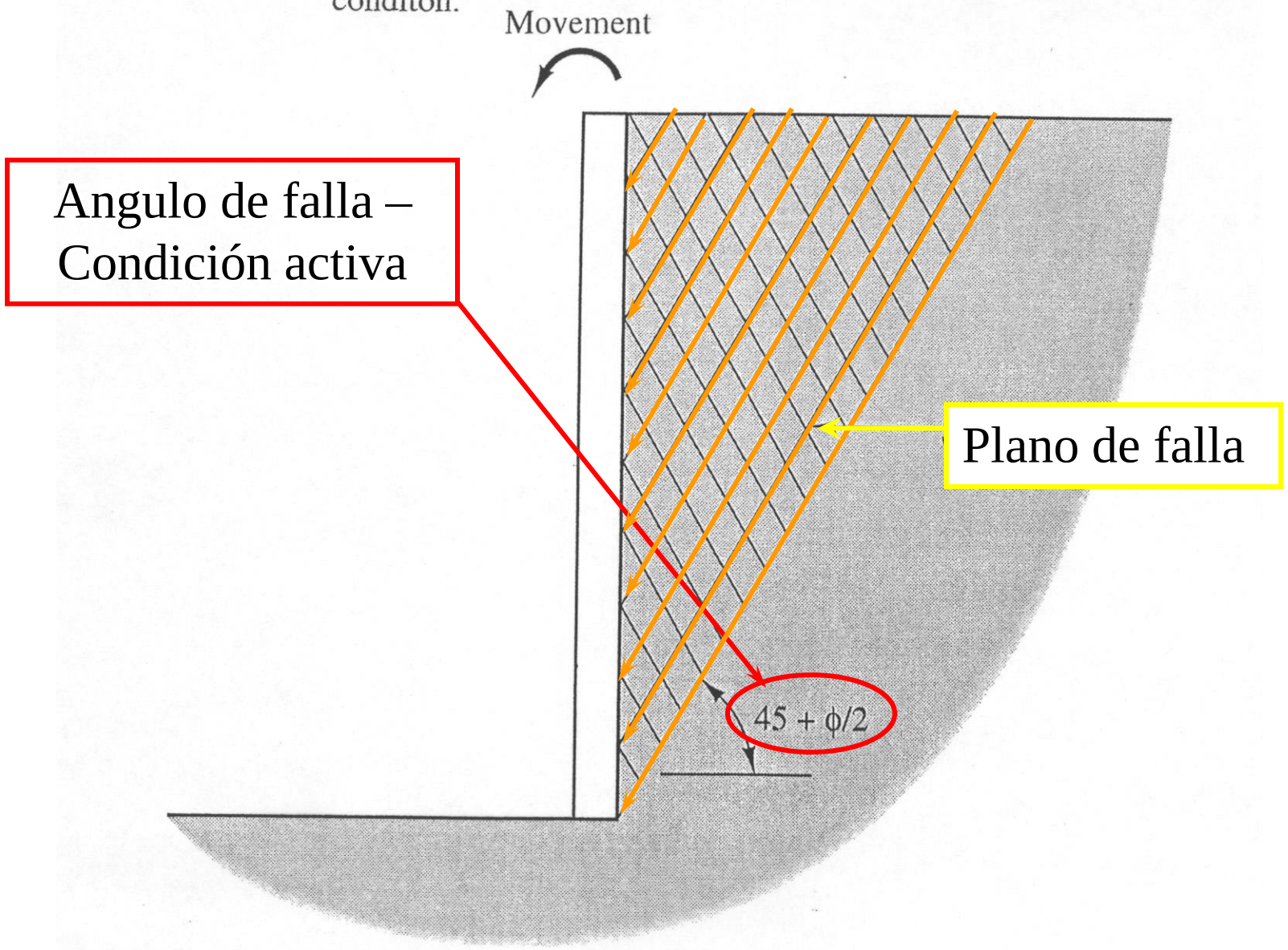

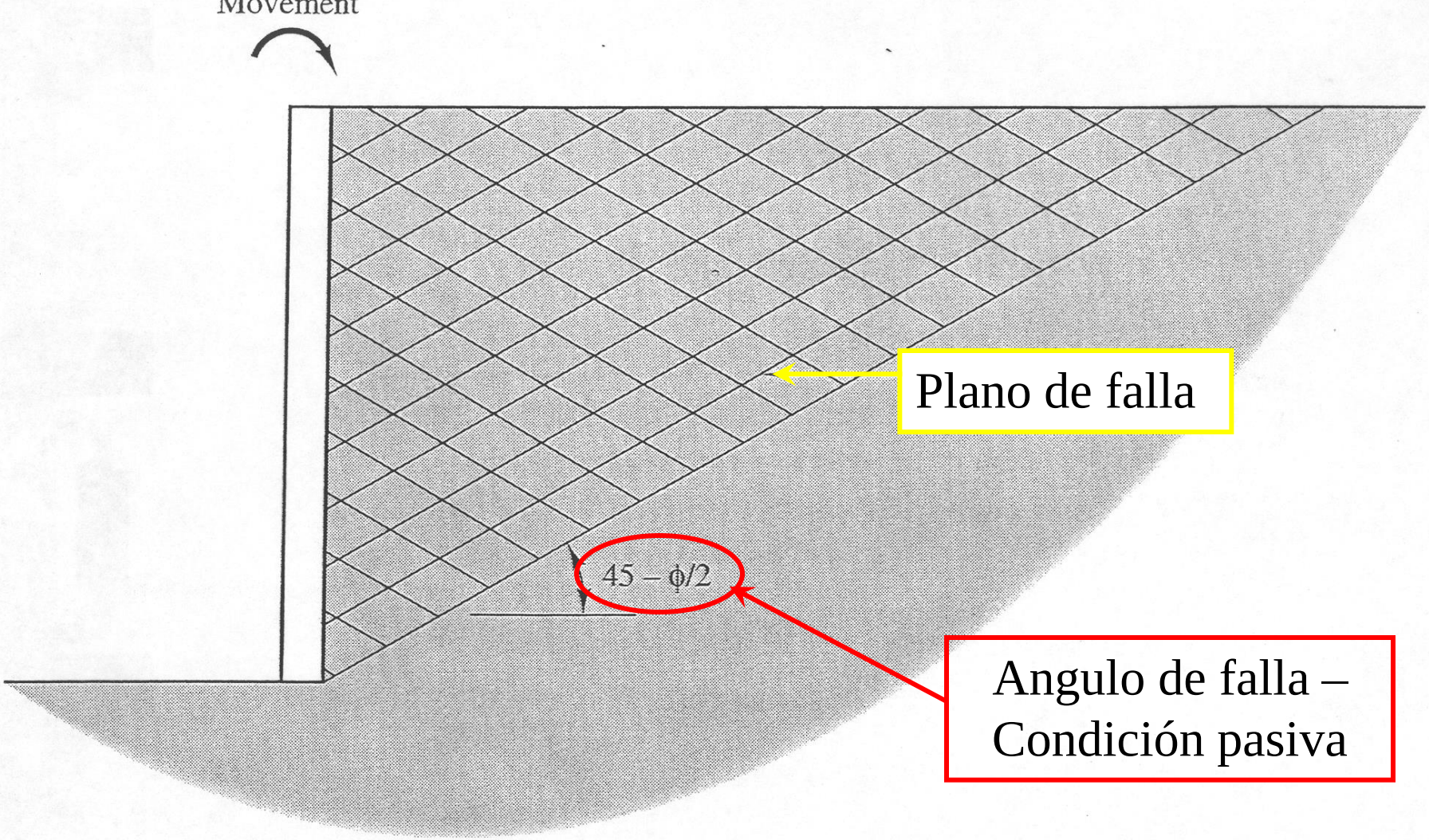

Figure 23.6 Development of shear failure planes in the soil behind a wall as it transitions from the at-rest condition to the passive condition.

Efecto del movimiento de la pared

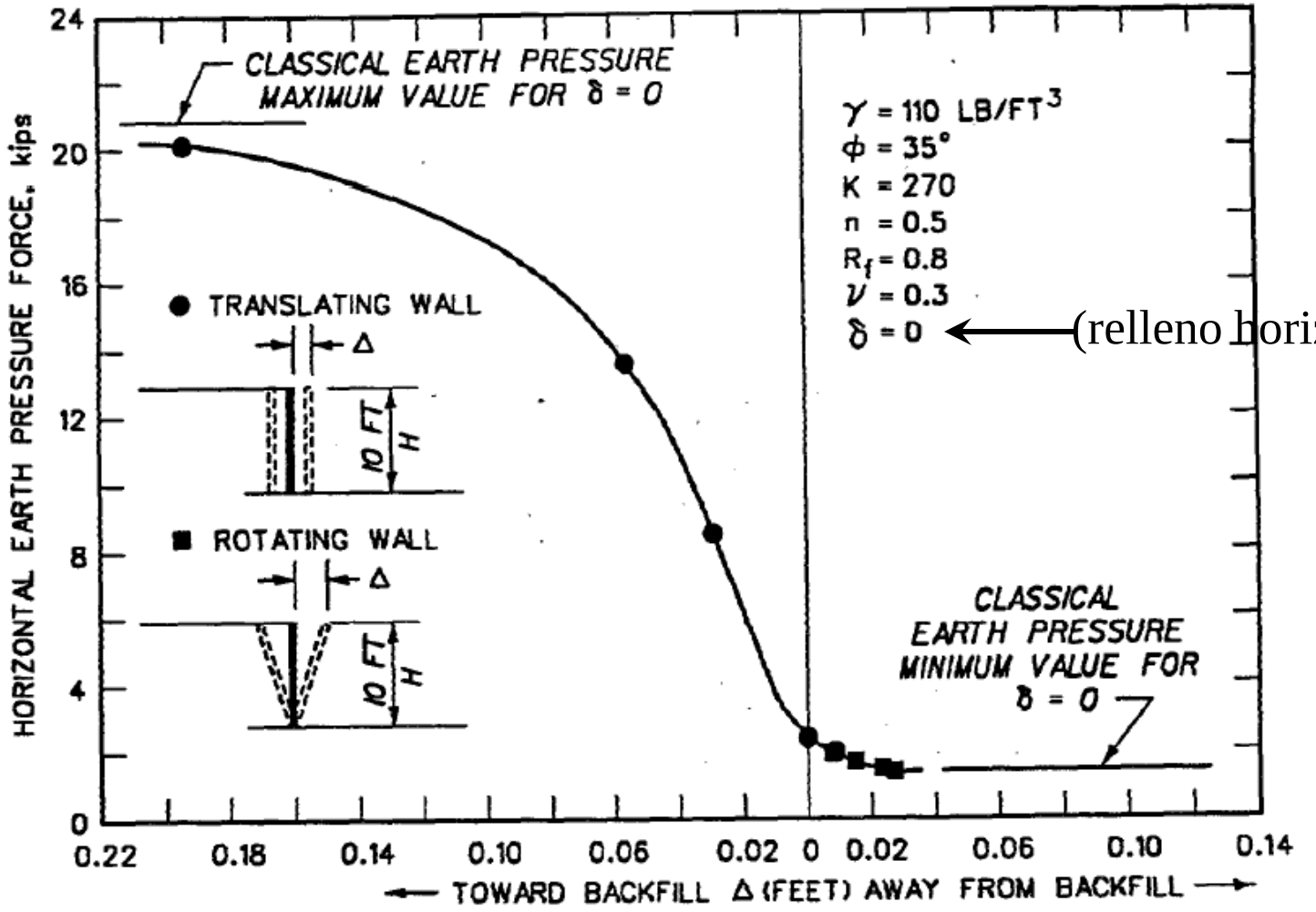

(relleno horizontal)

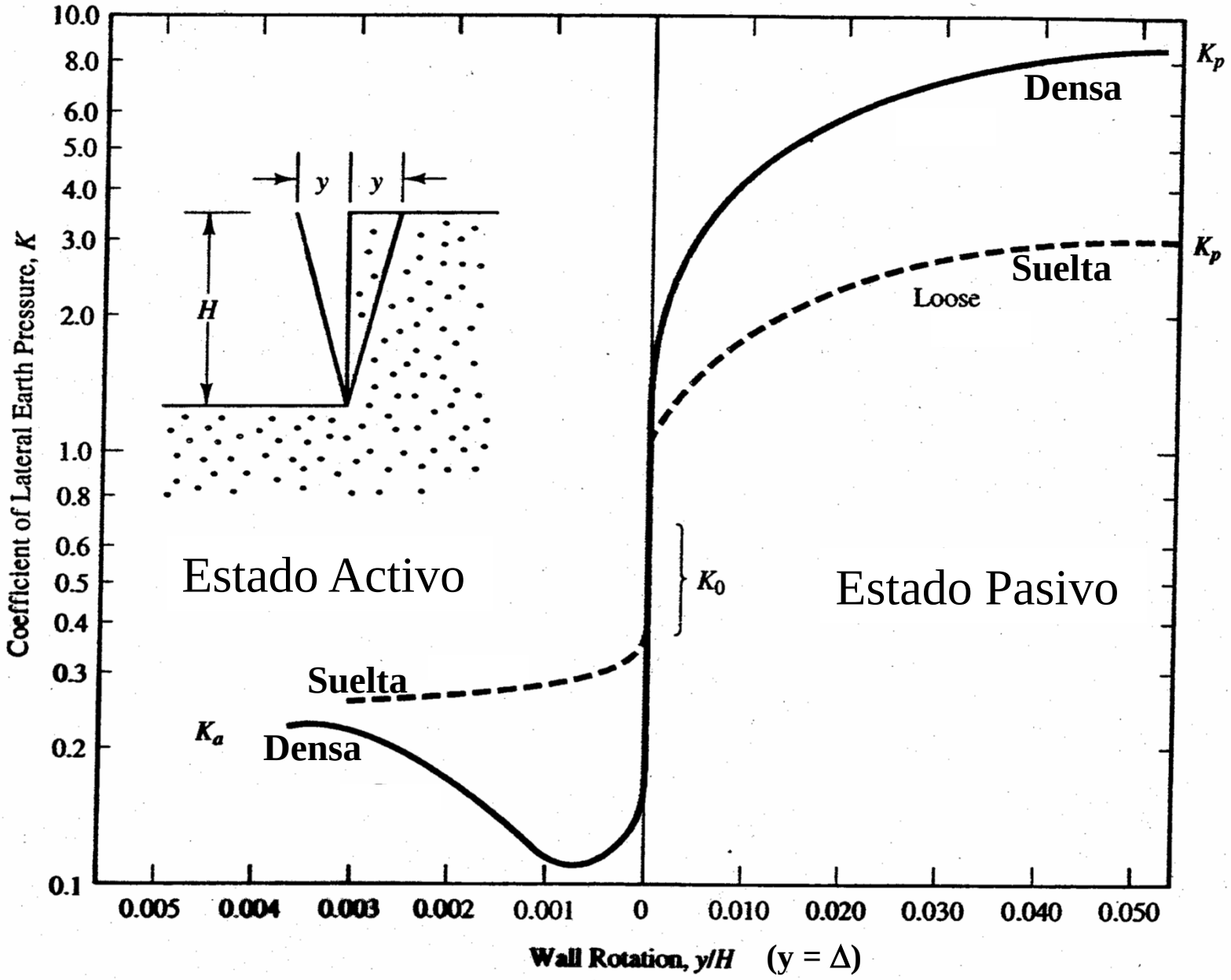

Figure 23.4 Effect of wall movement on lateral earth pressure in sand (Adapted from CGS, 1985).

Teoría de Rankine – Relleno Inclinado (Figura 12.10 Presiones Laterales)

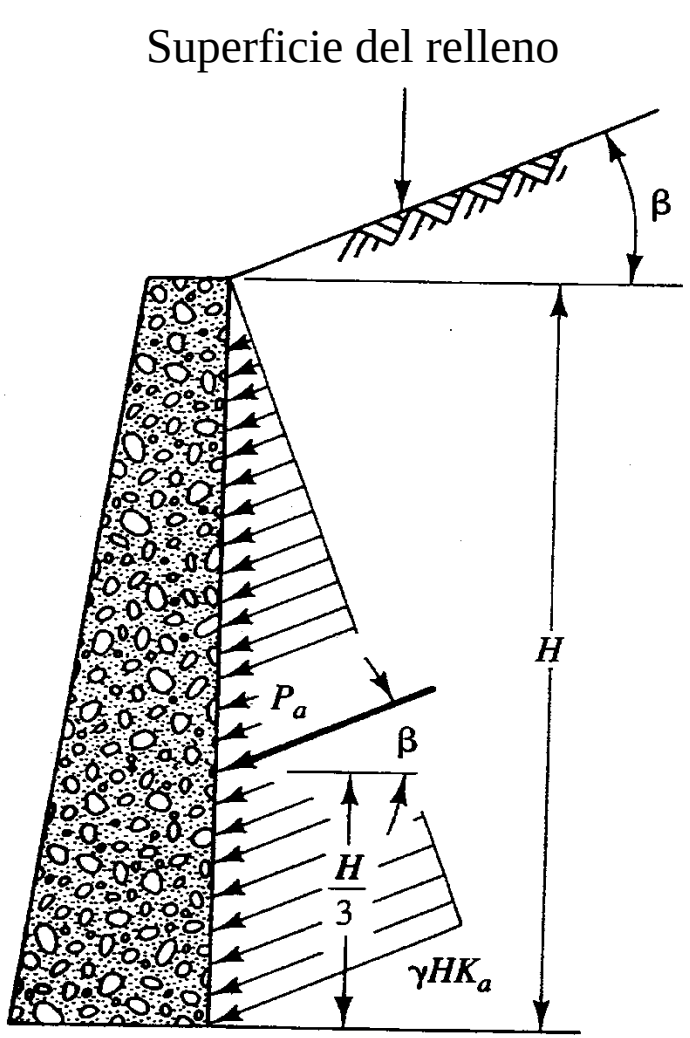

(a) cara posterior vertical

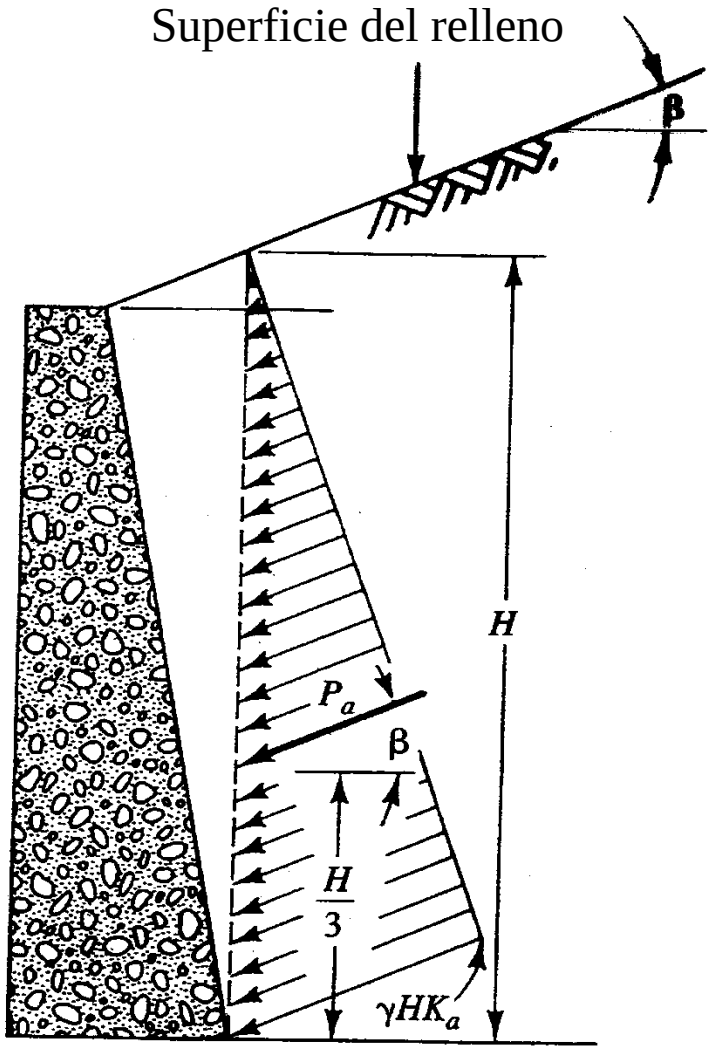

(b) cara posterior inclinada

Teoría de Rankine – Relleno Inclinado

Coeficiente de presión lateral activo (K_a):

$$K_a = \cos\beta \frac{\cos\beta - \sqrt{\cos^2\beta - \cos^2\phi}}{\cos\beta + \sqrt{\cos^2\beta - \cos^2\phi}}$$

Donde:

K_a= coeficiente de presión lateral activo,

ϕ = ángulo de fricción interna del suelo en el relleno

β = ángulo entre la superficie del terreno y la línea horizontal

- Si β=0 entonces,

$$K_a = \frac{1-\sin\phi}{1+\sin\phi} = \tan^2\left(45^\circ - \frac{\phi}{2}\right)$$

Teoría de Rankine – Relleno Inclinado (Fuerza Activa)

$$P_a = \frac{1}{2}\gamma H^2 K_a$$

Donde:

P_a= fuerza activa por longitud unitaria de pared

γ = peso unitario del suelo en el relleno

H = altura de la pared,

K_a = coeficiente de presión lateral activo

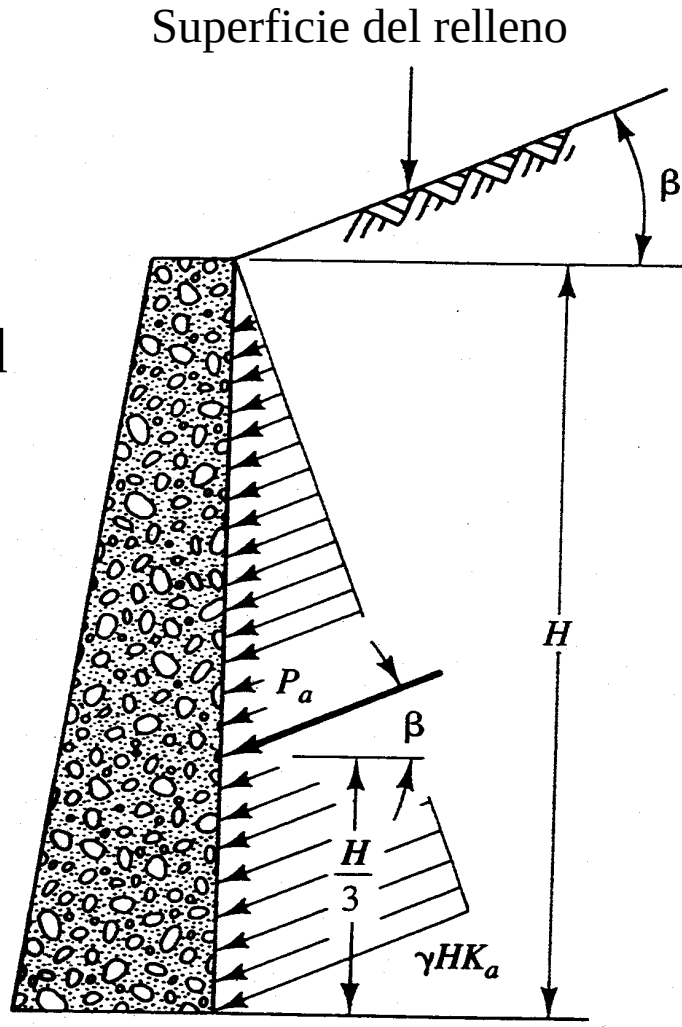

(a) cara posterior vertical

Teoría de Rankine – Relleno Inclinado

Coeficiente de presión lateral pasivo (K_p):

$$K_p = \cos\beta \frac{\cos\beta + \sqrt{\cos^2\beta - \cos^2\phi}}{\cos\beta - \sqrt{\cos^2\beta - \cos^2\phi}}$$

Donde:

K_p= coeficiente de presión lateral pasivo,

ϕ = ángulo de fricción interna del suelo en el relleno

β = ángulo entre la superficie del terreno y la línea horizontal

- Si β=0 entonces,

$$K_p = \frac{1+\sin\phi}{1-\sin\phi} = \tan^2\left(45^\circ + \frac{\phi}{2}\right) = \frac{1}{K_a}$$

Teoría de Rankine – Relleno Inclinado (Fuerza Pasiva)

$$P_p = \frac{1}{2}\gamma H^2 K_p$$

Donde:

P_p= fuerza pasiva por longitud unitaria de pared,

γ = peso unitario del suelo en el relleno

H= altura de la pared,

K_p= coeficiente de presión lateral activo

Teoría de Coulomb para suelos con $c = 0$ y $\phi \geq 0$

- Suposiciones
  - El suelo es homogéneo e isotrópico
  - La superficie mas critica es un plano
  - La superficie del terreno es un plano (no tiene que ser horizontal)
  - El movimiento de la pared es suficiente para desarrollar la condición activa o pasiva.
  - La fuerza lateral resultante esta inclinada a un ángulo igual a ϕ_w medido desde una linea perpendicular al muro
  - Existe fricción entre el suelo y la pared

Teoría de Coulomb-Coeficientes

$$K_a = \frac{\cos^2(\phi - \alpha)}{\cos^2 \alpha \cos(\phi_w + \alpha) + \left[1 + \sqrt{\frac{\sin(\phi + \phi_w)\sin(\phi - \beta)}{\cos(\phi_w + \alpha)\cos(\alpha - \beta)}}\right]^2}$$

Donde:

K_a= coeficiente de presión lateral activo,

ϕ = ángulo de fricción interna del suelo en el relleno,

β = ángulo entre la superficie del terreno y la línea horizontal,

α = ángulo de inclinación del interior de la pared medido desde la vertical, y

ϕ_w= ángulo de fricción en la interfase entre la pared y el relleno. Para paredes de concreto usar, ϕ_w 0.5ϕ y 0.67ϕ.

Nota: Esta ecuación es valida sólo para $\beta \leq \phi$

Figure 23.12 Parameters for Coulomb's active earth pressure equation. Walls inclined in the opposite direction have a negative α. V_a/b normally acts in the direction shown, thus producing a positive ϕ_w.

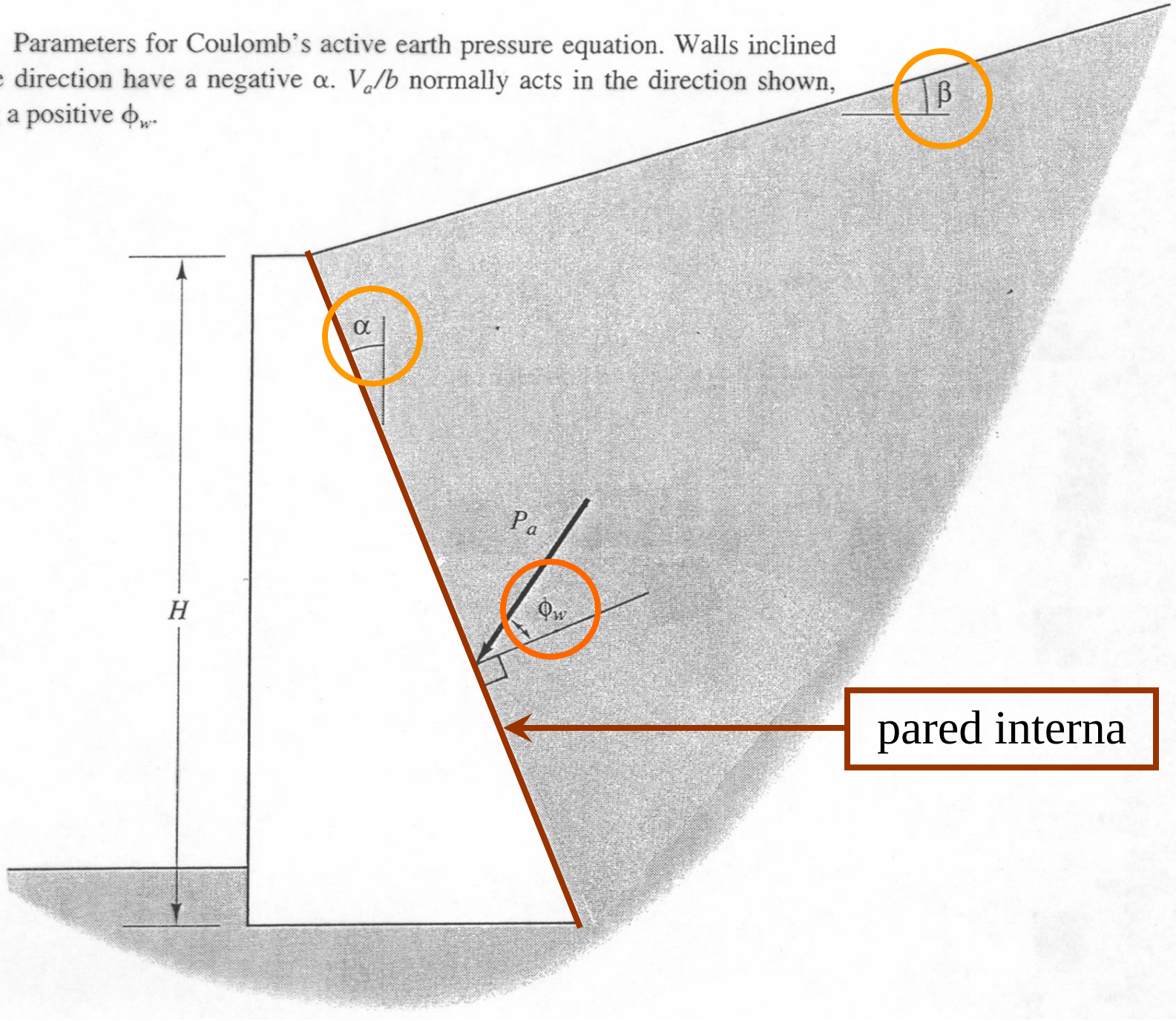

Fuerza Activa

$$P_a = \frac{1}{2}\gamma H^2 K_a$$

Donde:

P_a = fuerza activa por longitud unitaria de pared

γ = peso unitario del suelo

H = altura del muro

K_a= coeficiente de presión activa

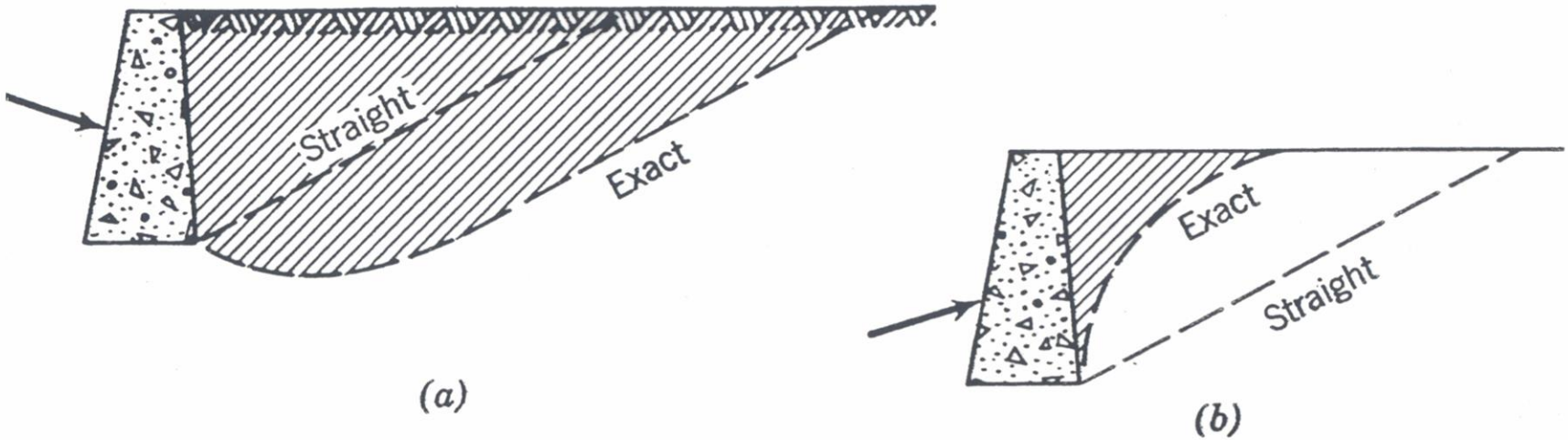

Fig. 13.19 Comparison of passive failure zone predicted by trial wedge method using straight and curved slip lines. (*a*) Positive wall friction. (*b*) Negative wall friction.

Valores Típicos para $\phi_w=\delta$ Fricción ente suelo y muro

Interface Materials	Friction Factor, tan δ	Friction angle, δ degrees
Mass concrete on the following foundation materials:		
Clean sound rock	0.70	35
Clean gravel, gravel-sand mixtures, coarse sand	0.55 to 0.60	29 to 31
Clean fine to medium sand, silty medium to coarse sand, silty or clayey gravel	0.45 to 0.55	24 to 29
Clean fine sand, silty or clayey fine to medium sand	0.35 to 0.45	19 to 24
Fine sandy silt, nonplastic silt	0.30 to 0.35	17 to 19
Very stiff and hard residual or preconsolidated clay	0.40 to 0.50	22 to 26
Medium stiff and stiff clay and silty clay	0.30 to 0.35	17 to 19
(Masonry on foundation materials has same friction factors.)		
Steel sheet piles against the following soils:		
Clean gravel, gravel-sand mixtures, well-graded rock fill with spalls	0.40	22
Clean sand, silty sand-gravel mixture, single size hard rock fill	0.30	17
Silty sand, gravel or sand mixed with silt or clay	0.25	14
Fine sandy silt, nonplastic silt	0.20	11
Formed concrete or concrete sheet piling against the following soils:		
Clean gravel, gravel-sand mixture, well-graded rock fill with spalls	0.40 to 0.50	22 to 26
Clean sand, silty sand-gravel mixture, single size hard rock fill	0.30 to 0.40	17 to 22
Silty sand, gravel or sand mixed with silt or clay	0.30	17
Fine sandy silt, nonplastic silt	0.25	14
Various structural materials:		
Masonry on masonry, igneous and metamorphic rocks:		
Dressed soft rock on dressed soft rock	0.70	35
Dressed hard rock on dressed soft rock	0.65	33
Dressed hard rock on dressed hard rock	0.55	29
Masonry on wood (cross grain)	0.50	26
Steel on steel at sheet pile interlocks	0.30	17

(from NAVFAC DM7.2 p.63)

Paredes con relleno cohesivo

- Por regla general, el relleno utilizado en estructuras de retención debe ser sin cohesión (granular), sin embargo en ocasiones no es posible evitar los rellenos de suelos cohesivos
- Suelos cohesivos utilizados para relleno presentan las siguientes debilidades:
  - Pobre drenaje (baja permeabilidad)
  - Deformación bajo esfuerzos constantes (Creep)
  - Propiedades expansivas
- La mayoría de las teorías de empuje lateral de tierra fueron desarrolladas para suelos puramente cohesivos (c=0), con el tiempo estas teorías se han modificado para suelos cohesivos.

Utilizar $\gamma_{equivalente}$ (discutido ayer)

Problemas con rellenos fino c >0

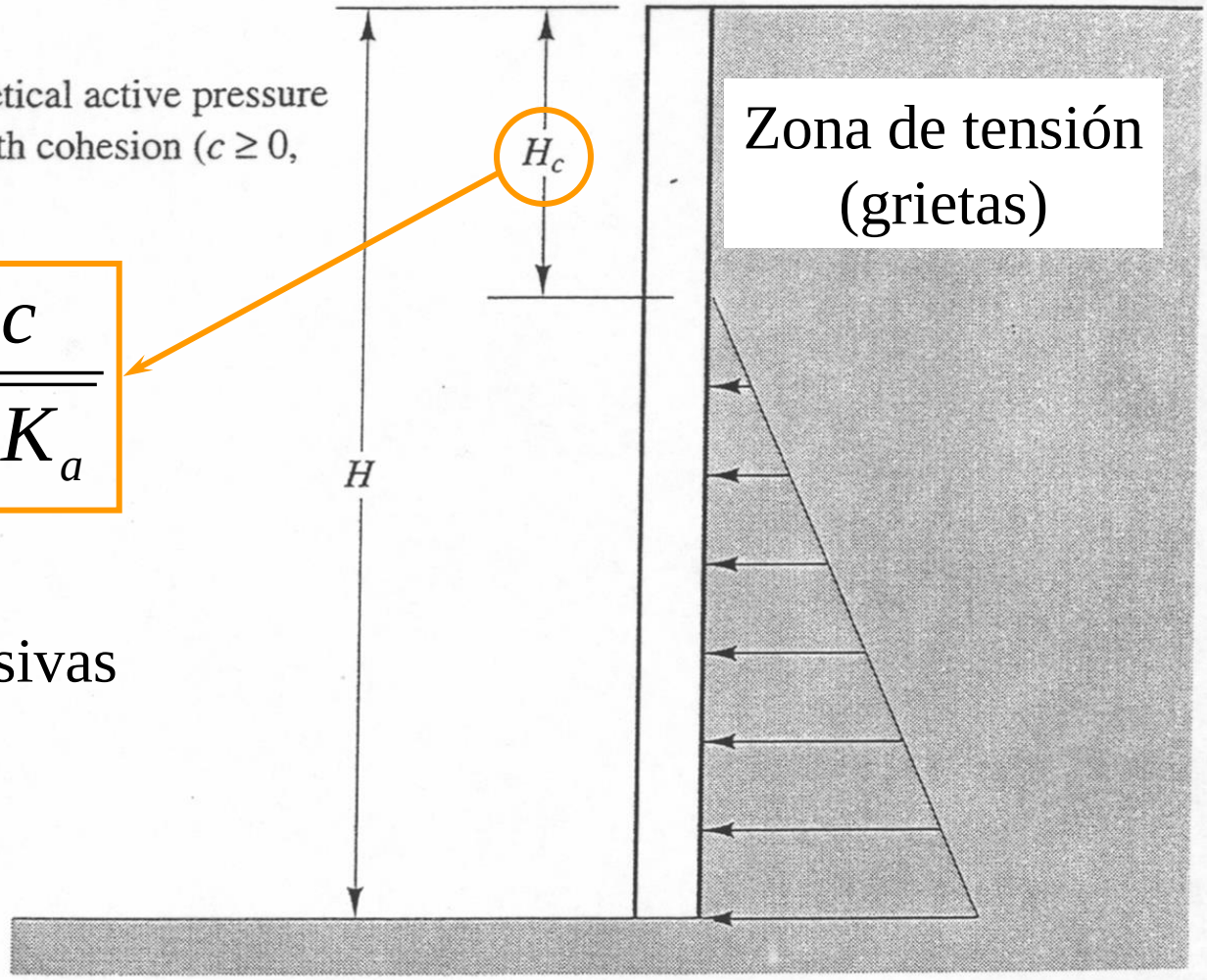

Figure 23.14 Theoretical active pressure distribution in soils with cohesion ($c \geq 0$, $\phi \geq 0$).

$$H_c = \frac{2c}{\gamma\sqrt{K_a}}$$

Propiedades expansivas

H_c = altura crítica. Es la altura máxima en la cual un suelo cohesivo puede mantenerse verticalmente sin la presencia de la pared.

Método de Fluido Equivalente

$$P_{a-h} = \frac{G_h H^2}{2}$$

$$P_{a-v} = \frac{G_v H^2}{2}$$

Donde:

$P_{a\text{-}h}$ = componente horizontal de la fuerza activa

$P_{a\text{-}v}$ = componente vertical de la fuerza activa por longitud unitara

G_h, G_v= densidad de fluido equivalente horizontal y vertical

Fluido Equivalente

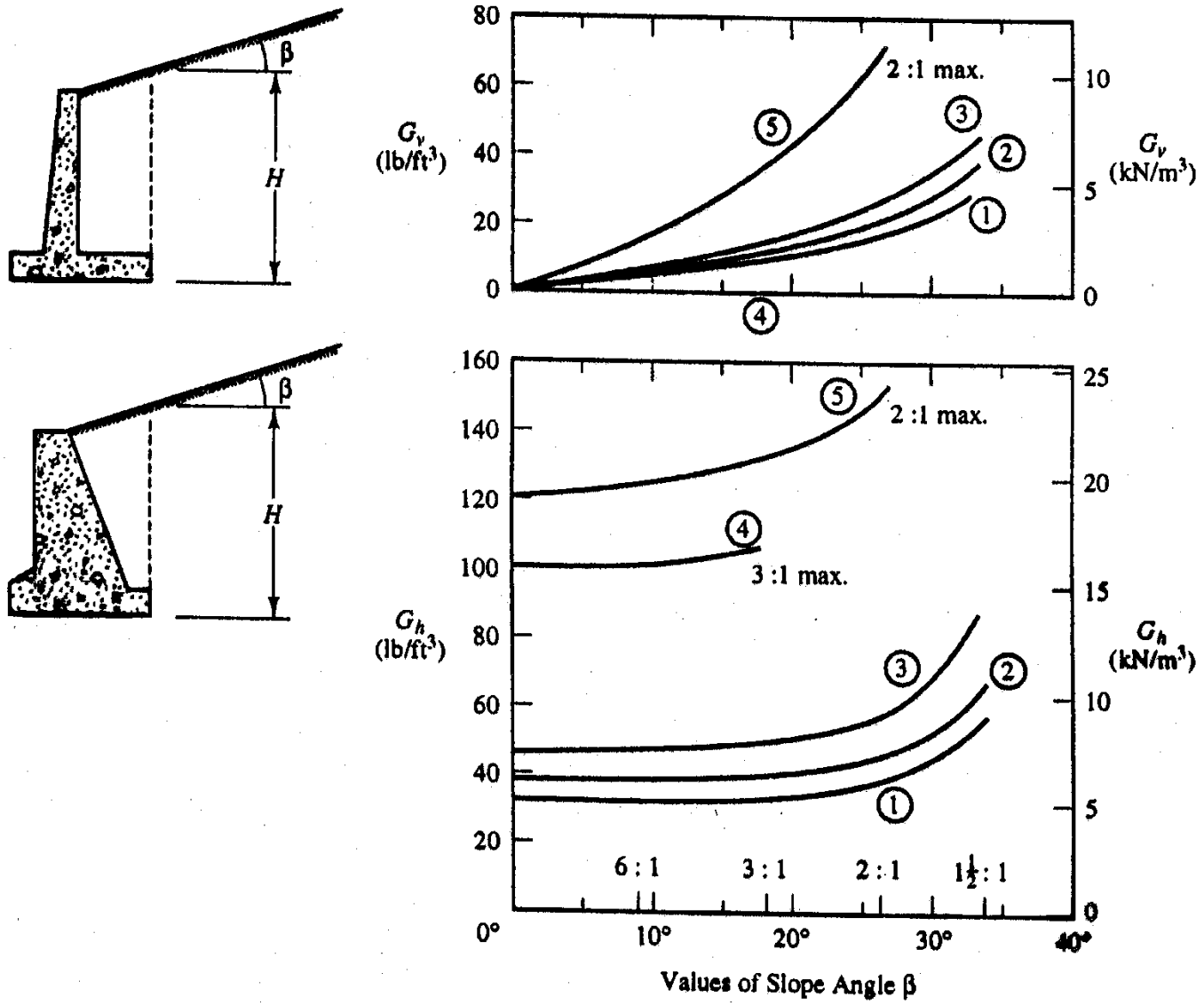

Figure 23.13 Charts for estimating the loads acting against a retaining wall beneath a planar ground surface (Adapted from Terzaghi and Peck, 1967).

Sobrecargas
(generan presiones adicionales sobre el muro)

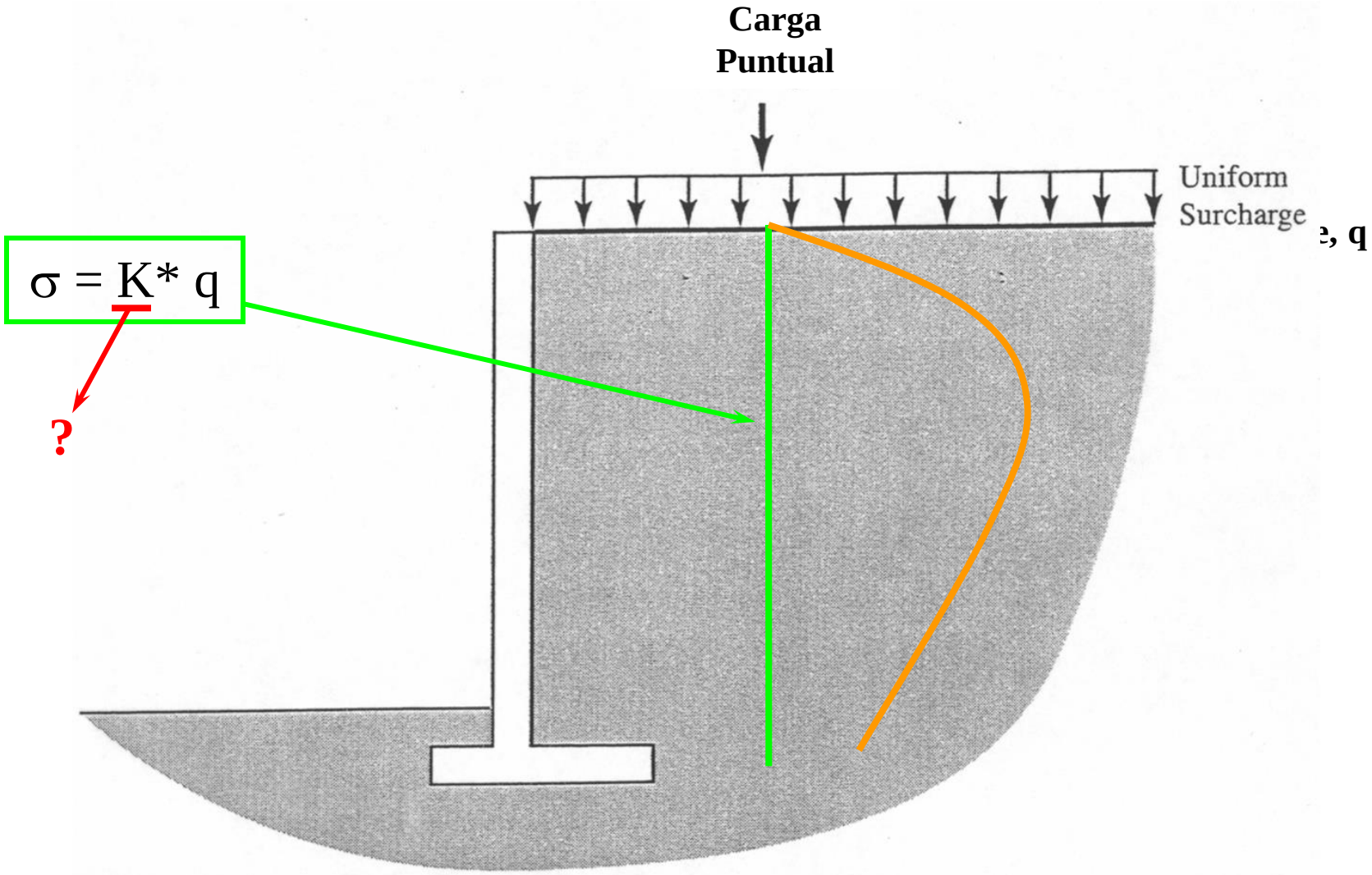

Figure 23.18 Typical surcharge loads near a retaining wall.

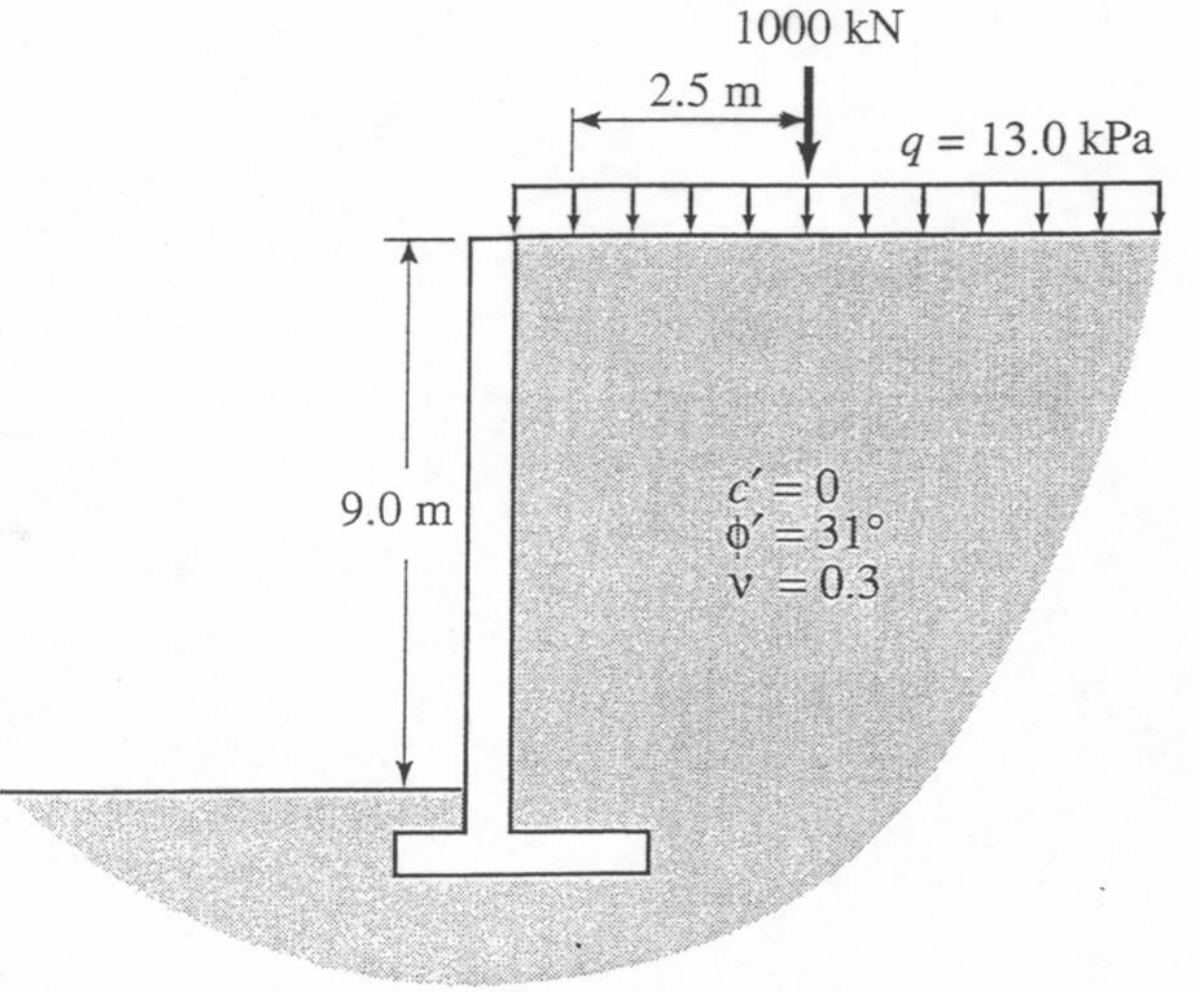
1000 kN
2.5 m
q = 13.0 kPa
9.0 m
c′ = 0
ϕ′ = 31°
ν = 0.3

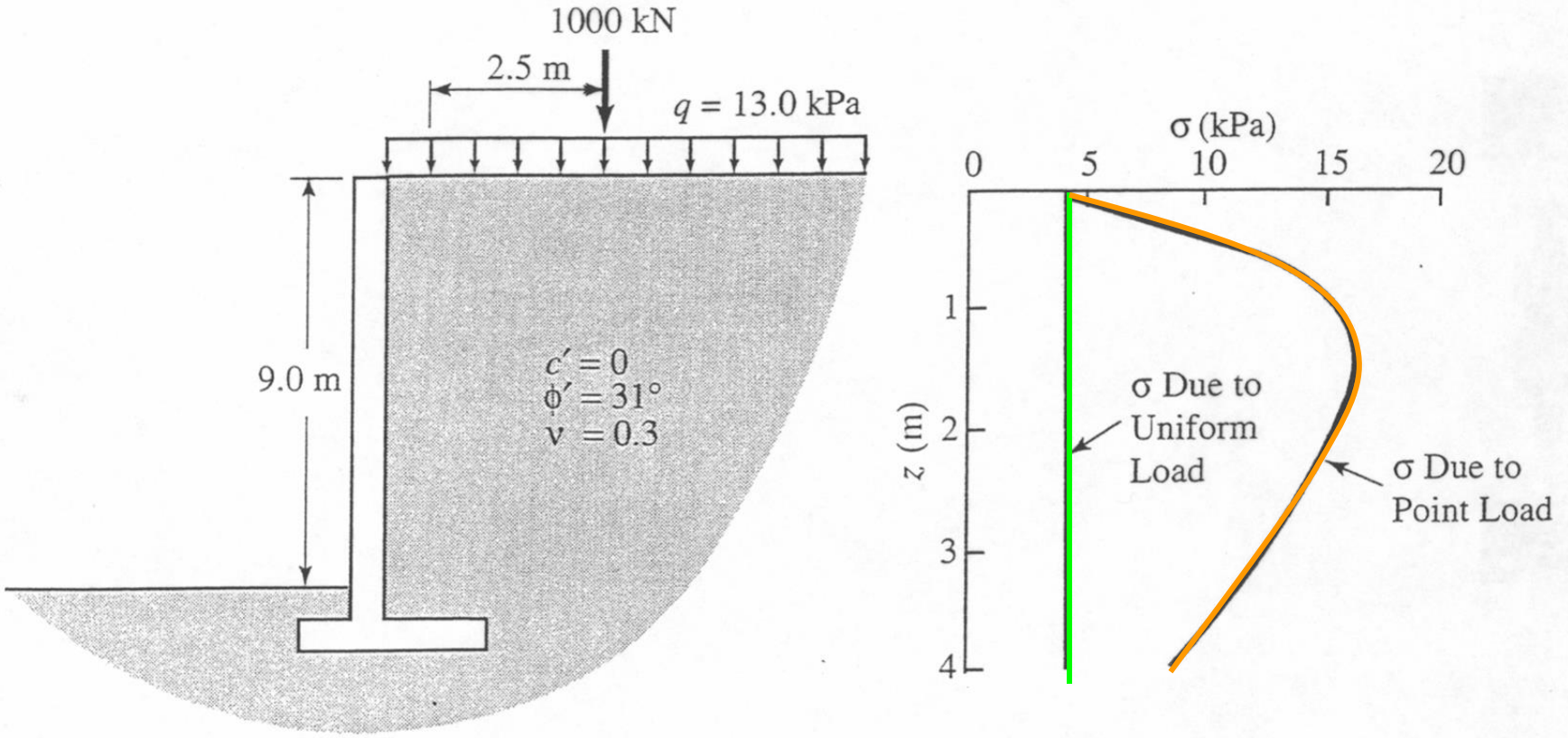

Figure 23.19 Proposed retaining wall with surcharge load for Example 23.6.

Efecto de sobrecarga, algunas ecuaciones

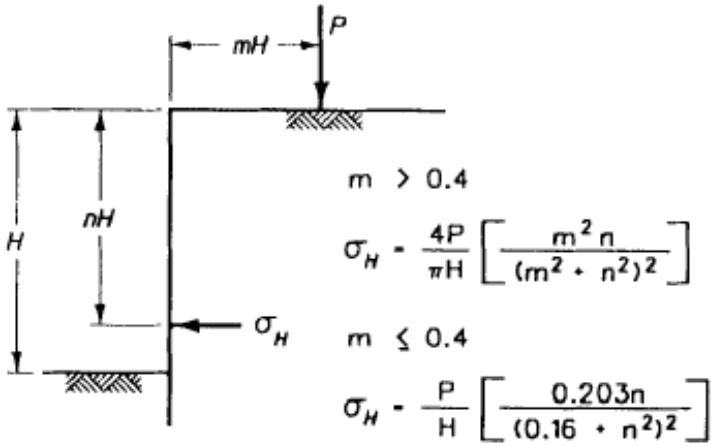

a. Line load (factor of two included)
from Terzaghi (1954)

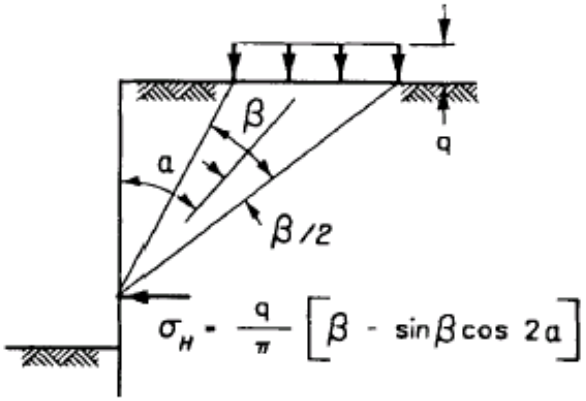

b. Strip load

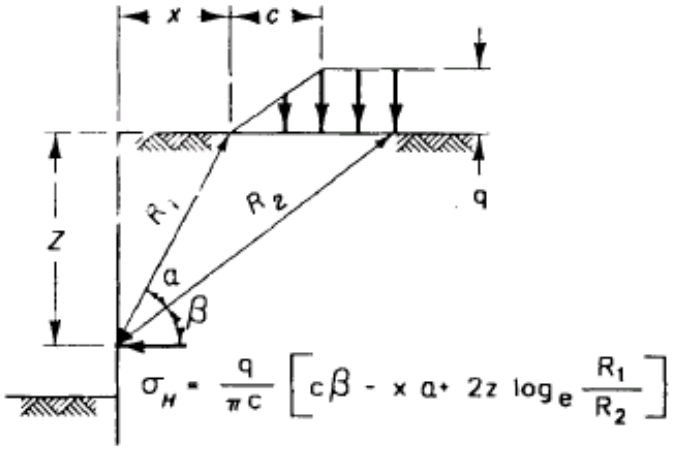

c. Ramp load

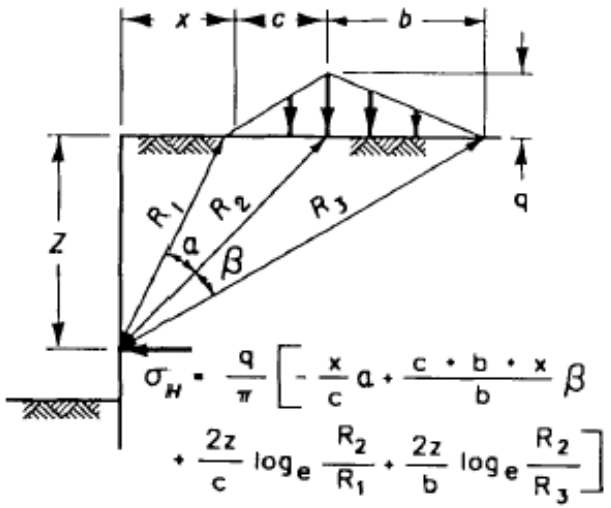

d. Triangular load

from Dawkins (1991)

NOTES:

(1) FOR FIGURES (c) AND (d) THE ANGLES α AND β ARE EXPRESSED IN UNITS OF RADIANS.

(2) NEGATIVE PRESSURES MAY BE COMPUTED AT SHALLOW DEPTHS (Z).

Efecto del Agua

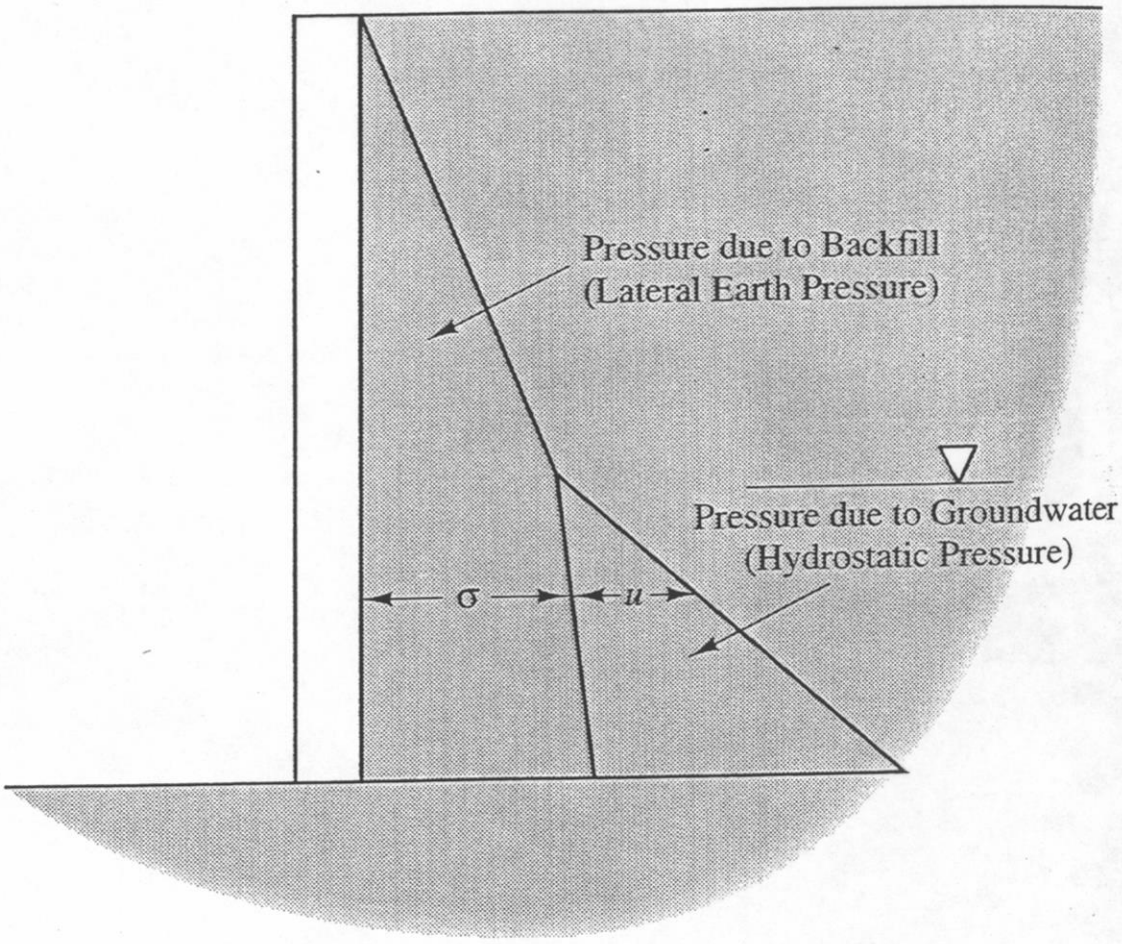

Figure 16.16 Theoretical lateral pressure distribution with shallow groundwater table.

Sobrecarga y nivel freático

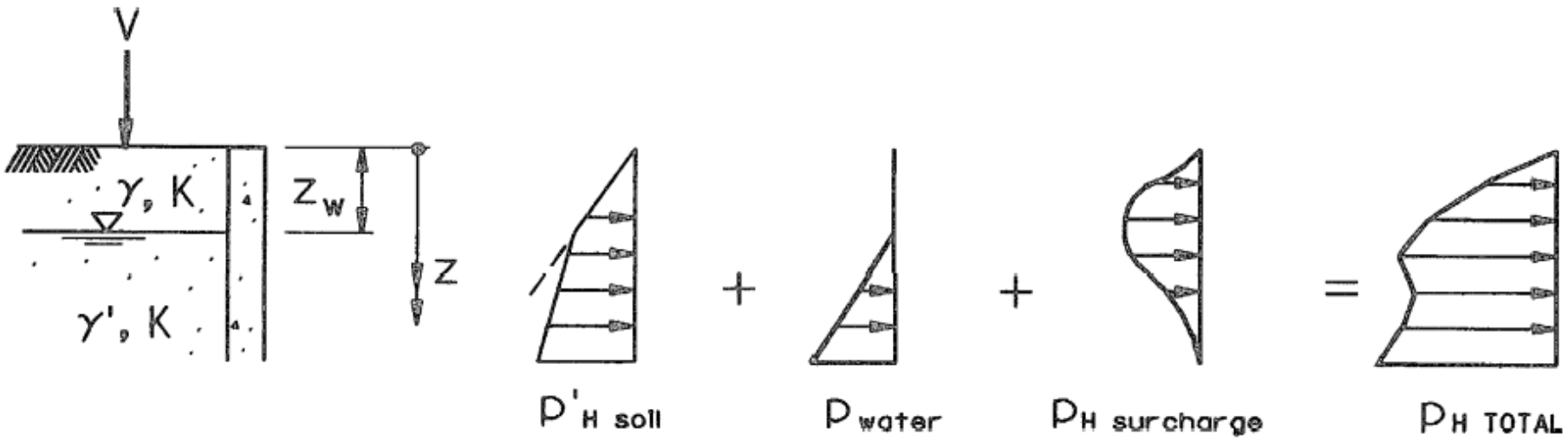

Figure 3-20 Lateral pressures, one soil, water, finite surcharge

Presión lateral de diseño - Activa

- Para casos donde el relleno o la fundación del muro contengan suelos arcillosos,
  - Las teorías clásicas de empuje lateral de tierra no toman en consideración la tendencia de estos suelos a deformarse bajo esfuerzos constantes (creep)
  - Utilizar el método de Terzaghi y Peck
- Para paredes con suelos granulares (arenas y gravas) en el relleno o bajo la fundación del muro.
  - Utilizar la teoría de Coulomb
  - Fijar ϕ_w = entre (0.5 ϕ) y (0.67 ϕ)
  - Otra opción es utilizar el método de Terzaghi y Peck.

Presión lateral de diseño - Pasiva

- Utilizar la teoría de Rankine
- Los ingenieros generalmente utilizan un valor menor al obtenido teóricamente por las siguientes razones,
  - El desplazamiento horizontal requerido para movilizar la presión pasiva en ocasiones es mayor a las deformaciones permisibles del muro. Se utiliza la mitad de los valores permisibles.
  - El suelo en la cara exterior del muro es generalmente alterado por “landscaping” o alguna otra actividad por lo que este generalmente no es tan resistente como se anticipa

MODOS DE FALLA
Estabilidad Externa e Interna

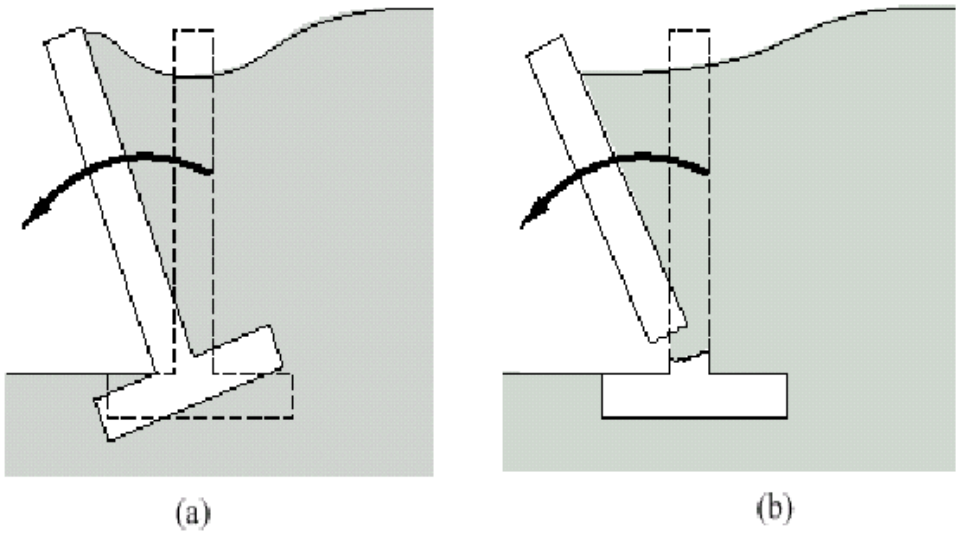

Figure 24.1 (a) A wall that lacks sufficient external stability moves away from its desired location because the soil fails; (b) A wall with inadequate internal stability (structural integrity) is unable to carry the necessary internal stresses and experiences a structural failure.

Modos de falla – Estabilidad Externa

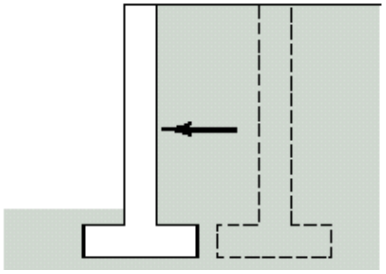

(a) Deslizamiento

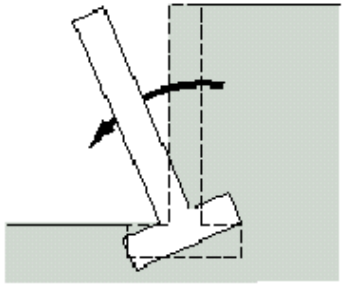

(b) Falla por vuelco

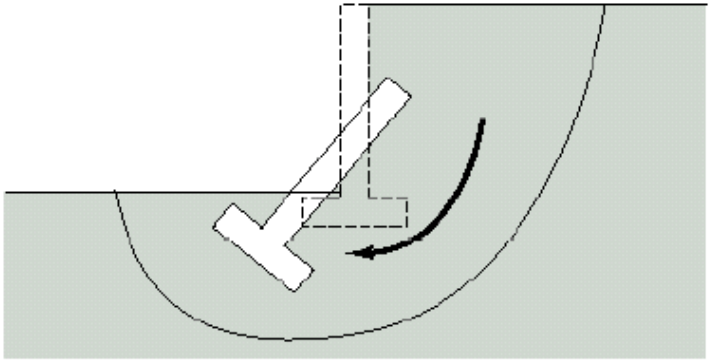

(c) Falla Global - estabilidad

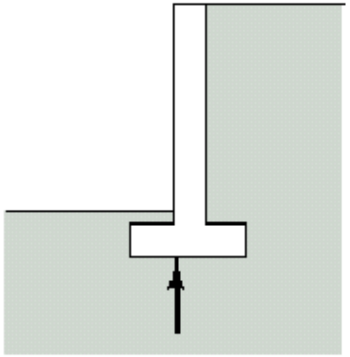

(d) Fuerzas de levantamiento

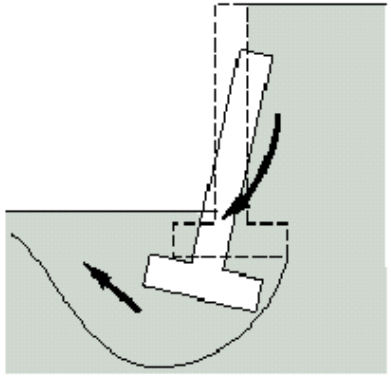

(e) Capacidad de Carga

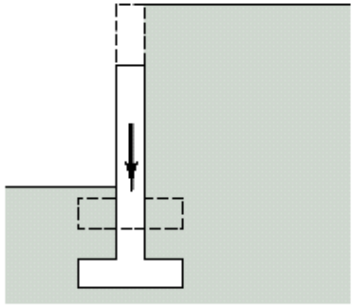

(f) Asentamientos excesivos

(a) Deslizamiento

Criterio de falla:

$$FS = \frac{\sum(fuerzas - resisten)}{\sum(fuerzas - causan)} = \frac{\sum(P_R / b)}{\sum(P_D / b)} \geq 1.5$$

Resiste – fuerza hidrostática en cara externa del muro

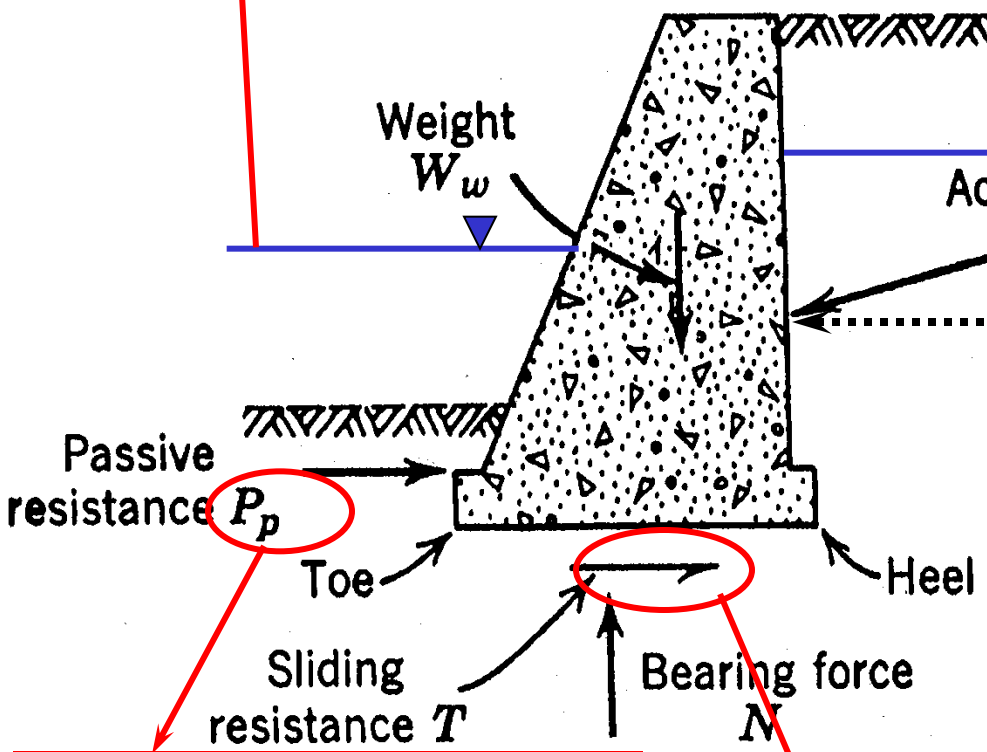

Causa – fuerza hidrostática actuando en la cara interna del muro

Causa – componente horizontal de la presión activa sobre el muro

Resiste – Presión lateral en cara externa del muro

Resiste – Fricción en la fundación (interfase muro el suelo)

Fuerza cortante V_f/b

$$V_f/b = (P_f/b) \tan(\phi_s)$$

Donde:

V_f/b = resistencia al corte generada a través de la fundación por longitud unitaria de muro.

P_f/b = fuerza normal entre la fundación y el suelo por longitud unitaria de muro.

ϕ_s = ángulo de fricción en la interfase fundación-suelo.

Angulo de Fricción Interfase Fundación-Suelo, ϕ_s

TABLE 23.4 DESIGN VALUES OF ϕ_f FOR CAST-IN-PLACE CONCRETE FOOTINGS

Soil or Rock Classification	ϕ_f (deg)
Clean sound rock	35
Clean gravel, gravel-sand mixtures, coarse sand	29 - 31
Clean fine to medium sand, silty medium to coarse sand, silty or clayey gravel	24 - 29
Clean fine sand, silty or clayey fine to medium sand	19 - 24
Fine sandy silt, nonplastic silt	17 - 19
Very stiff and hard residual or overconsolidated clay	22 - 26
Medium stiff and stiff clay and silty clay	17 - 19

Adapted from U.S. Navy (1982b).

(b) Vuelco

Criterio de falla:

$$FS = \frac{\sum(resisting\ moments)}{\sum(driving\ moments)} = \frac{\sum(M_R/b)}{\sum(M_D/b)}$$

Σ(moments) around the toe of the wall

Resiste – fuerza hidrostática en cara externa del muro

Resiste – Sobrecarga

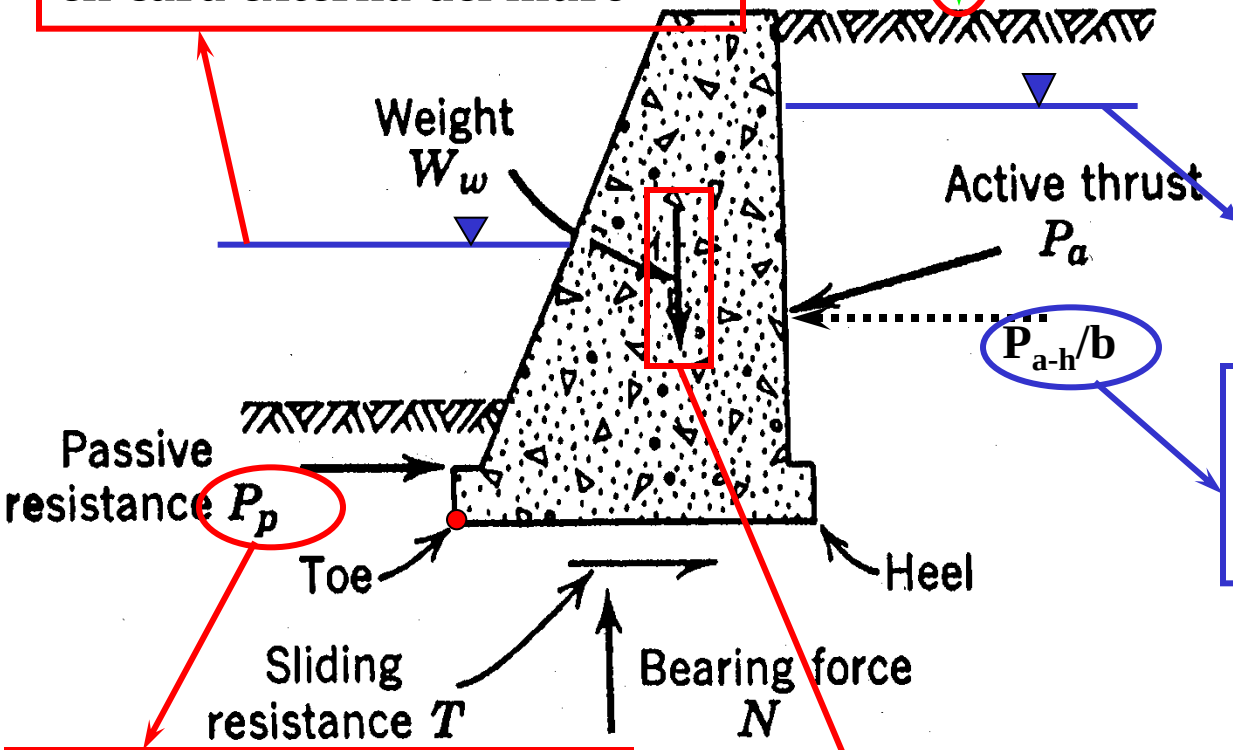

Causa – fuerza hidrostática actuando en la cara interna del muro

Causa – componente horizontal de la presión activa sobre el muro

Resiste – Presión lateral en cara externa del muro

Resiste – Peso del muro

Vuelco

- Criterio de falla

$$FS = \frac{\sum(resisting\ moments)}{\sum(driving\ moments)} = \frac{\sum(M_R / b)}{\sum(M_D / b)}$$

Para suelos sin cohesión FS ≥1.5
Para suelos cohesivos FS ≥2.0

(c) Capacidad portante

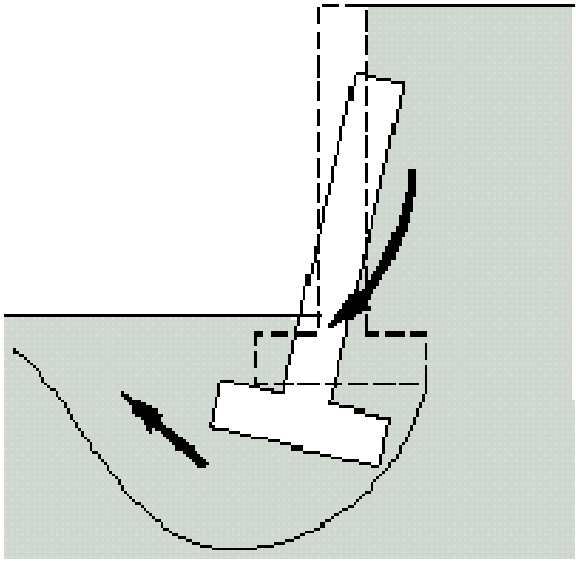

- Presiones en la zapata
  - Verificar no sobrepasar $q_{admisible}$ (repasar zapata)

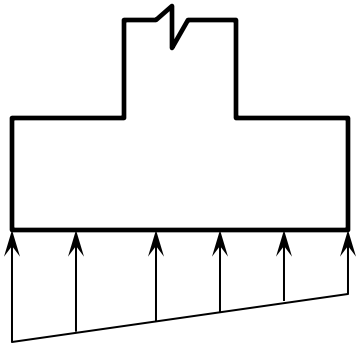

  - Verificar asentamientos admisibles, en ocasiones presión admisible se fija para cumplir con asentamientos admisibles

Recomendaciones Típicas de un Reporte Geotécnico

1) Material de Relleno: AASHTO A-2-4 o mejor
2) Ángulo de Fricción Interna del Material de Relleno, φ = 30 grados
3) Cohesión del Material de Relleno, c = 0 libras/pie^2 (psf.)
4) Ángulo de Inclinación del Relleno, β = 0 grados (a ser confirmado con los planos)
5) Peso Unitario del Material de Relleno = 125 libras/pie^3 (pcf.)
6) Capacidad de Carga Permitida = 2,000-psf
7) Profundidad Mínima para la Fundación = 3 pies

Incluye Capacidad Portante y Asentamientos

Dynamic Earth Pressure

Mononobe-Okabe

Dynamic Earth Pressure Approach

- During earthquakes, the soil behind a retaining wall exerts a horizontal dynamic thrust that is greater than the static force.
- Pseudo-static approach is suggested.
- The method was developed for dry cohesionless materials.

Dynamic Earth Pressure Approach, cont.

- Assumptions:
  - The wall yields sufficiently to produce the active pressure during earthquake.
  - The active failure wedge developed behind the wall behave as a rigid body. Pseudo-static inertial force are:
    - $k_h W_s$, $k_v W_s$, W_s = weight of the soil active failure wedge
  - The soil behind the wall is not saturated.

Fuerza Activa – Efecto Dinámico

Teoría de Mononobe-Okabe

$$P_{ae} = \frac{1}{2}\gamma H^2 (1 - k_v) K_{ae}$$

Donde:

P_{ae} = fuerza activa total dinámica por longitud unitaria de pared

γ = peso unitario del suelo

H = altura del muro

K_{ae}= coeficiente de presión lateral activo, incluyendo efecto dinámico

k_v= coeficiente de aceleración vertical

Teoría de Mononobe-Okabe

$$K_{ae} = \frac{\cos^2(\phi - \psi - \alpha)}{\cos\psi \cos^2\alpha \cos(\phi_w + \alpha + \psi) + \left[1 + \sqrt{\frac{\sin(\phi + \phi_w)\sin(\phi - \psi - \beta)}{\cos(\phi_w + \alpha + \psi)\cos(\alpha - \beta)}}\right]^2}$$

Donde:

K_{ae}= coeficiente de presión lateral activo, incluyendo efecto dinámico

ϕ = ángulo de fricción interna del suelo en el relleno,

β = ángulo entre la superficie del terreno y la línea horizontal,

α = ángulo de inclinación del interior de la pared medido desde la vertical,

ϕ_w= ángulo de fricción en la interfase entre la pared y el relleno. Para paredes de concreto usar, ϕ_w 0.5ϕ y 0.67ϕ.

$\psi = \tan^{-1}1(k_h/(1-k_v))$

k_h= coeficiente de aceleración horizontal

k_v= coeficiente de aceleración vertical

Teoría de Mononobe-Okabe

- La fuerza activa total dinámica consiste de dos componentes:
  - Presión estática activa, P_a
  - Incremento dinámico de la fuerza activa, ΔP_{ae}

$$P_{ae} = P_a + \Delta P_{ae} \quad \Rightarrow \quad \Delta P_{ae} = P_{ae} - P_a$$

  - ΔP_{ae} = aplicada a H/3
  - ΔP_{ae} = aplicada a 0.6H

Teoría de Mononobe-Okabe

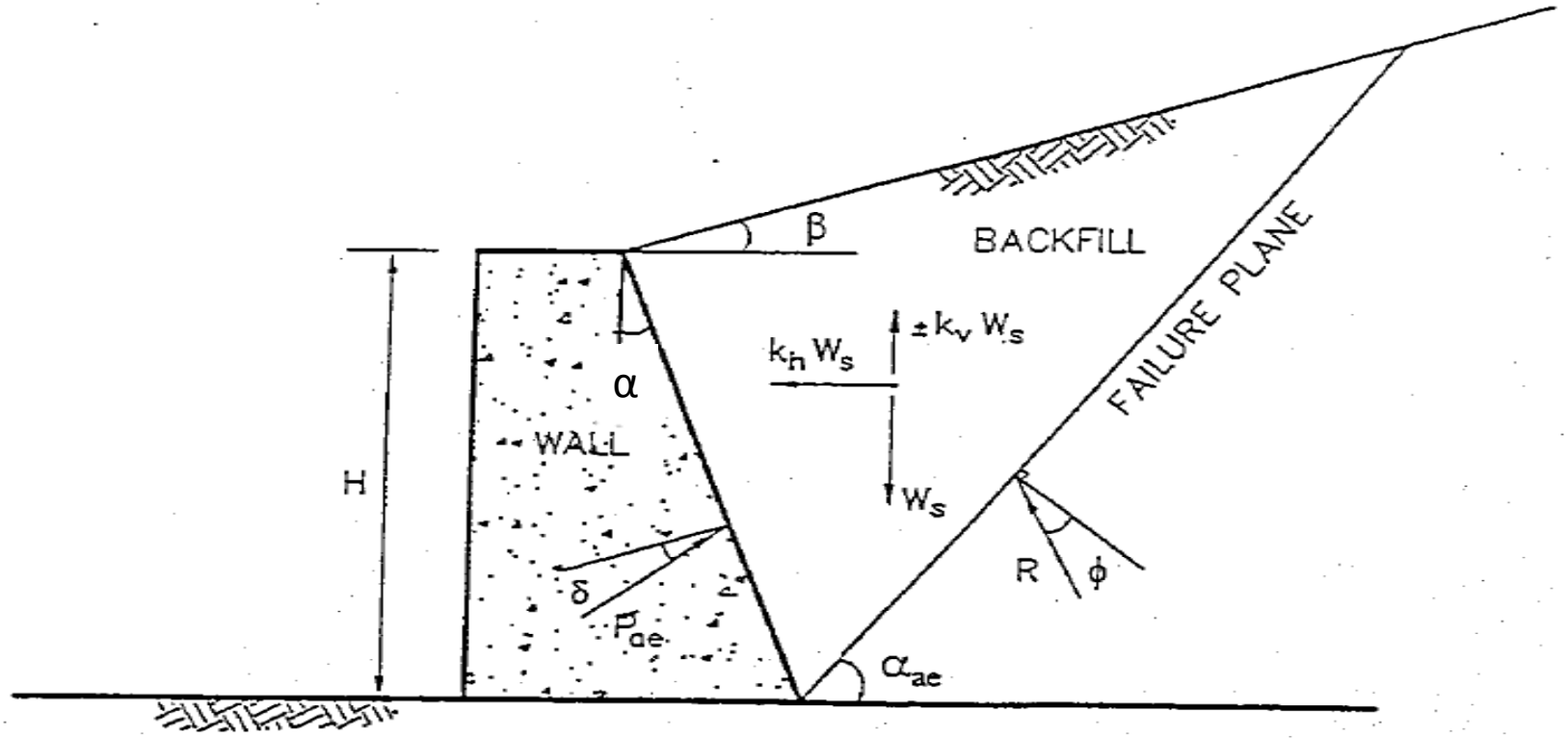

Procedimiento de Diseño – Teoría de Mononobe-Okabe

- Selecciones valores apropiados del coeficiente de aceleración horizontal, k_h. Valores pueden fluctuar entre 0 y 0.5. Típicamente se utiliza entre 0.15 y 0.2. Este valor depende de la aceleración pico generada por el terremoto.
- El valor del coeficiente de aceleración vertical típicamente se toma como cero, $k_v = 0$.
- Calcule las fuerzas inerciales del muro como el peso del muro multiplicado por el coeficiente de aceleración horizontal, $k_h W_{muro}$
- Calcule la fuerza activa dinámica total, P_{ae}
- Calcule el incremento dinámico de la fuerza activa, ΔP_{ae}
- Realice los cómputos de estabilidad

Procedimiento de Diseño – Teoría de Mononobe-Okabe

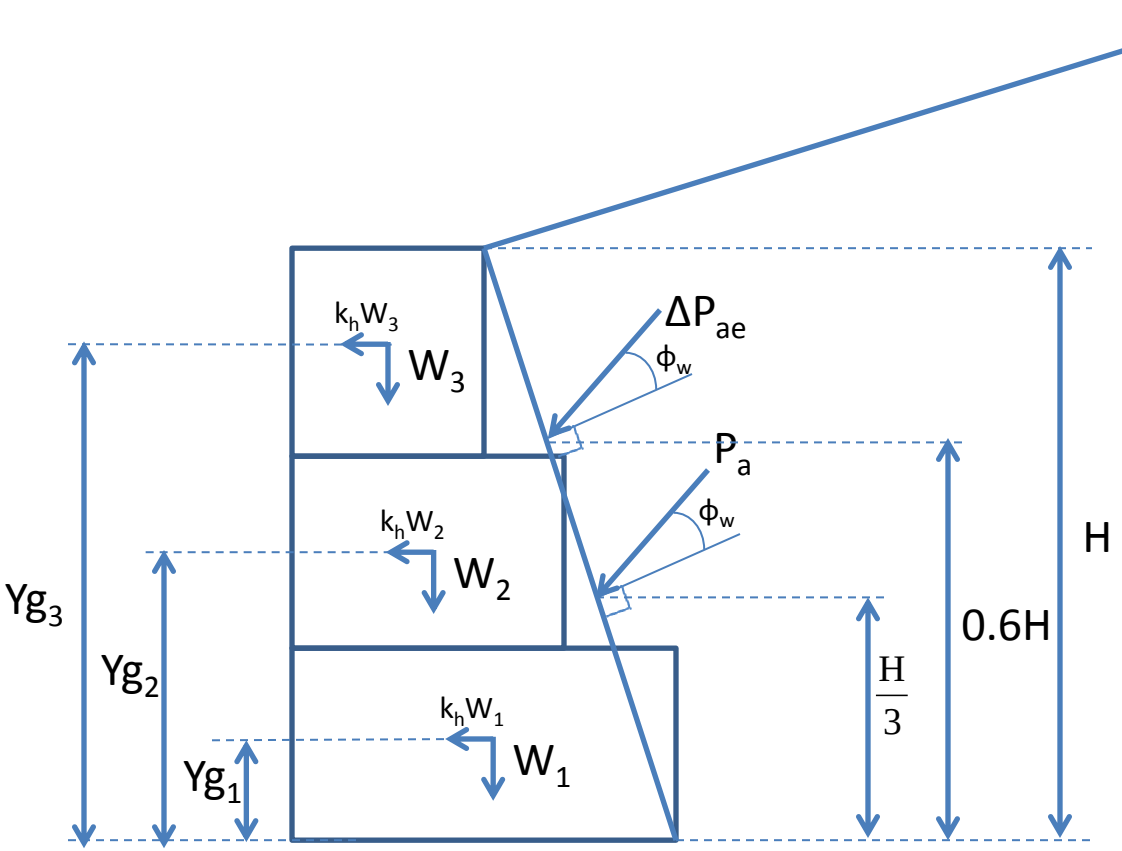

General Recommendations (FHWA)

- For critical facilities with walls that can accommodate very little deformations, use PGA.
  - Factor of safety
    - Bearing capacity and sliding - Factor of Safety between 1.0 and 1.1
    - Overturning stability – Factor of Safety between 1.3 and 1.5
- If the wall can accommodate some displacement, then a reduced seismic coefficient is used.
  - Factor of safety
    - Bearing capacity and sliding - Factor of Safety between 1.1 and 1.2
    - Overturning stability – Factor of Safety > 1.5

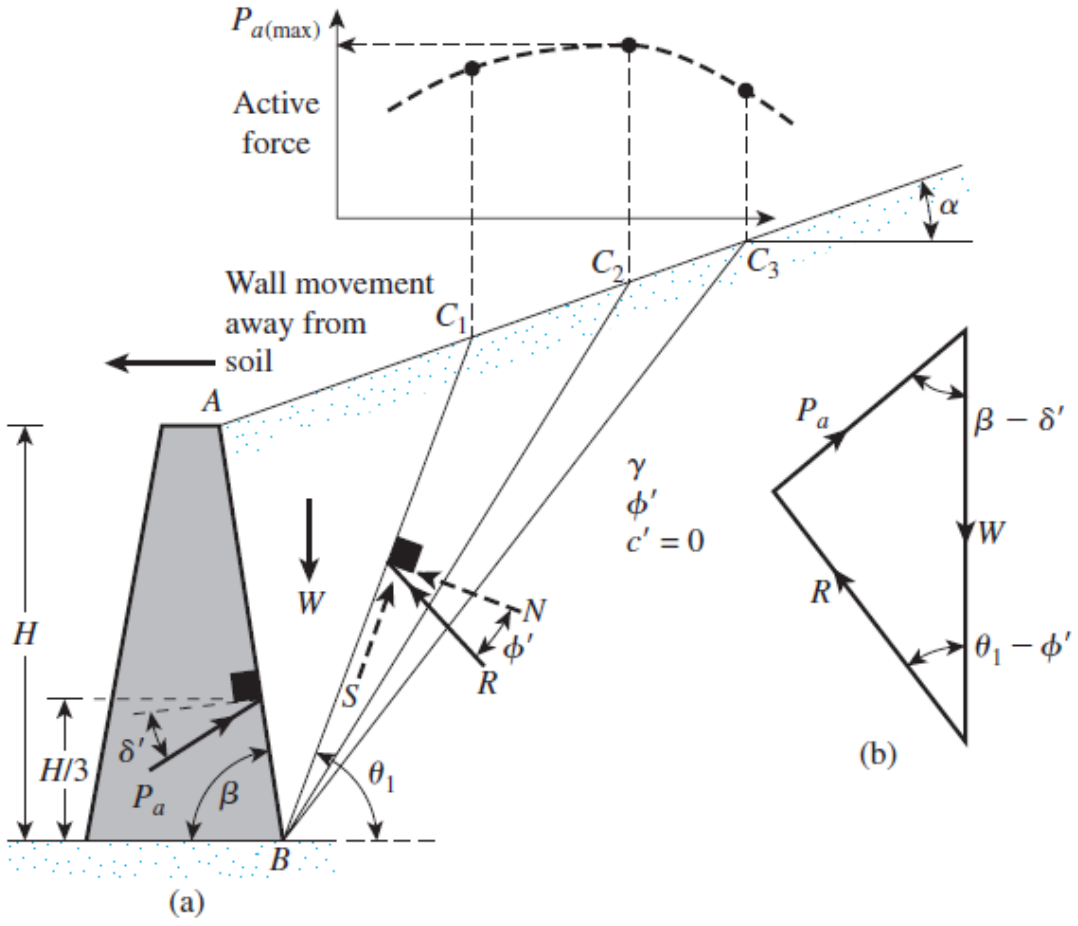
$P_{a(\max)}$
Active force
α
C_2
C_3
Wall movement away from soil
C_1
A
γ
ϕ'
$c' = 0$
W
N
ϕ'
R
S
H
δ'
H/3
P_a
β
θ_1
B
(a)
P_a
$\beta - \delta'$
W
R
$\theta_1 - \phi'$
(b)

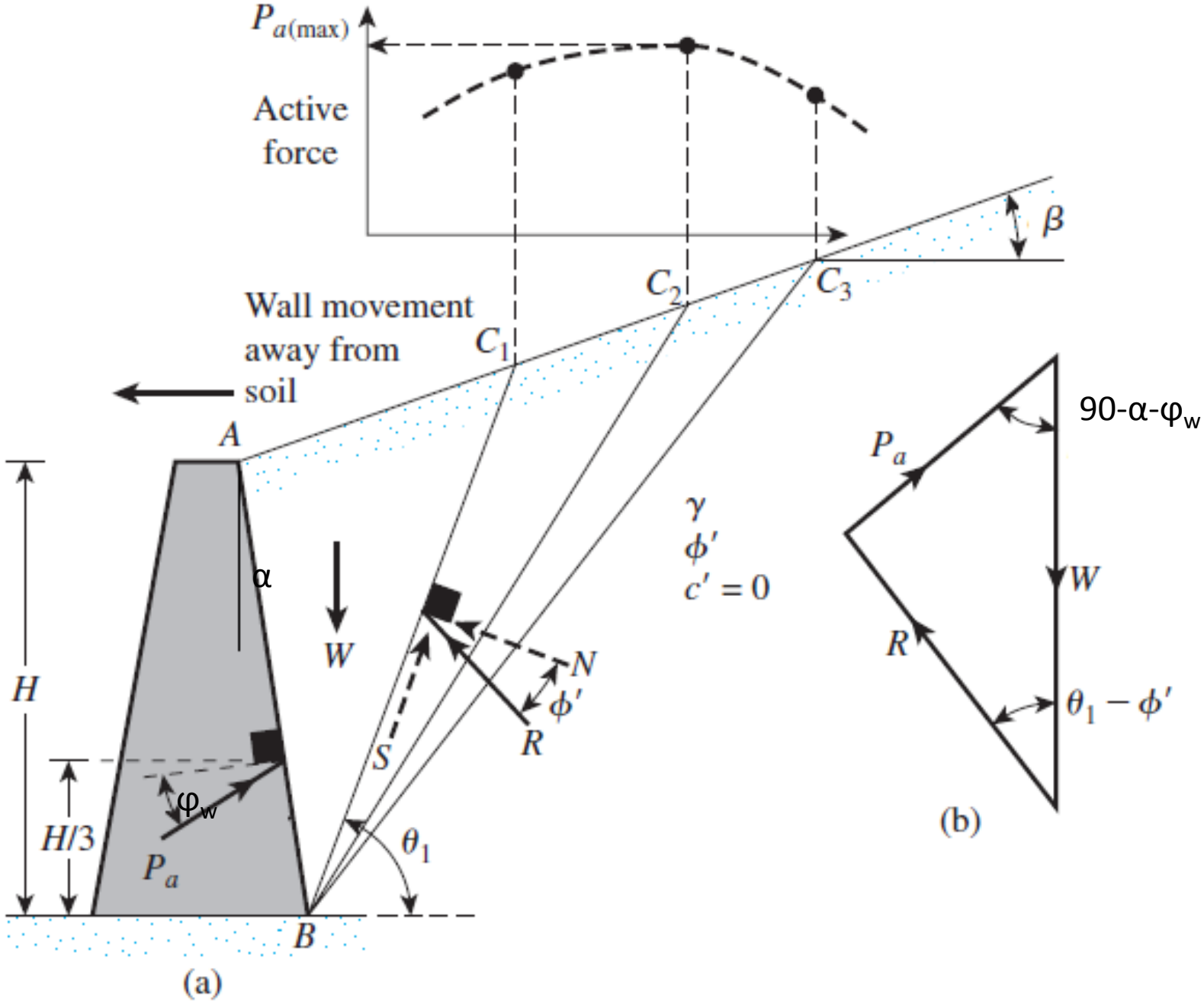
$P_{a(max)}$
Active force
β
C_2
C_3
Wall movement away from soil
C_1
A
α
W
H
γ
ϕ'
$c' = 0$
N
ϕ'
R
S
φ_w
H/3
P_a
θ_1
B
(a)
90-α-φ_w
P_a
W
R
$\theta_1 - \phi'$
(b)

Muro en gaviones

Tipos de Falla

- Deslizamiento sobre la base: ocurre cuando la resistencia al deslizamiento a lo largo de la base del muro, sumada al empuje pasivo disponible al frente de la estructura, es insuficiente para neutralizar el efecto del empuje activo actuante.

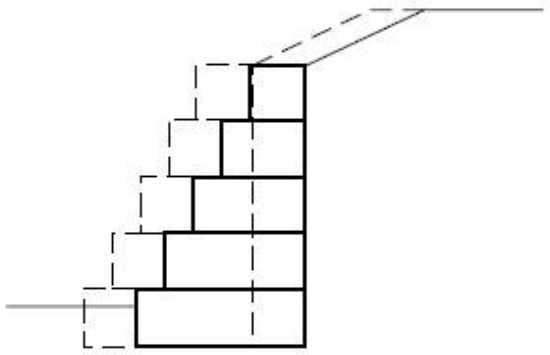

Deslizamiento

- Vuelco: ocurre cuando el momento estabilizante del peso propio del muro en relación al punto de vuelco es insuficiente para neutralizar el momento del empuje activo.

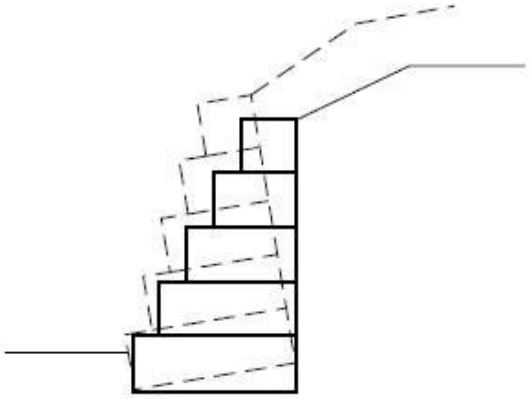

Vuelco

Tipos de Falla

- Rotura de la fundación o asentamientos excesivos: ocurre cuando las presiones aplicadas por la estructura sobre el suelo de fundación son superiores a su capacidad de carga.

- Rotura global del macizo: deslizamiento a lo largo de una superficie de rotura que envuelve a la estructura de contención.

- Rotura interna de la estructura: rotura de las secciones intermedias entre gaviones, que puede ocurrir tanto por deslizamiento como por exceso de presión normal.

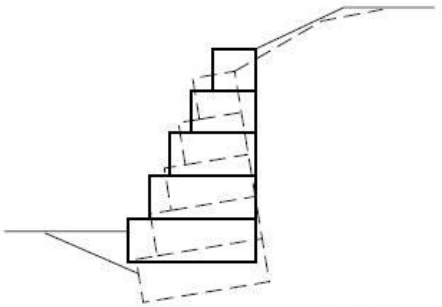

Rotura de la fundación

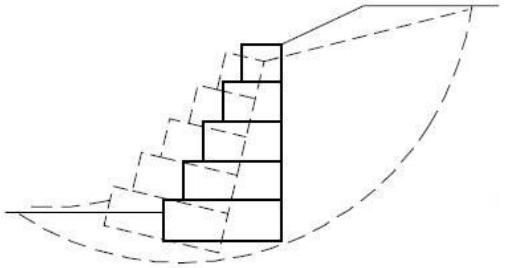

Rotura Global

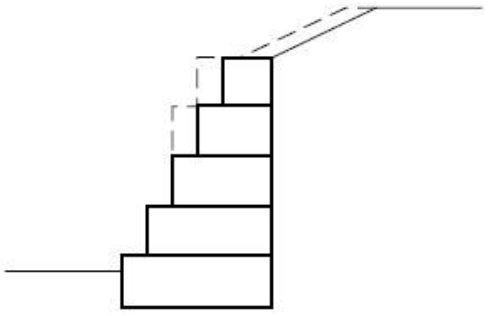

Rotura interna

Análisis y Diseño:

- Se aplica la misma teoría que a muros de gravedad.
- Literatura disponible:
  - Maccaferri y otros suplidores
  - NAVFAC Design Manual 7.2 Founation and Earth Structures (1982)

Análisis y Diseño:

Pasos a Seguir:

- Suponer dimensiones tentativas del muro.
  - Suelo con alta fricción: B/H ➔ 0.4- 0.5
  - Suelo con fricción moderada: B/H ➔ 0.5-0.7
  - Suelo con poca fricción o cohesivos: B/H ➔ 0.7-1.0
- Dibujar el diagrama de cuerpo libre del muro.
- Evaluar el empuje activo del suelo.
  - Teoría de Coulomb
  - Trial Wedge

Análisis y Diseño:
Pasos a Seguir:

- Analizar la estabilidad externa del sistema.
  - Deslizamiento
    - FS ≥ 1.5
  - Vuelco
    - FS ≥1.5 (suelos no cohesivos)
    - FE ≥ 2.0 (suelos cohesivos)
  - Capacidad de carga
  - Estabilidad global
    - Superficie de falla semicircular detrás y debajo del muro (falla profunda)

- Analizar la estabilidad interna del muro.
  - Verificación entre bloque y bloque aunque estos estén atados entre si
    - Deslizamiento
      - FS ≥ 1.5
    - Vuelco
      - FS ≥ 2.0

Análisis y Diseño
Consideraciones Especiales

- Peso especifico de rocas mas comunes para gaviones

Tipo de roca	(lb/ft^3)
Basalto	180
Granito	160
Caliza compacta	160
Traquita	155
Arenisca	140
Caliza tierna	138
Toba	105

- Para Gaviones se asume Angulo de fricción suelo-muro (Φw) ➔ (0.8 a 1) Φ
- Se recomienda inclinar el muro de gaviones unos 6° para aumentar la estabilidad del mismo.
- Despreciar fuerza pasiva frente al muro (conservador)

Análisis y Diseño:
Fuerzas Actuantes en Muro de Gaviones

Diagramas de Cuerpo Libre

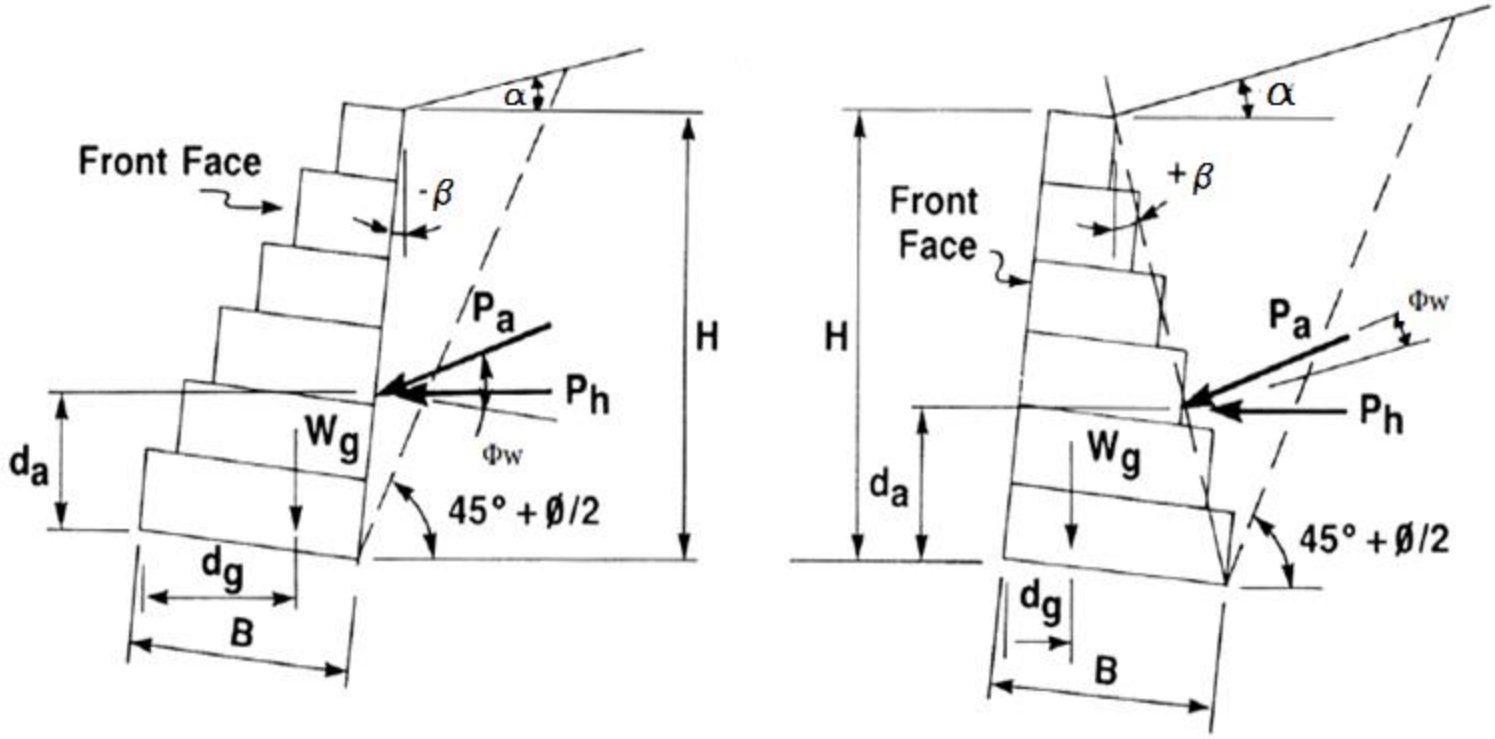

Análisis y Diseño:
Formulas

1. El empuje activo del suelo, P_a, se calcula usando la teoría de Coulomb.

$$P_a = \tfrac{1}{2}\ \gamma\ H^2\ K_a$$

γ = peso unitario del suelo
H = altura del muro
K_a = coeficiente de empuje activo de Coulomb $\rightarrow f(\varphi,\ \varphi_w,\ \beta,\ \alpha)$

$$K_a = \frac{\cos^2(\phi-\alpha)}{\cos^2\alpha\cos(\phi_w+\alpha)+\left[1+\sqrt{\frac{\sin(\phi+\phi_w)\sin(\phi-\beta)}{\cos(\phi_w+\alpha)\cos(\alpha-\beta)}}\right]^2}$$

2. Peso del muro, W

$$W = \gamma_{gaviones}\ x\ A$$

$\gamma_{gaviones}$ = peso unitario del gavión
A = área seccional del muro

Análisis y Diseño:
Formulas

3. Fuerzas normal y cortante en la base del muro, P_f y V_f

$$P_f = \Sigma \text{ fuerzas verticales}$$

$$V_f = (f \times P_f) + (c' \times B)$$

f = coeficiente de fricción suelo/muro
P_f = Σ fuerzas verticales que actúan en el plano de deslizamiento
c' = adhesión suelo-muro (0.67 x c)
B = ancho de la base del muro

En el caso de muros con gaviones, se ha determinado que $\varphi_w \approx (0.8 \text{ a } 1)\, \varphi$.

Análisis y Diseño: Ejemplo

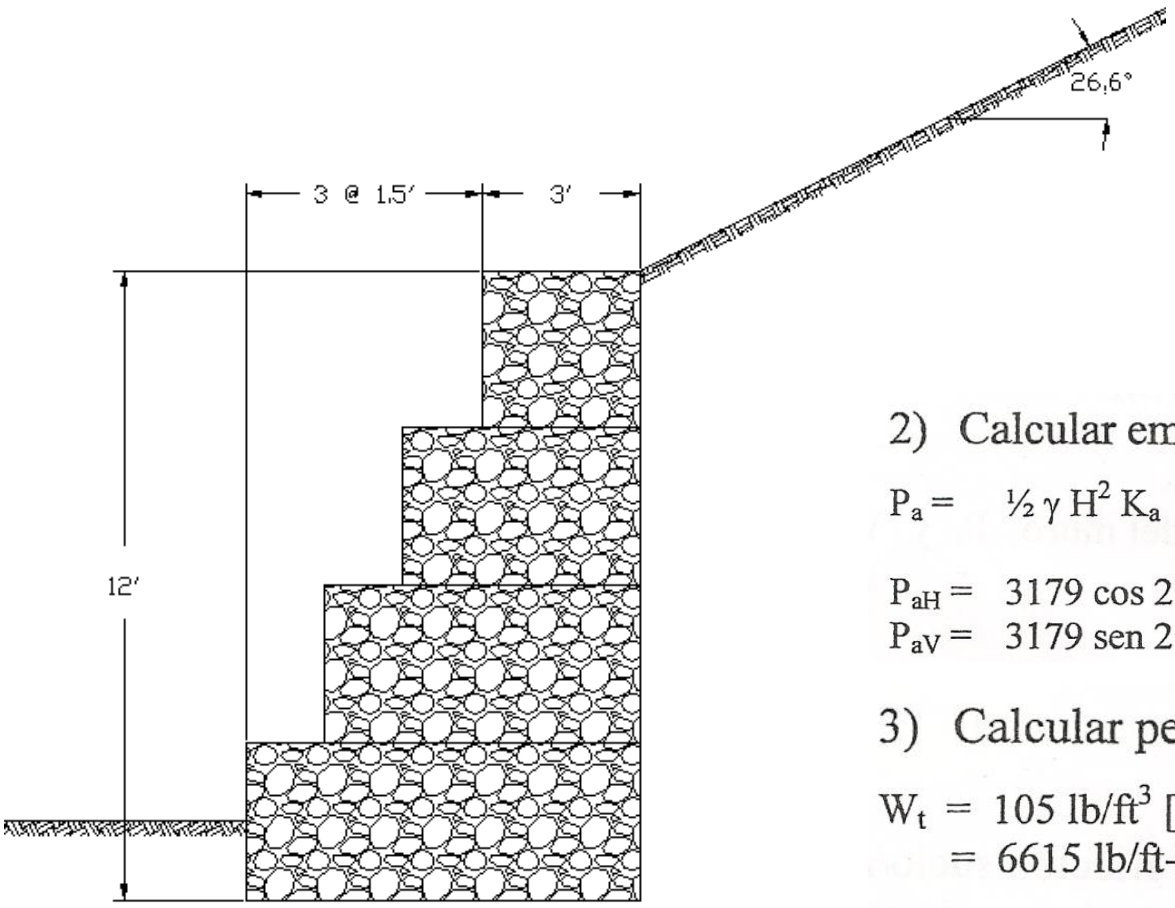

1) Calcular K_a

$\phi = 35^o$
$\beta = 26.6^o$
$\phi_w = 0.8\ \phi = 28^o$
$\alpha = 90^o$

$K_a \Rightarrow 0.384$ (Coulomb)

2) Calcular empuje activo de Coulomb

$P_a = \frac{1}{2}\gamma H^2 K_a = \frac{1}{2}(115)\,12^2\,(0.384) = 3179$ lb/ft-lin

$P_{aH} = 3179 \cos 28^o = 2807$ lb/ft-lin
$P_{aV} = 3179 \text{ sen } 28^o = 1492$ lb/ft-lin

3) Calcular peso total de gaviones

$W_t = 105\ \text{lb/ft}^3\ [\,(3x3) + (3x4.5) + (3x6) + (3x7.5)\,]$
$= 6615$ lb/ft-lin

Análisis y Diseño: Ejemplo

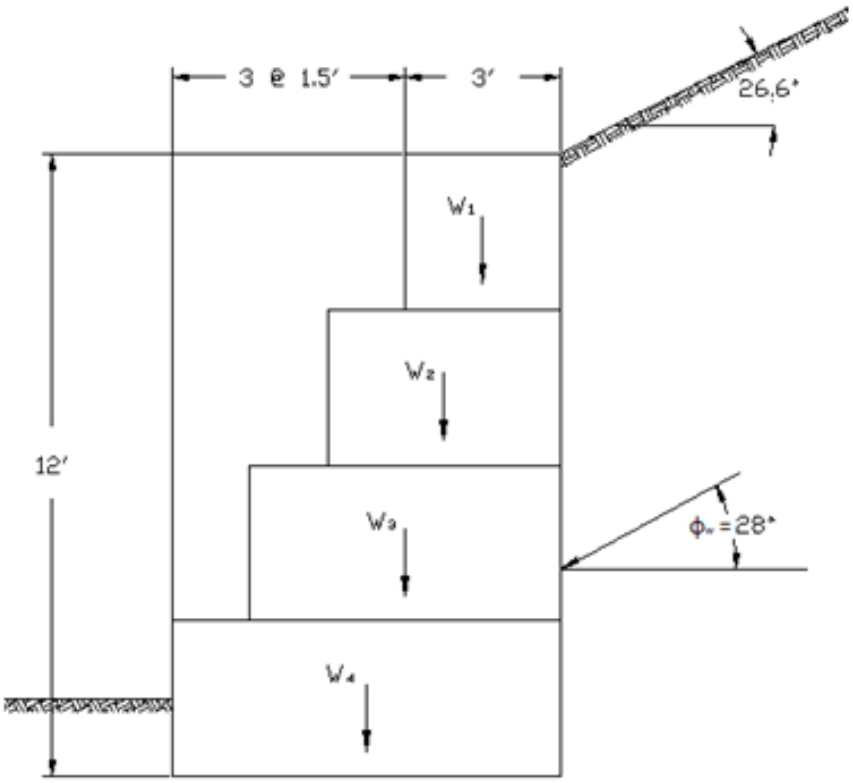

4) Dibujar diagrama de cuerpo libre y preparar cómputos en forma tabulada

Figura	A x γ = W	Brazo	Momento
1	3x3x105 = 945	4.5 + 3/2	5670
2	4.5x3x105 = 1417	3 + (4.5/2)	7439
3	6x3x105 = 1890	1.5 + (6/2)	8505
4	7.5x3x105 = 2362	7.5/2	8858
P_{av}	1492	7.5	11190
	ΣF_v 8106 lb	ΣM 41662	lb-ft/ft

5) Calcular factores de seguridad

a) Deslizamiento: $FS = [\Sigma F_v \times \tan \phi_w] / \Sigma P_h$
$= 8106\ (0.55) / 2807 = 1.59$

b) Vuelco: $FS = \overset{\curvearrowright}{M} / \overset{\curvearrowleft}{M} = 41662 / (2807 \times 12/3)$
$= 3.71$

Análisis y Diseño: Ejemplo

5) Calcular factores de seguridad (cont.)

c) Capacidad de carga:

$$\Sigma F_v \quad X = \overset{\curvearrowright}{M} - \overset{\curvearrowleft}{M}$$

$$X = (41662 - 11228) / 8106 = 3.75 \text{ ft}$$

$$e = B/2 - X = 7.5/2 - 3.75 = 0 \text{ ft}$$

$$q = \Sigma F_v / B' = 8106 / 7.5 = 1080 \text{ lb/ft}^2$$

$$q_{ult} = c N_c + \sigma'_{zD} N_q + \tfrac{1}{2} \gamma B N_\gamma$$

$$= \tfrac{1}{2} (110) \; 7.5 \; (28) = 11550 \text{ lb/ft}^2$$

Análisis y Diseño: Ejemplo

Si el muro tuviese escalones internos los resultados serían:

$K_a = 0.78$

$P_a = 6458$ lb/ft-lin

$FS_{des} = 1.48$

$FS_{vuel} = 2.82$

$e = 1.0$

$q_{equiv} = 2083$ lb/ft^3

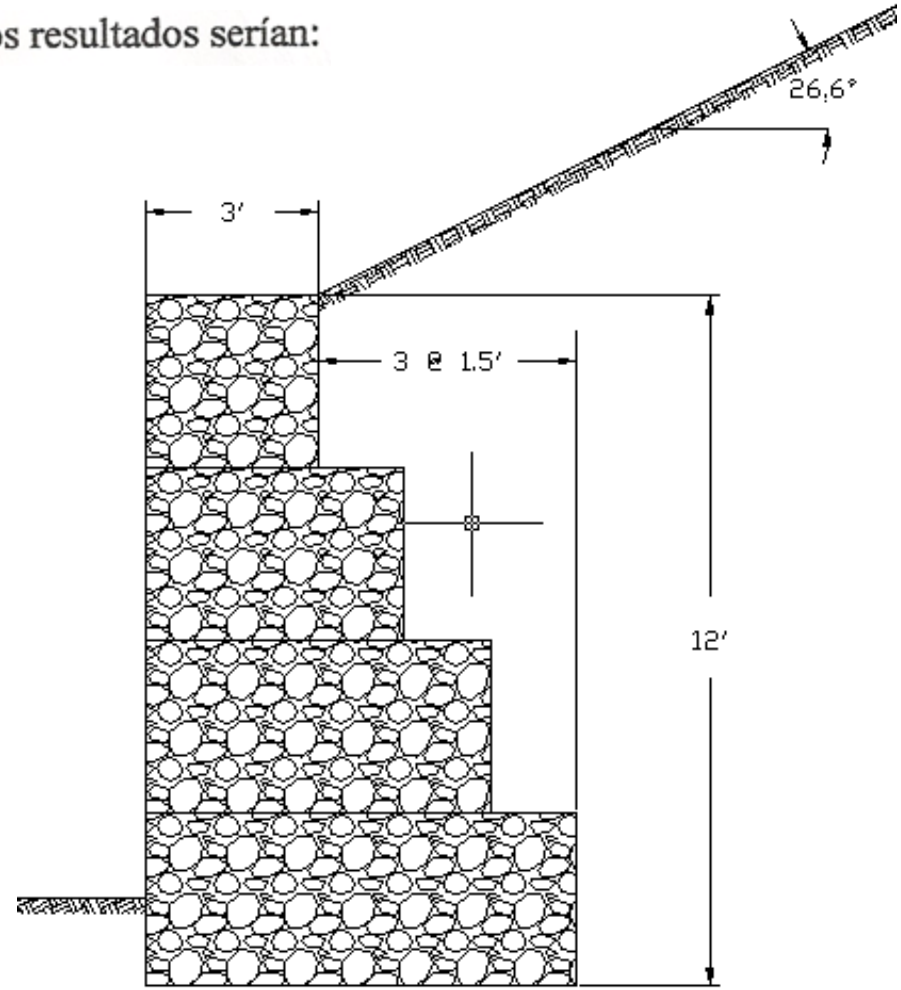

- Note que los factores de seguridad son menores para muros con escalones internos
  - Ka mayor
  - Palanca del peso de gaviones Mas pequeña

Estabilidad Interna

Primer Bloque

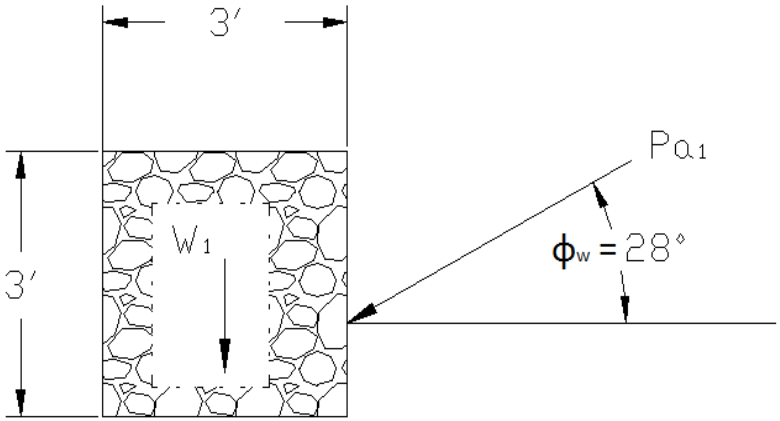

- $K_{a=.384}$ $\gamma=115^{lb}/_{ft^3}$

  $P_{a_1}= {}^1/_2\gamma H^2 K_a = {}^1/_2\,(115)(3^2)(.384)= 199\ lb$

- Factor de Seguridad Contra Vuelco
  - Momento Estabilizante:
    - $W_1= 3x3x105= 945\ lb$
    - $M_{E_1}=(W_1)\,({}^3/_2) =945\,({}^3/_2) =1417.5\ lb\text{-}ft$
  - Momento de Vuelco:
    - $M_{v_1}= P_{a_1}\,({}^1/_3\ x\ 3)= 199\ lb\text{-}ft$
  - FS Vuelco:
    - $FS_{v_1} = M_{E_1}/M_{v_1} = {}^{1417.5}/_{199} = 7.12 > 2$ ok

Estabilidad Interna

Primer Bloque (cont.)

- Factor de seguridad contra vuelco
  - $V_f = f \times P_f = 0.5 \times 1038 = 519\ lb$
    - $f = (0.5\text{-}0.7)$ *entre bloque y bloque*
    - $P_f = \sum Fv = Pav_1 + w_1 = 199 \sin 28 + 945 = 1038\ lb$
  - $FS_{desl} = \frac{V_f}{\sum P_h} = \frac{519}{P_{a_1} \cos \phi_\omega} = \frac{519}{199 \cos 28} = 2.95 > 1.5\ OK$

Estabilidad Interna

Segundo Bloque

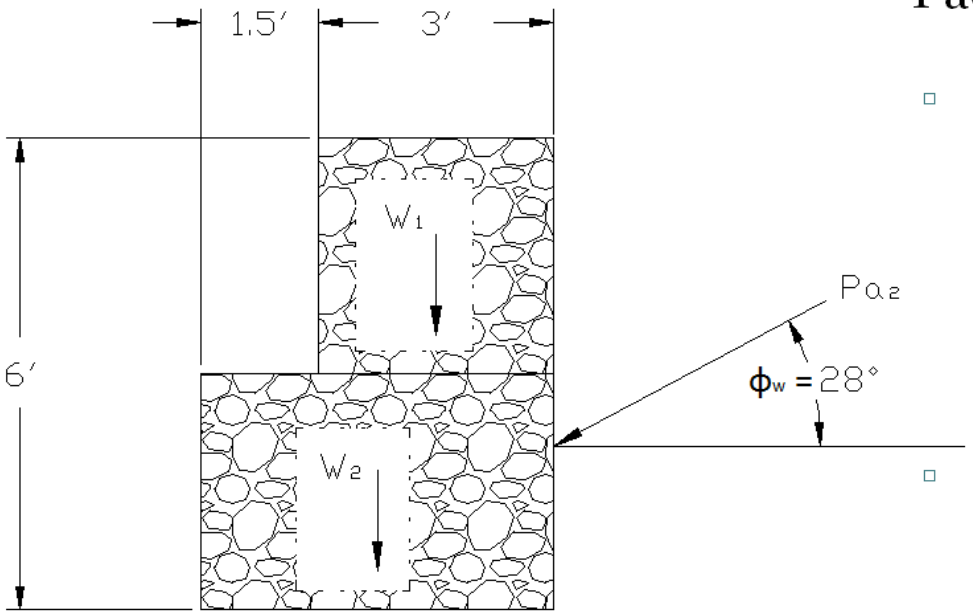

- $P_{a_1} = {}^1/_2 \gamma H^2 K_a = {}^1/_2 (115)(6^2)(.384) = 795\ lb$
- Factor de Seguridad Contra Vuelco
  - Momento Estabilizante:
    - $W_1 = 945\ lb$
    - $W_2 = 4.5x3x105 = 1418\ lb$
    - $M_{E_2} = (W_1)(3) + W_2 ({}^{4.5}/_2) + P_a \sin\phi_{\omega\ (4.5)}$
      $= 945\ (3) + 1418\ ({}^{4.5}/_2) + 795\ sin\ 28\ (4.5)$
      $= 7705\ lb\text{-}ft$
  - Momento de Vuelco:
    - $M_{v_2} = P_{a_2} \cos\phi_\omega ({}^1/_3\ x\ 6)$
      $= 795 \cos 28\ (2) = 1404\ lb\text{-}ft$
  - FS Vuelco:
    - $FS_{v_2} = M_{E_2} / M_{v_2} = {}^{7705}/_{1404} = 5.48 > 2$ ok

Estabilidad Interna

Segundo Bloque (cont.)

- Factor de seguridad contra vuelco
  - $V_f = f \times P_f = 0.5 \times 2736 = 1368\ lb$
    - $P_f = \sum Fv = Pav + w_1 + w_2$
      $= 795 \sin 28 + 945 + 1418$
      $= 2736\ lb$
  - $FS_{desl} = \frac{V_f}{\sum P_h} = \frac{1368}{P_{a_2} \cos \phi_\omega}$

    $= \frac{1368}{795 \cos 28} = 1.94 > 1.5\ OK$

Estabilidad Interna

Tercer Bloque

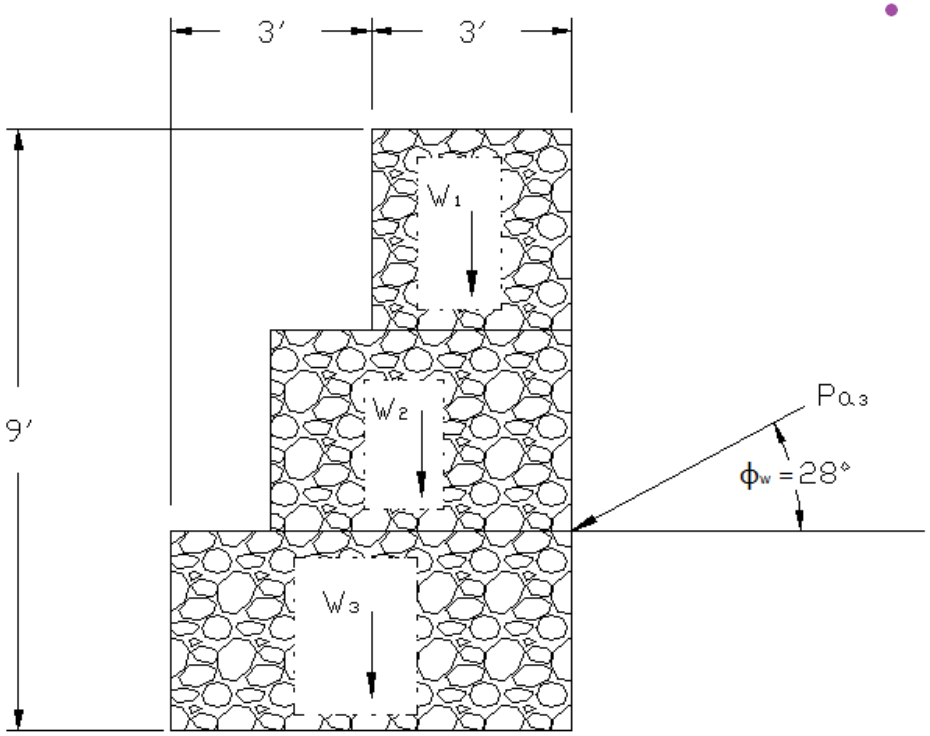

- $P_{a_1} = {}^1/_2 \gamma H^2 K_a = {}^1/_2 (115)(9^2)(.384) = 1789\ lb$
- Factor de Seguridad Contra Vuelco
  - Momento Estabilizante:
    - $W_1 = 945\ lb$
    - $W_2 = 1418\ lb$
    - $W_3 = 6x3x105 = 1890\ lb$
    - $M_{E_3} = (W_1)(4.5) + W_2(3.75) + W_3(3) + P_a \sin\phi_\omega (6)$
      $= 945(4.5) + 1418(3.75) + 1890(3) + 1789 \sin 28\ (6)$
      $= 20279\ lb\text{-}ft$
  - Momento de Vuelco:
    - $M_{v_3} = P_{a_3} \cos\phi_\omega ({}^1/_3 \times 9)$
      $= 1789 \cos 28\ (3) = 4739\ lb\text{-}ft$
  - FS Vuelco:
    - $FS_{v_2} = M_{E_2} / M_{v_2} = {}^{20279}/_{4739} = 4.28 > 2$ ok

Estabilidad Interna

Tercer Bloque (cont.)

- Factor de seguridad contra vuelco
  - $V_f = f \, x \, P_f = 0.5 \, x \, 5093 = 2546 \; lb$
    - $P_f = \sum Fv = Pav + w_1 + w_2 + w_3$
      $= 1789 \sin 28 + 945 + 1418 + 1890$
      $= 5093 \; lb$
  - $FS_{desl} = \frac{V_f}{\sum Ph} = \frac{2546}{P_{a_3} \cos \phi_\omega}$

$$= \frac{2546}{1789 \cos 28} = 1.61 > 1.5 \; OK$$

Estabilidad Interna

Notas Adicionales

- Para este caso en particular:
  - Escalones externos
  - Solo empuje de tierra
  - No cargas adicionales (lineales, distribuidas, etc.)
- FS vuelco y FS deslizamiento
  - Valor baja a medida que se analizan mas bloques profundos.
- Estabilidad interna no domina el diseño
  - Para escalones internos o muro con cargas adicionales, esto puede cambiar.

Análisis Y Diseño:
consideraciones adicionales

- Sobrecarga
  - Siempre se debe considerar una carga viva uniforme de al menos 40 psf.
    - $P_q = q * K_a * H$ (localizada a ½ H)
    - Considerar esta carga solo donde produzca vuelco (no considerar la contribución al momento estabilizante)
- Cargas Sísmicas
  - La teoría de Mononobe-Okabe se puede usar aunque esta se desarrolló para muros rígidos. Los gaviones son flexibles → se obtiene factor de seguridad adicional.
- Otras cargas adicionales
  - Cargas Puntuales o lineales, de trafico, estructuras cercanas, etc.

Drenaje

1 Gabion wall
2 Backfill
3 Drainage hardcore
4 Drain pipe
5 Concrete slab
6 Counterfort

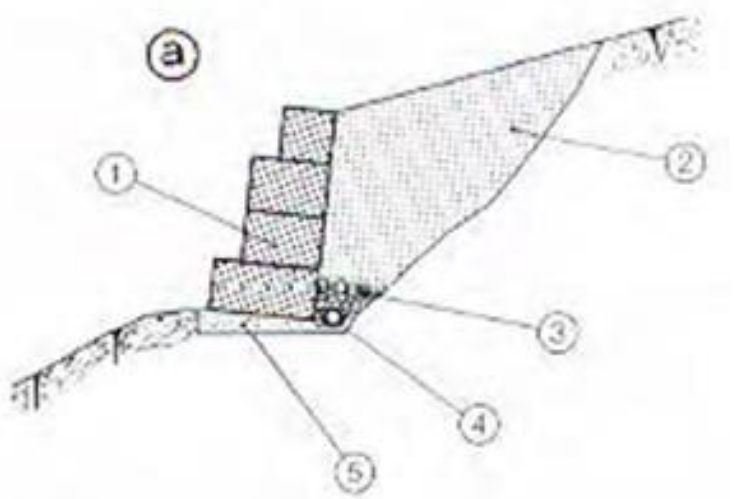

- El muro es prermeable → no requiere drenaje especial
  - No se generan presiones hidrostáticas adicionales
  - No hay peligro de socavación de la fundación por lavado
  - No obstante es recomendable colocar un tubo perforado rodeado por grava limpia para facilitar el transporte de las aguas
- Cuando el material de relleno es mayormente arena se requiere un filtro (geotextil o granular) en la cara interior del muro para evitar socavación (lavado) del suelo de relleno.

Drenaje

1 Gabion wall
2 Backfill
3 Drainage hardcore
4 Drain pipe
5 Concrete slab
6 Counterfort

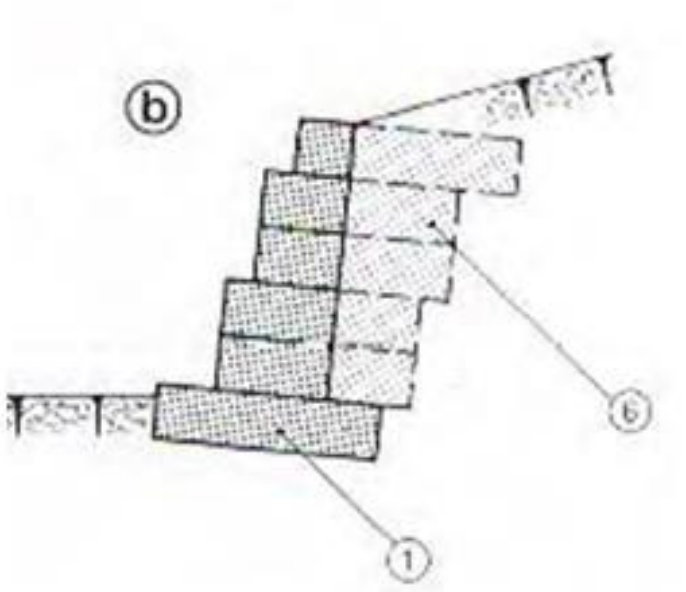

- Cuando el material de relleno es cohesivo (arcillas):
  - Se recomienda usar un sistema de contrafuertes drenantes en gaviones
    - Deben penetrar la totalidad de la cuña de falla
    - Pueden estar espaciados desde 13 ft (arcilla blanda) hasta 30 ft (arcilla rígida)
    - Estas adicionalmente ayudan a estabilizar el muro
  - Se requiere un filtro (geotextil) en la cara interior del muro para evitar que la arcilla bloquee el drenaje propio de los gaviones.
  - Se podría utilizar el método de fluido equivalente para determinar presiones de suelo.

Ejemplo 2: Muro de Gavión

Gabion Gravity Wall Design

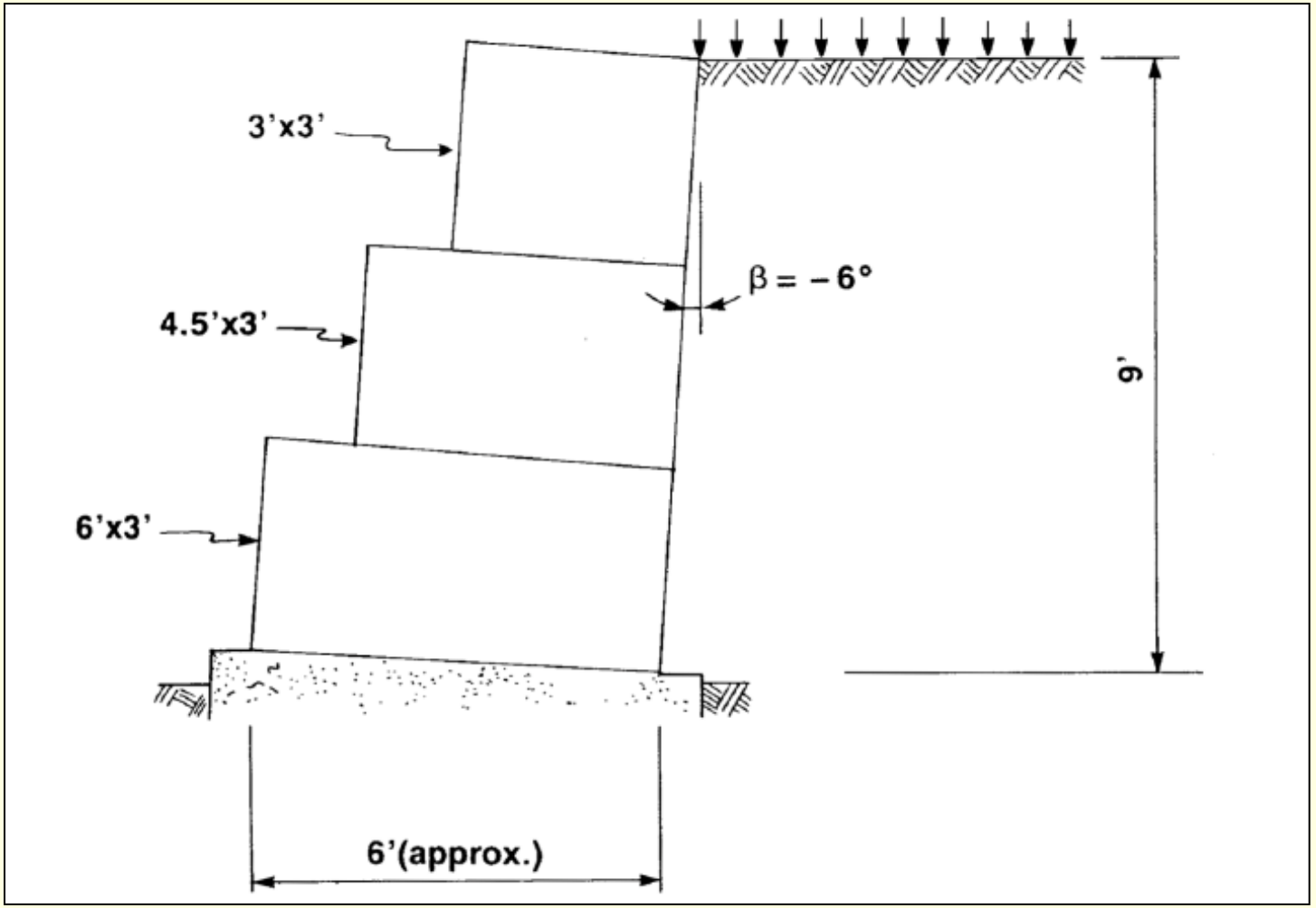

Gabion Gravity Wall Design

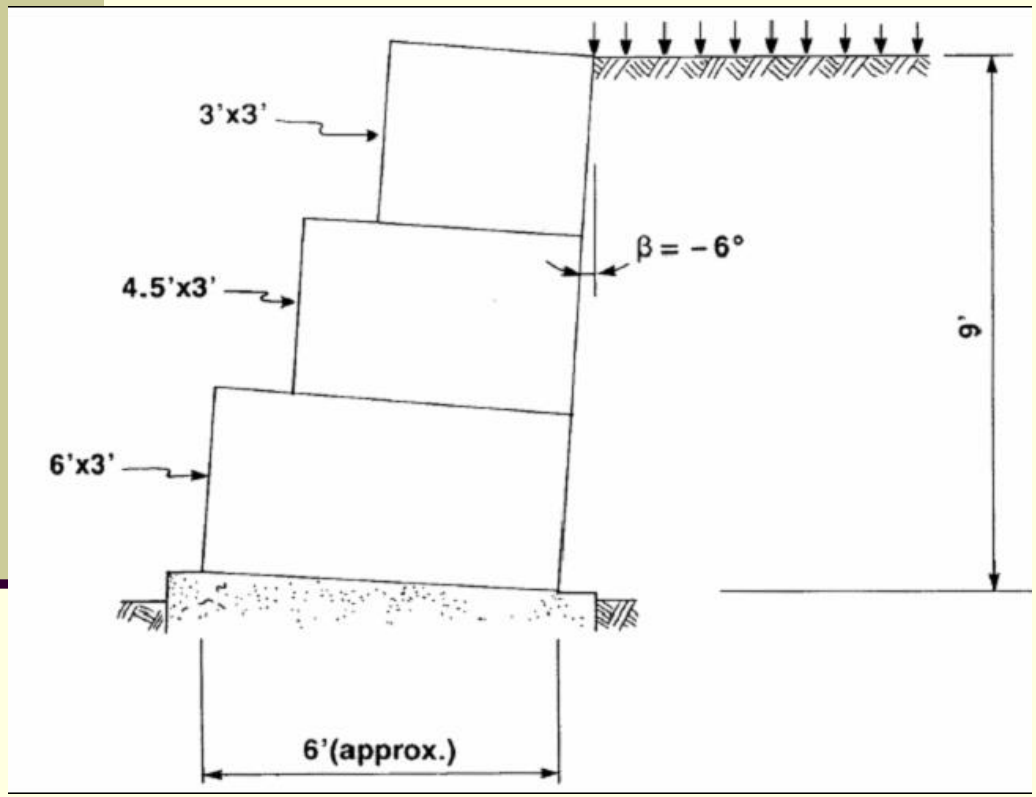

- **Given Data**
  - Wall Height, H = 9 ft
  - Surcharge, q = 300 psf
  - Backfill slope angle, α = 0°
  - Back Face slope angle, β = -6°
  - Soil friction angle, ϕ' = 35°
  - Soil density, γ_s = 120 pcf
  - Gabion fill density, γ_g = 100 pcf
  - Soil bearing pressure, P_b = 4000 psf (allowable = q_{ult}/FS)

Gabion Gravity Wall Design

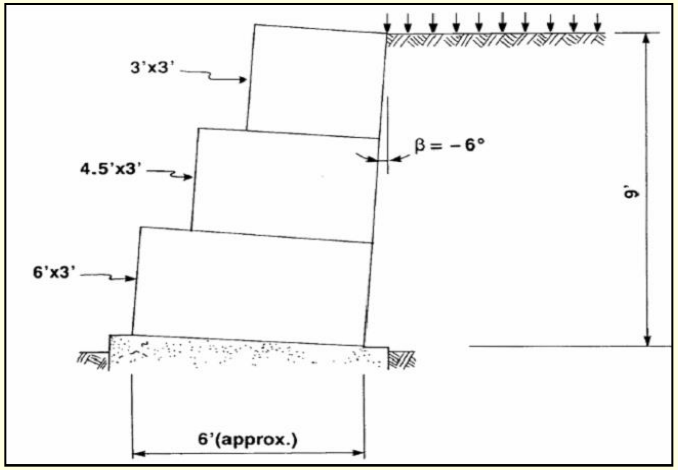

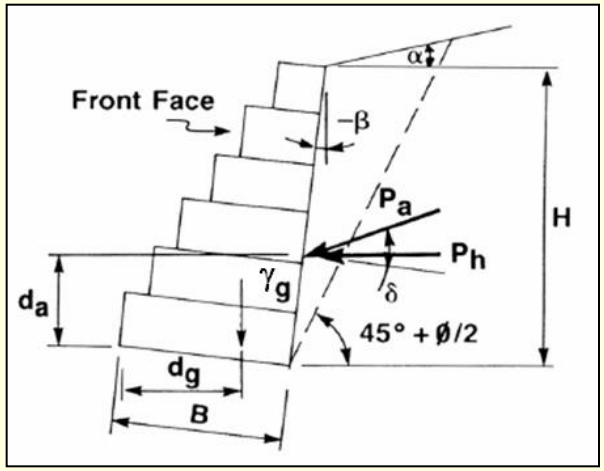

- **Forces Acting on the Wall**
  - $P_a = \frac{1}{2} K_a \gamma_s H^2$ **Eq. 1**

Where:

- γ_s = soil density
- H = wall height, and
- K_a = coefficient of active soil pressure.

$$K_a = \frac{\cos^2(\phi - \beta)}{\cos^2\beta\cos(\delta + \beta)\left[1 + \sqrt{\frac{\sin(\phi + \delta)\sin(\phi - \alpha)}{\cos(\delta + \beta)\cos(\alpha - \beta)}}\right]^2} \quad \textbf{Eq. 2}$$

Where:

- α = slope angle of backfill surface
- β = acute angle of back face slope with vertical
- δ = angle of wall friction
- φ = angle of internal friction of soil

- If a uniformly distributed surcharge pressure (q) is present on top of the backfill surface, Equation 1 is modified to:
- $P_a = K_a(\gamma_s H^2 / 2 + qH)$ **Eq. 1A**
- $P_h = P_a \cos\beta$ **Eq. 3**

Gabion Gravity Wall Design

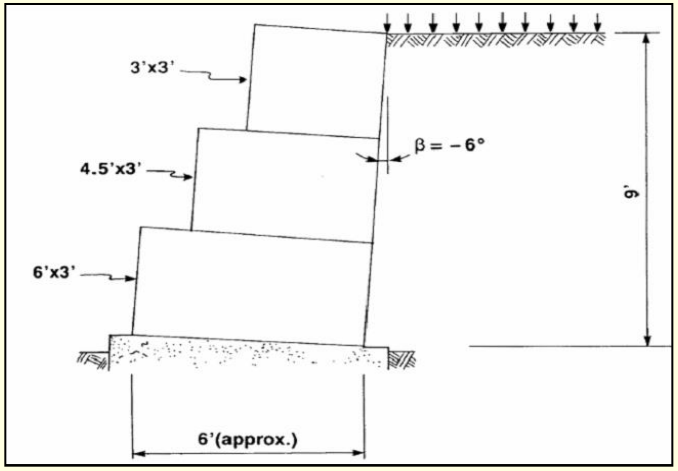

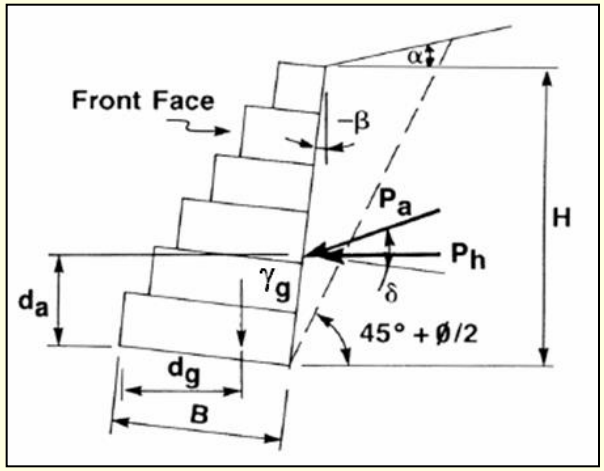

- **Forces Acting on the Wall**
  - Pressure coefficient from Eq. 2 is Ka=0.23
    - $P_a = K_a(\gamma_s H^2 / 2 + qH) =$
    - $P_a = 0.23(120(9)^2/2 + 300*9)$
    - $P_a = 1739$ *lb/ft*
  - Horizontal component from Eq. 3 is
    - $P_h = P_a \cos\beta$
    - $P_h = 1739*\cos(6)$

Gabion Gravity Wall Design

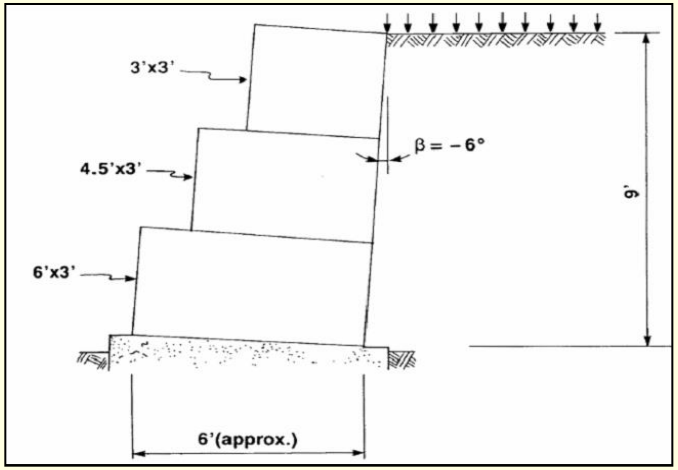

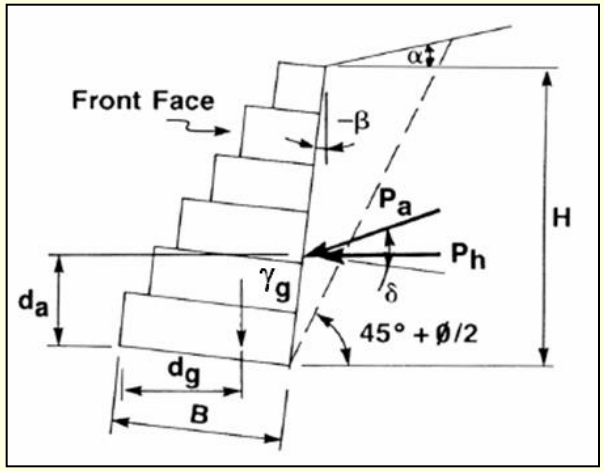

- **Overturning Moment Check**

  Using basic principles of statics, moments are taken about the toe of the wall to check overturning.

  - $M_r \geq SF_o M_o$ **Eq. 4**

  Where:

  - M_r = the resisting moment
  - M_o = the overturning moment, and
  - SF_o = the safety factor against overturning *(typically 2.0).*

  The active earth force acts normal to the slope of the back face at a distance H/3 above the base. When a surcharge is present, the distance of the total active force above the toe becomes

$$d_a = \frac{H(H + 3q/w_s)}{3(H + 2q/w_s)} + B\sin\beta \qquad \textbf{Eq. 5}$$

  - The overturning moment is
  - $M_o = d_a P_h$ **Eq. 6**
  - $M_r = \Sigma dW$ **Eq. 7**
  - $M_r = d_g W_g$ **Eq. 7A**

Gabion Gravity Wall Design

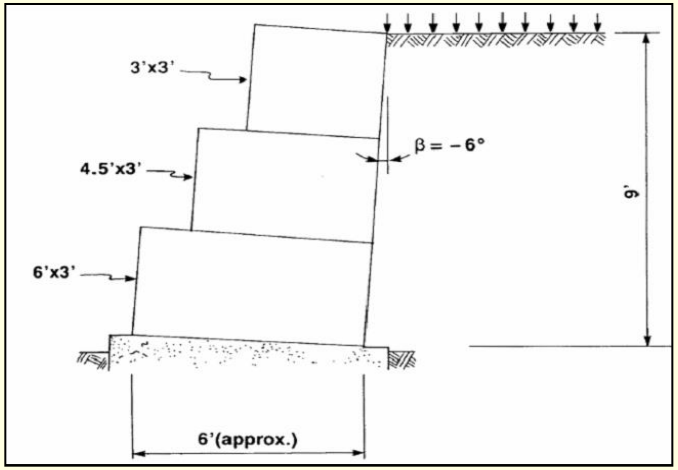

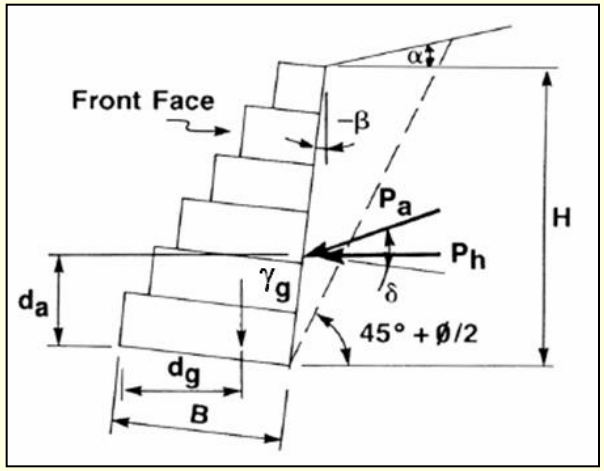

- **Overturning Moment Check**
  - Vertical distance to P_h from Eq. 5 is

$$d_a = \frac{9(9+3\times 300/120)}{3(9+2\times 300/120)} + 6\sin(-6)$$
$$= 2.91\,ft$$

  - Overturning moment from Eq. 6 is
    - $M_o = 2.91*1730 = 5034\ lb\cdot ft/ft$
  - Weight of gabion for a 1-ft unit length is
    - $W_g = (18 + 13.5 + 9)100$
    - $W_g = 4050$ lb/ft
  - Horizontal distance to W_g is

$$dg = \Sigma Ax / \Sigma A$$
$$= \left[\begin{matrix}18(3\cos 6 + 1.5\sin 6) + 13.5(3.75\cos 6 \\ +4.5\sin 6) + 9(4.5\cos 6 + 7.5\sin 6)\end{matrix}\right] / 40.5$$
$$= 3.96\,ft$$

  - Resisting moment from Equation 7 is
    - $M_r = 3.96*4050 = 16038\ lb\cdot ft/ft$
  - Safety factor against overturning from Eq. 4 is
    - $SF_o = M_r/M_o = 16038/5034$
    - $SF_o = 3.19$ ***ok***

Gabion Gravity Wall Design

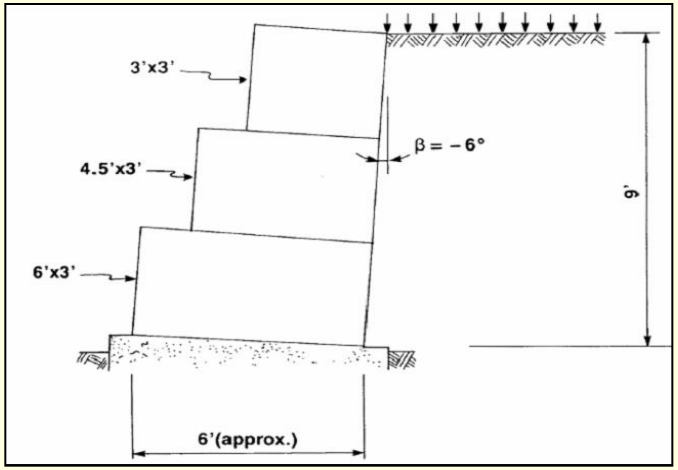

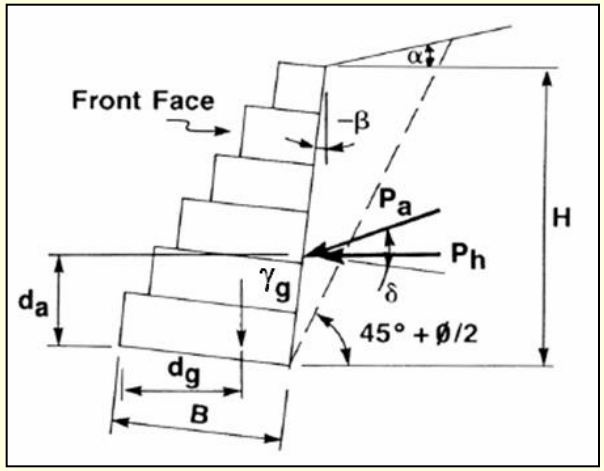

- **Sliding Resistance Check**
  - $\mu W_v \geq SF_s P_h$ **Eq. 8**

  Where:
  - μ = the coefficient of the sliding friction (tan of angle of friction of soil),
  - W_v = the sum of the vertical forces (W_g in this case), and
  - SF_s = the safety factor against sliding (typically 1.5).

  - Safety factor against sliding from Eq. 8 is
    - $SF_s = \mu W_g / P_h$
    - $SF_s = tan(35)*4050/1730$
    - $SF_s = 1.64$ ***ok***

Gabion Gravity Wall Design

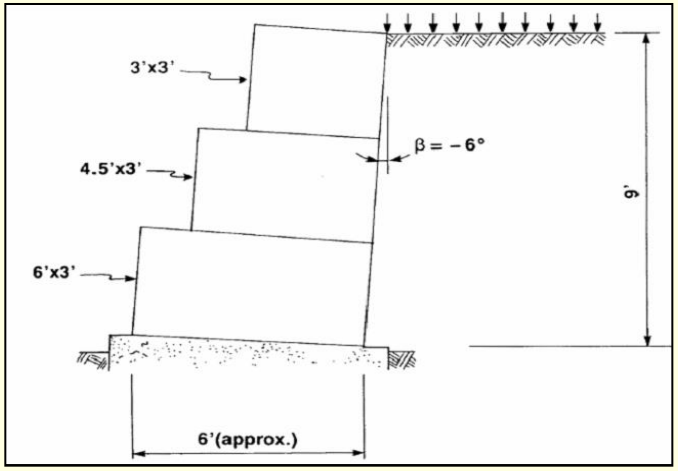

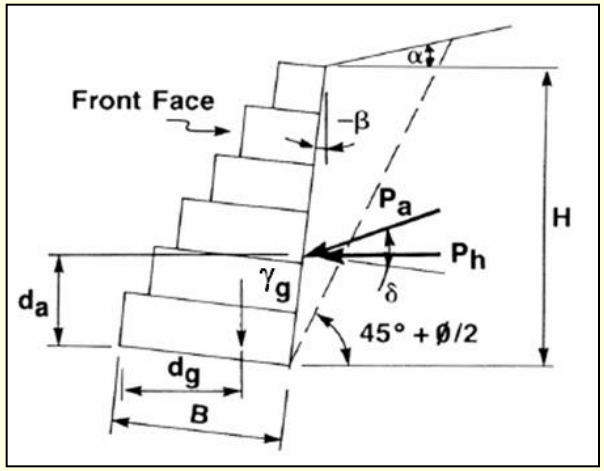

- **Check Bearing Pressure**

  First check to determine if the resultant vertical force lies within the middle third of the base. If B denotes the width of the base, the eccentricity, e, of the vertical force from the midwidth of the base is

  - $e = B/2 - (M_r - M_o)/W_v$ **Eq. 9**
  - For the resultant force to lie in the middle third:
  - $-B/6 \le e \le B/6$ **Eq. 10**
  - The maximum pressure under the base, P, is then
  - $P = (W_v/B)/(1 + 6e/B)$ **Eq. 11**
  - The maximum pressure must not exceed the allowable soil bearing pressure, P_b:
  - $P \le P_b$ **Eq. 12**

Gabion Gravity Wall Design

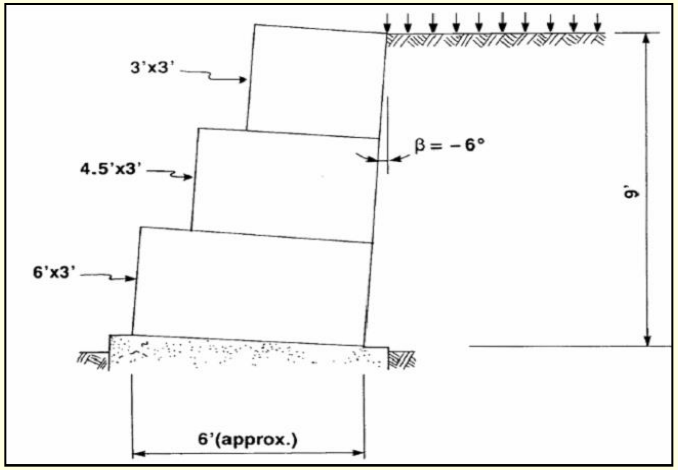

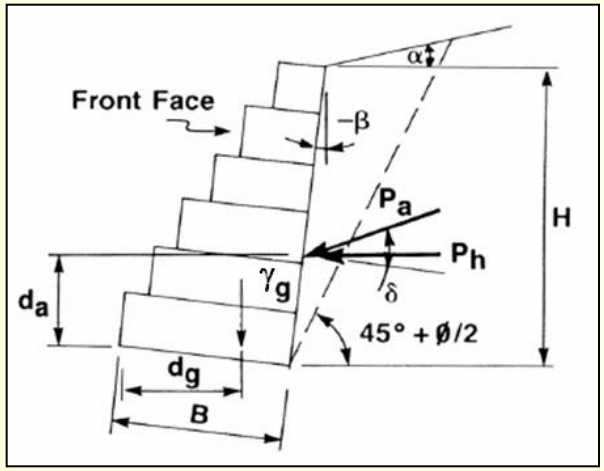

- **Check Bearing Pressure**
  - Reaction eccentricity from Eq. 9 is
    - *e = 6/ 2 – (16038 – 5034) / 4050*
    - *e = 0.283 ft*
  - Limit of eccentricity from Eq. 10 is
    - -1 ≤ *e* ≤ 1 *ft* ***ok***
  - Maximum base pressure from Eq. 11 is
  - *p = (4050/6)*(1 + 6*0.283/6)*
  - *p = 866 psf < 4000 psf* ***ok***

Falta:

- Estabilidad global (probar varias superficies)
- Estabilidad interna del muro
  - deslizamiento de cada canasta
  - Corrosión del alambre